A biosynthetic engineering approach to structural diversification of the enacyloxins

by

Jacob Sargeant

Thesis submitted in partial fulfilment of the requirements for the degree of Doctor of Philosophy in Chemistry

University of Warwick, Department of Chemistry

September 2021

Contents

List of figures

Figure 2.4 Formation of desired plasmid containing the Ser-Ala mutation. Restriction sites used for digestion and ligation are shown. Km^R and Tp^R indicate kanamycin and trimethoprim resistance markers respectively.

Figure 2.5 Workflow for the tri-parental mating procedure used to incorporate the mutated 1 kb ACP region into the genome of *B.ambifaria* BCC0203. Tp^R and Tc^R indicate trimethoprim and tetracycline resistance markers respectively

Figure 2.6 Agarose gel from the PCR of the first tri-parental mating event confirming the presence of the 1 kb mutated ACP fragment. (Lane 1 = HR ladder, lane 2 = MR ladder, lanes 3-12 = PCR products. Observed bands in lanes 8, 9 and 11 correspond to expected 1 kb band expected for the mutated 1 kb region. Primers used can be found in table **6.6**.

Figure 2.7 Agarose gel from the PCR of the second tri-parental mating event confirming the presence of the 1 kb mutated ACP fragment. (Lane 1 = HR ladder, lane 2 = MR ladder, lanes 3-14 = PCR products. Observed bands in lanes 3-14 correspond to expected 1 kb band expected for the mutated 1 kb region. Primers used can be found in table **6.6**.

Figure 2.8 Phenotype screen to monitor for loss of production of wild-type enacyloxin IIa. (**A**) wild-type production confirmed by the presence of characteristic yellow streaks, (**B**) second cross-over product containing the desired mutation in the ACP region shown by the appearance of white streaks indicating the loss of enacyloxin IIa production.

Figure 2.9 UV chromatogram at 360 nm from LC-MS analysis of ethyl acetate extracts of *Burkholderia ambifaria* BCC0203 and a mutant blocked in enacyloxin biosynthesis grown on BSM media (**top**) enacyloxin IIa (**bottom**) second cross-over mutant product blocked in enacyloxin IIa biosynthesis.

Figure 2.10 8 % SDS-PAGE gel of purified proteins and deconvoluted MS. (**A**) KS domain, (**B**) KR-ACP di-domain (* = +178 Da expected for gluconylation) Lane 1 contains pre-stained protein ladder for initial size determination of purified proteins.

Figure 2.11 MS of the phosphopantheine ejection assay (**A**) Control with no NADPH, (**B**) Reaction with NADPH addition

Figure 2.12 Deconvoluted intact protein MS of the stand-alone KS domain and the incubation product of the KS with NAC thioester **95**. * indicates gluconylation

Figure 2.13 8 % SDS-PAGE gel of purified proteins and deconvoluted MS. (**A**) C218A KS variant, (**B**), C699A KS variant (* = gluconylation) Lane 1 contains pre-stained protein ladder for initial size determination of purified proteins

Figure 2.14 Deconvoluted intact protein MS of the KS cysteine mutants and the products when incubated with NAC thioester **95**. (**A**) C218A variant (**top**) and incubation product (**bottom**), (**B**) C699A variant (**top**) and incubation product (**bottom**). * indicates gluconylation.

Figure 2.15 Deconvoluted intact protein MS of the KS C218A + C699A double variant and the product when incubated with NAC thioester **95**.

Figure 2.16 LC-MS analysis of supernatant from *in vitro* assay compared to an authentic standard, (**top**) chemically synthesised authentic standard, (**middle**) +ve reaction, (**bottom**) -ve control

Figure 3.1 Enacyloxin IIa biosynthetic gene cluster with highlighted deleted genes responsible for DHCCA biosynthesis and enacyloxin analogue **77** containing a more rigid unsaturated DHCCA ring with the most potent activity to date (MIC = 0.5 µg/mL).

Figure 3.2 Previously produced enacyloxin analogue isolated from the feeding of **60** to *B.ambifaria* BCC0203 Δ5912-14 (Dr. Joleen Masschelein).

Figure 3.3 Structure of enacyloxin analogue **132** with a linear DHCCA moiety from the feeding of **131** with *B. ambifaria* BCC0203 Δ5912-14

Figure 3.4 (above) NOE spectrum with irradiation of the proton at 2.79 ppm (H_A) causing a positive NOE correlation to the proton at 1.50 ppm (H_B). (below) configurations of the *anti*- and *syn*- diastereomers where the *anti*-configuration orientates the protons within a distance of each other to induce an NOE. The *syn*-

configuration is unable to induce an NOE effect due to the >4-5 Å distance between the protons H_A and H_B.

Figure 3.5 Structure of enacyloxin analogue **145** containing the 7-membered DHCCA ring with the *anti*- configuration isolated from feeding of compound **143** to the *B.ambifaria* BCC0203 Δ5912-14 mutant strain.

Figure 3.6 HPLC chromatograms at 360 nm from extracts of the *B. ambifaria* mutant blocked in DHCCA biosynthesis grown on BSM media supplemented with 7-membered DHCCA analogues **143** and **144**. (top) mixture of enacyloxin analogues with *syn*- and *anti*- relationships between the acid and diol. (bottom) enacyloxin analogue with *anti*-conformation. (R = enacyloxin backbone)

Figure 3.7 Separated products from feeding of diastereomeric mixture of **143** and **144** to *B. ambifaria* BCC0203 Δ5912-14 blocked in DHCCA biosynthesis. The stereochemistry for each product was determined by HPLC comparison of a single analogue with known stereochemistry to a mixture of analogues **145** and **146**.

Figure 3.8 Structures of enacyloxin analogues containing the 7-membered DHCCA ring with *trans*-diol configurations proposed to be formed from the feeding of compounds **148** and **151** to *B. ambifaria* BCC0203 Δ5912-14.

Figure 3.9 Structures of biologically active compounds tazobactam **154**, rufinamide **155** and a vancomycin homodimer **156** formed from copper catalysed click reactions (Van = Vancomycin, VSEF = vancomycin susceptible *Enterococcus faecali*s, VRE = vancomycin resistant *Enterococcus*)

Figure 3.10 Structures of PEG-azides to be used in copper-catalysed click reactions to improve the aqueous solubility of the enacyloxins

Figure 3.11 (**A - top**) UV chromatogram at 360 nm of ethyl acetate extracts of the crude product from *B. ambifaria* BCC0203 Δ5912-14 blocked in DHCCA biosynthesis supplemented with **178**, (**A-bottom**) EIC for m/z = 740.2604 (corresponding to $[M+H]^+$ for **163**) from UHPLC-HRMS (**B**) HRMS data of species at 17 minutes.

Figure 4.9 ESI mass spectra of *E. coli* EF-Tu sprayed from ammonium acetate showing preferential binding of enacyloxin IIa (5 μM) to the EF-Tu•GDPNP complex (**A**) compared to the EF-Tu•GDP complex (**D**). Charge states of each species are shown above the m/z values. Figure provided by Professor Neil J. Oldham (University of Nottingham).

Figure 4.10 Enacyloxin analogues selected for native mass spectrometry studies at the University of Nottingham. Antimicrobial activities against *A. baumannii* are provided alongside the binding affinities for EF-Tu•GDPNP. (Values in brackets correspond to binding to EF-Tu•GDP when binding to EF-Tu•GDPNP was below <0.5 μM.)

Figure 4.11 ESI mass spectrum of the 12+ charge state (*m/z* = 3735.2) of the EF-Tu•GDPNP complex. Bound to enacyloxin analogue **163**, following isolation using the quadrupole. Activation of this complex results in ejection of the enacyloxin analogue **163**, which can be observed at *m/z* = 762.3 and displays the expected isotopic distribution (inset). Figure provided by Professor Neil J. Oldham (University of Nottingham).

Figure 5.1 Example of halide incorporation pattern of analogues offering insights in the halide preference of the two halogenase enzymes halogenases.

Figure 5.2 Structures of potential NAC thioester mimics to be used in the *in vitro* assay.

Figure 5.3 Structures of potential analogues produced by a combination of domain swapping and previously discussed backbone modification strategies.

Figure 5.4 Structure of potential analogues by mutating the DH domains of module 8 and 9 in the enacyloxin PKS.

List of schemes

Scheme 1.12 Thioesterase catalysed chain release via macrocylisation (top) and hydrolysis (bottom). (X = OH or NH_2)

Scheme 1.13 Reductase domain catalysed chain release to produce either an aldehyde or primary alcohol product

Scheme 1.14 Manipulation of the erythromycin PKS where the TE domain has been repositioned to the terminus of module 2 to afford the expected lactone product **21**

Scheme 1.15 Mutagenesis within the monensin PKS system. (Top) pre-modified PKS responsible for pre-monensin production, (bottom) Mutagenesis (Gly, Gly → Ser, Pro) of ER domain in module 2 responsible for the production of ER2-A. Only module 2 of the PKS is shown for clarity

Scheme 1.16 Early steps in rhizoxin biosynthesis with a mutasynthesis approach to the production of rhizoxin analogues. Oxazole formation by the HC and OXY domains is blocked due to an in-frame deletion of the HC domain. Feeding of a NAC thioester mimics of the intermediate assembled on module 1 of the PKS-NRPS results in rhizoxin and novel analogue production. (A = adenylation domain, OXY = oxidase domain; scheme adapted from Kusebauch *et al*.

Scheme 1.17 Cycle for the transportation of t-RNA to the ribosome using the EF-Tu•GTP complex. Binding of enacyloxin IIa locks EF-Tu in its GTP bound state preventing bacterial protein synthesis (highlighted).

Scheme 1.18 Proposed biosynthetic pathway for production of the polyketide enacyloxin IIa.

Scheme 1.19 Transacylation of the enacyloxin polyketide chain from the Bamb_5919 ACP domain to the Bamb_5917 PCP domain followed by chain release catalysed by the Bamb_5915 condensation domain and DHCCA (R represents the fully assembled polyketide chain). The domain marked with a '?' is of unknown function.

List of tables

Table 6.27 NMR assignments for Δ5912-14 enacyloxin analogue **132** (d_4-MeOH, ^1H 500 MHz, ^{13}C 125 MHz)

Acknowledgements

Firstly I would like to thank my supervisor Professor Greg Challis for the opportunity to work on such an exciting and interesting project within a fantastic research group. His support and guidance has been invaluable during my time at Warwick. Thanks are also owed to Dr Lona Alkhalaf for all her support and guidance throughout my project and for reading and editing countless thesis drafts.

Special thanks also go to Christian Hobson, Helen Smith, Dr Xinyun Jian, Ioanna Nakou, Dr Matt Beech, Dr Jinlian Zhao, Dr Chuan Huang, Dr Matthew Jenner and Fang Pang for all the knowledge and guidance they have offered over the years. I could not have done any of this without them. Thanks to everyone in Challis group for making the time during my PhD so enjoyable and for keeping me going through the hardest of days.

I would also like to thank Dr Lijiang Song and Dr Ivan Prokes for the countless mass spectrometry and NMR samples that they have run for me over the years.

Thanks are owed to MIBTP and BBSRC for funding.

I would like to thank my family who have helped and supported me throughout my endeavours. My brother Sam, sister-in-law Alison and Fiancée Hannah have always been there to cheer me on and I can't tell them enough what that means to me.

Finally, I would like to thank my parents, Kim and Jonathan who have always loved and supported me in whatever I set out to achieve. They both mean so much to me and I will never be able to thank them enough for what they have done for me over the years.

Declaration

This thesis has been prepared in accordance with the university's guidelines on the presentation of a research thesis for the degree of Doctor of Philosophy. The experimental work reported in this thesis is original research carried out by myself, unless otherwise stated. No material has been submitted in any application for any other degree.

Results from other authors are referenced in the usual manner throughout the thesis.

Date: 29/09/2021

Jacob Sargeant

Abbreviations

A	Adenylation domain
Å	Angstrom
ACP	Acyl carrier protein
AMR	Antimicrobial resistance
AT	Acyl transferase
ATP	Adenosine triphosphate
ATR	Attenuated total reflection
Bcc	*Burkholderia cepacia* complex
BSM	Basal salts medium
CAN	Ceric ammonium nitrate
cbz	Carboxybenzyl
CFU	Cell forming units
CoA	Coenzyme A
COSY	Correlation Spectroscopy
Da	Daltons
DEBS	6-deoxyerythronolide B synthase
DH	Dehydratase
DHCCA	Dihydroxycyclohexane carboxylic acid
DMF	Dimethylformamide
DMSO	Dimethylsulfoxide
DNA	Deoxyribonucleic acid
DPCK	Dephospho-CoA kinase
EDTA	Ethylenediaminetetraacetic acid
EF-Tu	Elongation factor thermo unstable
EIC	Extracted Ion chromatogram
ER	Enoyl reductase
ESI	Electrospray ionisation
EU	European Union
FAD	Flavin adenine dinucleotide
FDA	Food and Drug Administration
FP	Forward primer
FSM	Fully synthetic macrolide
GDP	Guanosine diphosphate
GDPNP	Guanylyliminodiphosphate
GNAT	GCN5-related *N*-acetyl-transferase
GSK	GlaxoSmithKline
GTP	Guanosine triphosphate
HC	Heterocylisation domain
HCl	Hydrochloric acid

HDD	Hairpin docking domain
HMBC	Heteronuclear multiple bond correlation
HMPA	Hexamethylphosphoamide
HPLC	High performance liquid chromatography
HR	High-range
HRMS	High resolution mass spectroscopy
HSQC	Heteronuclear single quantum coherence
HTS	High throughput screening
Hz	Hertz
ICU	Intensive care unit
IP	Intraperitoneal
IPTG	Isopropyl β-D-1-thiogalactopyranoside
IR	Infrared
KG	Ketoglutarate
KLD	Kinase, ligase and Dpn1
KPSI	Kilo pounds per square inch
KR	Ketoreductase
KS	Ketosynthase
L	Litre
LB	Luria-Bertani
LC-MS	Liquid chromatography mass spectrometry
LiHMDS	Lithium bis(trimethylsilyl)amide
m-CPBA	*Meta*-chloroperoxybenzoic acid
MDR	Multi-drug resitant
mg	Milligram
MH	Mueller Hinton
MIC	Minimum inhibitory concentration
mL	Millilitre
MR	Mid-range
MRSA	Methicillin-resistant *Staphylococcus aureus*
MS	Mass spectrometry
MT	Methyl transferase
NAC	*N*-acetylcysteamine
NADH	β-Nicotinamide adenine dinucleotide
NADPH	β-Nicotinamide adenine dinucleotide 2'-phosphate
nm	Nanometre
NMR	Nuclear magnetic resonance
NOE	Nuclear overhauser effect
NRPS	Non ribosomal peptide synthase
OD	Optical density

Omp	Outer membrane protein
OXY	Oxidase domain
PAGE	Polyacrylamide gel electrophoresis
PANK	Pantetheine kinase
PCC	Pyridinium chlorochromate
PCP	Peptidyl carrier protein
PCR	Polymerase chain reaction
PDB	Protein data bank
PDP	Penicillin binding protein
PEG	Poly(ethylene) glycol
PKS	Polyketide synthase
PPAT	Phosphopantetheine adenylyltransferase
ppm	Parts per million
PPTase	Phosphopantetheinyl transferase
PQQ	Pyrroloquinoline quinone
R	Reductase domain
RNA	Ribonucleic acid
RP	Reverse primer
rpm	Revolutions per minute
RT	Room temperature
SAM	S-adenosylmethionine
SAR	Structure activity relationship
SDS	Sodium dodecyl sulfate
SLiM	Short linear motif
TAE	Tris-acetate-EDTA
TB	Tuberculosis
TBAF	Tetrabutylammonium fluoride
TBE	Tris-borate-EDTA
TBS	*tert*-butyldimethylsilyl
TE	Thioesterase
TEMED	Tetramethylethylenediamine
THCCA	Trihydroxycyclohexane carboxylic acid
THF	Tetrahydrofuran
TLC	Thin layer chromatography
TOF	Time of flight
UHPLC	Ultra-high performance liquid chromatography
USA	United States of America
UTI	Urinary tract infection
VRSA	Vancomycin-resistant *Staphylococcus aureus*
WHO	World Health Organisation
WT	Wild-type

Abstract

As anti-microbial resistance becomes increasingly concerning, it is imperative that drug discovery efforts are focussed on combatting it. Natural products have historically been crucial in the fight against pathogenic bacteria. However, their recent use has been in steady decline. An increased understanding of natural product biosynthesis presents an exciting opportunity to produce novel pharmaceuticals capable of tackling this growing threat. One such potential compound is the polyketide enacyloxin IIa, produced by *Burkholderia ambifaria,* which is active against the multi-drug resistant pathogen *Acinetobacter baumannii*.

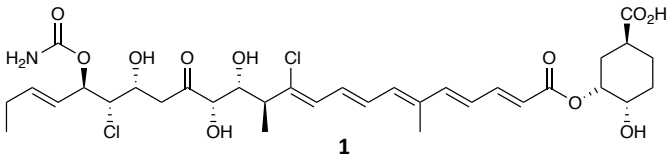

1

Figure 1 Structure of enacyloxin IIa

Several approaches were used to produce analogues of enacyloxin IIa. Brominated analogues were generated by swapping all sources of chloride in the media with bromide, and analogues with modifications to the dihydroxycyclohexane carboxylic acid (DHCCA) moiety were generated by mutasynthesis. The possibility of using *N*-acetylcisteamine (NAC) thioester analogues as mimics of polyketide synthase linked intermediates was also investigated both *in vivo* and *in vitro.* The MIC of novel analogues against *A. baumanii* gave useful insights into the structure activity relationship (SAR) of enacyloxin with its microbial target, elongation factor Tu (EF-Tu).

Finally, via collaboration with Monash University and Nottingham University, a selection of analogues were used to investigate *in vivo* efficacy and toxicity in mouse models, and binding to EF-Tu using in-tact protein mass spectrometry, respectively.

Chapter 1 - Introduction

1.1 Antibiotics

1.1.1 History of antibiotics

Use of antibiotics can be traced back to ancient Sudanese Nubia[1] with skeletal remains found to contain the antibiotic tetracycline. Despite limited knowledge of what chemical entity was involved in combatting infectious diseases, naturally occurring materials have historically been used for therapeutic effect. It wasn't until the second half of the twentieth century that antibiotic discovery was at the forefront of infectious disease control (figure **1.1**).

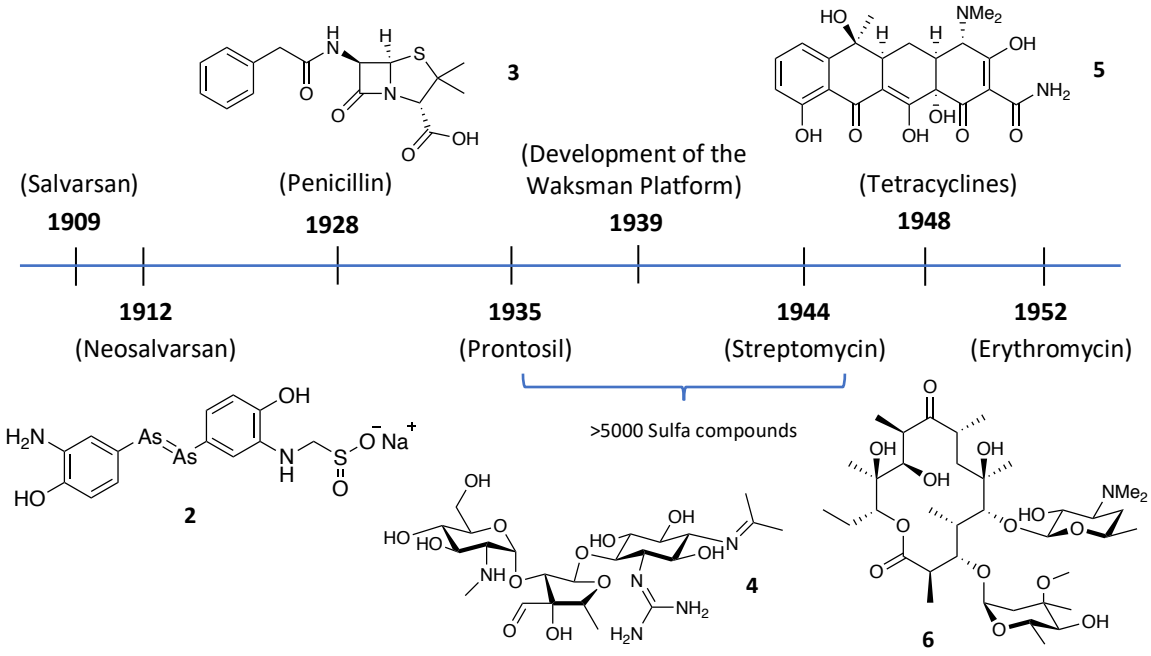

Figure 1.1 Timeline of key discoveries in the field of antibiotic drug discovery with chemical structures for key compounds; Neosalvarsan **2**, penicillin G **3**, streptomycin **4**, tetracycline **5** and erythromycin A **6**.

In the early 1900s, Paul Ehrlich came up with the concept of a 'magic bullet' to selectively eliminate pathogenic bacteria whilst leaving the host intact.[2,3] This revolutionary idea led to the search for compounds to combat the prevalent and near incurable sexually transmitted disease syphilis.[4,5] In 1909 a compound sold under the name Salvarsan whose structure has only recently been solved[6]- was seen to be

active against syphilis[7] and was further modified into the more soluble and less toxic drug Neosalvarsan (figure **1.1**).[3,8] These became the most prescribed drugs until the serendipitous discovery of penicillin by Sir Alexander Fleming.[9] Fleming observed a zone of inhibited Staphylococcus bacterial growth around a fungus/mould contaminant on an agar plate. Isolation of the mould identified it as a *Penicillium* active against Gram-positive pathogens. However, Fleming struggled to produce the compound on a sufficient scale due to purification and stability issues.[3] It wasn't until 1939 that Sir Howard Florey and Ernst Chain were able to purify the penicillin in sufficient quantities for clinical testing and mass distribution. This enabled the elucidation of the structure in 1942, with confirmation by Dorothy Hodgkin in 1945.[10] For their efforts into the discovery and development of penicillin **3** as an antibiotic, Fleming, Chain and Florey were each awarded the Nobel Prize in Physiology and medicine in 1945 with Hodgkin being awarded the Nobel Prize in Chemistry in 1964.

Prior to the widespread use of penicillin **3** towards the end of World War II, other examples of antibiotic production had emerged. In 1935 Gerhard Domagk reported his findings of a new class of antibiotics from his research into the antibacterial properties of synthetic dyes.[11] The red dye chemical known as Prontosil became commercially available as a treatment for bacterial infections. However, it was later realised that when consumed, Prontosil was metabolised into sulphanilamide. This contained the key sulphonamide functional group responsible for the observed antibacterial activity which soon became a platform in the development of over 5000 broad spectrum antibiotic compounds known as the sulfa drugs.[3,5,7,12,13]

During this period of sulfa-compound development, Selman Wakesman and Harold Woodruff developed what is now commonly referred to as the Waksman Platform.[14] This revolutionary method was used to detect for the presence of soil-borne antibiotics with particular interest to those active against Gram-negative bacteria.[15–17] Observed zones of bacterial growth inhibition on agar plates, surrounding samples of soil microbes incubated with a variety of bacterial cultures, were used to identify potential sources for novel antimicrobials. The microbes resulting in growth inhibition were used to further test against a range of pathogens for specific activity

and the active substances identified and isolated. This platform let to the discovery of streptomycin **4** in 1944 which is active against *Mycobacterium tuberculosis*.[18,19] At the time, penicillin **3** and a variety of sulfa drugs were available, however none were active against tuberculosis (TB) which was a problematic pathogen responsible for many deaths.[17] Since the discovery of streptomycin **4** the Waksman Platform has been used by many including the pharmaceutical industry in the production of a vast quantity of novel antibiotics during a period coined as the 'golden era' or antibiotic production.[3,16] Antibiotics currently in use today but developed during the golden era (figure **1.1**) include the macrolide erythromycin **6**, used for the treatment of Gram-positive respiratory tract and skin infections and tetracycline **5**, active against both Gram-positive and Gram-negative bacterial infections such as pneumonia and urinary tract infections (UTIs).[20]

In the 21st century, antibiotics remain heavily relied upon for treatment of ailments ranging from mild pain relief to life threatening diseases. In 2009, the global antibiotics market saw sales of $42 billion demonstrating the importance of these essential drugs.[21] However, since the 'golden era' of antibiotic production between the 1940-1960s, very few novel antibiotics have been developed. This has become increasingly worrying due to the presence of anti-microbial resistance (AMR) and the devastating knock-on effects caused.

1.1.2 Anti-microbial Resistance (AMR)

Since the inception and widespread implementation of penicillin in the 1940s, AMR has become of increasing concern to the scientific community due to the development of natural resistance mechanisms. Bacteria can reduce the efficacy of antibiotics by a variety of mechanisms including target site modifications, control of intracellular antibiotic concentrations via efflux pumps and production of antibiotic deactivating enzymes.[22–24]

One such problematic pathogen is *Staphylococcus aureus*.[22] Resistance against the β-lactam penicillin **3** emerged in strains containing a gene encoding a β-lactamase, resulting in the hydrolysis of the β-lactam ring responsible for antimicrobial activity.[25,26] To overcome this issue a semi-synthetic alternative was produced in 1959 called methicillin. This penicillin derivative contains a methoxy-disubstituted phenol ring, with increased steric hindrance on the lactam ring which inhibits lactamase efficacy.[27] However, soon after methicillin became available, methicillin-resistant *S. aureus* (MRSA) strains were identified, in which the target of β-lactams, penicillin binding protein (PDP), is mutated. This results in a structural change to the protein which relocates the active site into an inaccessible deep pocket resulting in resistance to all β-lactam antibiotics.[22] The glycopeptide vancomycin **7** can be used as an alternative since it targets bacterial cell wall biosynthetic intermediates. However, emergence of vancomycin-resistance *S.aureus* (VRSA) has already been observed.[26] Combination drugs such as quinupristin / dalfopristin marketed as Synercid® are now used to combat VRSA, but in 2015, over 148,000 infections and over 7000 deaths in the EU were as a direct result of MRSA.[28]

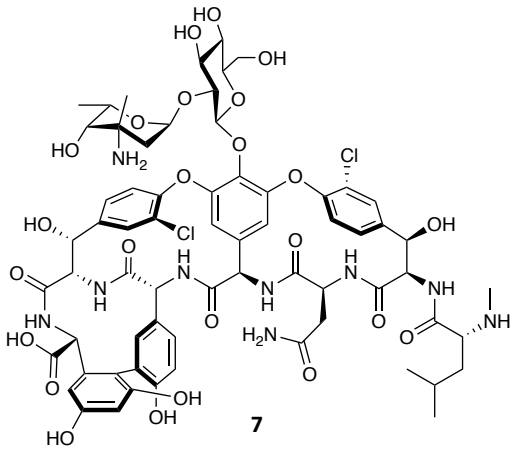

7

Figure 1.2 Structure of the antibiotic vancomycin used in the treatment of MDR Gram-negative pathogens

This demonstrates the urgent need for novel antimicrobials to combat AMR and the resultant economic cost within the healthcare industry. However, in order to do this we need to drastically change our current relationship with antibiotics.

Throughout the period of antibiotic availability there has been a serious issue of misuse of antibiotics for human and "nontherapeutic animal use".[29] Over-prescription of common antibiotics, due to pressures on doctors to have a positive impact on patients, combined with fear of overlooking treatable bacterial infections[30] and self-medication play a role in the rise of AMR.[3,31] Abuse of antibiotics can be seen within the agricultural industry as it's estimated that 80 % of antibiotics in the USA are for use in animals,[31–33] where their primary use was growth promotion with the added benefit of infection control. This practice was banned by the European Union (EU) in 2006[3,33] due to the concern of the effect on AMR due to the transfer of these compounds into the environment and humans via secretion and other means.[3,24,32–34] It is therefore vital that in parallel to the investment into the production of novel antibiotics, we play an active role in the stewardship of current and future antibiotics.

1.2 WHO priority pathogens

With the rise in anti-microbial resistance, a list of six nosocomial pathogens exhibiting multi-drug resistance was formed.[35] These pathogens, commonly referred to as the "ESKAPE" pathogens include; *Enterococcus faecium, Staphylococcus aureus, Klebsiella pneumoniae, Acinetobacter baumannii, Pseudomonas aeruginosa* and *Enterobacter* spp and are frequently used to determine the efficacy of novel drugs. Due to the threat posed by antibiotic resistance the World Health Organisation (WHO) has recently published a list of 12 priority pathogens requiring urgent research and development.[35,36] These are separated into 3 priority categories; Critical, High and Medium and contain multiple ESKAPE pathogens.

Within the critical category are the pathogens *Acinetobacter baumannii, Pseudomonas aeruginosa* and *Enterobacteriaceae*. Of particular concern and focus of this work is *Acinetobacter baumannii*, a Gram-negative multi-drug resistant pathogen responsible for numerous hospital acquired infections and deaths across the world.[37]

1.2.1 *Acinetobacter baumannii*

Acinetobacter baumannii belongs to the genus *Acinetobacter* and was first isolated in 1911 by a Dutch microbiologist named Martinus Beijerinck from soil enriched with a calcium acetate minimal media.[38] This genus was originally named *Micrococcus calcoaceticus,* but later changed to, *Acinetobacter* following studies by Brisou and Prevot[39] and Baumann *et al*.[40] The *Acinetobacter* genus contains 34/35 species with most found within common soil and surface water sources.[37,41] Whilst *A. baumannii* is not prolific, the severity of an acquired infection within a hospital environment, or in an already vulnerable individual, makes it of significant concern. One area *A. baumannii* is particularly problematic is in the dry and sandy conditions of conflict zones such as Iraq, earning it the nickname 'Iraqibacter'.[37,42–45] The return of wounded military personal to the UK and US can then cause outbreaks of further infections within a hospital environment.

A. baumannii is an opportunistic nosocomial pathogen that poses a significant risk to patients, especially those that are immunocompromised in the intensive care unit (ICU). The ability of the pathogen to form biofilms due to influences such as outer membrane proteins (Omp) allows the pathogen to survive on hospital surfaces and medical devices causing further outbreaks and infections.[23,37,43,46–48] Despite being treatable up until the early 1970s, high levels of resistance means many previously active antimicrobials are now considered ineffective.[49] Due to the survivability and high rate of spread of *A. baumannii*, in the EU in 2015 over 30,000 infections were attributed to antibiotic resistant strains with over 2,500 deaths.[28] Current treatments for *A. baumannii* infections include the drug Sulbactam – a ß-lactamase inhibitor-used synergistically with ampicillin, carbapenems and others.[50–53] The most effective treatments reported involve the use of colistin-based combinatory methods however these are generally used as last resort approaches due to unwanted side-effects such as nephrotoxicity and to minimise overuse.[22,29,52,54] Despite this last resort approach to minimise antimicrobial resistance, 2015 saw over 1000 infections and almost 100 deaths caused by colistin-resistant strains of *A. baumannii*.[28]

These alarming figures outline the urgent requirement for the discovery of novel antimicrobials to combat this devasting and life-threatening pathogen which will in turn relieve some of the economic burden our healthcare systems currently face.[55–57]

1.3 Novel drug discovery

Despite the rise of anti-microbial resistance, anti-bacterial drug discovery efforts within pharmaceutical companies has declined in recent years.[58,59] Following the success of the Waksman platform, discovering new antibiotic classes became increasingly difficult, with frequent rediscovery of known compounds. Furthermore, previous wide spread successes of antibiotics led to complacency in the belief that further research was not required.[60]

A new found interest in drug discovery was seen following the report in 1995 of the first complete DNA sequence for the bacterial genome from *Haemophilus influenzae*. After the fading success of traditional screening methods, this paved the way for a promising genomics-based target-led high-throughput screening (HTS) approach for the production of novel targets as potential antimicrobials. Gene sequencing comparisons to both Gram-positive and -negative pathogens, followed by gene deletion strategies, identified target genes essential for bacteria survival. Between 1995-2001, GlaxoSmithKline (GSK) identified 160 possible proteins as targets for novel antibacterials.[61,62] 67 HTS campaigns were completed against a synthetic collection of 260,000-530,000 compounds. Only 15 out of the 67 campaigns generated hits, for which only 5 resulted in leads. Due to failings of target-led strategies they attempted to use a whole cell screening approach. Another 3 HTS campaigns against a synthetic compound library of around 500,000 once more produced disappointing results.

The overall outcomes of such an intensive and high financial investment with limited results was not confined to GSK. Difficulties were seen in another 34 companies, further highlighting the challenges associated with novel drug discovery efforts.[63]

These failings can be associated to a number of factors including the types of synthetic libraries used. Most synthetic libraries for drug discovery are based around Lipinski's rule of 5, despite active compounds generally deviating from them.[61,64] Poor cell penetration of *in vitro* targets especially in Gram-negative species made it difficult for industries to justify further financial investment into an already struggling field.[65]

1.3.1 Re-emergence of Natural Products as antibiotics

Since the aforementioned 'golden age' of antibiotic discovery, natural products as a rich source of novel pharmaceuticals have been in steady decline. The genomic era opened up a variety of options for novel natural product discovery including the development of new screening methods, moving away from typical phenotype based screens.[66] Other methods such as genome mining coupled with a growing knowledge of natural product biosynthesis helped to drive a revitalised natural product drug discovery effort.[67–69] Despite the previous success of natural products as novel antimicrobial agents producers, very few possess the required physical properties to be effective without structural modifications.[70,71] Semi- and total synthesis methods have both been used to produce compounds with more suitable pharmacological properties.

1.3.1.1 Total Synthesis

Total synthesis has been used to make approved drugs and antibiotics, such as the quinolones, carbapenems and oxazolidinones (figure **1.3**).[72] There have been vast improvements in synthetic methodology since the early days of sulfa-drug

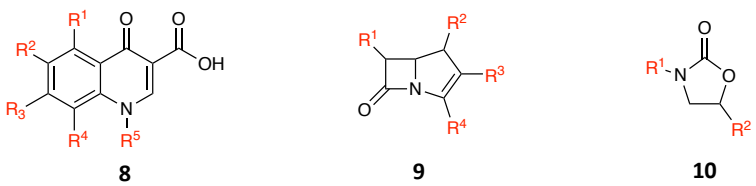

8 **9** **10**

Figure 1.3 General structures for quinolones **8**, carbapenems **9** and oxazolindones **10** with highlighted sites of functionalisation

production, allowing for the synthesis of much more complex and functionally diverse compounds.

For example, Myers *et al*[71] created a platform for the production of novel macrolide antibiotics active against a panel of pathogenic bacteria in the hope of combatting resistance to macrolide antibiotics.[73] Using a highly convergent synthetic strategy, a library of over 300 fully synthetic macrolide (FSM) compounds were produced, using individual building blocks to create a vast array of complex structural analogues (figure **1.4**).[71]

Compound testing revealed many exhibited promising activity against bacterial strains resistant to erythromycin, including MRSA. Notably FSM-100573 displayed good activity against Gram-negative strains including *A. baumannii*.

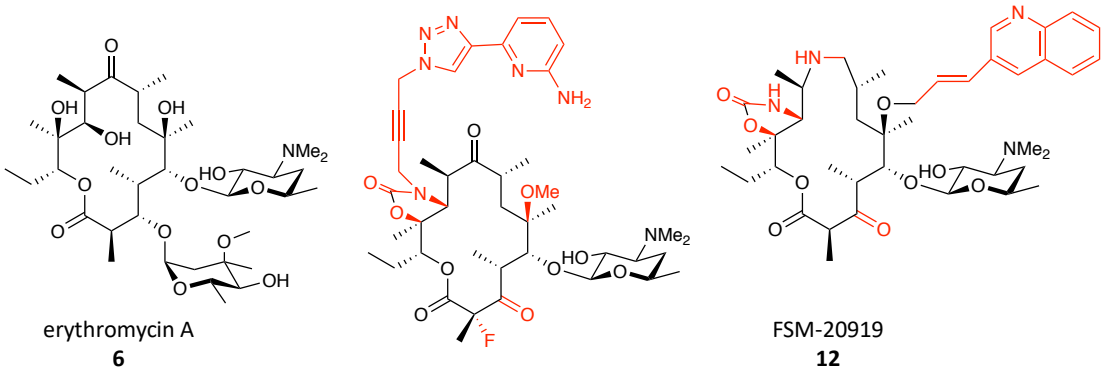

Figure 1.4 Chemical structures of a selection of fully synthetic macrolides (FSM) with the structural differences, compared to the natural product erythromycin A **6**, highlighted.

A similar approach was used to access over 3000 fully synthetic tetracycline analogues, including the clinical candidate eravacycline (figure **1.5**).[74,75] Presence of the fluoro substituent at carbon-7 alongside the introduction of the pyrrolidiniacetamido sidechain at carbon-9 results in good broad spectrum activity of eravacycline against multi-drug resistance pathogens.[74,76]

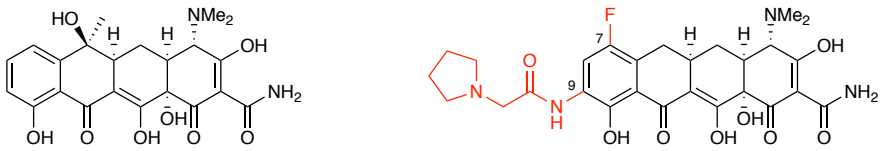

tetracycline
5

eravacycline
13

Figure 1.5 Chemical structures of the natural product tetracycline **5** and the fully synthetic analogue eravacycline **13** with highlighted key structural modifications

Whilst total synthesis can also benefit the drug discovery pipeline by aiding stereochemical assignment, with the exception of a few examples, including those described above, it is not an efficient way to make natural product analogues. Due to the structural diversity, complex stereochemistry and multiple functional groups, complete syntheses are often long and poor yielding. The total synthesis of the natural product etnangien, for example, was achieved in 23 steps (linear) with an overall yield of 0.25%.[77] Although this method of drug discovery can access otherwise difficult to attain structures, creating libraries of compounds is a long and arduous task with no guarantee of the production of a new commercial drug.

1.3.1.2 Semi-Synthesis

Semi-synthesis is the modification of fermentation product scaffolds/ backbones.[7] The antimicrobial activity is preserved with functional side group modifications tuning the antibiotic properties such as bioavailability, efficacy and safety.[78]

The discovery of erythromycin A **6** from *Saccharopolyspora erythraea*, and subsequent widespread clinical use for the treatment of Gram-positive infections, soon revealed issues regarding poor oral availability, stability and resultant side-effects. The semi-synthetic compound clarithromycin contains a methoxy group at C-6 in the place of the hydroxyl group of erythromycin.[79] This six-step transformation, required for simple O-methylation, prevents the acid catalysed interaction of the C-6 hydroxyl and C-9 keto group seen in erythromycin at gastric pH, whilst maintaining good levels of activity.[80,81] Since the discovery of the structural instability of erythromycin A **6**, many semi-synthetic analogues have been produced

such as azithromycin[82] – four steps from the natural product – and the clinical candidate solithromycin – sixteen steps from the natural product (scheme **1.1**).[83]

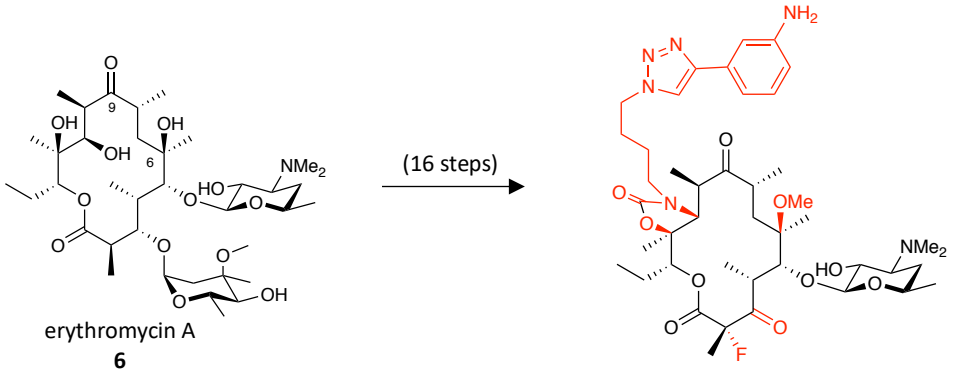

Scheme 1.1 Semi-synthetic analogue solithromycin **14** from the naturally occurring erythromycin with highlighted structural modifications. The number of synthetic steps required from erythromycin are also shown.

Other antibiotics produced by semi-synthesis include, dihydrostreptomycin[84] **16** and tetracycline[85] **5** (later discovered as a natural product),[86] which both result from the catalytic hydrogenation of their respective natural product precursors (scheme **1.2**). Both were seen to retain their antimicrobial properties with increased stabilities compared to the natural product.

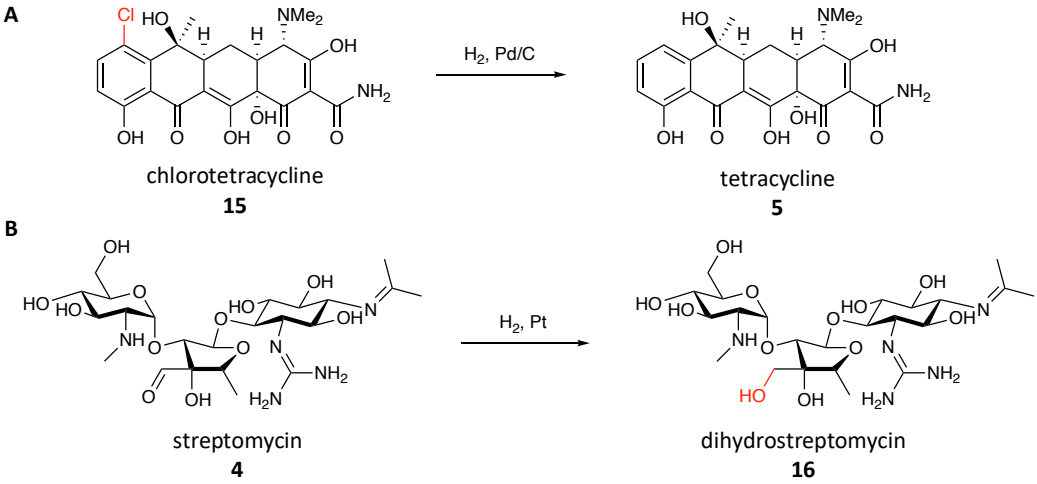

Scheme 1.2 Catalytic hydrogenation of chlorotetracyline (**A**) and streptomycin (**B**) to afford the semi-synthetic products tetracycline and dihydrostreptomycin respectively. Structural changes are highlighted for clarity.

Resistance mechanisms such as β-lactamases (discussed briefly in section **1.1.2**) can also be overcome through semi-synthesis. Enzymatic hydrolysis of the natural

product penicillin G affords 6-aminopenicillanic acid (6-APA) which can be chemically modified to produce a variety of semi-synthetic penicillins.[87,88] This includes the production of methicillin, used to combat penicillin resistant *S.aureus* strains before MRSA strains emerged.

Due to the complexity of natural product scaffolds, selective modifications through semi-synthetic measures can be difficult, especially if the compound itself is inherently unstable. Semi-synthesis is extremely useful however as a method of functionalising known compounds despite the limitation of being unable to generate novel drug scaffolds.

1.4 Polyketide Synthases

Polyketides are a group of chemically diverse and structurally complex molecules that display a range of biological activities (figure **1.6**).[89]

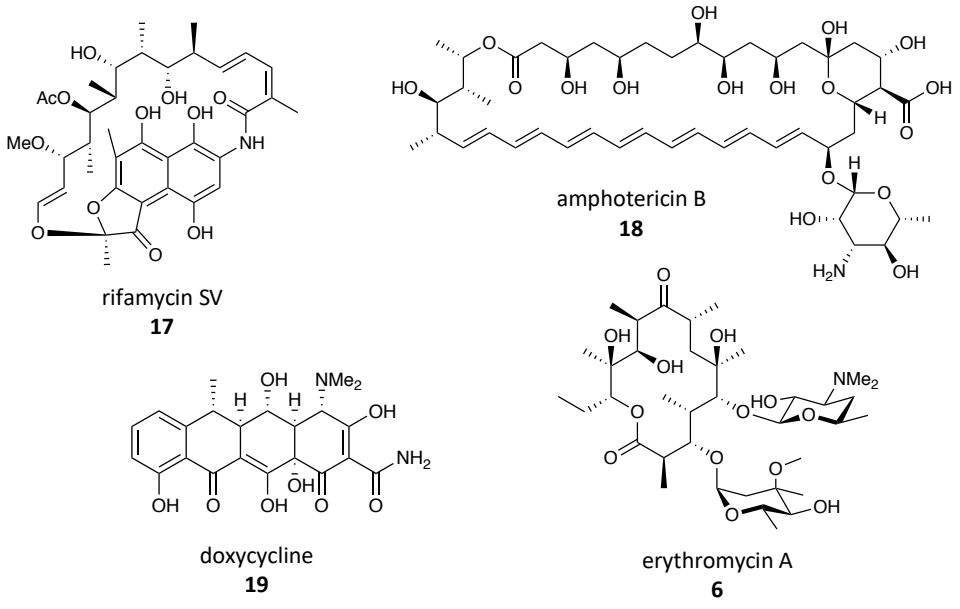

Figure 1.6 Chemical structures of the polyketides; rifamycin SV **17**, amphotericin B **18**, doxycycline **19**, and erythromycin A **6**.

The total synthesis of polyketides is challenging. However nature has fashioned remarkable biosynthetic machinery called polyketide synthases (PKSs) for the efficient production of this molecule class. PKSs can be classified into three distinct

categories; type I, II and III. Type I PKSs are large multifunctional proteins containing modular arrangement of domains, type II PKSs contain distinct monofunctional proteins that act in an iterative manner. Type III PKSs also act in an iterative manner, however the acyl-carrier protein (ACP) domain present in type I and II systems is absent.

1.4.1 Type I modular PKSs

Type I modular PKSs require a minimal set of catalytic domains responsible for polyketide chain elongation. These are the acyl-transferase (AT), acyl-carrier protein (ACP) and the ketosynthase (KS) domains. Following a single round of chain elongation additional catalytic domains, such as ketoreductase (KR), dehydratase (DH), enoyl reductase (ER) and methyl transferase (MT) domains can further modify the β-ketothiosester. Once the polyketide chain has been assembled a thioesterase domain (TE) is often responsible for the polyketide thioester cleavage, providing the scaffold for the polyketide product. In addition to the optional domains a series of tailoring enzymes may also be present which can further modify the polyketide either during or post assembly (section **1.4.1.4**).

1.4.1.1 Erythromycin Biosynthetic pathway

A well-characterised example of a type I modular PKS is the 6-deoxyerthronolide B synthase (DEBS) (scheme **1.3**). DEBS uses a single starter unit of propionyl CoA followed by six rounds of chain elongation using methylmalonyl-CoA as the extender unit.[90–92] Sequence analysis indicated three large multi-functional proteins denoted as DEBS 1, 2 and 3. There are six modules within the DEBS system responsible for the polyketide assembly. The terminal TE domain catalyses chain release via a macrolactonisation producing the macrolide 6-deoxyerthronolide B. This is further modified by tailoring enzymes to produce erythromycin A **6**.

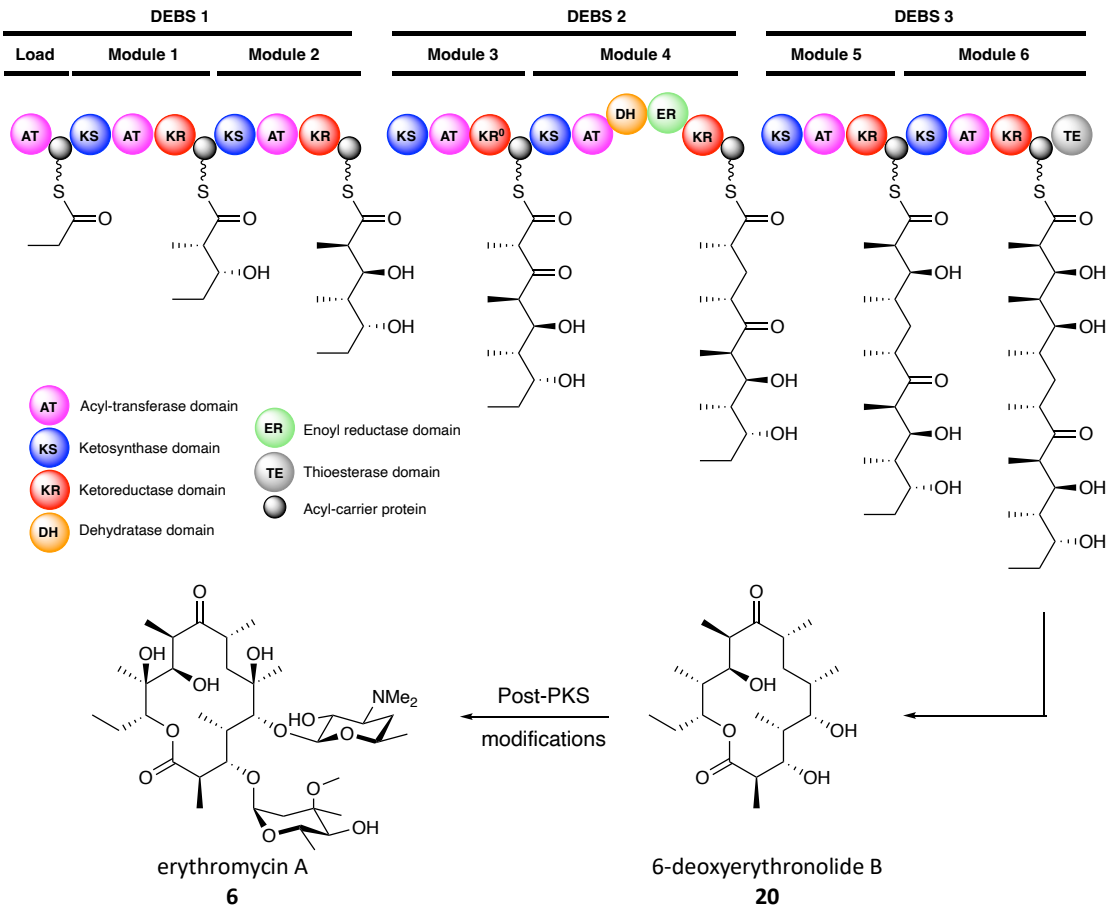

Scheme 1.3 Biosynthetic pathway for the assembly of erythromycin A. 6-deoxyerthronolide is first assembled by a modular PKS that follows the rules of co-linearity and is further modified to produce erythromycin A.

1.4.1.2 *Cis*- and *trans*-AT PKSs

Assembly of 6-deoxyerythronolide B **20** obeys the co-linearity principle meaning that the observed polyketide product correlates to the order and specific functions of the catalytic domains within the PKS. This is typical of *cis*-AT PKSs due to the presence of a catalytic AT domain within each module, therefore making it simpler to predict the polyketide structure from sequence analysis. Generally, systems in which there is an absence of embedded AT domains are known as *trans*-AT PKSs, as the AT domain acts *in trans* during each elongation step (figure **1.7**), although this is not always the case. It is also seen that within *trans*-AT systems there is greater biosynthetic diversity such as non-elongating modules caused by the presence of KS^0 domains. These KS^0 lack the histidine required for the decarboxylative Claisen condensation facilitating chain elongation.[93,94] Due to such unusual structural features the

co-linearity rule cannot always be applied in *trans*-AT PKSs making structural predictions and understanding of these systems challenging.

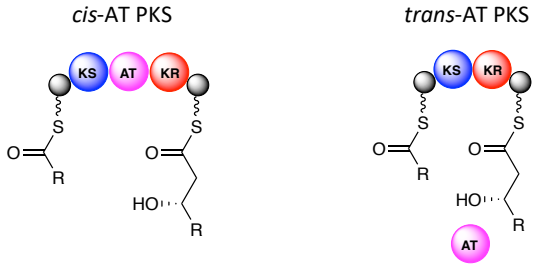

Figure 1.7 Examples of the architecture found in simple *cis*-AT and *trans*-AT PKS modules.

1.4.1.3 PKS catalytic domain functions

1.4.1.3.1 Acyl-carrier protein domain

The function of the acyl-carrier protein is to transfer the polyketide chain between different domains within the PKS. To facilitate this process, conversion of inactive *apo*-ACP to active *holo*-form is required. This occurs through the transfer of the phosphopantetheine arm from coenzyme A (CoA) to the conserved serine residue of an ACP mediated by a phosphopantetheinyl transferase (PPTase) (scheme **1.4**).[95–98]

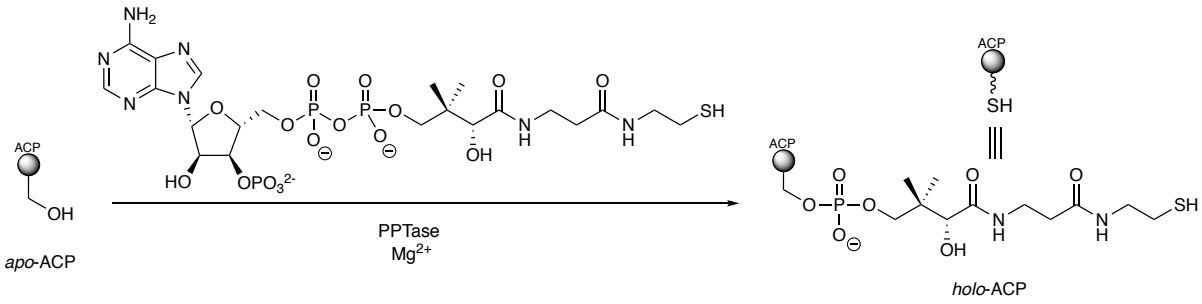

Scheme 1.4 Activation of *apo*-ACP to *holo*-ACP through use of coenzyme A, a phosphopantetheinyl transferase (PPTase) and a magnesium cofactor

1.4.1.3.2 Acyl-transferase domain

The function of the AT domain is to load the downstream activated *holo*-ACP domain with an appropriate acyl starter or extender unit. Deprotonation of the AT active site serine hydroxyl group, by an active site histidine residue, facilitates a nucleophilic addition elimination reaction loading the AT domain with the appropriate acyl unit[99] followed by acyl transfer to the downstream activated *holo*-ACP domain (scheme **1.5**). The starter units are usually acetyl-CoA or propionyl-CoA [100] whereas extender

units are generally malonyl-CoA or methylmalonyl-CoA. However examples of alternative starter and extender units are also known.[101]

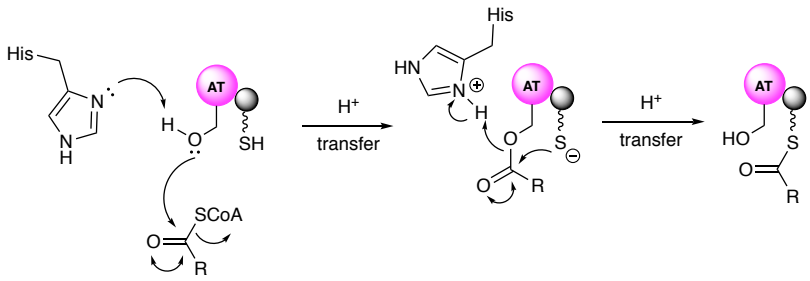

Scheme 1.5 AT domain mechanism: The AT domain is loaded with an acyl unit followed by transacylation onto the activated downstream holo-ACP

1.4.1.3.3 Ketosynthase domain

The KS domain catalyses translocation of the polyketide chain onto its active site cysteine residue from the upstream ACP. This facilitates chain elongation via a proposed histidine mediated decarboxylative Claisen condensation with a downstream ACP domain pre-loaded with an extender unit by the AT domain (scheme **1.6**).[99,102]

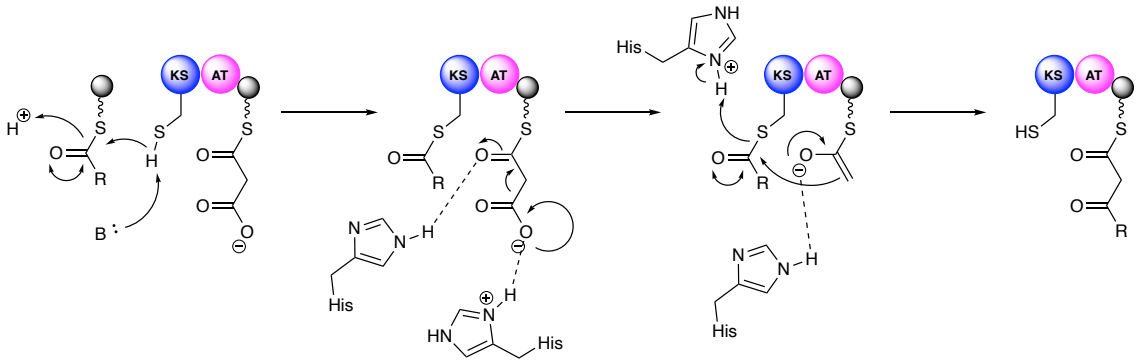

Scheme 1.6 Proposed mechanism for the KS domain-mediated translocation of the polyketide chain to the active site cysteine of the KS domain, followed by a decarboxylative Claisen condensation with malonyl-ACP to generate the β-keto-ACP.

1.4.1.3.4 Ketoreductase domain

Following polyketide chain extension by the AT, ACP and KS domains, further modifications can occur. The newly incorporated β-keto thioester can undergo stereospecific β-keto reduction in the presence of an active KR domain using nicotinamide adenine dinucleotide phosphate (NADPH) (scheme **1.7**).[103]

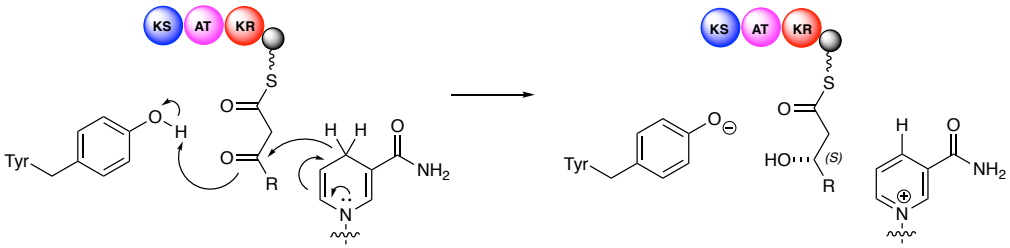

Scheme 1.7 Mechanism of an A1 type ketoreductase using NADPH mediated by a tyrosine residue producing the *(S)*-configured hydroxyl product.

Sequence analysis of the KR domain can be used to predict the stereochemistry of the reduced product.[104,105] Conserved tryptophan residues in A-type KR domains result in an (*S*)-configured hydroxyl group, whereas the presence of a Leucine, Aspartic acid, Aspartic acid (LDD) motif in B-type KR domains results in an *(R)*-configured product.[105,106] If a methyl substituent is present at the C-2 position the stereochemical outcome of the methyl group is dependent on base mediated α-proton abstraction resulting in a tautomerisation event. These are given the additional descriptors (A1, A2, B1 or B2 type) (scheme **1.8**). Ketoreduction can also be classified as a C1/2-type if the KR domain lacks any functionality due to an absence of the required tyrosine residue or to describe when only epimerisation occurs at the C-2-methly group.[106] As illustrated by Keatinge-Clay *et al*, sequence analysis of the catalytic regions of KR domains helps to distinguish between individual KR types. The presence of a proline within the catalytic region alongside the conserved LDD motif for example, is indicative of a B2 type KR whereas proline absence suggests B1 type.[105,107]

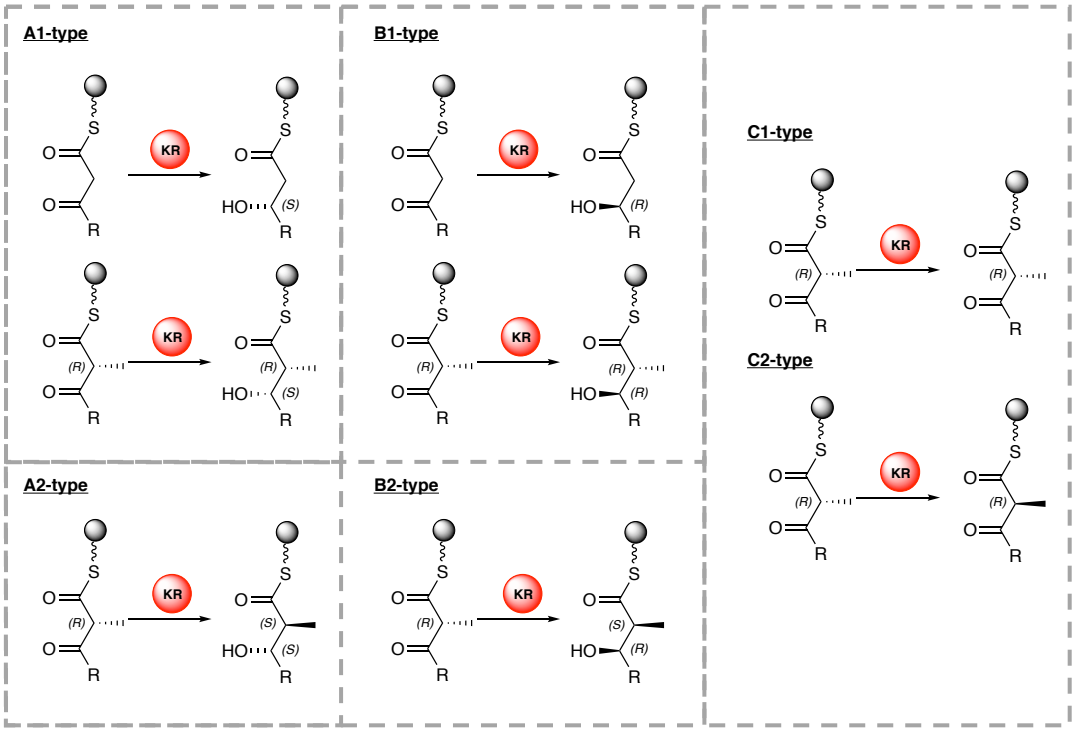

Scheme 1.8 Overview of the types of ketoreductases found within PKS systems

1.4.1.3.5 Dehydratase domain

Following ketoreduction of the β-keto group, the dehydratase domain can catalyse dehydration of the β-hydroxyl group to form either a *cis*- or *trans*-configured α/β-double bond. An active site histidine residue deprotonates the α-proton producing an enolate intermediate which facilitates the C-O bond cleavage and resultant *syn*-elimination of water. A conserved aspartic/glutamic acid residue is believed to help orientate the hydroxyl group and direct the stereochemical outcome (scheme **1.9**).[99,108] Dehydration of an *(R)*-configured hydroxyl group resulting from a B-type ketoreduction affords the *(E)*-configured double bond whereas dehydration of an *(S)*-hydroxyl group affords a *(Z)*-double bond.[109]

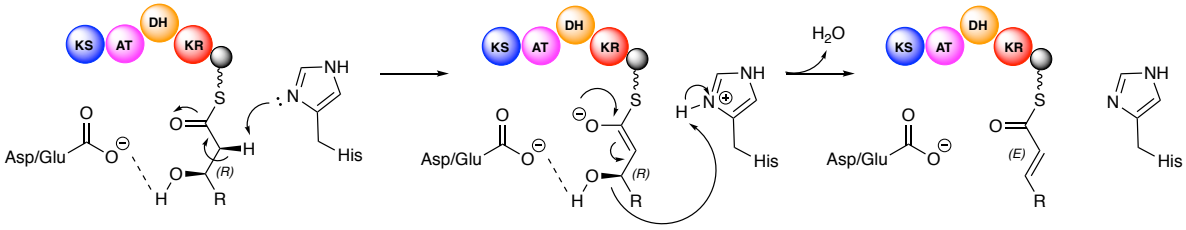

Scheme 1.9 Mechanism of a DH domain catalysed *syn*-elimination from an *(R)*-configured hydroxy group to form the corresponding *(E)*-configured double bond polyketide product.

1.4.1.3.6 Enoyl reductase domain

Enoyl reductase (ER) domains catalyse reduction of the double bond formed by the DH domain using NADPH as a hydride source. An enolate intermediate is formed followed by protonation from an unknown proton source (scheme **1.10**).[110] If a methyl substituent is presence at the C-2 position the resultant stereochemistry can be predicted using sequence analysis. The presence of a conserved tyrosine in the active site indicates formation of an *(S)*-configured methyl group whereas absence of this tyrosine suggests an *(R)*-configured product.[111]

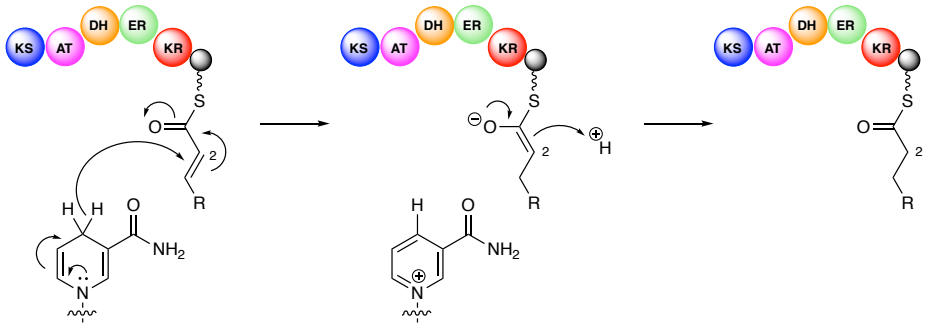

Scheme 1.10 ER domain mechanism

1.4.1.3.7 Methyl Transferase domain

A methyl transferase domain is able to methylate the C-2 position (C-MT) following chain elongation or the β-hydroxyl group (O-MT) formed following ketoreduction using *S*-adenosylmethionine (SAM) as the methyl donor.[112,113] Further studies are required to fully understand how these transferases function.[114–117]

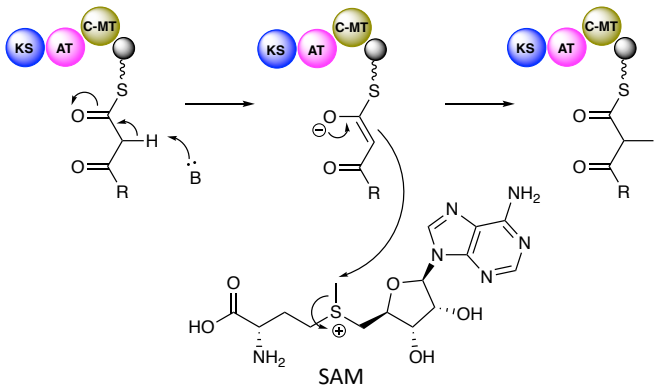

Scheme 1.11 C-MT mechanism following deprotonation using methyl donor S-adenosylmethionine (SAM)

1.4.1.3.8 Thioesterase domain and chain release mechanisms

Following assembly of the polyketide chain, release from the polyketide synthase is usually catalysed by a thioesterase domain. A conserved histidine mediates the transfer of the polyketide chain onto a conserved serine of the TE domain. Following this, either hydrolysis or macrocylisation occurs through nucleophilic attack resulting in either a linear or cyclic macrolactone product (scheme **1.12**, adapted from the literature[118–120]).

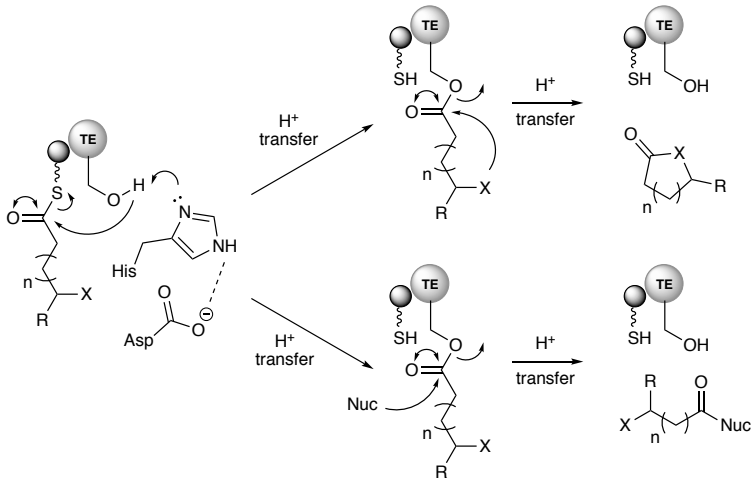

Scheme 1.12 Thioesterase catalysed chain release via macrocylisation (top) and hydrolysis (bottom). (X = OH or NH_2)

Alongside TE catalysed chain release are other less common methods. Reductase (R) domains are also responsible for polyketide chain release producing either an aldehyde or primary alcohol product following a two or four-electron reduction respectively (scheme **1.13**).[121–123]

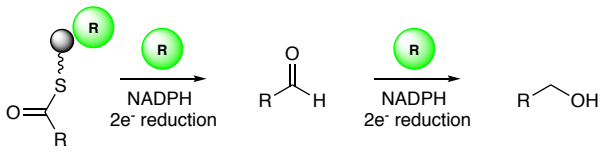

Scheme 1.13 Reductase domain catalysed chain release to produce either an aldehyde or primary alcohol product

Other unusual chain release mechanisms include the use of oxygenases and the recently discovered dual transacylation mechanism by Challis and co-workers (section **1.5.2.2**).[123–125]

1.4.1.4 PKS Tailoring Enzymes

Modifications to the polyketide backbone can arise from a variety of tailoring enzymes and can occur during or post polyketide assembly. These include halogenases which catalyse the halogenation of substrates, with chlorination being the most common. Bromination is also seen, however iodination and fluorination are less common.[126,127] Two of the most frequently seen halogenase types are flavin-dependent and non-heme iron-dependent halogenases. These are understood to halogenate electron rich species and unactivated aliphatic carbons respectively.[127–129] Oxidoreductase enzymes such as oxygenases, oxidases, peroxidases, reductases and dehydrogenases are responsible for the most common polyketide chain modifications.[126] Other tailoring enzymes include a host of transferases which further decorate the polyketide chain with a variety of functional groups such as carbamoyl, methyl, acyl and glycosyl groups. Specific tailoring enzymes are discussed in more detail in section **1.5.2.3**.

1.4.2 Manipulation of biosynthetic pathways

Due to increased understanding of how polyketide synthases function, new methods of natural product analogue production have become available. Cortes *et al*[130] used a relocation strategy to manipulate the biosynthetic pathway of erythromycin A **6**. Repositioning of the TE domain onto DEBS1 prevents chain extension by blocking the interaction between DEBS1 and DEBS2, resulting in early chain release. This completely abolished erythromycin production alongside production of the anticipated lactone **21** (scheme **1.14**).

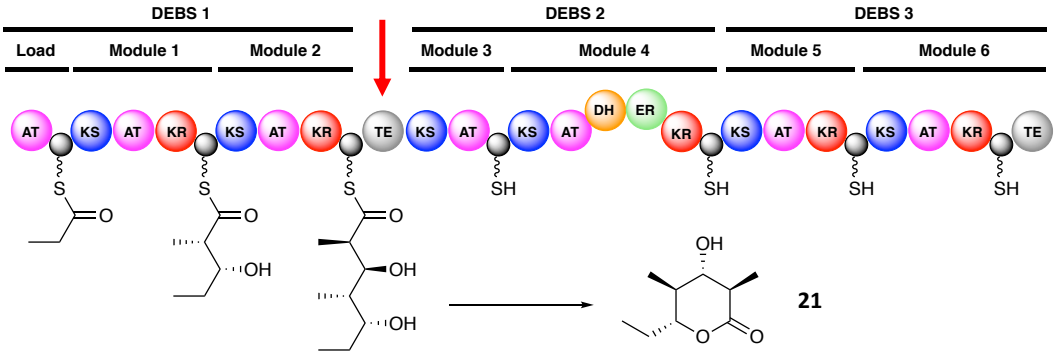

Scheme 1.14 Manipulation of the erythromycin PKS where the TE domain has been repositioned to the terminus of module 2 (red arrow) to afford the expected lactone product **21**

The same relocation strategy was adopted using modules 3 and 5 in DEBS 2 and DEBS 3 respectively, affording the lactone products **22** and **24** respectively.[131–133] The presence of **23** indicates a competing hydrolysis event in module 3 followed by cyclisation.

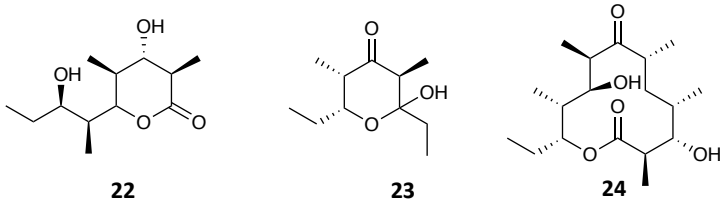

Figure 1.8 Structures of the products formed from the erythromycin PKS relocation strategy where the TE domain was relocated to the terminus of module 3 (**22**) and module 5 (**23** and **24**)

Kushnir and colleagues used mutagenesis to prepare novel natural product analogues by engineering the monensin PKS from *Streptomyces cinnamonensis*.[134] Using a modified pathway, in which post-PKS oxidative cyclisation is blocked, they created a series of point mutations in individual ER, KR and DH domains.[135] This led to the production of a library of natural product analogues including ER2-A, formed following inactivation of the ER domain of module 2 PKS (scheme **1.15**). ER2-A (minimum inhibitory concentration (MIC) = 1.8 µg/mL) exhibits an increase of two orders of magnitude in antibacterial activity against the Gram-negative pathogen *Pseudomonas aeruginosa* compared to pre-monensin (MIC = 228 µg/mL).

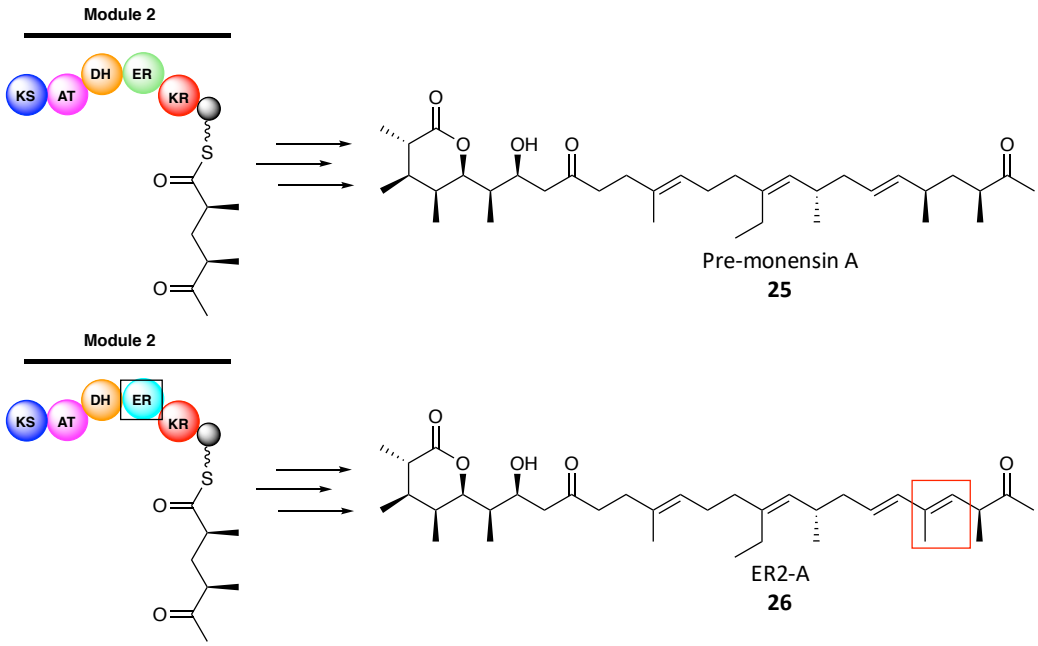

Scheme 1.15 Mutagenesis within the monensin PKS system. (**Top**) pre-modified PKS responsible for pre-monensin production, (**bottom**) Mutagenesis (Gly, Gly → Ser, Pro) of ER domain in module 2 responsible for the production of ER2-A. Only module 2 of the PKS is shown for clarity

Other approaches such as mutasynthesis utilise *N*-acetylcysteamine (NAC) thioesters to produce natural product analogues. *N*-acetylcysteamine (NAC) thioesters can act as mimics of the phosphopantetheine arm present on an ACP domain within a PKS (figure **1.9**). This feature of can be exploited and used to feed synthetic mimics of PKS intermediates to mutant strains blocked in natural product biosynthesis.

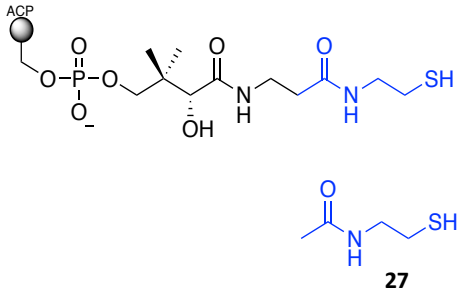

Figure 1.9 Structures of the phosphopantetheine arm tethered to an ACP domain and *N*-acetylcysteamine **27**. The similarities between the two are highlighted demonstrating how NAC can act as a suitable mimic.

This approach was used by Kusebauch and colleagues within the rhizoxin system to produce analogues of the macrolide rhizoxin S2, isolated from *Burkholderia rhizoxinica.*[136] Rhizoxin is assembled by a hybrid *trans*-AT PKS-nonribosomal peptide synthase (NRPS). NRPSs are similar to PKSs in that they are modular multi-enzymes,

but differ in that they use amino acids as building blocks instead of (alkyl)malonyl thioesters. The rhizoxin PKS-NRPS hybrid contains a heterocylisation (HC) domain, which catalyses the condensation of an acetyl thioester with a serinyl thioester and subsequent cyclodehydration to form an oxazoline. Subsequent oxidation of the oxazoline affords the oxazole. Kusebauch and colleagues found that an in-frame deletion of the HC domain abolished rhizoxin production.[136] A NAC thioester mimic of the intermediate assembled by module 1 of the PKS was fed to the deletion mutant resulting in restoration of rhizoxin production at a reduced titre. Analogues of the NAC thioester mimic were also fed to the mutant, resulting in the production of novel rhizoxin analogues (scheme **1.16**).

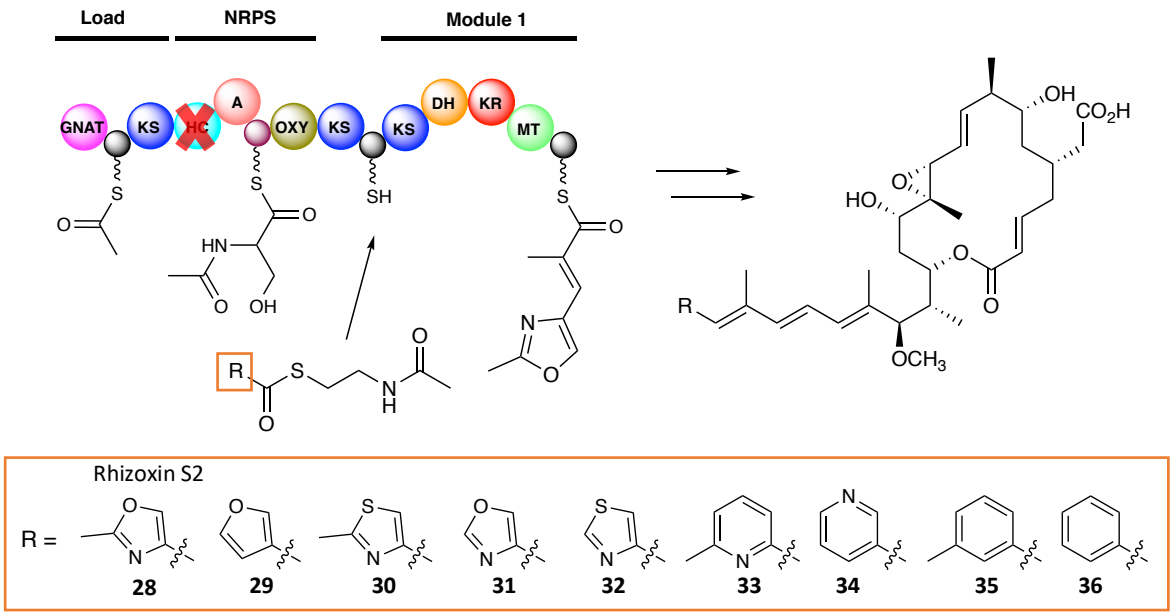

Scheme 1.16 Early steps in rhizoxin biosynthesis with a mutasynthesis approach to the production of rhizoxin analogues. Oxazole formation by the HC and OXY domains is blocked due to an in-frame deletion of the HC domain. Feeding of a NAC thioester mimics of the intermediate assembled on module 1 of the PKS-NRPS results in rhizoxin and novel analogue production. (A = adenylation domain, OXY = oxidase domain; scheme adapted from Kusebauch *et al*.

These methods demonstrate that biosynthetic engineering of PKSs is a powerful tool in the development of novel natural products and potentially new commercial pharmaceutical agents.[137]

1.5 Enacyloxin IIa

Enacyloxin IIa belongs to a group of antibiotics called the enacyloxins, first isolated from *Frateuria sp*. W-315 by Watanabe *et al*.[138,139] Subsequent studies elucidated the structure of enacyloxin IIa and several other enacyloxin compounds that were active against Gram-positive and -negative bacteria.[140–145]

An antimicrobial activity screen of Gram-negative *Burkholderia cepacia complex* (Bcc) isolates against cystic fibrosis bacterial pathogens identified enacyloxin IIa as a metabolite of *Burkholderia ambifaria* AMMD with activity against *Burkholderia multivorans*.[146] Enacyloxin IIa also has promising activity against the MDR Gram-negative pathogen *Acinetobacter bauamnnii* (MIC = 2 μg/mL) however is prone to light induced isomerisation leading to the formation of *iso*-enacyloxin **37**, a significantly less active compound than the natural product (MIC = 7 μg/mL).

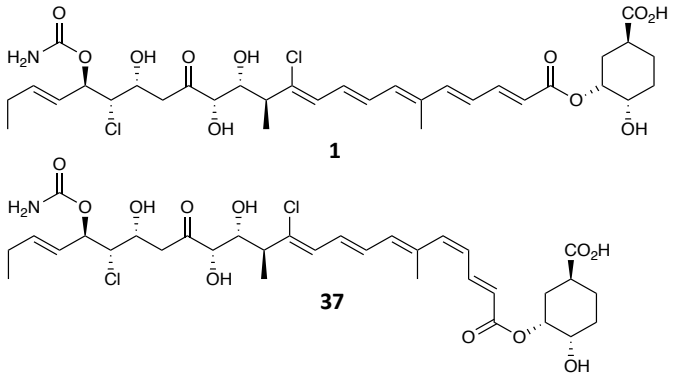

Figure 1.10 Structure of the recently rediscovered polyketide enacyloxin IIa **1** and its' structural isomer *iso*-enacyloxin **37**.

Enacyloxin IIa acts by binding to ribosomal elongation factor thermo unstable (EF-Tu).[147–150]

1.5.1 Mechanism of EF-Tu inhibition

EF-Tu bound to guanosine triphosphate (GTP) carries aminoacyl-tRNA to the ribosome which, upon hydrolysis of GTP to guanosine diphosphate (GDP), triggers the release of the EF-Tu•GDP complex promoting peptide bond formation and bacterial protein synthesis (scheme **1.17**). Binding of enacyloxin IIa to EF-Tu prevents release of the EF-Tu•GDP complex by locking EF-Tu in its GTP bound state preventing protein synthesis.[149–151] This mode of action can also be seen in the structurally different polyketide antibiotic kirromycin.[149,151]

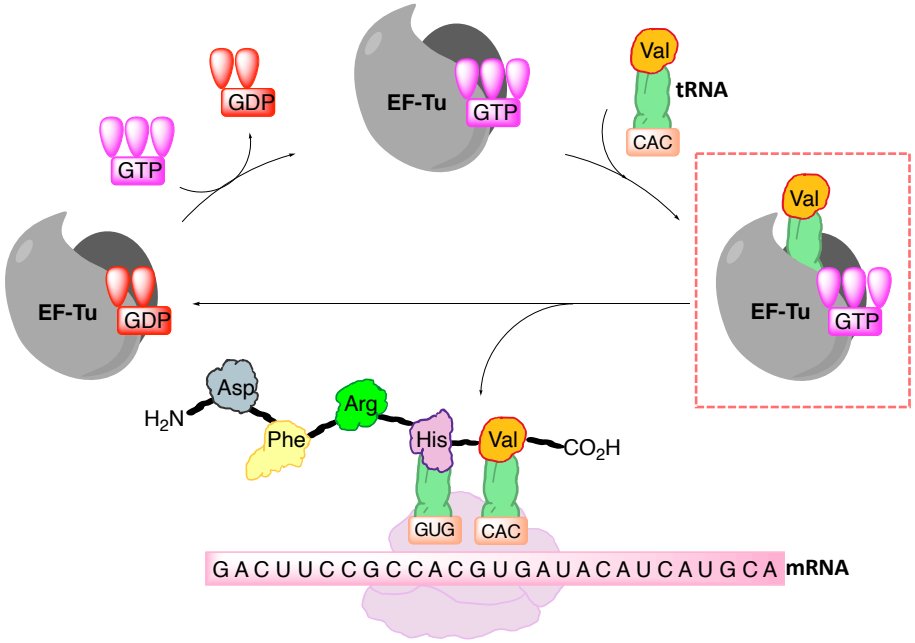

Scheme 1.17 Cycle for the transportation of t-RNA to the ribosome using the EF-Tu•GTP complex. Binding of enacyloxin IIa locks EF-Tu in its GTP bound state preventing bacterial protein synthesis (highlighted).

A crystal structure of *E.coli* EF-Tu bound to enacyloxin IIa and the non-hydrolysable GTP analogue guanylyliminodiphosphate (GDPNP) has been reported by Parmeggiani and colleagues (figure **1.11**).[149] This revealed a number of residues that interact with enacyloxin IIa in the binding site.

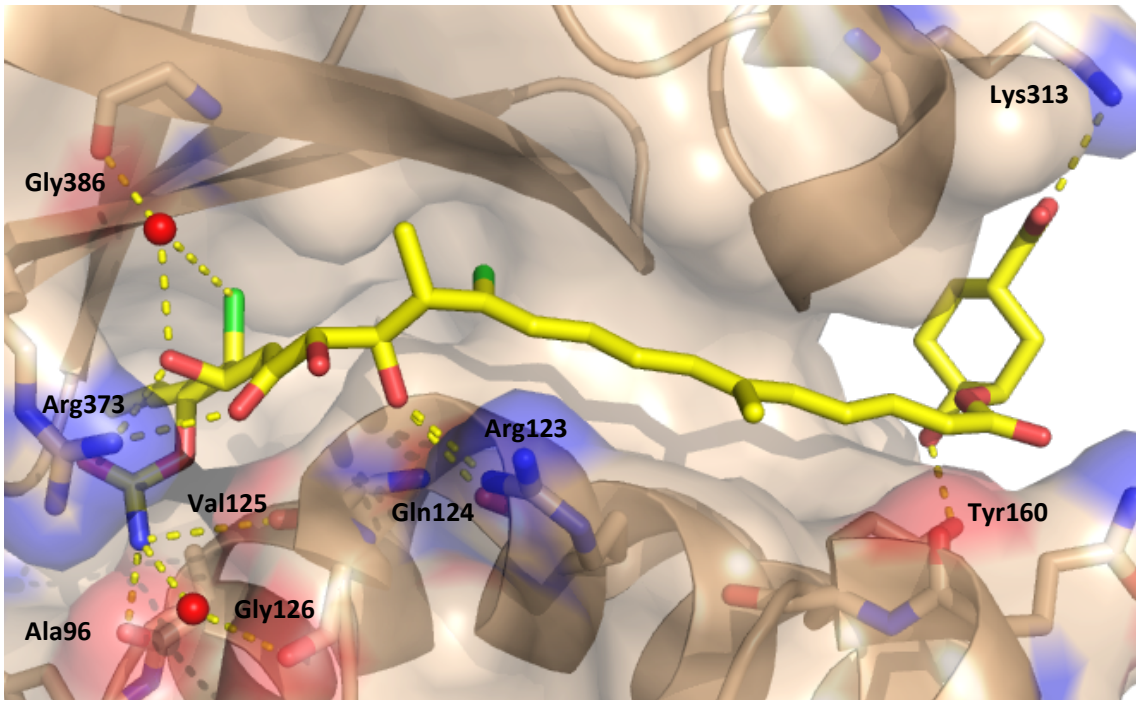

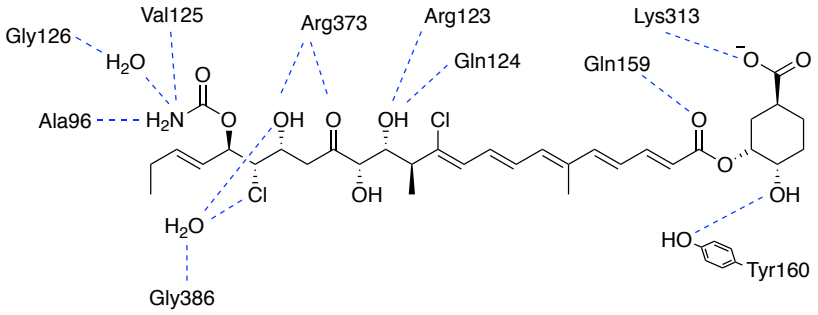

Figure 1.11 The solved crystal structure and polar contacts of enacyloxin IIa bound to EF-Tu.

1.5.2 Enacyloxin Biosynthesis

1.5.2.1 Polyketide assembly

With the rediscovery of enacyloxin IIa from *Burkholderia ambifaria* AMMD, a biosynthetic pathway has also been proposed using sequence analysis of the biosynthetic gene cluster (scheme **1.18**). Genes within the enacyloxin PKS are described using the notation, Bamb followed by the gene number.

A hybrid *cis*/*trans*-AT type I modular PKS is responsible for the production of the large polyketide thioester. Bamb_5925-5920 show sequence similarity to *cis*-AT PKS genes with Bamb_5919 having *trans*-AT sequence similarity. Interestingly only modules 1

and 6 encode AT domains despite modules 2-5 and 7-9 showing resemblance to *cis*-AT PKSs. This suggests that either the AT domain within modules 1 and 6 is responsible for catalysing *in trans* loading of the ACP domains in modules missing an AT domain or catalysis is mediated by an AT domain outside of the enacyloxin gene cluster such as one responsible for fatty acid synthesis.[146]

Polyketide chain assembly is initiated by a GCN5-related *N*-acetyl-transferase (GNAT) which catalyse the decarboxylation of malonyl-CoA followed by transfer of the acetyl-CoA to an adjacent ACP domain.[152] The presence of the MT and ACP domain alongside the GNAT domain in the loading module therefore results in the generation of a propionyl starter unit tethered to ACP 1 withing Bamb_5925.[153]

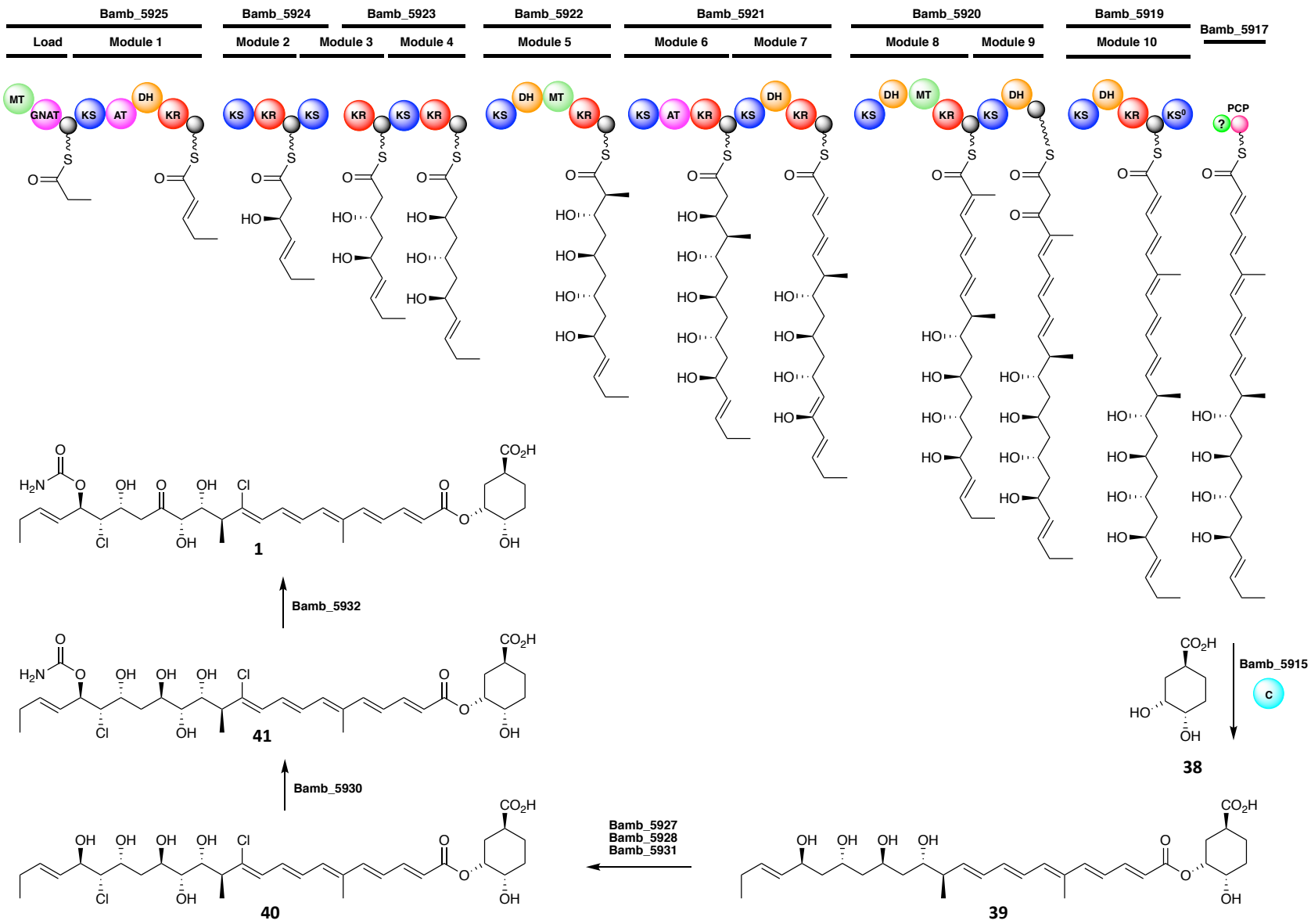

Scheme 1.18 Proposed biosynthetic pathway for production of the polyketide enacyloxin IIa.

1.5.2.2 Polyketide chain release

Following the assembly of the polyketide chain across modules 1-10, chain release is mediated by a recently reported unusual dual transacylation mechanism.[124]

The KS^0 domain present in module 10 of the PKS transfers the fully-assembled polyketide chain from the upstream ACP domain of Bamb_5919 to the downstream peptidyl carrier protein (PCP) domain of Bamb_5917. Condensation of the PCP tethered thioester with dihydroxycyclohexane carboxylic acid (DHCCA) is subsequently catalysed by the non-ribosomal peptide synthetase (NRPS)-like condensation (C) domain of Bamb_5915, producing what has been previously described as pre-enacyloxin.[146] In order for condensation to occur, chain transfer from the ACP of Bamb_5919 to the PCP of Bamb_5917 is essential, suggesting that specific protein-protein interactions may be responsible for site recognition and condensation. This interaction was confirmed to be mediated between a short linear motif (SLiM) on the PCP domain and a ß-hairpin docking domain (ßHDD) appended to the C-domain of Bamb_5915 (scheme **1.19**).[125]

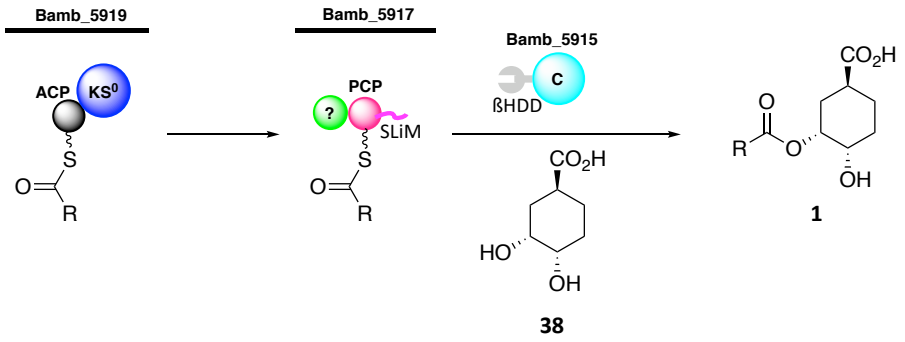

Scheme 1.19 Transacylation of the enacyloxin polyketide chain from the Bamb_5919 ACP domain to the Bamb_5917 PCP domain followed by chain release catalysed by the Bamb_5915 condensation domain and DHCCA (R represents the fully assembled polyketide chain). The domain marked with a '?' is of unknown function.

1.5.2.3 Modifications to the polyketide chain

The condensation product of the enacyloxin polyketide chain and DHCCA leads to the production of pre-enacyloxin (**39**). Within the enacyloxin biosynthetic gene cluster a

series of tailoring enzymes are encoded and are responsible for modifications to the polyketide chain (figure **1.12**).

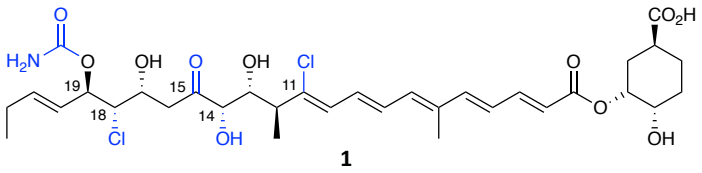

1

Figure 1.12 Enacyloxin IIa with structural modifications as a result of the tailoring enzymes highlighted

These tailoring genes were identified as; a hydroxylase (Bamb_5927), a flavin-dependent halogenase (Bamb_5928), a carbamoyl transferase (Bamb_5930), an Fe(II) α-ketoglutarate-dependent halogenase (Bamb_5931) and a PQQ-dependent dehydrogenase (Bamb_5932).[146,154] It is uncertain whether these tailoring steps occur on or post-PKS but for clarity they have been represented as acting post-PKS.

1.5.2.3.1 Hydroxylation

Hydroxylation of C-14 is catalysed by the Fe(II) and α-ketoglutarate-dependent Bamb_5927 hydroxylase. The proposed mechanism demonstrates binding of dioxygen to the Fe(II) species upon loss of water followed by hydrogen abstraction from the substrate which is then hydroxylated by the Fe(III) complex. Regeneration of the inital Fe(II) complex occurs through loss of a succinate unit and addition of α-ketoglutarate (α-KG).

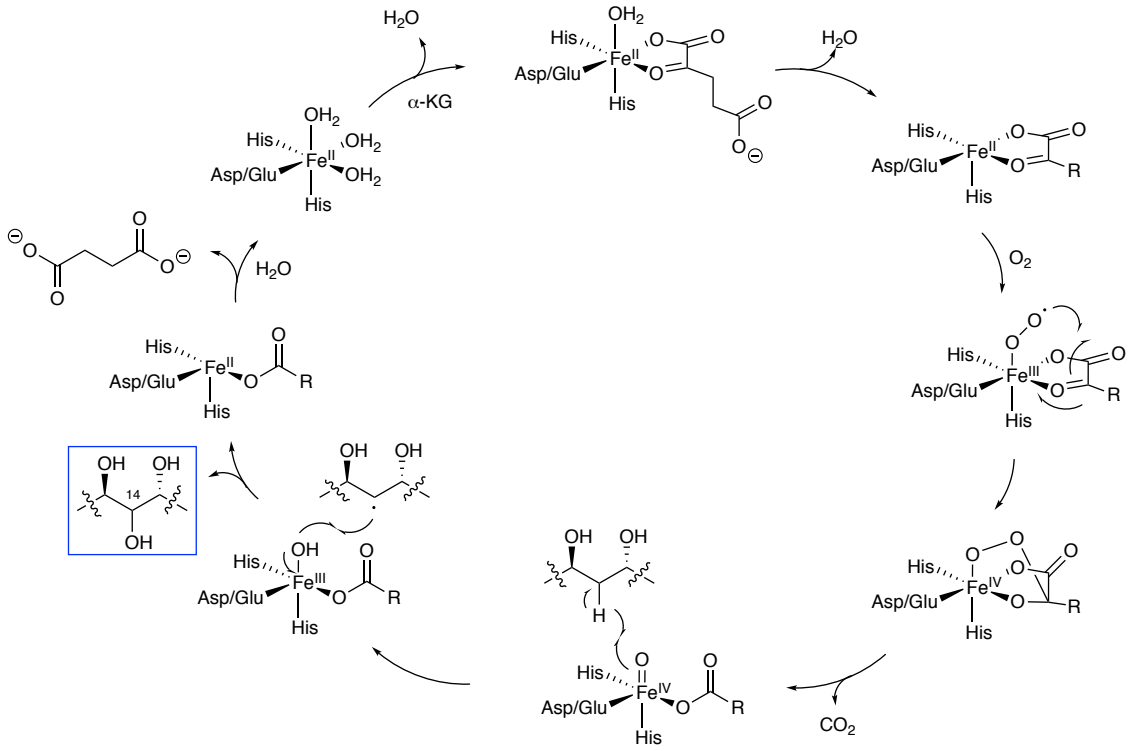

Scheme 1.20 Proposed mechanistic formation of the hydroxylated enacyloxin polyketide backbone (Blue box) using an Fe(II) and α-ketoglutarate dependent hydroxylase.

1.5.2.3.2 Halogenation

Within the gene cluster are two halogenases, one of which is Bamb_5928, a flavin-dependent halogenase. This catalyses the chlorination of C-11 through a reduced flavin co-factor, $FADH_2$, which reacts with molecular oxygen to form an FAD-hydroperoxide intermediate. This is attacked by the halide to generate the hypochlorous acid (HOCl) which is essential for halogenation (scheme **1.21A**). The hypochlorous acid is required to migrate to the substrate binding site located 10 Å from the halide binding site. The free HOCl species is unable to chlorinate the substrate directly and is therefore dependent on interactions with lysine and glutamic acid residues located within the binding site. Uncertainties remain whether chlorination occurs due to activation of the HOCl species by H-bonding to the lysine residue increasing its' electrophilicity (scheme **1.21B** , blue) or by generation of a known active chlorinating lysine *N*-chloroamine species (scheme **1.21B**, red).[127,128,155,156]

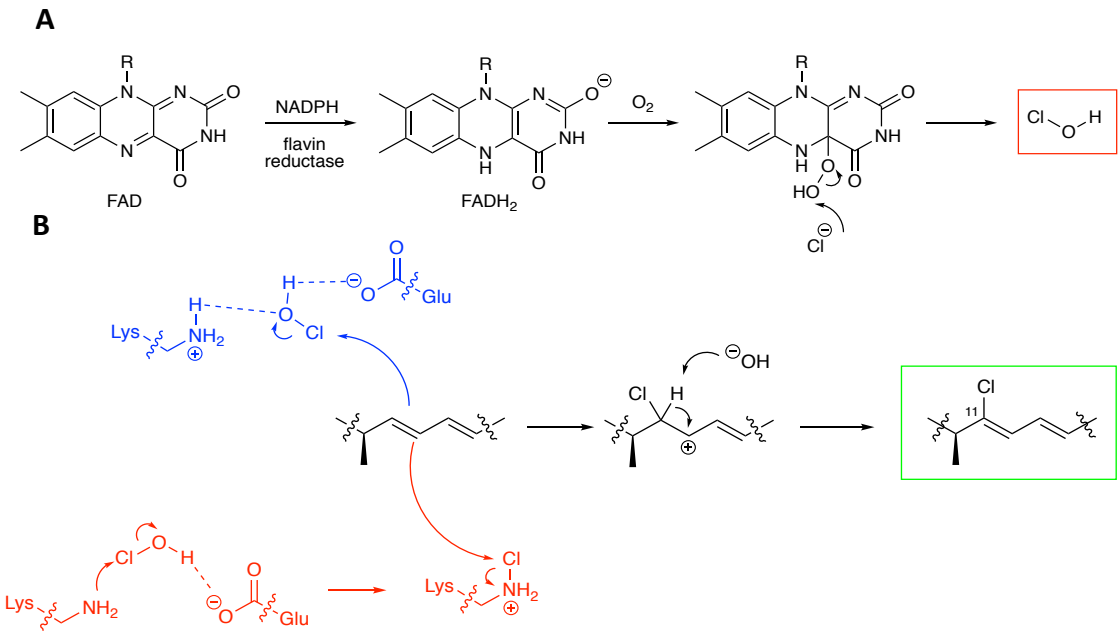

Scheme 1.21 Proposed enacyloxin C-11 chlorination by a flavin-dependent halogenase. (**A**) formation of hypochlorous acid from flavin adenine dinucleotide (FAD) via an FAD-hypochlorous intermediate, (**B**) chlorination of C-11 of enacyloxin backbone using an activated HOCl species (blue) or lysine N-chloroamine (red).

The second halogenation event is mediated by an Fe(II) and α-ketoglutarate-dependent Bamb_5931 halogenase. The proposed mechanism is similar to that of hydroxylation. Formation of the highly reactive Fe^{IV}=O species results in hydrogen radical abstraction followed by homolytic cleavage of the Fe^{III}-Cl bond and formation of the C-18 chlorinated enacyloxin backbone (scheme **1.22**).[127,128,157,158]

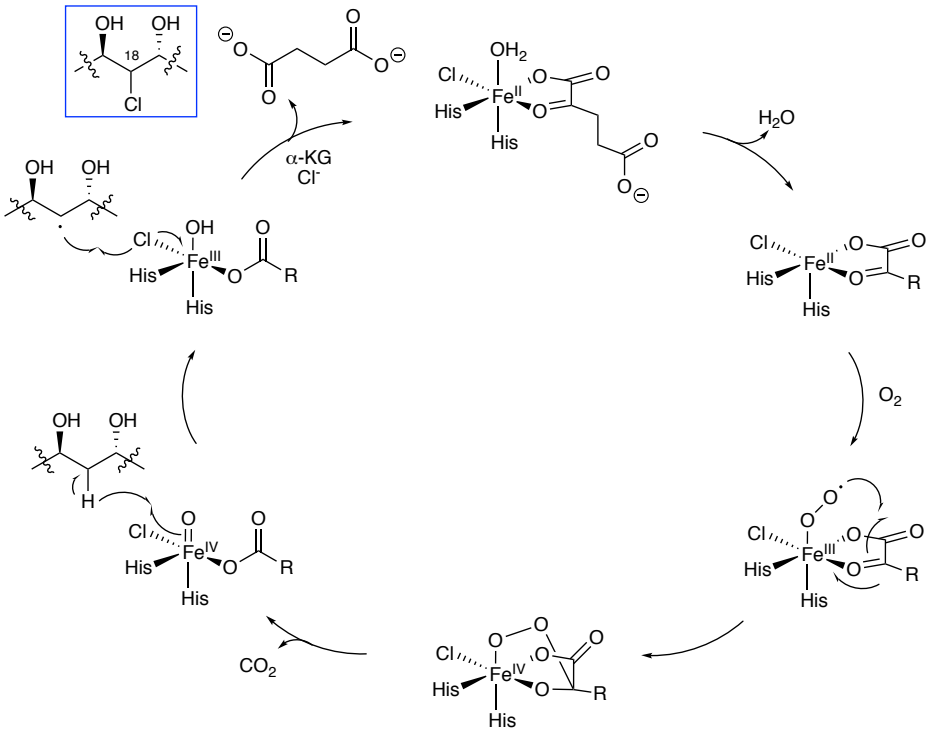

Scheme 1.22 Proposed mechanistic formation of the chlorinated enacyloxin polyketide backbone using an Fe(II) and α-ketoglutarate dependent halogenase.

1.5.2.3.3 Carbamoylation

Addition of the carbamoyl moiety is catalysed by the Bamb_5930 carbamoyl transferase using carbamoyl phosphate formed from ammonia, bicarbonate and adenosine triphosphate (ATP) (scheme **1.23**).

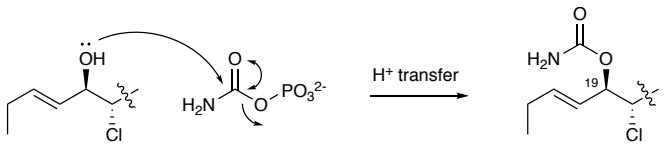

Scheme 1.23 Mechanism of carbamoylation of the enacyloxin backbone by a carbamoyl transferase

1.5.2.3.4 Oxidation

The final structural modification which generates enacyloxin IIa (**1**) is the oxidation of the C-15 secondary alcohol by Bamb_5932, a pyrroloquinoline quinone (PQQ) dependent oxidase. Regeneration of the PQQ species is proposed to be through an electron transfer process mediated by a disulphide bridge formed between neighbouring cysteine residues.[154,159–161]

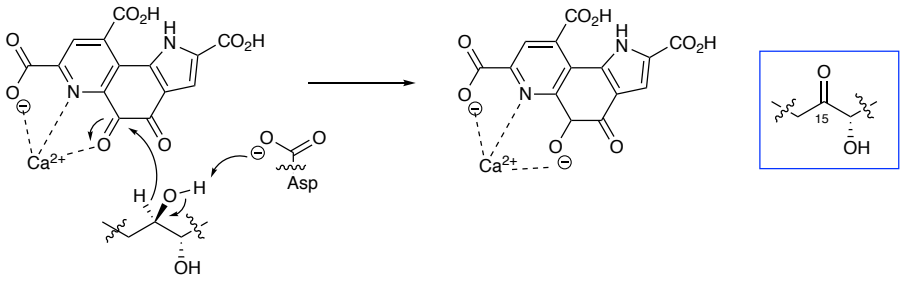

Scheme 1.24 Oxidation of the C-15 secondary hydroxyl group by a PQQ dependent oxidase

1.5.2.4 DHCCA biosynthesis

The DHHCA biosynthetic pathway was originally proposed by Mahenthiralingham and co-workers.[146,162] However, sequential deletion of the genes proposed to be involved did not result in the expected shunt metabolites. Unfortunately an *in vitro* approach was initially unsuccessful because the required proteins were insoluble. Genome mining led to the discovery of an enacyloxin homologous gene cluster within *Vibrio rhizosphaerae* MSSRF3 responsible for the production of vibroxin (**42**).

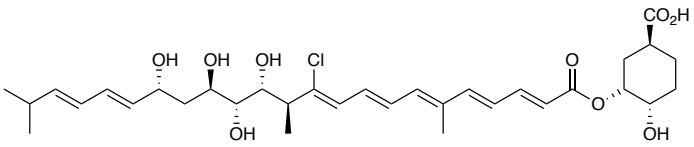

42

Figure 1.13 Structure of vibroxin, a polyketide natural structurally similar to enacyloxin IIa that has a homologous gene cluster

Production and isolation of vibroxin revealed it is structurally similar to enacyloxin IIa and is also active against *A. baumannii* (MIC = 1-2 µg/mL). Therefore, homologues from the vibroxin biosynthetic gene cluster were used to further investigate the DHCCA biosynthetic pathway (table **1.1**).

Table 1.1 Genes responsible for the biosynthesis of DHCCA in both enacyloxin IIa and vibroxin

Enacyloxin Gene	Homologous Vibroxin Gene
bamb_5912	*VbxL*
bamb_5913	*VbxM*
bamb_5914	*VbxN*
bamb_5916	*VbxP*
bamb_5918	*VbxK*

The homologous vibroxin genes were overproduced and *in vitro* assays with the proposed substrates, or substrate analogues, were used to elucidate the biosynthesis of DHCCA (scheme **1.25**).[162] The proposed route is consistent with the metabolites produced following *in vivo* gene deletions in *B. ambifaria*.

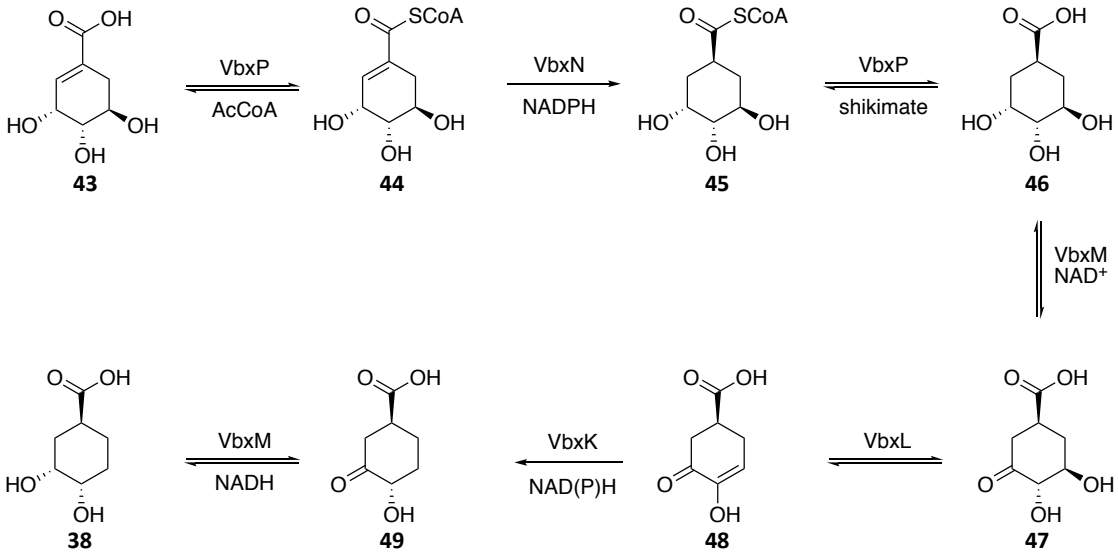

Scheme 1.25 Proposed DHCCA biosynthetic pathway

Shikimate conversion to shikimate CoA **43** is catalysed by CoA transferase, VbxP, and reduced by the enoyl reductase, VbxN to afford **45**. VbxP catalyses the production of trihydroxy-cyclohexanecarboxylic acid (THCCA) **46** using shikimate and **45** as a CoA donor. Oxidation of **46** is catalysed by the dehydrogenase, VbxM to produce the ketone intermediate **47** followed by its dehydration to **48** by the dehydratase, VbxL. Enoyl reduction of **48** is catalysed by enoyl reductase, VbxK to produce the

penultimate product **49** which is reduced by VbxM to afford the final DHCCA unit used in vibroxin and enacyloxin IIa biosynthesis.

1.5.3 Enacyloxin IIa analogue production within the Challis group

A greater understanding of the structure activity relationship (SAR) of enacyloxins has been possible due to the production of a wide range of novel analogues using a combination of mutagenesis and mutasynthesis strategies.[163]

Using a gene deletion strategy a series of tailoring gene 'knock-out' mutants were created in *B. ambifaria* BCC0203 and used to create a library of enacyloxin analogues with modified polyol regions. This led to the production of 11 enacyloxin analogues with activities ranging from 1 to >64 µg/mL containing either single gene deletions for each tailoring gene or a combination of multiple tailoring gene deletions. The antimicrobial activities were tested against *Acinetobacter baumannii* and all structures were confirmed by HRMS and NMR spectrometry (figure **1.14** and **appendices** section)

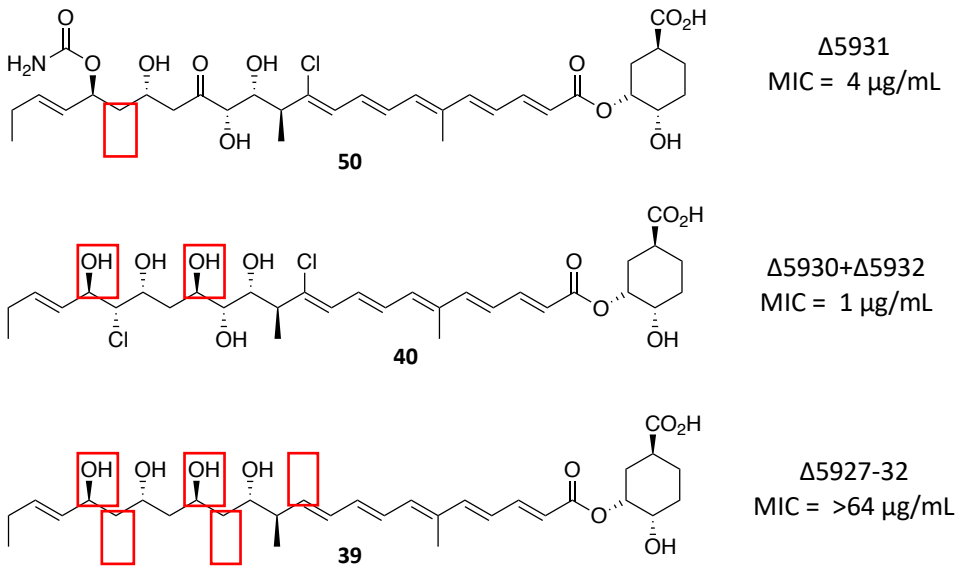

Figure 1.14 Enacyloxin analogues produced using a gene deletion strategy with antimicrobial activity data against *A. baumannii*. A complete library of analogues can be found in **appendices** section.

The substrate tolerance of the Bamb_5915 condensation domain was initially investigated using an *in vitro* assay approach. A range of DHCCA analogues were

incubated with Bamb_5915 and the acetylated Bamb_5917 PCP domain, seen to be a suitable mimic for the complex polyketide chain, without the need for a complicated near total synthesis. Of the twenty-two DHCCA analogues tested, thirteen were successfully acetylated *in vitro,* as confirmed by UHPLC-ESI-Q-TOF-MS (scheme **1.26**).[124] These experiments demonstrated a relaxed substrate tolerance, however a 1,3 relationship of nucleophile and carboxylic acid was essential for acceptance by the Bamb_5915 condensation domain.[124]

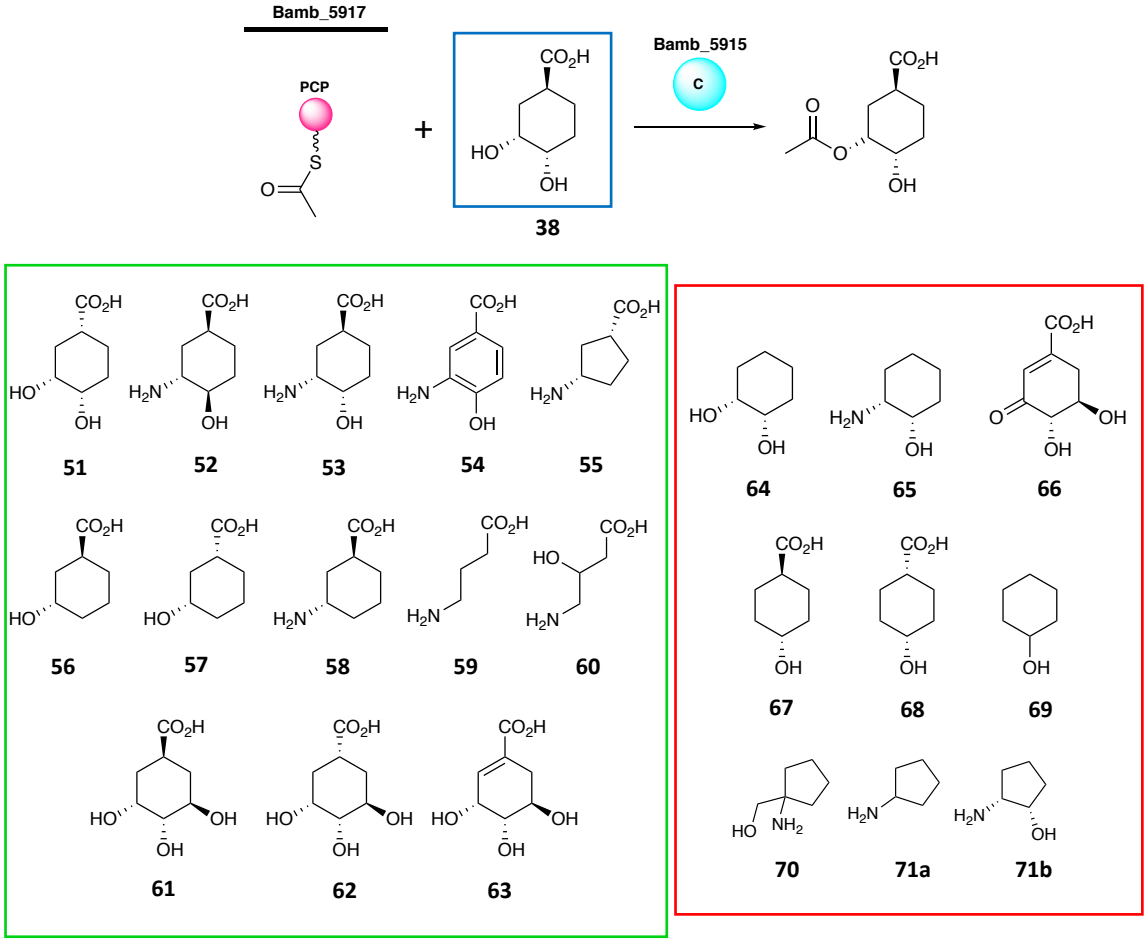

Scheme 1.26 *In vitro* investigations into the tolerance of the Bamb_5915 condensation domain using DHCCA analogues (Green = tolerated, red = not tolerated).

Genes responsible for the biosynthesis of the DHCCA moiety, (Bamb_5912-14), were deleted, abolishing production of enacyloxin IIa. Growth of *B. ambifaria* BCC0203 Δ5912-14 (blocked in DHCCA biosynthesis) on BSM media supplemented with commercially available/synthesised DHCCA analogues generated novel enacyloxin analogues with a range of activities against *A. baumannii* (figure **1.15**).

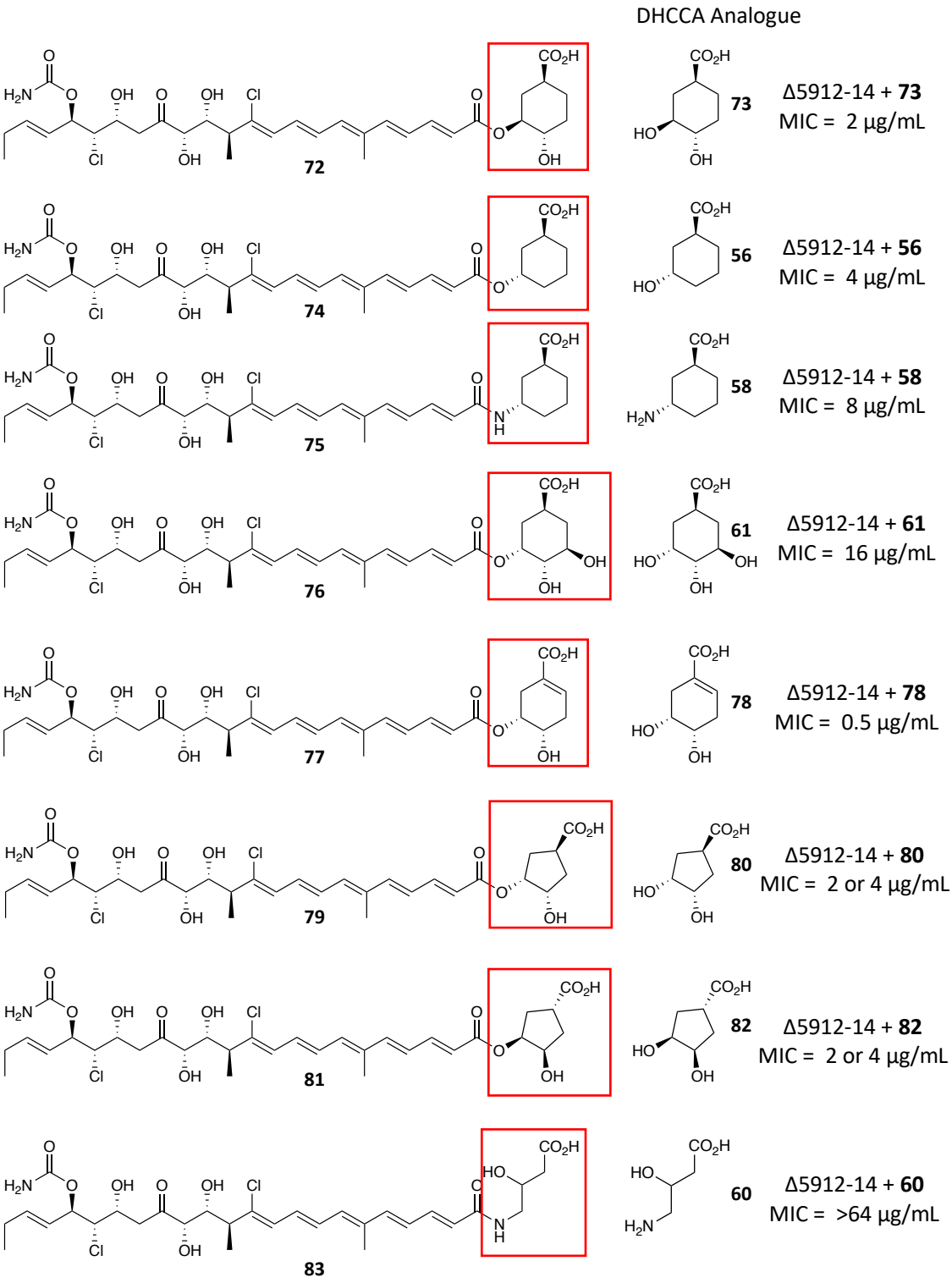

Figure 1.15 Enacyloxin analogues produced from feeding of DHCCA analogues to *B. ambifaria* BCC0203 Δ5912-14 blocked in DHCCA biosynthesis.

Different strategies could also be combined to obtain analogues with modifications at both the DHCCA moiety and on the backbone.[163] For example analogue **84** was produced by growth of a mutant strain containing deletions of the genes responsible

for; installation of the carbamoyl moiety (Bamb_5930), oxidation of the secondary alcohol (Bamb_5932), DHCCA biosynthesis (Bamb_5912-14) and supplemented with DHCCA analogue **78** (figure **1.16**). Unfortunately no improvement in MIC was seen when these modifications were combined.

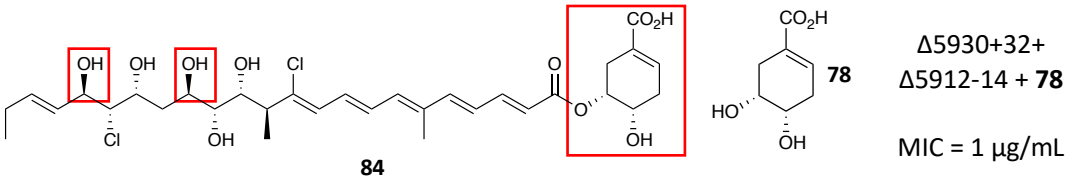

Figure 1.16 Enacyloxin analogue **84** produced using a combination of knock-out mutagenesis and mutasynthesis strategies with corresponding activity data.

1.6 Project Aims and Objectives

With a greater understanding of the enacyloxin IIa biosynthetic gene cluster and an established methodology for the preparation of novel analogues, the aim of this project was to further expand the library of enacyloxin analogues. This will provide a greater understanding of SAR and aid in the design and production of more active and stable compounds (figure **1.17**).

The first aim was to make further modifications to the polyol region. Previous reports by Watanabe *et al* suggest chlorinases will accept bromine as a halide source if bromine is provided in the growth media.[141,143] The aim was therefore to produce brominated analogues of enacyloxin in both wild type and mutant strains. We next aimed to use a mutasynthesis approach to inactivate the biosynthesis of the natural product and feed a NAC thioester mimic of the polyketide chain to re-establish production, to establish whether feeding novel NAC thioesters could produce novel analogues.

The second aim was to further investigate incorporation of DHCCA analogues into enacyloxin by making modifications to the DHCCA unit including introducing a linear analogue and an analogue containing a 7-membered ring. Additionally, it was aimed

to investigate whether a DHCCA analogue containing an alkyne moiety could be incorporate, which could later be used as a synthetic handle.

The final aim was to obtain bioactivity data for a selection of analogues including; Antimicrobial activity data for any analogues produced in this project; Testing enacyloxin IIa and some promising analogues in *A. baumannii* mouse infection models; measuring binding affinity with EF-Tu by in-tact mass spectrometry with relevant analogues.

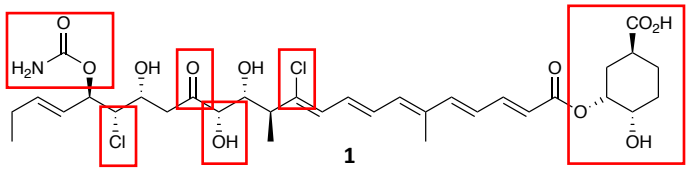

Figure 1.17 Structure of enacyloxin IIa with regions targeted for modification within this project highlighted

Chapter 2 - Results and Discussion I

2.1 Modifications to the enacyloxin acyl chain

This chapter explores structural modifications to the enacyloxin polyketide backbone using a variety of methods. Initially, tolerance of the halogenases was investigated followed by the use of NAC thioester mimics using a strategy similar to Kusebauch *et al*.[136]

2.1.1 Investigations into the halogenase domains

2.1.1.1 Production of brominated enacyloxin IIa

Within the biosynthetic gene cluster responsible for the production of enacyloxin IIa (**1**) are two genes encoding halogenases. A flavin-dependent halogenase (*bamb*_5928) and an Fe(II) α-ketoglutarate-dependent halogenase (*bamb*_5931) are responsible for the chlorination at C-11 and C-18 respectively (figure **2.1**).

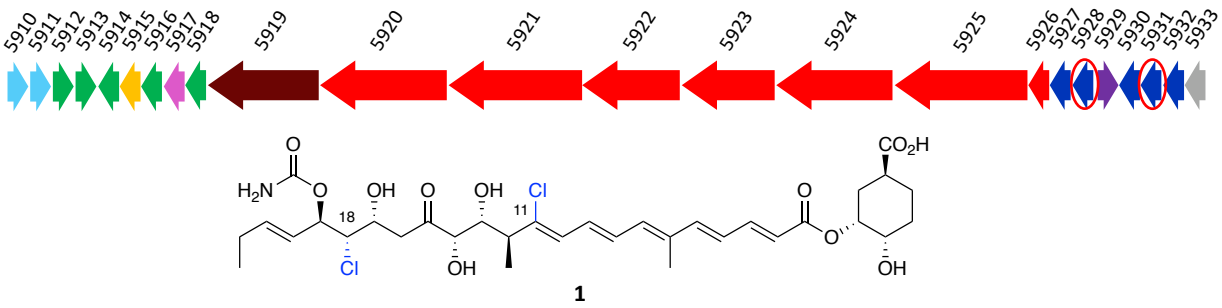

Figure 2.1 Enacyloxin IIa biosynthetic gene cluster with halogenase enzymes and halogenated positions highlighted

It has been reported by Furukawa *et al*[141] and Watanabe *et al*[143] that the use of media containing bromide in place of chloride results in the production of mono-brominated enacyloxin analogues. However, the compounds were only characterised by mass spectrometry, they were not isolated and characterised by NMR spectrometry. To produce brominated enacyloxin IIa, *Burkholderia ambifaria* BCC0203 was grown on BSM media in which ammonium chloride was replaced with ammonium bromide (section **6.2.13**). LC-MS analysis of ethyl acetate extracts from

the growth plates indicated three enacyloxin analogues were produced (figure **2.2**, **Appendices** section).

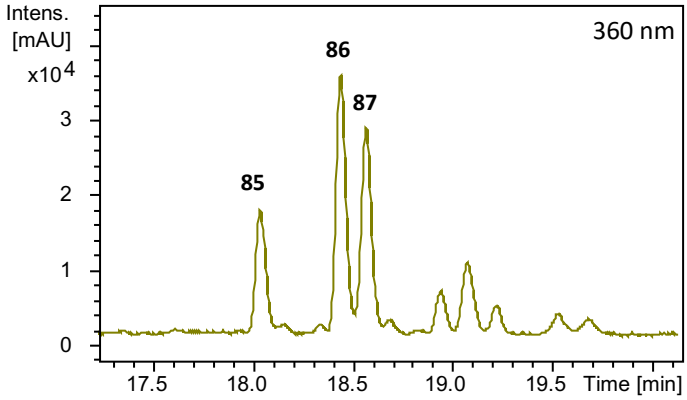

Figure 2.2 UV chromatogram at 360 nm from LC-MS analysis of extracts of *Burkholderia ambifaria* BCC0203 grown on BSM media supplemented with ammonium bromide in the place of ammonium chloride (See **Appendices** section for MS data).

The analogues were purified by HPLC and their structures determined by ^{1}H and ^{13}C NMR spectroscopy. In all three compounds C-11 is brominated, whilst C-18 contained a hydrogen, chlorine or bromine in **85**, **86** and **87** respectively (figure **2.3**, **Appendices** section). The structures of the isolated analogues indicates that the flavin-dependent halogenase has a greater halide tolerance than the Fe(II) α-ketoglutarate-dependent halogenase. Although halogenases that accept bromide as well as chloride have been identified from both halogenase families, they generally have a reduced efficiency for bromide.[128,164,165] However, a few flavin-dependent halogenases have been identified that have preference for bromide in the place of chloride, [166–168] which could explain the consistent bromination at C-11. Further *in vitro* studies would be needed for a more comprehensive understanding of the selectivity of the halogenase enzymes within the enacyloxin gene cluster. Interestingly, despite the replacement of chloride in the media, chlorination at C-18 still occurs due to an inability to completely avoid any source of chloride. Media components such as CAS amino acids contain sodium chloride at low concentrations which is sufficient to facilitate chlorination.

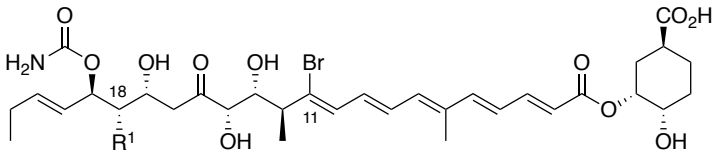

R^1 = H **85**

R^1 = Cl **86**

R^1 = Br **87**

Figure 2.3 Enacyloxin analogues isolated from *Burkholderia ambifaria* BCC0203 when bromide supplemented BSM media was used

Having established that the halogenase enzymes accept bromide as a halogen source and that production of novel compounds from the wild-type strain is possible, this method for novel analogue production was further investigated using mutant strains previously prepared in the Challis group.

2.1.1.2 Production of novel brominated analogues from mutant *B. ambifaria* BCC0203

As a large number of mutant strains and resultant analogues have previously been made in the group (section **1.5.3**), brominated analogues were only targeted for those with a low MIC against *A. baumannii*. The selected strains were; *B. ambifaria* BCC0203_Δ5927, *B. ambifaria* BCC0203_Δ5930 and *B. ambifaria* BCC0203_Δ5930+Δ5932 containing deletions in the genes encoding the α-ketoglutarate dioxygenase responsible for hydroxylation at C-14, the carbamoyl transferase responsible for the addition of the carbamoyl moiety on the hydroxyl on C-19 and both the carbamoyl transferase and the PQQ-dependent dehydrogenase responsible for oxidation of the secondary alcohol at C-15 respectively. As previously, the strains were grown on BSM media supplemented with bromide in place of chloride, the agar was extracted with ethyl acetate and the compounds purified by HPLC following LC-MS analysis. The produced compounds are shown in table **2**.

Table 2.1 Isolated enacyloxin analogues from bromide supplemented media from mutated strains of *B. ambifaria* BCC0203. Structural modifications from the gene deletions are highlighted.

Mutant Strain	Structure	R^1	R^2	Compound
B. ambifaria BCC0203 Δ5927	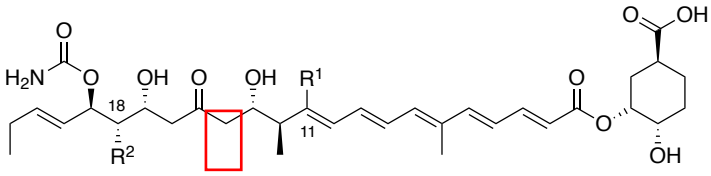	Br Br	Br Cl	**88** **89**
B. ambifaria BCC0203 Δ5930	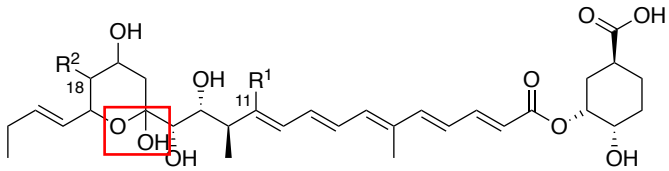	Br	Br	**90**
	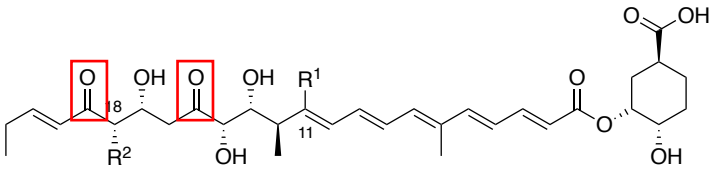	Br	H	**91**
B. ambifaria BCC0203 Δ5930 + Δ5932	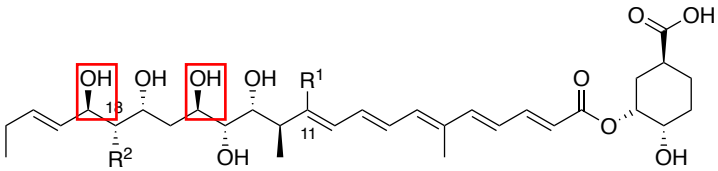	Br Br Br	Br Cl H	**92** **93** **94**

Bromide incorporation at C-11 was seen across all strains used. However, incorporation at C-18 varied between strains. None of the analogues isolated from *B. ambifaria* BCC0203_Δ5927 contained a hydrogen at C-18, but compounds **88** and **89** were isolated. The di-brominated cyclised ether analogue **90** was isolated from *B. ambifaria* BCC0203_Δ5930. The hemi-ketal is formed by reaction of the de-carbamoylated C-19 hydroxyl and the keto group at C-15. Interestingly, having hydrogen instead of a halogen at C-18 results in the hydroxyl at C-19 getting oxidised to a ketone. This could be due to a keto-enol tautomerism where the product exists as the more stable keto form, inhibiting formation of the cyclised ether resulting in the production of **91**. Alternatively, the PQQ dependent dehydrogenase could be able to oxidise the alcohol due to the reduced steric hindrance caused by the absence of a halogen. Bromide incorporation in analogues isolated from *B. ambifaria*

BCC0203_Δ5927 + Δ5932 was similar to the WT strain, with all the analogues containing bromine at C-11 and either hydrogen, chlorine or bromine at C-18.

2.1.2 Use of NAC thioesters to create novel enacyloxin analogues

2.1.2.1 Use of NAC thioesters in mutasynthesis

Within the PKS, inactive *apo*-ACP must first be converted to its active *holo*-form through the transfer of the phosphopantetheine arm from Coenzyme A (CoA) to the conserved ACP serine residue. This reaction is mediated by a PPTase as described in section **1.4.1.3.1**.[95,96,98] As discussed in section **1.4.2**, NAC thioesters can act as mimics of the phosphopantetheine arm present in an ACP within a PKS (scheme **2.1**).

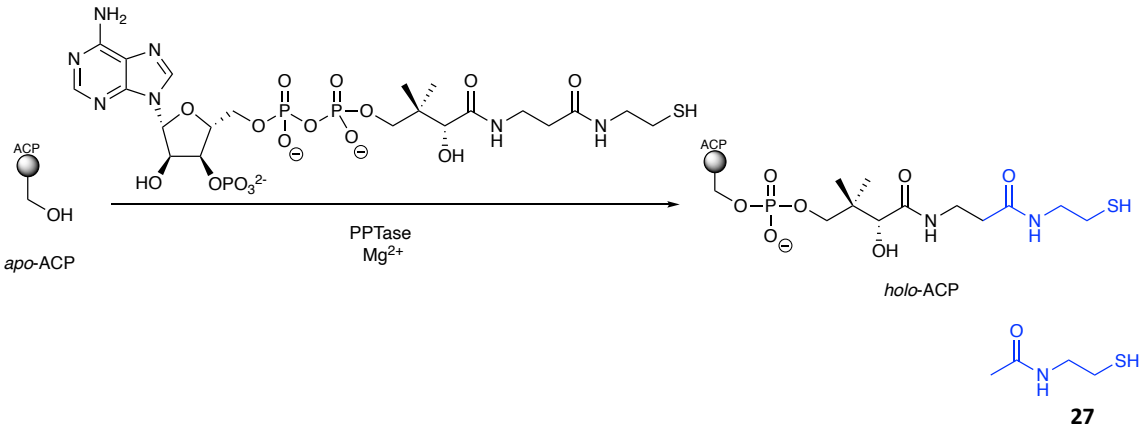

Scheme 2.1: Activation of *apo*-ACP to *holo*-ACP through use of coenzyme A, a phosphotransferase and a magnesium cofactor. Similarities between the structures of the phosphopantetheine arm tethered to an ACP domain and N-acetylcysteamine are highlighted demonstrating how NAC can act as a suitable mimic.

Mutation of the serine residue within the ACP domain of a module to an alanine residue prevents activation of the ACP as the free hydroxy is no longer present to facilitate the phosphopantetheine arm transfer inhibiting natural product biosynthesis. Feeding of a synthetic NAC mimic of PKS chain assembly can then be used to restore production, as the downstream KS domain recognises the NAC thioester mimic, allowing biosynthesis to continue (scheme **2.2**). Synthetic analogues of the natural mimic can then be used to create novel enacyloxin analogues in a similar approach used by Kusebauch and co-workers[136] in the rhizoxin system (section **1.4.2**). Module 2 of the enacyloxin system was selected due to its proximity

to the beginning of the biosynthetic pathway meaning that synthesis of the required NAC thioester would not be too complex. Also the production of novel NAC thioesters should be possible by simple functionalisation if the hydroxyl group.

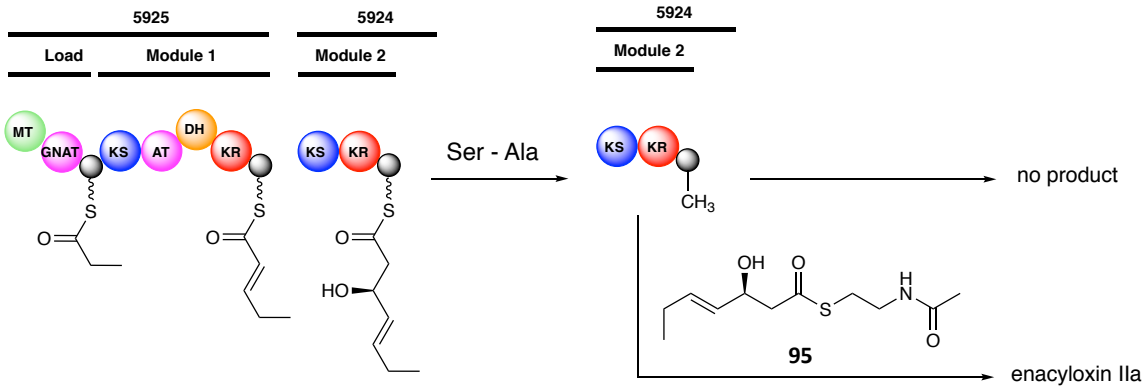

Scheme 2.2: Work-flow for creation of novel enacyloxin analogues using a mutasynthesis approach. (**A**) Inactivation of the ACP domain from module 2 of the enacyloxin biosynthetic pathway. (**B**) Idealised feeding experiment of a synthetic NAC-thioester mimic of a PKS intermediate to re-establish production of enacyloxin IIa.

2.1.2.2 Creation of a *B. ambifaria* mutant blocked in enacyloxin IIa production

The desired *B. ambifaria* BCC0203 mutant strain was created by double homologous recombination approach, using the tri-parental mating procedure outlined in section **6.2.12.4** and the suicide plasmid pGPI-*Sce*I, containing an *Sce*I endonuclease restriction site and trimethoprim resistance marker which are both essential for successful integration into the genome.

A 1 kb fragment of the ACP domain of module 2 about the active serine residue was PCR amplified from *B. ambifaria* BCC0203 genomic DNA and ligated into linearised pGPI-*Sce*I. Site-directed mutagenesis experiments were initially unsuccessful, likely due to the size of the plasmid, so the PCR product was first inserted into the smaller vector, pCR-Blunt, containing a kanamycin resistance marker. The Ser-Ala mutation was then made in the plasmid and the gene fragment was excised and reinserted into pGPI-*Sce*I to give the desired plasmid, containing the mutation (figure **2.4**).

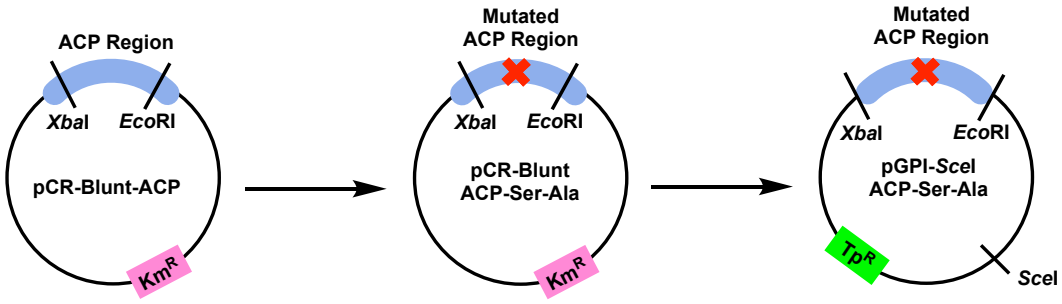

Figure 2.4 Formation of desired plasmid containing the Ser-Ala mutation. Restriction sites used for digestion and ligation are shown. Km^R and Tp^R indicate kanamycin and trimethoprim resistance markers respectively.

The plasmid containing the mutated ACP region was incorporated into the genome of *B. ambifaria* BCC0203 through a series of triparental mating procedures (figure **2.5**).

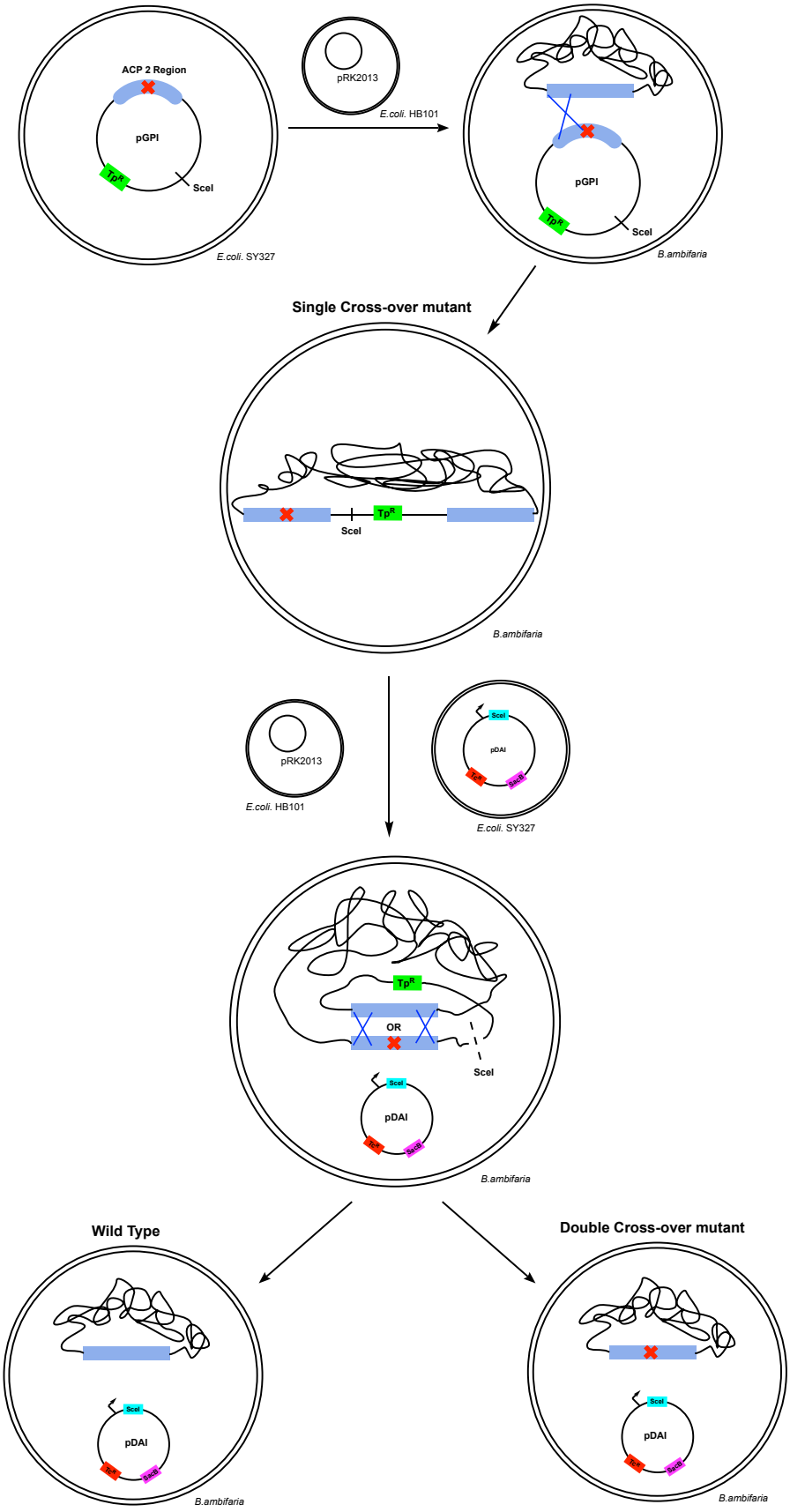

Figure 2.5 Workflow for the tri-parental mating procedure used to incorporate the mutated 1 kb ACP region into the genome of *B. ambifaria* BCC0203. Tp^R and Tc^R indicate trimethoprim and tetracycline resistance markers respectively

The plasmid containing the mutated DNA was introduced into *E. coli* SY327 by electroporation and the construct confirmed by sequencing. Plasmid integration into *B. ambifaria* BCC0203 occurred from the first tri-parental mating procedure using the *E.coli* SY327 donor strain containing the ACP mutant pGPI-*Sce*I plasmid, *E.coli* HB101 helper strain containing the pRK2013 plasmid and *B. ambifaria* BCC0203. The recombinant event can be selected for by the addition of trimethoprim and gentamycin. The first cross-over (recombination) event occurs due to the addition of trimethoprim as the *B. ambifaria* strain does not have resistance against this and must therefore integrate the pGPI-*Sce*I construct containing trimethoprim resistance in order to survive. Addition of gentamycin selects against any *E.coli* strains, leaving only the single crossover product which was confirmed using PCR (figure **2.6**).

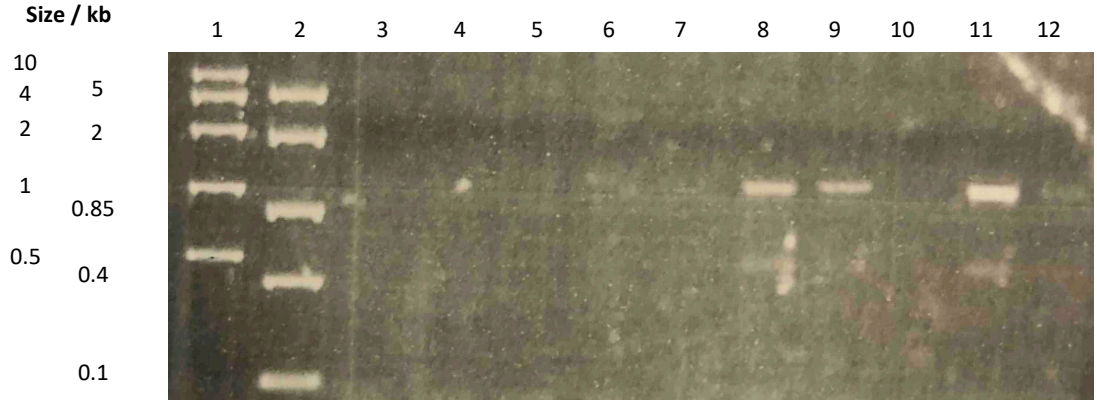

Figure 2.6 Agarose gel from the PCR of the first tri-parental mating event confirming the presence of the 1 kb mutated ACP fragment. (Lane 1 = HR ladder, lane 2 = MR ladder, lanes 3-12 = PCR products. Observed bands in lanes 8, 9 and 11 correspond to expected 1 kb band expected for the mutated 1 kb region. Primers used can be found in table **6.6**.

To the single cross-over product was introduced an *E.coli* SY327 donor strain containing the plasmid pDAI and the *E.coli* HB101 helper strain containing the pRK2013 plasmid. The recombinant event can be selected for by the addition of tetracycline and gentamycin. The second cross-over (recombination) event occurs due to the addition of the pDAI plasmid encoding a *Sce*I endonuclease causing a double strand break at the *Sce*I recognition site now found within the single cross-over product. Recombination repairs the damage and removes the pGPI-*Sce*I plasmid. However, this results in the production of a mixture of both the wild-type *B. ambifaria* BCC0203 strain and the mutated strain containing the Ser-Ala mutation

within the ACP of module 2. As before, from addition of tetracycline this recombination event can be selected for as both double cross-over products comprise the plasmid pDAI containing tetracycline resistance. Addition of gentamicin again selects against *E.coli* strains leaving only the double cross-over product which was confirmed using PCR (figure **2.7**).

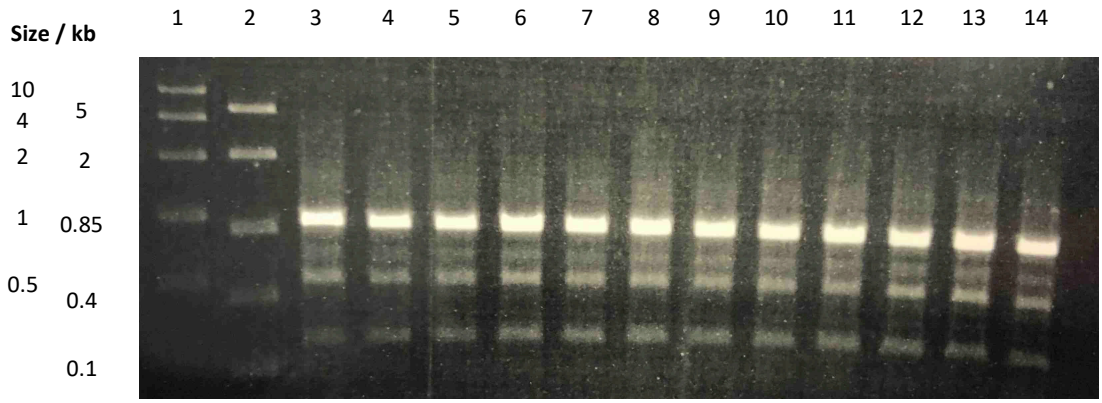

Figure 2.7 Agarose gel from the PCR of the second tri-parental mating event confirming the presence of the 1 kb mutated ACP fragment. (Lane 1 = HR ladder, lane 2 = MR ladder, lanes 3-14 = PCR products. Observed bands in lanes 3-14 correspond to expected 1 kb band expected for the mutated 1 kb region. Primers used can be found in table **6.6**.

To confirm the presence of the desired mutation a phenotype screen was performed to monitor for the disappearance of the characteristic yellow pigment seen when WT enacyloxin is grown on BSM production media (figure **2.8**).

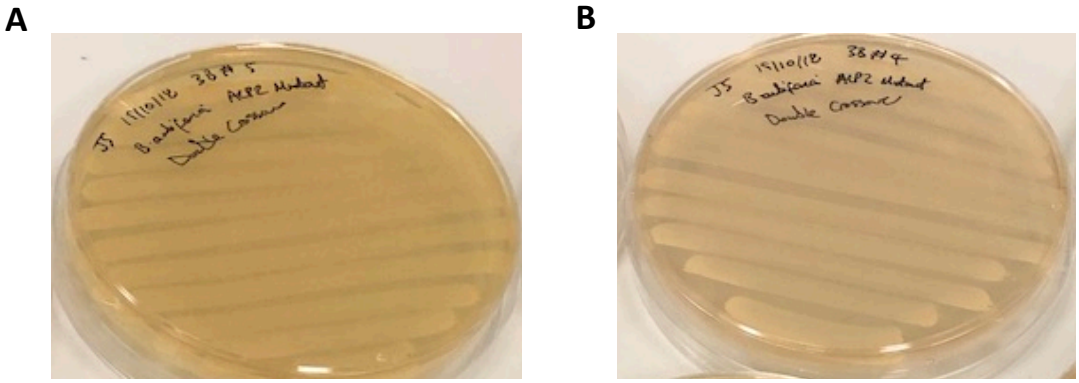

Figure 2.8 Phenotype screen to monitor for loss of production of wild-type enacyloxin IIa. (**A**) wild-type production confirmed by the presence of characteristic yellow streaks, (**B**) second cross-over product containing the desired mutation in the ACP region shown by the appearance of white streaks indicating the loss of enacyloxin IIa production.

Production of a successful second cross-over product containing the desired ACP mutation was also confirmed by sequence analysis of the mutated fragment. The

pDAI plasmid was removed by growth on 15% sucrose LB plates and confirmed by the loss of tetracycline resistance. To confirm the loss of enacyloxin production, both the *B. ambifaria* BCC0203 wild-type strain and the mutated strain (*B. amb*_M2_ΔACP) were grown on BSM media and the ethyl acetate extracts analysed by LC-MS (figure **2.9**).

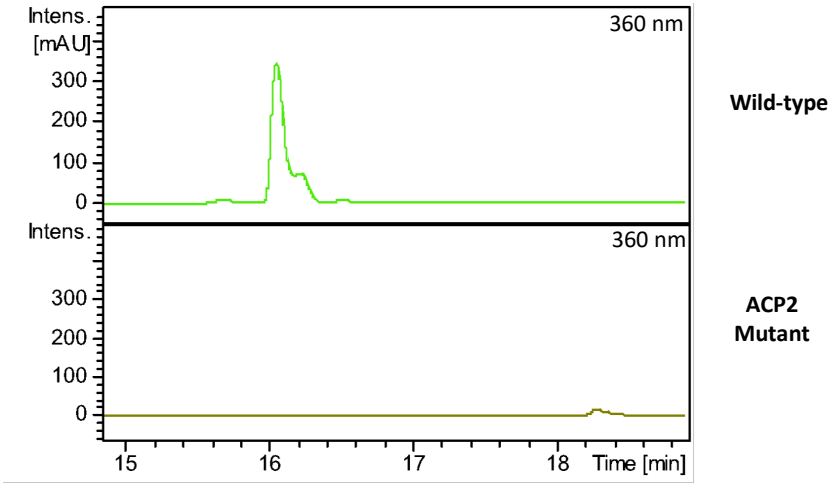

Figure 2.9 UV chromatogram at 360 nm from LC-MS analysis of ethyl acetate extracts of *Burkholderia ambifaria* BCC0203 and a mutant blocked in enacyloxin biosynthesis grown on BSM media (**top**) enacyloxin IIa (**bottom**) second cross-over mutant product blocked in enacyloxin IIa biosynthesis.

Enacyloxin production is abolished in the mutant so we next investigated whether enacyloxin IIa **1** production can be restored through the use of *N*-acetylcysteamine (NAC) thioesters.

2.1.2.3 Chemical synthesis of a NAC thioester mimic for feeding experiments

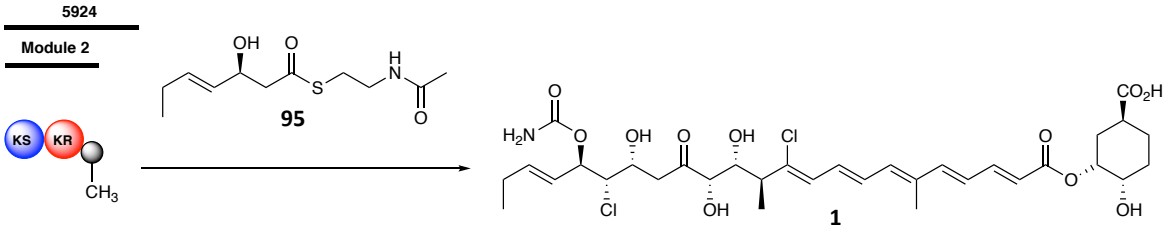

Scheme 2.3 Feeding of a synthesised NAC thioester to the mutated *B. ambifaria* strain blocked in enacyloxin IIa biosynthesis with the aim of restoring production of the natural product.

To establish whether restoration of the natural product is possible (scheme **2.3**) a NAC thioester mimicking the intermediate assembled by module 2 of the PKS was synthesised, including the stereoselective installation of the secondary hydroxyl group (scheme **2.4**).

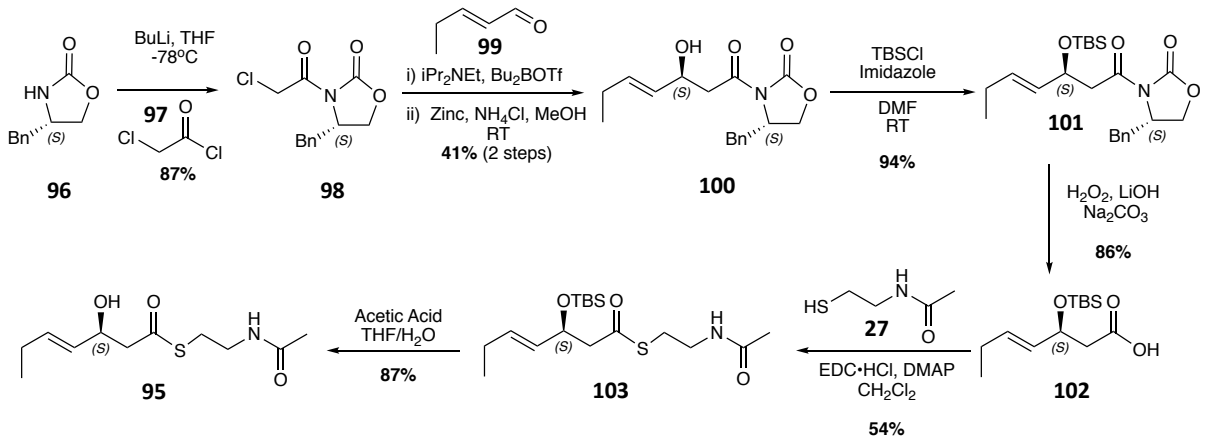

Scheme 2.4 Chemical synthesis of a NAC thioester to be used in feeding experiments to restore enacyloxin IIa production from a mutant blocked in natural product biosynthesis.

Acetylation of (*S*)-configured Evan's auxiliary **96** with chloroacetyl chloride affords compound **98** which can be used in the following stereoselective aldol reaction with Hünig's base and dibutylboryl trifluoromethanesulfonate to afford the chlorinated aldol product. Dehalogenation occurs in the presence of activated zinc affording **100** as the major product with the unwanted formation of the α/β-unsaturated compound as a by-product.[169,170] Chlorination at the α-position is essential for the desired reaction to proceed as elimination of the installed hydroxyl occurs in the absence of chlorine. The stereochemistry of the installed hydroxyl group was confirmed by Mosher's ester analysis[171–173] followed by the TBS protection of the alcohol. Hydrolysis of the auxiliary using LiOOH generated in situ afforded acid **102** which was coupled to freshly prepared *N*-acetylcisteamine (**27**). The deprotection of the hydroxyl group on the coupled product **103** afforded the desired NAC thioester mimic from module 2 of the PKS.

2.1.2.4 Feeding experiments to restore enacyloxin IIa production

The synthesised NAC thioester **95** was added to the production media in a variety of solvents (methanol, water, BSM, DMSO) and concentrations. The mutated *B. ambifaria* strain (*B. amb*_M2_ΔACP) described in section **2.1.2.2** was grown on the NAC thioester supplemented BSM agar plates and ethyl acetate extracts analysed by LC-MS. Although the mutation abolished enacyloxin production, it was not restored upon addition of **95**. However it was uncertain whether this was because the KS domain did not accept the SNAC substrate or as a result of poor cell permeability.

Current production of enacyloxin IIa uses solid BSM production media and liquid media was used in the production of novel rhizoxin analogues using a similar NAC thioester feeding method. It was thought that if enacyloxin IIa **1** can be produced using liquid media, improved uptake of **95** might be observed. Production studies revealed that enacyloxin IIa **1** can be produced in liquid media but at a reduced titre. Using 1 L of liquid production media, only 1 mg of the natural product was isolated, compared to the 10 mg produced on solid media following HPLC purification. Feeding experiments using liquid media were therefore not further explored as work by Kusebauch and colleagues demonstrated that using a NAC thioester feeding method to restore natural product production decreased the yield from 50 mg L^{-1} to 1.5 mg L^{-1}.[136] If this significant decrease in yield was seen within in the enacyloxin system, this method for producing novel analogues would be severely limited. Further investigations into increasing enacyloxin production in liquid media are required before significant progress in this area can be made.

To determine whether production of enacyloxin was not restored because the NAC thioester mimic was not accepted by the KS domain of module 3 of the PKS, the relevant modules were heterologously overproduced and their activity reconstituted *in vitro*.

2.1.2.5 Module 3 *in vitro* reconstitution

An *in vitro* assay was designed to determine whether feeding of NAC thioesters is a viable process for restoring enacyloxin production and creating novel analogues (scheme **2.5**). The assay can be divided into four separate reactions; malonyl loading of the KR-ACP di-domain, KS loading with synthesised NAC thioester (**95**), chain elongation of the malonylated KR-ACP di-domain and ketoreduction to generate the final ACP tethered product. Over-production and purification of the KR-ACP di-domain and KS domain from module 3 are required to conduct the necessary *in vitro* experiments.

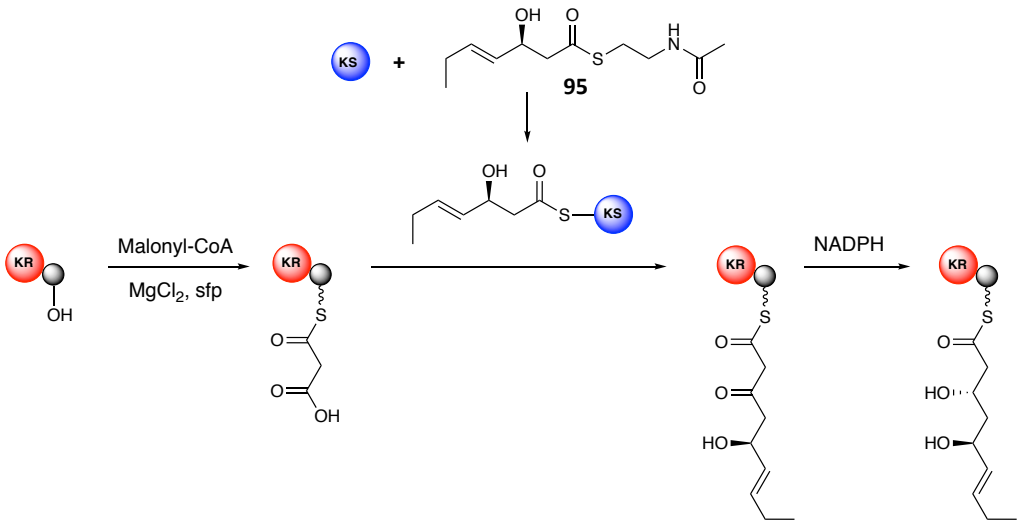

Scheme 2.5 *In vitro* assay used to probe the tolerance of the KS domain of module 3 to the synthesised PKS intermediate NAC thioester mimic and whether chain elongation can occur if tolerated.

2.1.2.5.1 Isolation of the KR/ACP and KS domains of module 3 of the PKS

The KR-ACP didomain and KS domain were separately amplified by PCR using primers containing the restriction enzymes *Hin*dIII or *Nde*I, cloned into the vector pET28a(+) and the constructs confirmed by sequence analysis. The expression vector contains a kanamycin resistance gene, a T7lac promotor that is induced by IPTG and a *N*-terminal His_6-tag allowing for protein purification using a nickel affinity column. Both proteins were overproduced and purified followed by analysis using protein MS (figure **2.10**).

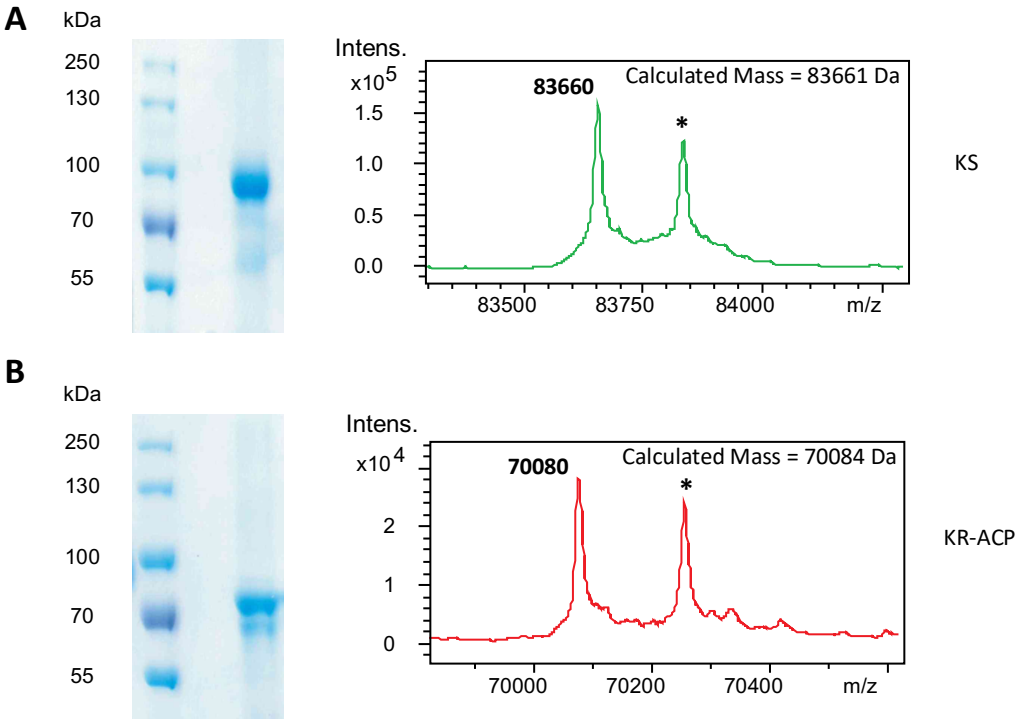

Figure 2.10 8 % SDS-PAGE gel of purified proteins and deconvoluted MS. (**A**) KS domain, (**B**) KR-ACP di-domain (* = +178 Da expected for gluconylation) Lane 1 contains pre-stained protein ladder for initial size determination of purified proteins.

2.1.2.5.2 Activity of the KR-ACP didomain.

The inactive *apo*-KR-ACP di-domain was incubated at RT for 1 hour with acetoacetyl-CoA, $MgCl_2$ and Sfp to convert it to the active acetoacetyl *holo*-KR-ACP. This mimics the natural PKS intermediate allowing the functionality of the KR domain to be probed. Addition of NADPH facilitates ketoreduction.

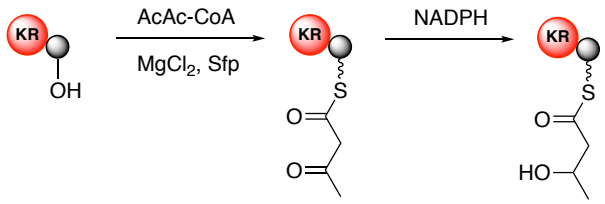

Scheme 2.6 *In vitro* assay used to probe the activity of the KR domain on a simple acetoacetyl unit mimicking the natural PKS chain intermediate

Monitoring of the expected 2 Da mass shift utilised a phosphopantetheine ejection assay developed by Kelleher *et* al.[174]

The substrate bound to the phosphopantetheine arm is ejected to release a protonated imine species detectable by mass spectrometry (scheme **2.7**).[174,175]

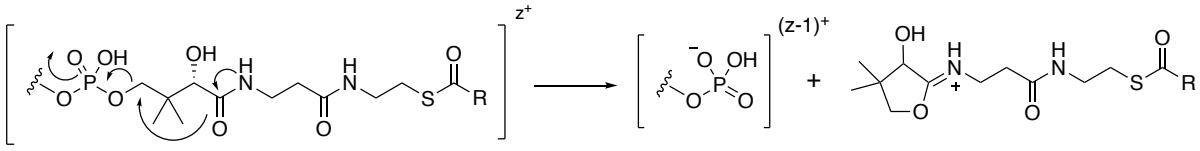

Scheme 2.7 Mechanism of formation of a phosphopantetheine ejection ion for detection of ACP bound PKS intermediates by MS

Upon addition of NADPH a 2 Da mass increase can be seen in the ejection ion species indicating that ketoreduction has taken place, the KR domain is active and the KR-ACP di-domain is functional (figure **2.11**).

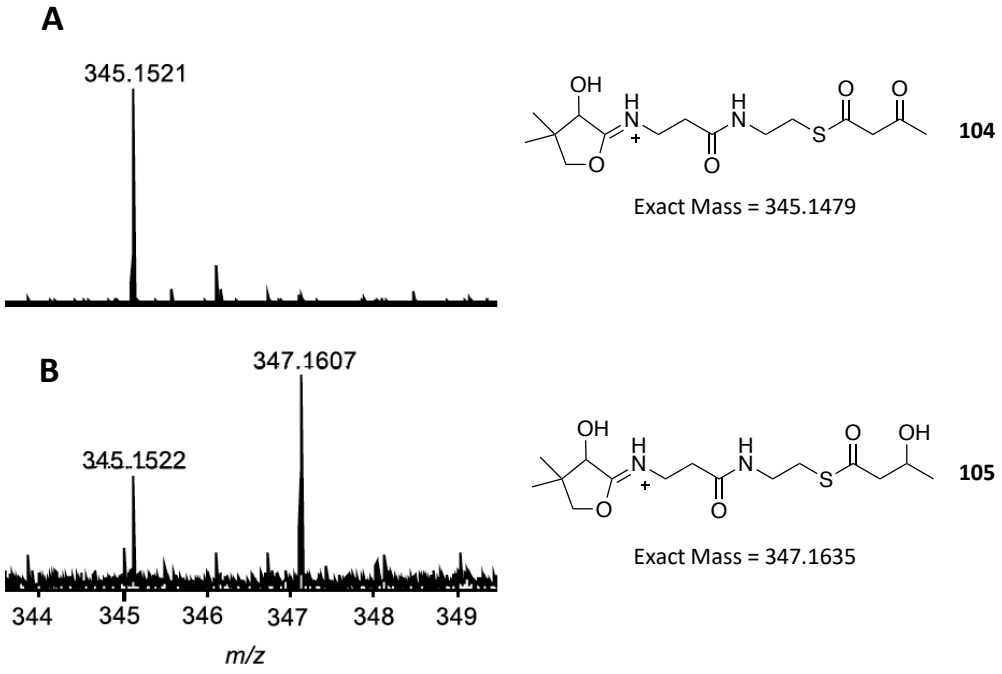

Figure 2.11 MS of the phosphopantheine ejection assay (**A**) Control with no NADPH, (**B**) Reaction with NADPH addition

2.1.2.5.3 Acylation of the KS domain with the NAC thioester

Assessing whether the KS domain can accept the NAC thioester **95** as a substrate is crucial in determining whether feeding NAC thioester analogues is a viable method of producing novel enacyloxin analogues.

The KS domain and NAC thioester mimic **95** were incubated at RT for 3 hours followed by intact protein MS analysis (figure **2.12**).

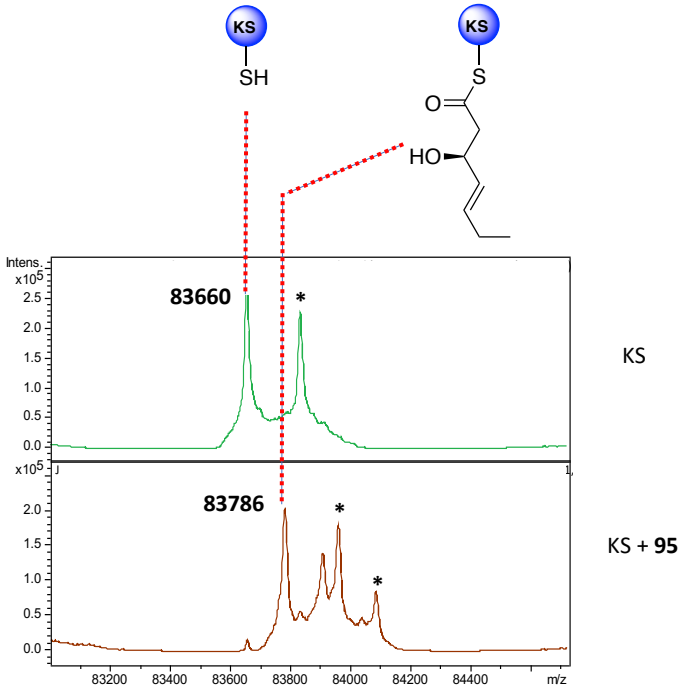

Figure 2.12 Deconvoluted intact protein MS of the stand-alone KS domain and the incubation product of the KS with NAC thioester **95**. * indicates gluconylation

Following incubation with **95**, acylation of the KS domain can be seen due to the expected 126 Da mass increase indicative of the acylated cysteine residue and the disappearance of the KS peak. However, there is evidence of a second acylation event occurring, indicated by the second peak at 83912 Da suggesting one or more other cysteine residues, likely on the surface of the protein, are also being acylated by the NAC thioester.

To investigate this further, a homology model (section **6.2.17.3** and **Appendices** section) of the KS domain was created and one surface cysteine residue was identified (Cys699). To determine whether acylation was occurring on the active site residue (Cys218) or on Cys699, both residues were separately mutated to alanine and the effect on acylation was determined.

2.1.2.5.3.1 Creation of cysteine mutants to determine the acylation site within the KS domain

Initial investigations to produce the desired mutation using a site directed mutagenesis approach on the KS_pET28a(+) construct failed so an overlap PCR approach was used (scheme **2.8**).

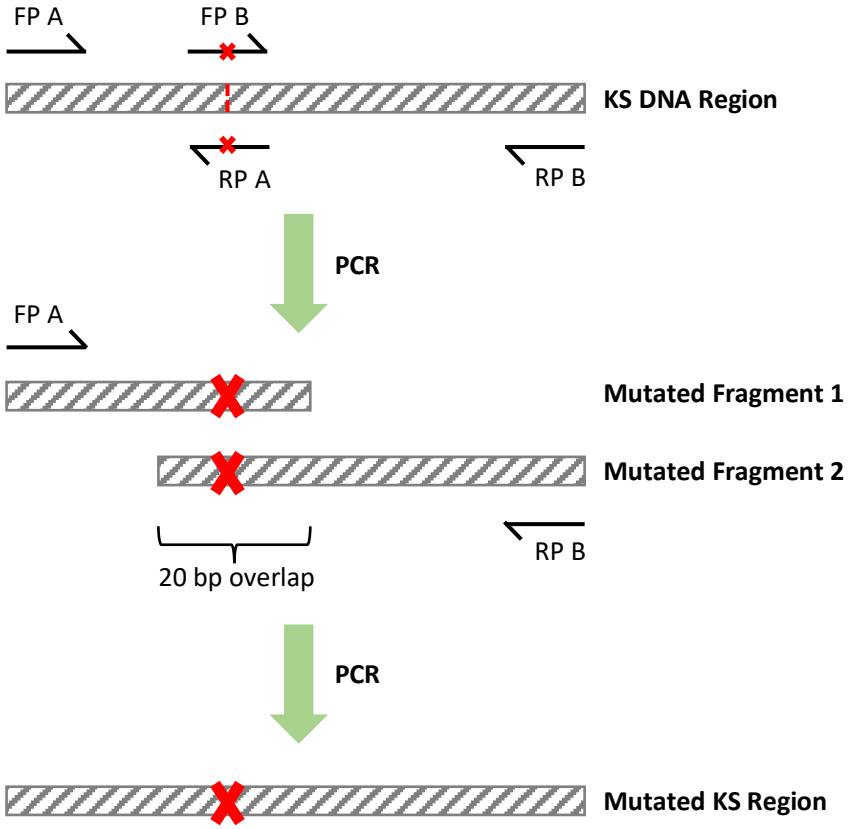

Scheme 2.8 General work-flow for the creation of cysteine to alanine mutants within the KS region of module3. FP A/B and RP A/B refers to forward and reverse primers used in each step with the corresponding primer pair indicated by either A or B. The red cross denotes the site of mutation

This approach splits the DNA region of interest into two sections with a 20 bp overlap at the point of desired mutation through two PCR reactions. Primers are designed (section **6.2.17.4**, table **6.1**) to create the mutation in the overlapping region within each fragment. These two fragments are then PCR amplified to produce one complete fragment containing the desired mutation using the flanking primers. This can then be cloned into the vector pET28a(+) using restriction sites introduced by the primers to give the desired mutated construct which was confirmed by sequence

analysis. Using this method both C218A and C699A variant constructs were prepared and used to overproduce and purify the respective proteins (figure **2.13**).

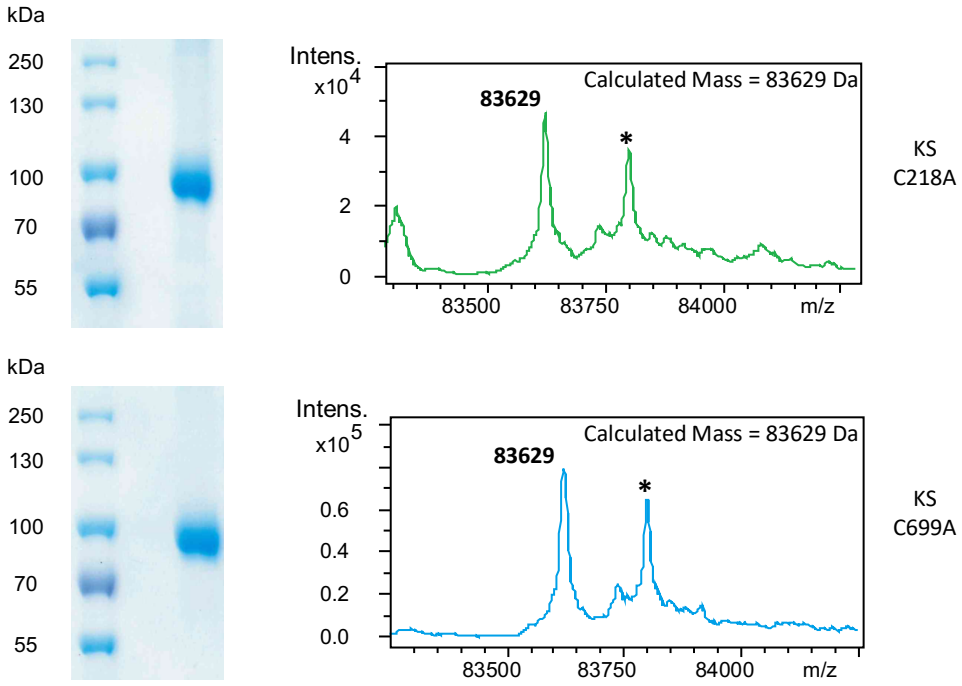

Figure 2.13 8 % SDS-PAGE gel of purified proteins and deconvoluted MS. (**A**) C218A KS variant, (**B**), C699A KS variant (* = gluconylation) Lane 1 contains pre-stained protein ladder for initial size determination of purified proteins

The mutated KS domains were incubated with **95** as before and analysed by intact protein MS (figure **2.14**).

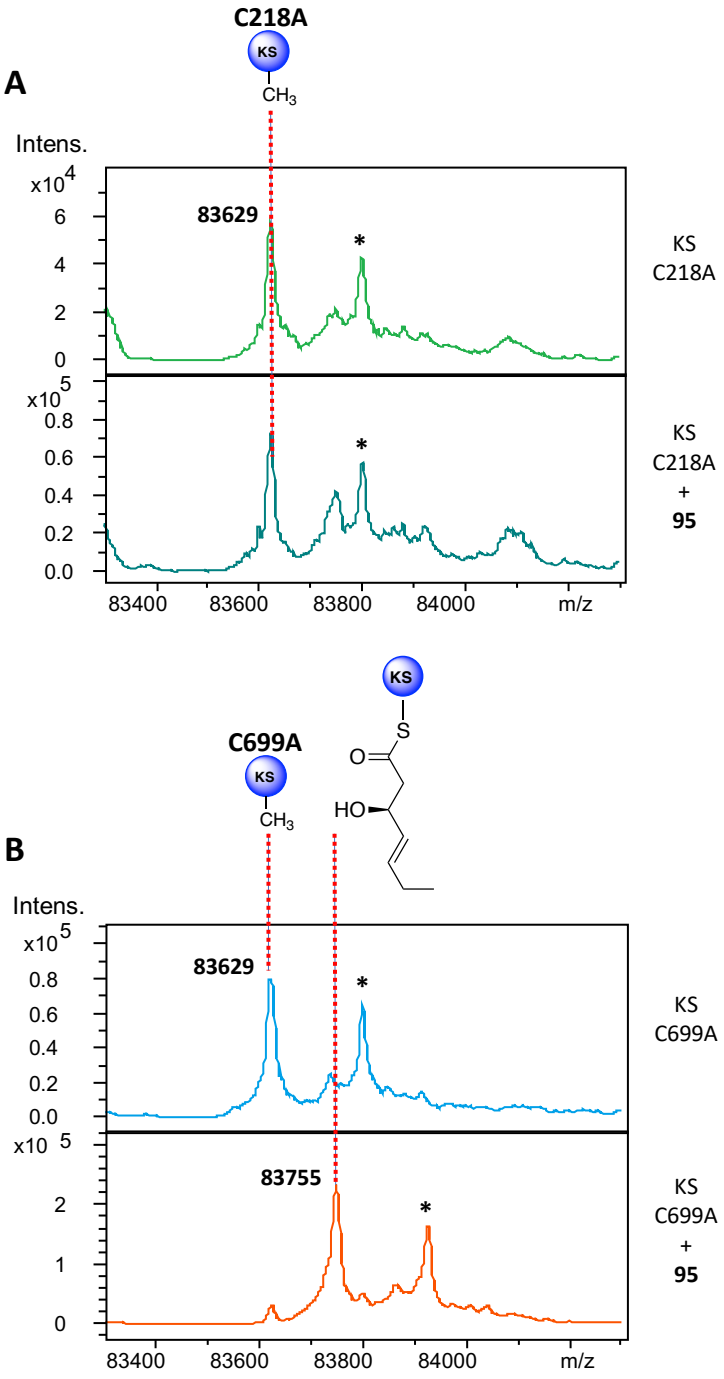

Figure 2.14 Deconvoluted intact protein MS of the KS cysteine mutants and the products when incubated with NAC thioester **95**. (**A**) C218A variant (**top**) and incubation product (**bottom**), (**B**) C699A variant (**top**) and incubation product (**bottom**). * indicates gluconylation.

Upon incubation of **95** with the C699A variant, a single acylated product was observed with a 126 Da mass increase, with negligible secondary acylation observed, indicating that this was the likely site of non-catalysed acylation. Incubation of the active site C218A variant with NAC thioester **95** abolished all acylation, confirming the active site residue is being acylated and suggesting that acylation of the active

site may cause a conformational change which makes C699 more solvent exposed and prone to acylation.

Incubation of NAC thioester **95** with a KS domain containing both the C218A and C699A mutations (figure **2.15**) prepared using overlap PCR, also did not result in any acylation, further supporting that these two positions were the only ones acylated in the original experiment.

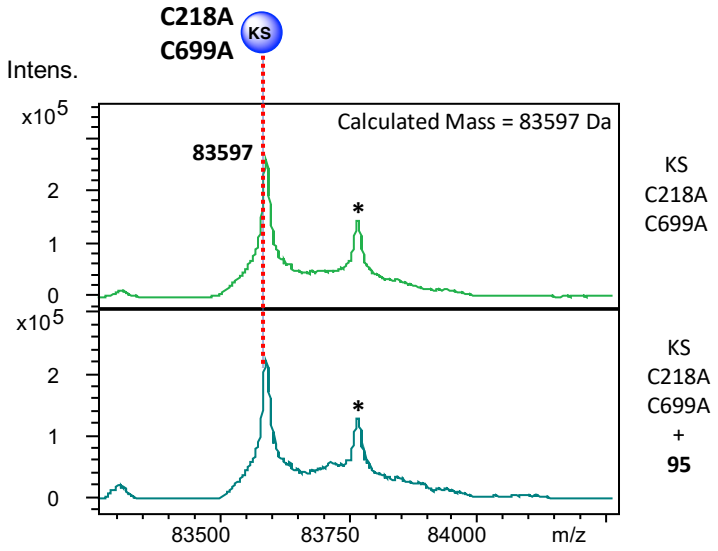

Figure 2.15 Deconvoluted intact protein MS of the KS C218A + C699A double variant and the product when incubated with NAC thioester **95**.

Having established the KS domain can be successfully loaded, its ability to catalyse chain extension was investigated.

2.1.2.5.4 Investigations into chain elongation of the malonylated KR/ACP di-domain

The *apo*-KR-ACP di-domain was first incubated with malonyl-CoA, Sfp and $MgCl_2$ at RT for 1 hour, to convert it from the *apo*-form to the active malonylated *holo*-form. Loading was confirmed by intact protein MS followed by addition of the wild-type acylated-KS domain was added. Both were incubated at RT for 1 hour and the intact protein MS repeated (scheme **2.9**).

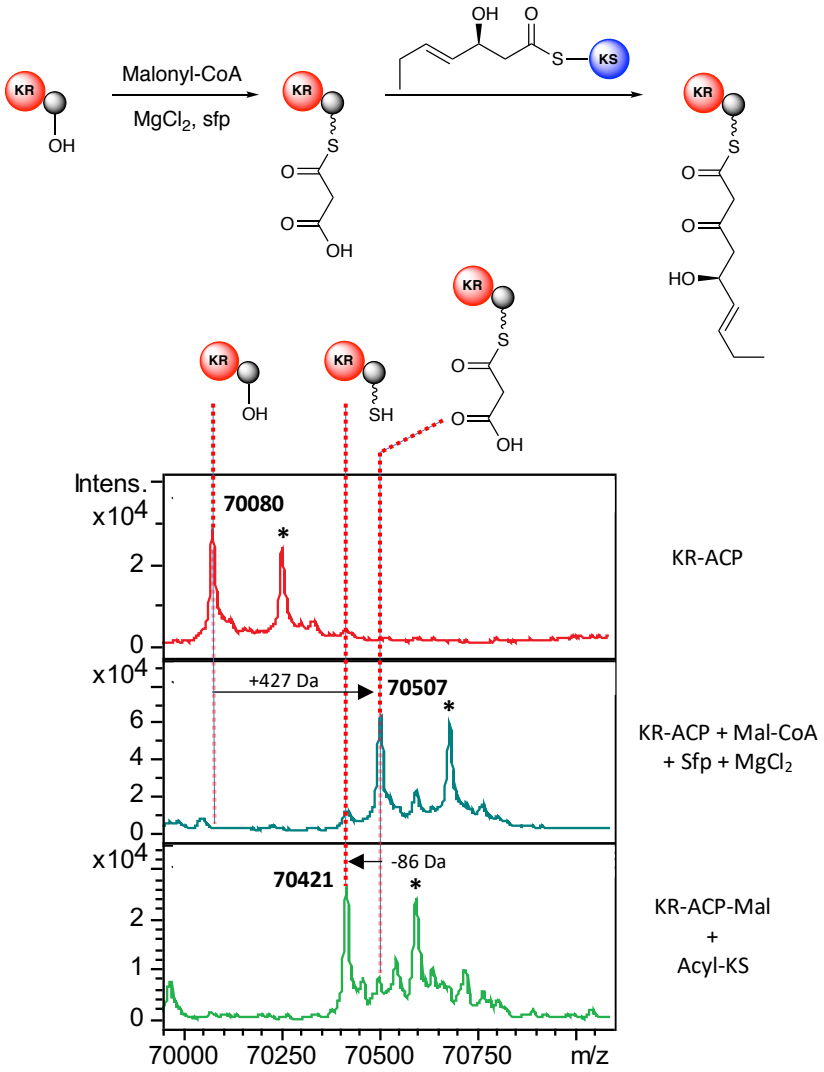

Scheme 2.9 (**Top**) *In vitro* assay used to determine if chain elongation can occur using KS loaded with NAC thioester **95** (**Bottom**) Deconvoluted intact protein MS of the *in vitro* assay investigations into the use of NAC thioester **95** as a means of restoring PKS functionality. (**top**) *Apo*-KR-ACP di-domain, (**middle**) formation of malonylated *holo*-KR-ACP di-domain, (**bottom**) product of maolonated *holo*-KR-ACP and acylated-KS domain incubation

Conversion of the *apo*-KR-ACP didomain to the malonylated *holo*-KR-ACP didomain was confirmed by the +427 Da mass shift. Addition of the acylated KS domain caused a -86 Da shift, suggesting the formation of the *holo*-KR-ACP didomain and not the desired elongated PKS intermediate. It is possible that following elongation of the polyketide chain, the substrate cyclises, affording a lactone and the *holo*-KR-ACP didomain observed by MS (scheme **2.14**). Thioesters are inherently labile and prone to nucleophilic attack and formation of the stable 6-membered lactone ring would drive the reaction.

To mitigate the issue of cyclisation and resultant cleavage of the KS-bound substrate, an alternative substrate analogue, containing an amide in place of the thioester, was targeted.

2.1.2.5.5 Use of non-hydrolysable substrate analogues to monitor KR-ACP chain elongation

The use of non-hydrolysable probes both *in vitro* and *in vivo,* to monitor and characterise polyketide intermediates has been previous used on both type I (DEBS)[176,177] and type III (stilbene) PKSs. [178,179] However, these have primarily focused on the offloading of polyketide intermediates 'trapping' them for LC-MS analysis (scheme **2.10**). Using a non-hydrolysable mimic of the malonyl unit would allow intact protein MS analysis of the elongated polyketide chain.

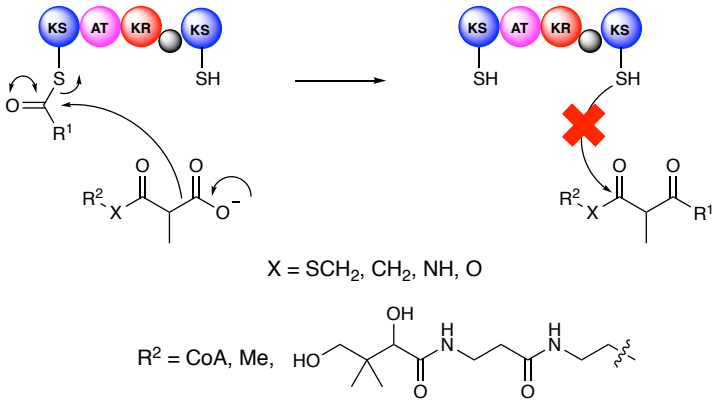

Scheme 2.10 Current literature methods for the trapping of PKS intermediates using methyl malonyl derived non-hydrolysable analogues (scheme adapted from the literature)

Formation of the *N*-malonyl-KR-ACP didomain required the synthesis of pantetheine substrate **111** (scheme **2.11**).

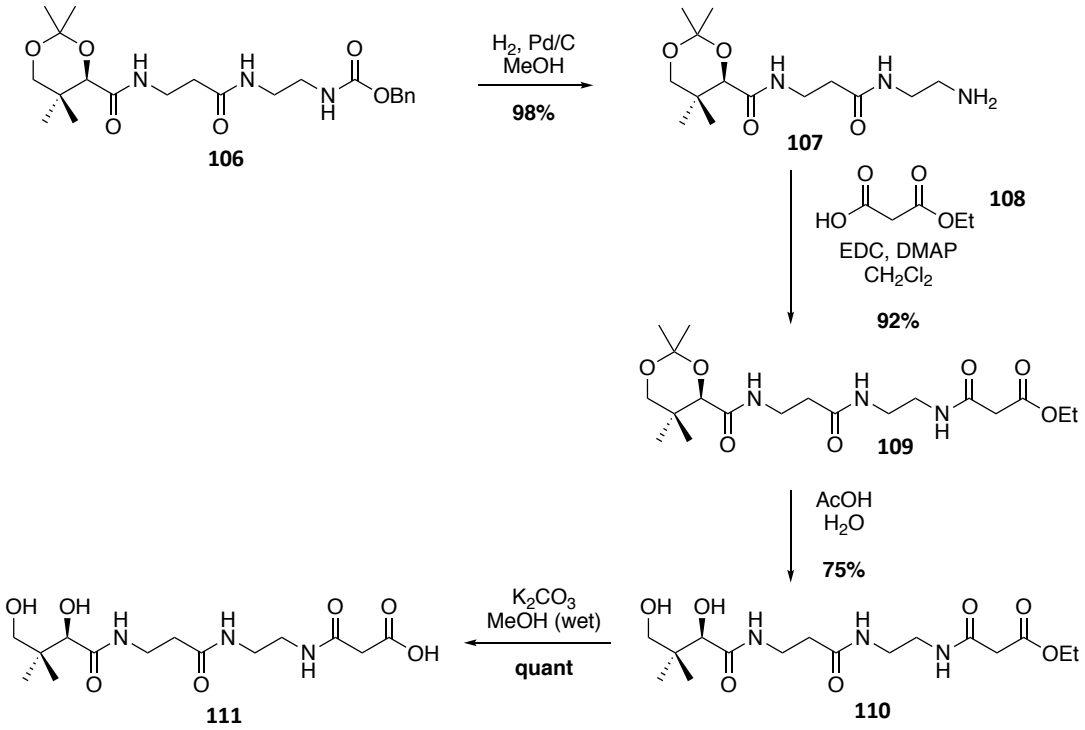

Scheme 2.11 Synthetic route for the production of the pantetheine substrate required for N-malonyl-KR-ACP formation in an *in vitro* assay.

Hydrogenation of carboxybenzyl (cbz) protected amine **106** (previously synthesised in the Challis group) afforded intermediate **107** which could be coupled to commercially available acid **108**. Deprotection of the acetonide in **109** using acetic acid afforded the desired diol **110**. Finally, ester hydrolysis under basic conditions afforded the desired pantetheine derivative **111**.

To prepare the *N*-malonyl-KR-ACP didomain a one-pot reaction was used in which pantetheine substrate **111** was incubated with pantetheine kinase (PANK), phosphopantetheine adenylyltransferase (PPAT), dephospho-CoA kinase (DPCK) and adenosine triphosphate (ATP) to convert it into the corresponding *N*-malonyl CoA, which can be loaded onto the ACP domain with Sfp as previously described (scheme **2.12**).

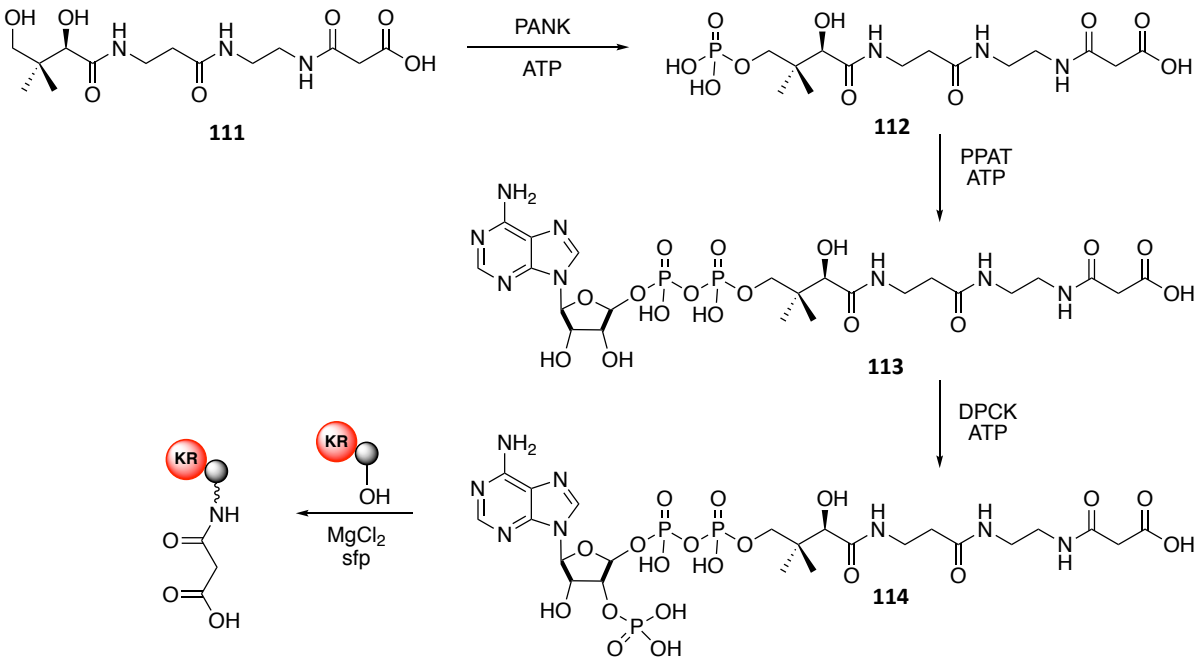

Scheme 2.12 Enzymatic formation of *N*-malonyl loaded KR-ACP from chemically synthesised substrate **111**.

Conversion of *apo*-KR-ACP didomain to the *N*-malonylated *holo*-KR-ACP didomain was confirmed by a +410 Da mass shift in the deconvoluted mass spectrum. However, addition of the acylated-KS domain did not result in formation of the elongated PKS intermediate. Cleavage of the malonylated intermediate to give the free amine was also not observed. (scheme **2.13**).

It is possible the presence of the amide prevents the decarboxylation required for chain elongation, due to the donation of electron density to carbonyl group. Exchanging the nitrogen for the more electronegative oxygen, to give an ester, may be a suitable alternative. However, this has yet to be investigated.

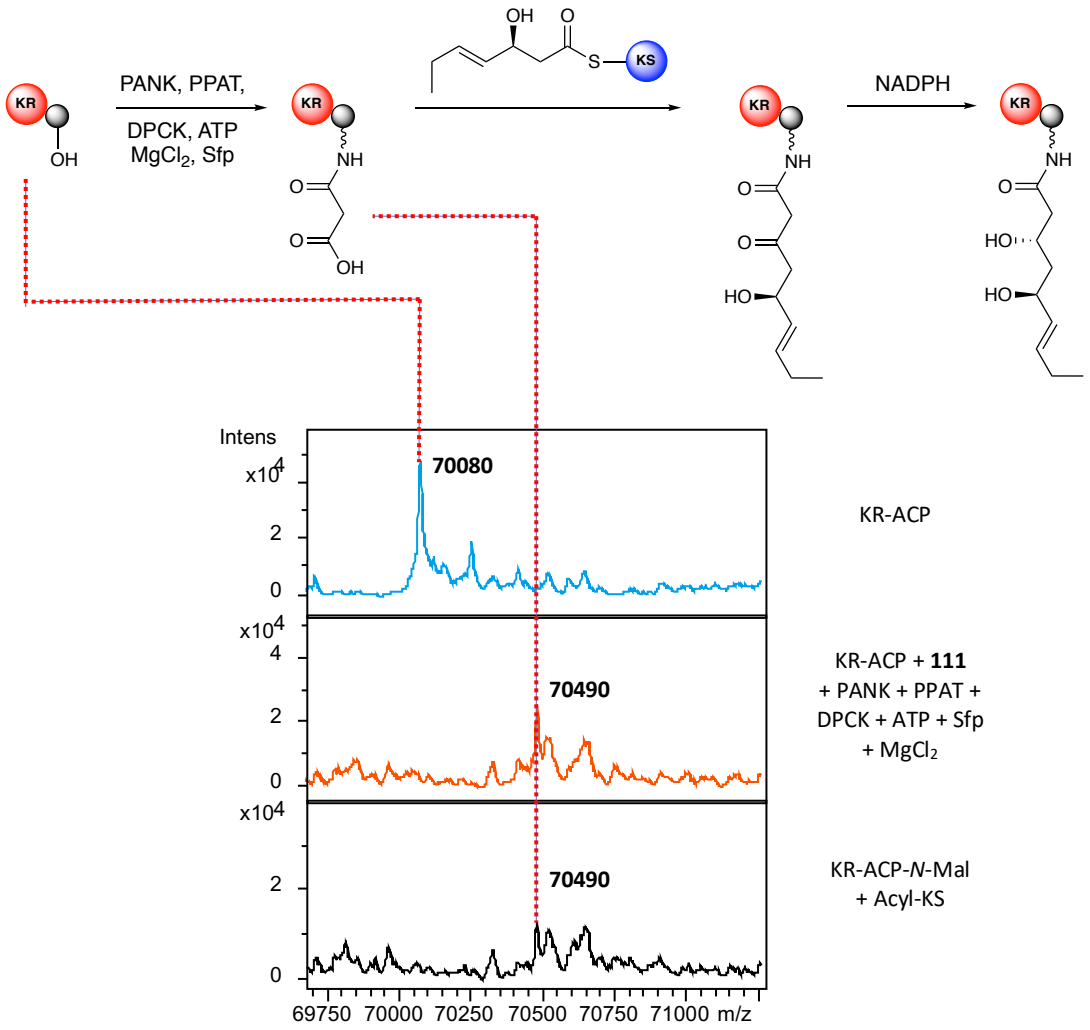

Scheme 2.13 (**Top**) Revised *In vitro* assay with a non-hydrolysable tethered intermediate to probe whether chain elongation can occur. (**Bottom**) Deconvoluted intact protein MS of the *in vitro* assay investigations into the use of a non-hydrolysable intermediate to monitor chain elongation. (**top**) *Apo*-KR-ACP di-domain, (**middle**) formation of *N*-malonylated *holo*-KR-ACP di-domain, (**bottom**) product of maolonated *holo*-KR-ACP and acylated-KS domain incubation.

2.1.2.5.6 Monitoring of *in vitro* assay off-loaded by-products

Since monitoring of PKS tethered intermediates proved challenging, small molecule LC-MS to search for proposed off-loaded lactone **115** was investigated.

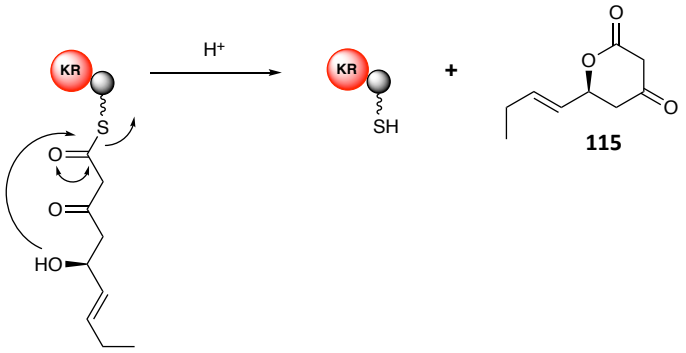

Scheme 2.14 Proposed mechanistic production *holo*-KR-ACP and the lactone by-product

The lactone was therefore chemically synthesised to be used as a standard for LC-MS comparison. Treatment of methyl acetoacetate with sodium hydride followed by ^{n}BuLi and *trans*-2-pentenal afforded the desired lactone product **117** as a racemic mixture (scheme **2.15**).

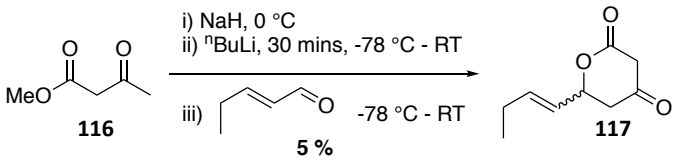

Scheme 2.15: Synthesis of lactone **117** for use in LC-MS studies to evaluate the success of *in vitro* chain elongation

The assay described in section **6.2.18.5** was repeated, the protein was precipitated and the supernatant extracted with EtOAc, followed by analysis by LC-MS (figure **2.16**).

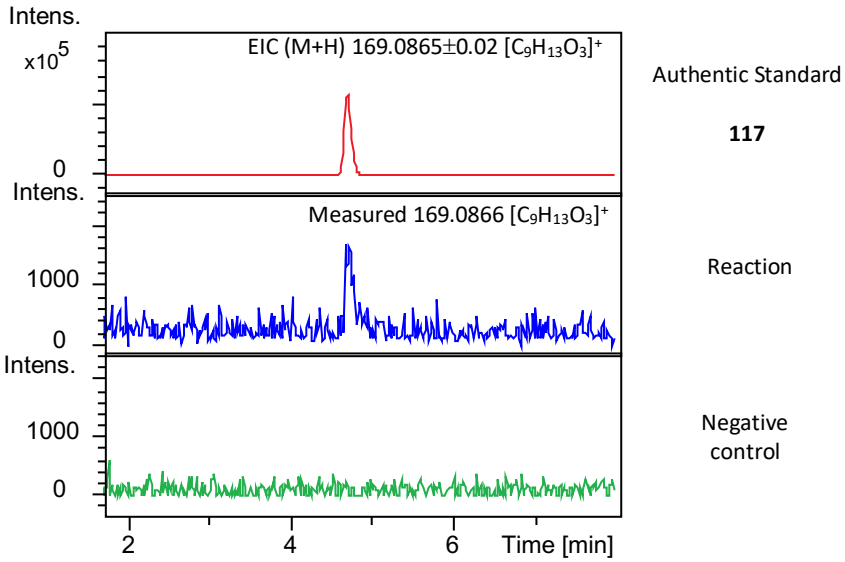

Figure 2.16 LC-MS analysis of supernatant from *in vitro* assay compared to an authentic standard, (**top**) chemically synthesised authentic standard, (**middle**) +ve reaction, (**bottom**) -ve control

The peak observed from the *in vitro* assay has an identical retention time to the authentic standard and was not observed in the negative control. This confirms that the chain elongation does occur, but that due to the labile thioester, the products are rapidly hydrolysed. Within the PKS it is likely however that this intermediate is translocated to the next module before cyclisation can occur.

This suggests that using NAC thioesters for semi synthesis would be a viable method for the production of novel analogues if the problems with cell uptake could be overcome.

2.2 Conclusions

In this chapter the production of several enacyloxin analogues with modifications to the acyl chain has been discussed. Substitution of halide sources was successful in producing novel brominated analogues using both the natural producing *B. ambifaria* BCC0203 WT strain and mutated strains previously produced in the Challis group. The bioactivity of these analogues is discussed in chapter **4.**

A mutasynthesis approach for the production of novel enacyloxin analogues was also investigated. The creation of an ACP point mutation within module 2 of the PKS blocked enacyloxin biosynthesis, but feeding of a chemically synthesised NAC thioester mimic failed to restore natural product production.

An *in vitro* assay was designed to determine whether the downstream KS domain can accept the NAC thioester substrate analogue and catalyse chain elongation. From this it was shown that KS acylation using a NAC thioester is possible. However the chain elongation product was prone to lactonization which was confirmed through LC-MS comparison of the off-loaded product to a synthetic lactone standard. The activity of the KR domain was also confirmed. The complete reconstitution of module 3 can be confirmed if the elongation assay is repeated in the presence of NADPH and the reduced off-loaded reduced lactone observed by LC-MS. This would be the first example of complete *in vitro* reconstitution of a module with this type of unusual split architecture. This would allow interesting questions about the nature of the interaction between the KS and KR domain to be investigated such as whether it is mediated by docking domains or direct catalytic interaction of the two domains.

With an *in vitro* assay established with a system whereby chain extension can be monitored by LC-MS of off-loaded products, the tolerance of the KS and KR domain towards NAC thioester analogues could be further investigated. The free hydroxyl group of NAC thioester **95** could be functionalised with groups able to hydrogen bond with the key residues within the active site. Synthesis of the NAC thioester containing the (*R*)-configured alcohol may also help determine whether the alternative configuration affects the acceptance by the KS and whether the carbamoylation by the Bamb_5930 carbamoyl transferase is stereospecific. Synthesis of a NAC thioester without a nucleophilic group able to cleave the labile thioester should also allow for chain extension to be observed on the KR-ACP di-domain.

If it is shown that the KS domain will accept analogues of the natural biosynthetic intermediate, further work is needed to get the NAC thioester into the cell. One way

in which this could be achieved is to clone and express the enacyloxin cluster into a heterologous host known to be permeable to NAC thioesters.

A non-hydrolysable intermediate was also used to try and prevent the hydrolysis of the thioester however the amide linkage may have prevented the decarboxylation required for chain elongation. Therefore production of the ester linked intermediate may be a suitable alternative that would allow intact protein MS of *in vitro* assay products without hydrolysis concerns (scheme **2.16**).

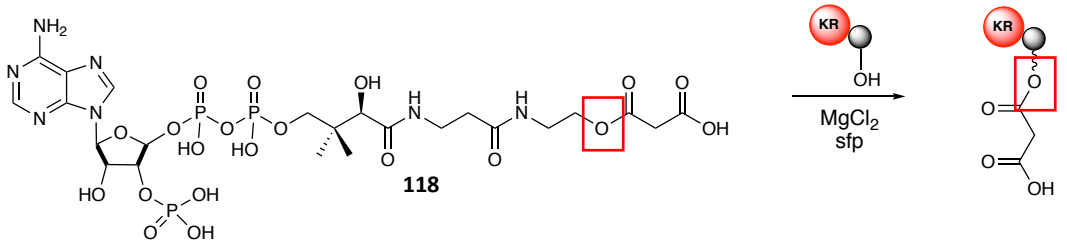

Scheme 2.16 Formation of a non-hydrolysable intermediate able to facilitate decarboxylation and resultant chain elongation.

Chapter 3 - Results and Discussion II

3.1 Modifications to the DHCCA unit

The DHCCA region of enacyloxin IIa **1** has yet to be further explored in this project. Therefore using a previously established mutasynthesis approach, investigations into changes to the DHCCA ring size and further structural modifications were undertaken.

3.1.1 A mutasynthesis approach towards the production of novel enacyloxin analogues

3.1.1.1 Re-creation of enacyloxin analogue 77

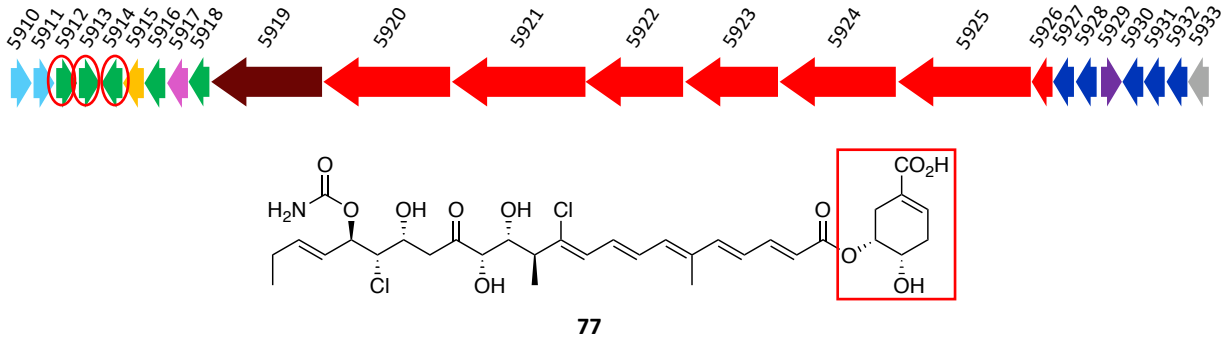

77

Figure 3.1 Enacyloxin IIa biosynthetic gene cluster with highlighted deleted genes responsible for DHCCA biosynthesis and enacyloxin analogue **77** containing a more rigid unsaturated DHCCA ring with the most potent activity to date (MIC = 0.5 µg/mL).

As described previously, gene deletion of *bamb*_5912, *bamb*_5913 and *bamb*_5914, (figure **3.1**) to prevent the biosynthesis of DHCCA, followed by supplementation of the *B. ambifaria* BCC0203 Δ5912-14 growth media with DHCCA analogues, is a successful method of enacyloxin analogue generation. This strategy was used to produce the most potent enacyloxin analogue to date (**77**). The first objective was to resynthesize DHCCA analogue **78** from D-(-)-quinic acid (**119**), and feed it to *B. ambifaria* BCC0203 Δ5912-14 to obtain enough **77** for the bioactivity assays discussed in section **4.1**.

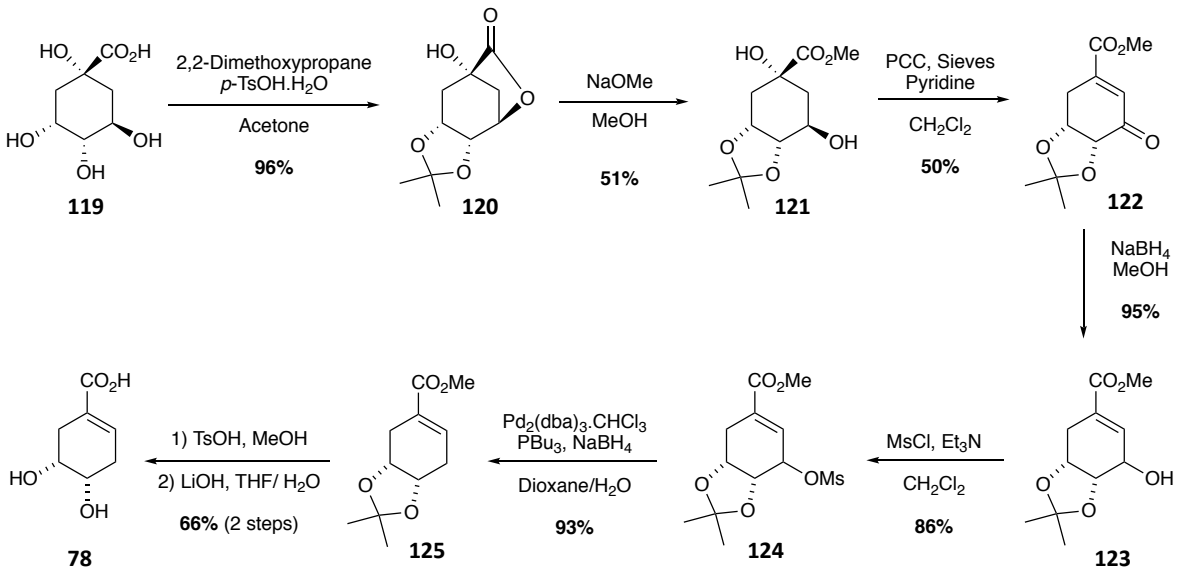

Scheme 3.1 Synthetic route for the preparation of DHCCA analogue **78** to be used in the production of the enacyloxin analogue **77**.

Quinic acid **119** was protected as an acetonide and converted to lactone **120**, which, under basic conditions was ring opened to form the methyl ester **121**. Elimination of the tertiary alcohol was promoted by oxidation of the secondary alcohol to a ketone with pyridinium chlorochromate (PCC), which was then reduced back to the alcohol non-stereoselectively to give **123**. Mesylation of **123**, followed by a palladium catalysed elimination afforded ester **125** which, upon deprotection of the acetonide and hydrolysis of the ester, produced the DHCCA analogue **78**. Feeding of **78** to *B. ambifaria* BCC0203 Δ5912-14 blocked in DHCCA biosynthesis produced the desired enacyloxin analogue **77**. Analogue production was confirmed by NMR spectroscopy (section **6.3**) and LC-MS analysis (**Appendices** section).

3.1.1.2 Chemical synthesis of a linear DHCCA analogue and production of a novel enacyloxin IIa analogue

Most of the enacyloxin IIa analogues produced within this and previous projects have contained a cyclic moiety in place of DHCCA. The effect of incorporation of linear DHCCA analogues was therefore investigated. The only linear analogue previously produced was **83**, obtained by feeding **60** to *B. ambifaria* BCC0203 Δ5912-14. This

analogue had significantly decreased activity against *A. baumannii* (MIC = >64 µg/mL) (figure **3.2**).

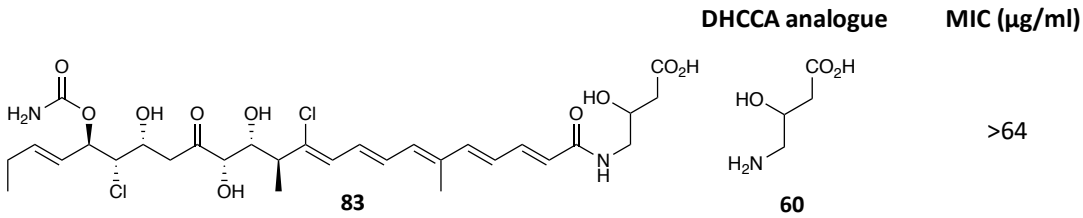

Figure 3.2 Previously produced enacyloxin analogue isolated from the feeding of **60** to *B. ambifaria* BCC0203 Δ5912-14 (Dr. Joleen Masschelein).

To more accurately mimic the DHCCA unit, a similar substrate was synthesised which contained an additional carbon unit (scheme **3.2**).

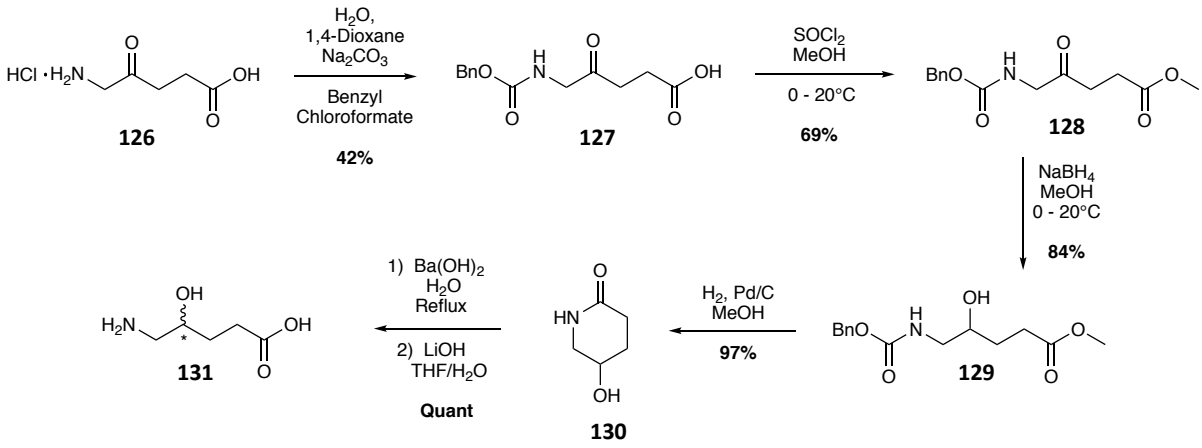

Scheme 3.2 Synthetic route for the preparation of a linear DHCCA analogue to be used in the production of novel enacyloxin analogues

Commercially available 5-aminolevulinic acid hydrochloride **126** was carboxybenzyl protected to afford intermediate **127** which was then converted to methyl ester **128**. Ketone reduction using sodium borohydride was followed by hydrogenation of the carboxybenzyl group affording lactam **130**. Under basic conditions the lactam was ring opened to form the linear DHCCA analogue mimic **131** which was fed to *B. ambifaria* BCC0203 Δ5912-14 blocked in DHCCA biosynthesis. The enacyloxin analogue was isolated by ethyl acetate extractions of BSM growth plates, purified by HPLC analysis and characterised by LC-MS and NMR spectroscopy to afford compound **132**.

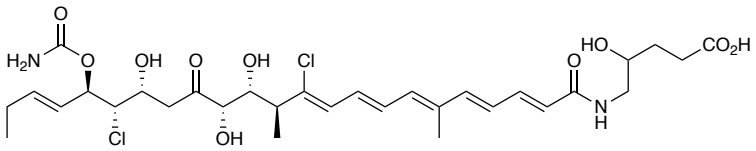

132

Figure 3.3 Structure of enacyloxin analogue **132** with a linear DHCCA moiety from the feeding of **131** with *B. ambifaria* BCC0203 Δ5912-14

3.1.1.3 Production of enacyloxin analogues containing a 7-membered DHCCA unit

Production of 7-membered analogues was completed in collaboration with MChem student Caitlin Heffernan and visiting student Nesrine Bali.

Previous efforts within the Challis group focused on five and six membered rings with one example of a linear chain analogue. Incorporation of 7-membered rings has yet to be explored. The added degree of freedom gained from the extra carbon linker may benefit the interaction with Lys313 and Tyr160 residues within the active site providing an interesting target for SAR studies. Therefore a 7-memebered DHCCA analogue was chemically synthesised and used to feed into *B. ambifaria* BCC0203 Δ5912-14 blocked in DHCCA biosynthesis.

3.1.1.3.1 Chemical synthesis of a 7-membered DHCCA analogue and production of novel enacyloxin analogues

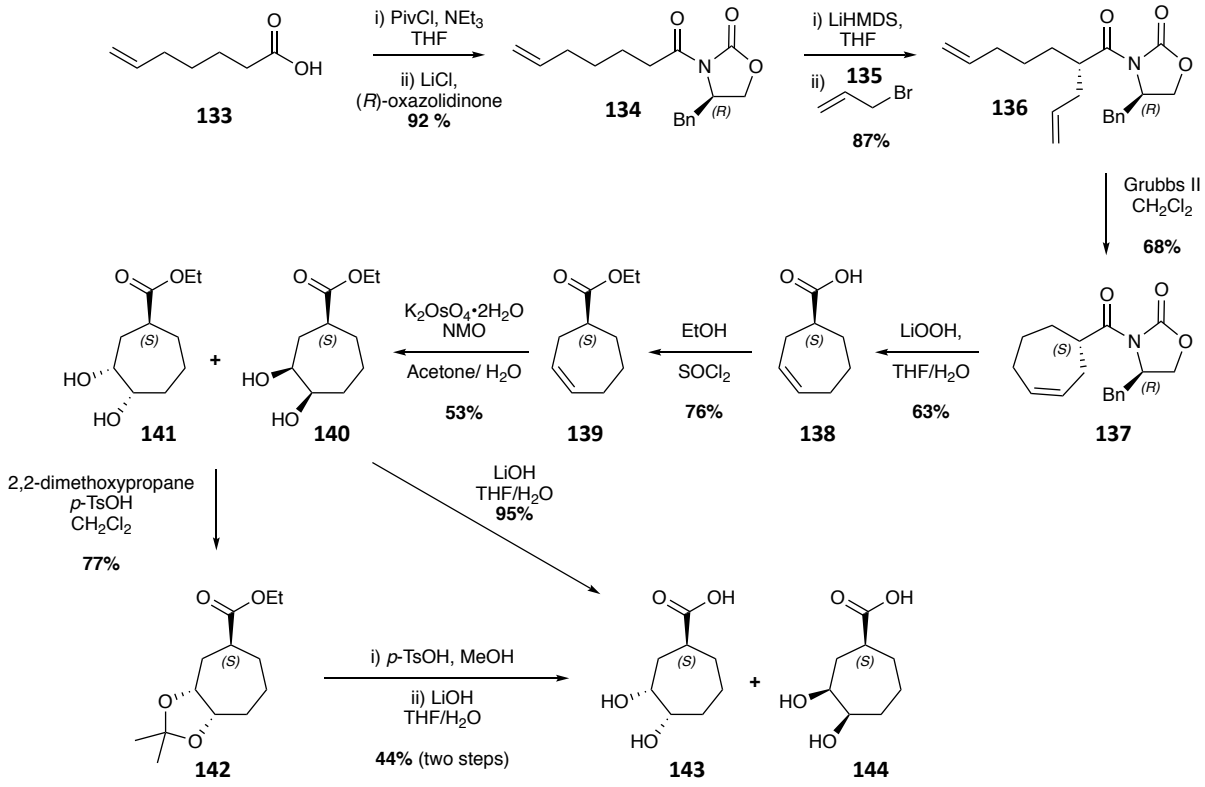

Scheme 3.3 Synthetic route for the preparation of 7-membered DHCCA analogues to be used in the production of novel enacyloxin analogues.

Addition of the *R*-configured Evans' auxiliary to 6-heptenoic (**133**) allowed for the stereoselective allyation of **134** producing the diene intermediate **136**. Subsequent metathesis using Grubb's 2nd generation catalysis afforded the desired 7-membered backbone of the DHCCA analogue. Removal of the auxiliary via hydrolysis yielded the acid **138**, which was protected as the corresponding ethyl ester **139**. An Upjohn dihydroxylation using potassium osmate dihydrate resulted in production of both diastereomers of the desired *cis*-diol product, **140** and **141**. Separation of the diastereomers was not possible at this stage.

Following hydrolysis of the mixture of diastereomers **140** and **141** with LiOH, **143** and **144** were fed as a mixture to *B. ambifaria* BCC0203 Δ5912-14 mutant strain blocked in DHCCA biosynthesis and both enacyloxin analogues were purified by HPLC,

characterised by LC-MS and NMR spectroscopy to give **145** and **146** with the stereochemistry for each analogue undetermined.

To confirm the stereochemistry of each analogue, acetonide **142** and its diastereomer were synthesised and separated by silica column chromatography which yielded diastereomer **142** as a single product and the other as an inseparable mixture of diastereomers. Nuclear Overhauser Effect (NOE) NMR analysis revealed a correlation between H_A and H_B in compound **142** indicating an *anti*-relationship between the acid and acetonide (figure **3.4**).

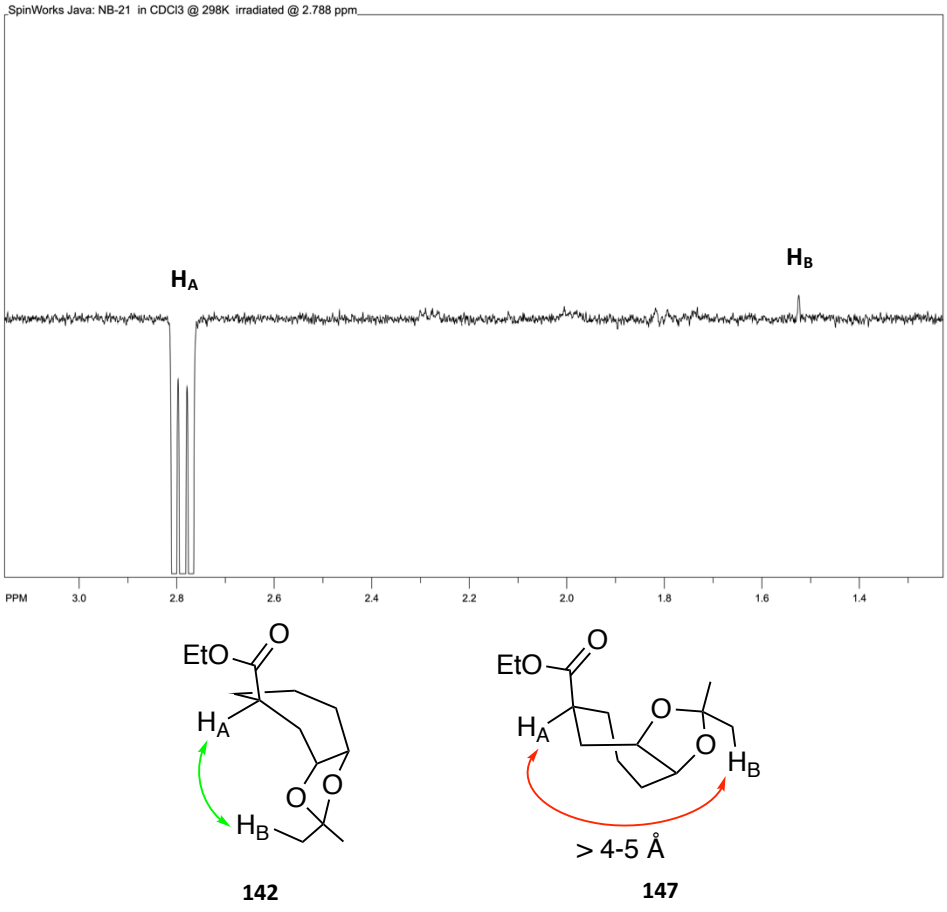

Figure 3.4 (above) NOE spectrum with irradiation of the proton at 2.79 ppm (H_A) causing a positive NOE correlation to the proton at 1.50 ppm (H_B). (below) configurations of the *anti*- and *syn*- diastereomers where the *anti*-configuration orientates the protons within a distance of each other to induce an NOE. The *syn*-configuration is unable to induce an NOE effect due to the >4-5 Å distance between the protons H_A and H_B.

Following stereochemical assignment of acetonide **142**, it was converted to the corresponding diol **143** and fed into the *B. ambifaria* BCC0203 Δ5912-14 mutant strain blocked in DHCCA biosynthesis to afford compound **145** of known

stereochemistry at a reduced titre compared to production of WT enacyloxin using this method. Comparison of ^{1}H NMR coupling constants to that of 6-membered ring containing compounds suggest the regiochemistry shown.

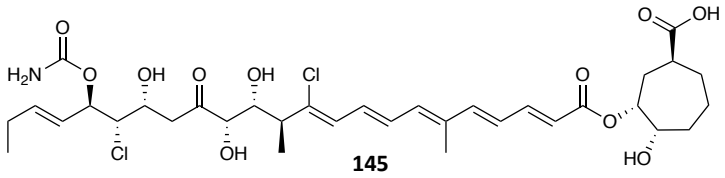

145

Figure 3.5 Structure of enacyloxin analogue **145** containing the 7-membered DHCCA ring with the *anti*-configuration isolated from feeding of compound **143** to the *B. ambifaria* BCC0203 Δ5912-14

HPLC comparison of the product mixture with analogue **145** of known stereochemistry allowed for stereochemical assignment of each product (figure **3.6** and **3.7**).

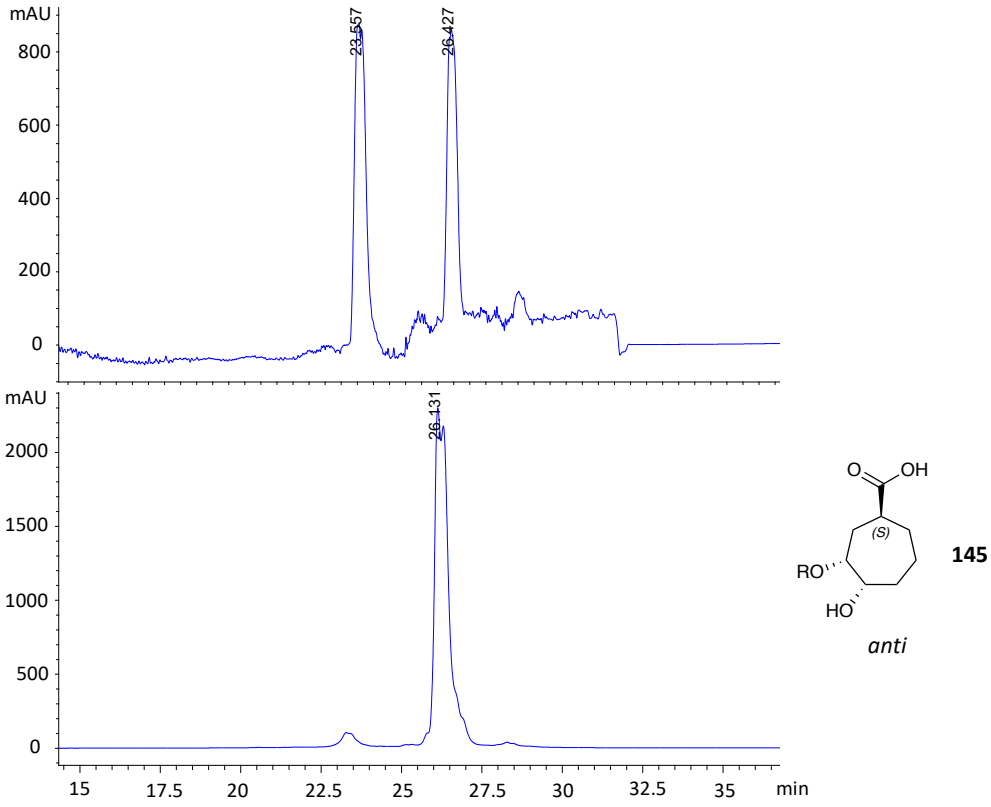

Figure 3.6 HPLC chromatograms at 360 nm from extracts of the *B. ambifaria* mutant blocked in DHCCA biosynthesis grown on BSM media supplemented with 7-membered DHCCA analogues **143** and **144**. (top) mixture of enacyloxin analogues with *syn*- and *anti*- relationships between the acid and diol. (bottom) enacyloxin analogue with *anti*-conformation. (R = enacyloxin backbone)

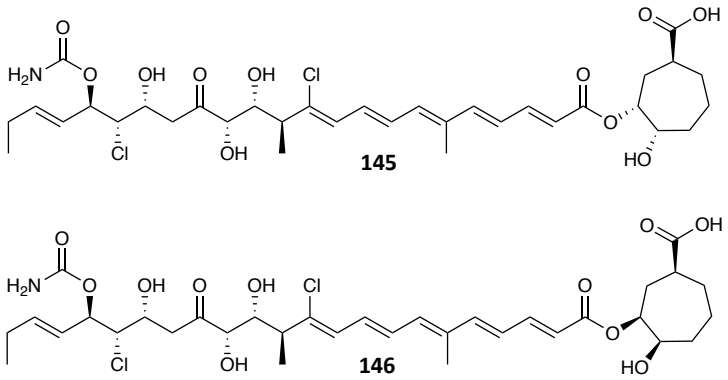

Figure 3.7 Separated products from feeding of diastereomeric mixture of **143** and **144** to *B. ambifaria* BCC0203 Δ5912-14 blocked in DHCCA biosynthesis. The stereochemistry for each product was determined by HPLC comparison of a single analogue with known stereochemistry to the mixture of analogues **145** and **146**.

3.1.1.3.2 Chemical synthesis of 7-membered trans-diol DHCCA analogues and attempted production of novel enacyloxin analogues

As incorporation of a 7-membered ring mimicking the natural DHHCA unit was successful, the relationship between the diols within this system was also investigated. The 7-membered DHCCA analogues containing a *trans*-diol relationship (**148** and **151**) were chemically synthesised and fed to *B. ambifaria* BCC0203 Δ5912-14, blocked in DHCCA biosynthesis (scheme **3.4**).

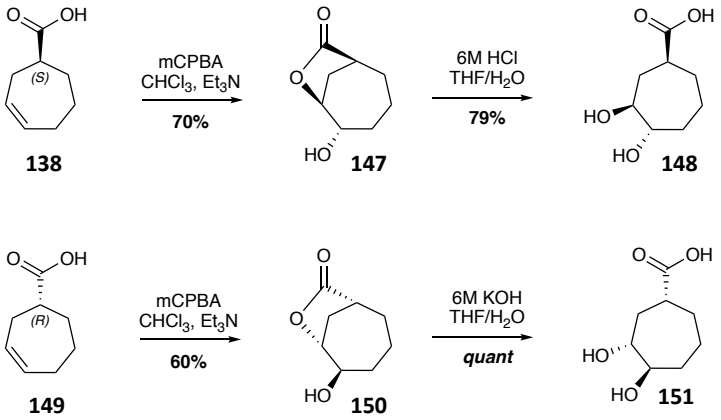

Scheme 3.4 Synthetic route for the preparation of 7-membered *trans*-diol DHCCA analogues to be used in the production of novel enacyloxin analogues. Compound **149** was prepared in the same manner as **138** with the (*S*)-oxazolidinone used as the Evan's auxiliary and the final step undertaken using KOH.

Addition of m-CPBA to the least hindered face of **138** afforded an epoxide which, upon nucleophilic attack of the acid, produced lactone **147**. Ring opening under acidic conditions afforded the desired *trans*-diol **148**. Enantiomer **151** was also synthesised

via the same route but using *S*-oxazolidinone as the Evans auxiliary in the initial step shown in scheme **3.3**. The final ring opening to afford **151** occurred under basic conditions (scheme **3.4**). Basic conditions were used as under acidic conditions, lactone ring opening was unsuccessful.

Both diols (**148** and **151**) were fed to *B. ambifaria* BCC0203 Δ5912-14, blocked in DHCCA biosynthesis, but only analogue **153** could be observed by LC-MS. Compound **148** was either not accepted by the *Bamb*_5915 condensation domain or was not able to enter the cells. Unfortunately, compound **153** appeared to have degraded upon purification.

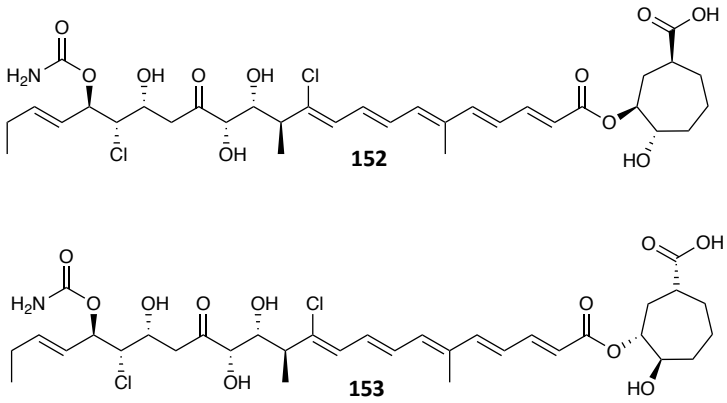

Figure 3.8 Structures of enacyloxin analogues containing the 7-membered DHCCA ring with *trans*-diol configurations proposed to be formed from the feeding of compounds **148** and **151** to *B. ambifaria* BCC0203 Δ5912-14.

Investigations into the 7-membered DHCCA ring system were not studied further as the expanded ring system does not appear to be key to antimicrobial activity (See section 4.1). A combination of the 7-membered DHCCA system along with other potent analogues may offer greater insights into the SAR but were not pursued further at this time.

3.1.1.4 Enacyloxin analogues with an alkyne linker for click chemistry.

3.1.1.4.1 Click chemistry as a means of producing a library of novel analogues

Chemical transformations are often sensitive to air and/or water, produce unwanted side products, require purification to isolate the desired product and have variable

yields. 'Click' chemistry describes versatile linking reactions that follow a general set of guidelines. They must be very high yielding with a wide substrate scope, require minimal or no purification and be easily performed with an insensitivity to external factors.[180–182] Sharpless and co-workers have identified four reaction categories that can be classified as 'click' reactions; cycloadditions, nucleophilic ring openings, non-aldol carbonyl chemistry and carbon-carbon multiple bond additions.[183] The most successful and widely used example is Huisgen's 1,3-dipolar cycloaddition of azides and alkynes to produce 1,2,3-triazoles (scheme **3.5**). This method was further optimised by Rostovtsev *et al* and Tornøe *et al* through the use of $Cu^{(I)}$ catalysis.[184,185] The exact mechanism is unclear however mechanistic studies have revealed a potential pathway.[181,186–189]

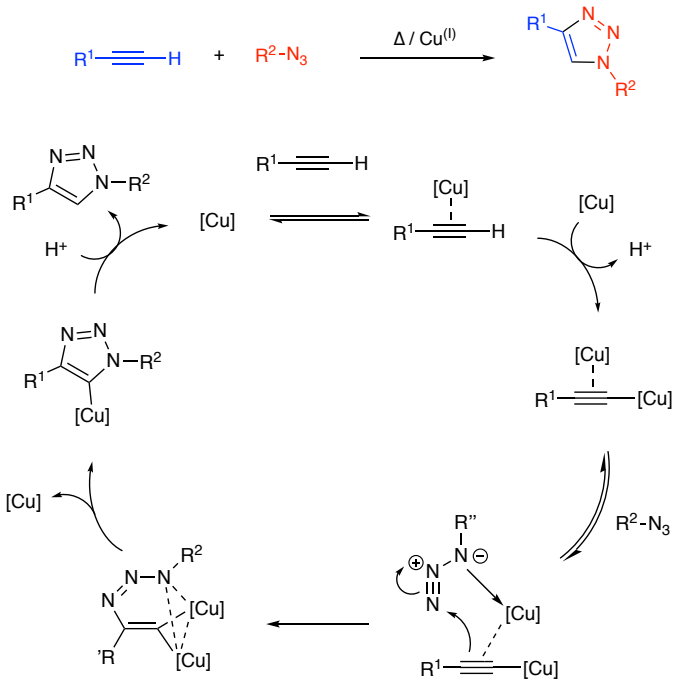

Scheme 3.5 General reaction scheme (above) and mechanism (below) for the 1,3-dipolar copper-cataylsed cycloaddition of azides and alkynes to produce a range 1,2,3-triazole products in a highly efficient manner. (scheme sourced from Worrell *et al*.)

Compounds containing 1,2,3-triazoles exhibit a range of biological activities including antimicrobial and anti-viral.[190–193] Copper-catalysed click reactions have been increasingly used in medical chemistry research due to the simplified approach to pharmacophore design. This method has led to the production of the β–lactamase inhibitor tazobactam **154**, the commercially available antiepileptic rufinamide, sold under the name Banzel **155** and other biologically active compounds.[194–196] Multiple

semi-synthetic vancomycin homodimers have also been produced with many exhibiting improved activity against resistant bacteria compared to the natural product (figure **3.9**).[197]

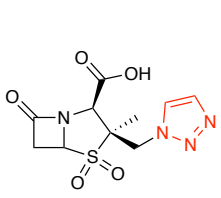

154

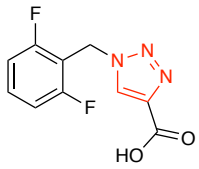

155

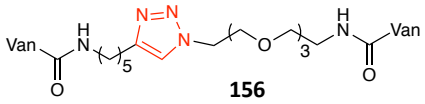

156

Compound	MIC / μg/ml VSEF	MRSA	VRE
Vancomycin	2.5	2.5	2.5
156	0.5	0.6	0.8

Figure 3.9 Structures of biologically active compounds tazobactam **154**, rufinamide **155** and a vancomycin homodimer **156** formed from copper catalysed click reactions (Van = Vancomycin, VSEF = vancomycin susceptible *Enterococcus faecalis*, VRE = vancomycin resistant *Enterococcus*)

Use of a 1,2,3-triazole linker provides a synthetic handle for the production of a range of analogues. A variety of natural product paulownin analogues were produced using a range of azides, to improve its' cytotoxicity (scheme **3.6**).[198]

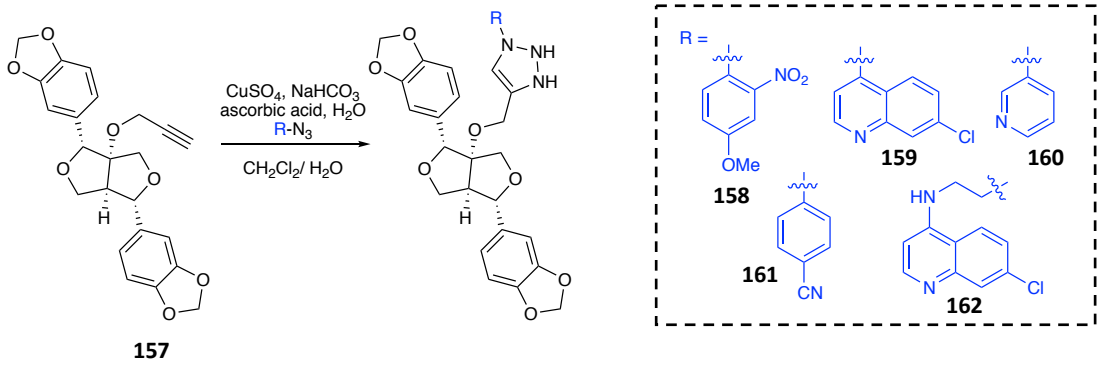

157

Scheme 3.6 Production of novel paulownin analogues using click chemistry between a propargylated paulownin derivative and a selection of azides. (scheme adapted from Pereira *et al.*)

There is therefore the potential to create novel compound libraries using this strategy for any substance harbouring the appropriate linkers. However, functionalisation of the secondary hydroxyl group on the DHCCA moiety has yet to be explored.

The crystal structure of EF-Tu bound enacyloxin IIa indicates a hydrogen bond between the DHCCA secondary hydroxyl group and tyrosine 160.[149] Depending on whether the hydroxyl group acts as the hydrogen bond acceptor or donator,

alkylation at this site may or may not inhibit binding. Introduction of a 1,2,3-triazole linker at this position offers a novel method of producing enacyloxin analogues, whilst combatting a property of enacyloxin currently hindering its' potential as a drug candidate - poor aqueous solubility - as triazoles are highly water soluble. We therefore proposed to isolate propargylated enacyloxin analogue **163** for use as a substrate in copper-catalysed click chemistry (scheme **3.7**).

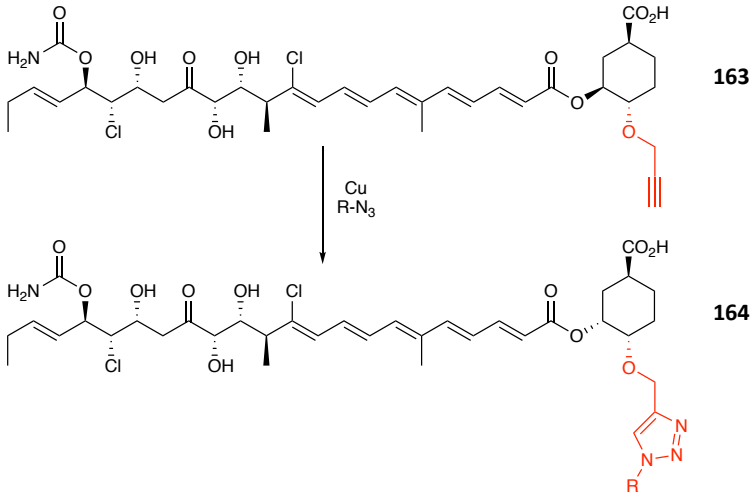

163

164

Scheme 3.7 Proposed use of 'click' chemistry to produce novel enacyloxin analogues harbouring a 1,2,3-triazole with variety of R groups

A variety of poly(ethylene) glycol (PEG) azides would act as suitable substrates for the required click reaction and could act as solubility tags on the natural product (figure **3.10**). PEG has been shown to improve pharmacological properties such as aqueous solubility whilst being non-toxic and Food and Drug Administration (FDA) approved.[199] The crystal structure shows that the DHCCA moiety resides at the end of the active site suggesting that there would be sufficient room for further functionalisation such as the use of PEG compounds with a range of chain lengths.

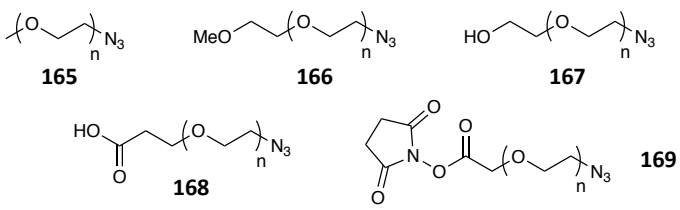

165 **166** **167** **168** **169**

Figure 3.10 Structures of PEG-azides to be used in copper-catalysed click reactions to improve the aqueous solubility of the enacyloxins

3.1.1.4.2 Synthesis of a propargylated DHCCA analogue

Synthesis of DHCCA analogue **178** used similar strategies to those used in the production of **148** and **151** (scheme **3.8**). The *R*-configured Evans' auxiliary was coupled to 6-hexanoic acid (**170**), followed by stereoselective allyation using ally bromide to afford the diene **172**. Grubbs metathesis afforded the 6-membered cyclic intermediate **173** which was hydrolysed to produce acid **174**. Production of lactone **175** was mediated by *m*-CPBA and addition of triethylamine. Lactone **175** is the key intermediate in the production of hydroxyl-functionalised enacyloxin analogues and until this point yields were excellent. Alkylation of the hydroxyl group was conducted by deprotonation with sodium hydride in DMF, followed by addition of propargyl bromide. This proceeded in a relatively poor yield due to issues associated with the work-up and purification. DMF was seen to be challenging to remove without also removing the desired alkylated product resulting in poor product isolation. Attempts to improve this yield are discussed in section **3.1.1.4.4**. Finally LiOH was used to hydrolyse the lactone and open the ring affording the alkylated DHCCA analogue **178** with a *trans*-hydroxyl group and alkyne ester. Attempts to epimerise the free hydroxyl under standard Mitsunobu conditions were unsuccessful. DHCCA analogue **178** was believed to be a suitable substrate since both *cis*- and *trans* DHCCA are accepted by the C-domain, and the resultant enacyloxin analogues have the same MIC against *A. baumannii.*

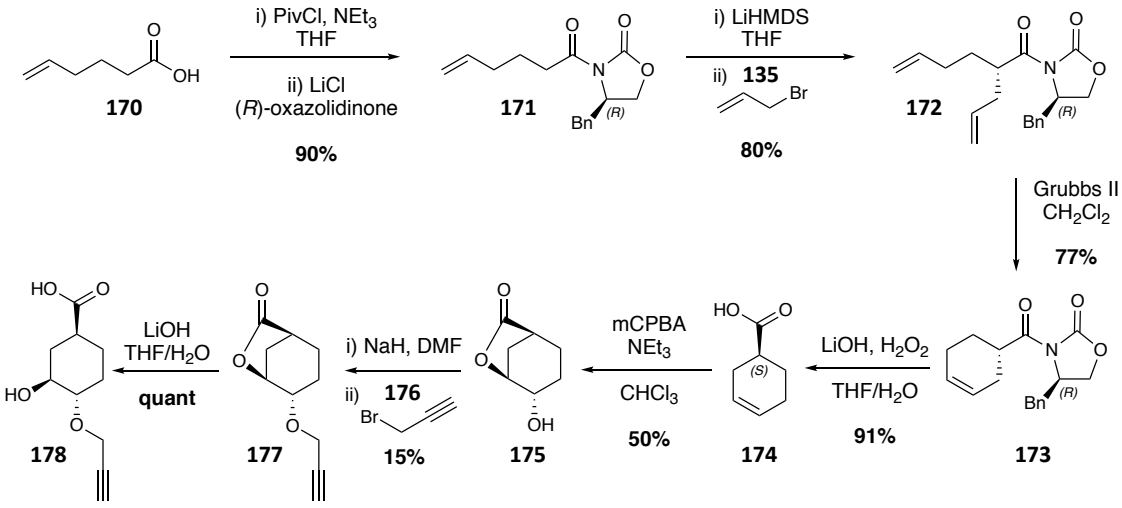

Scheme 3.8 Synthetic route for the preparation of DHCCA analogue **178**

3.1.1.4.3 Small scale feeding experiment using DHCCA analogue 178

Following chemical synthesis, **178** was fed on a small scale into *B. ambifaria* Δ5912-14 blocked in DHCCA biosynthesis. Following incubation, the BSM plates were extracted with ethyl acetate and analysed by UHPLC-HRMS. A peak in the LC-MS chromatogram with the correct molecular weight and isotopic pattern for **163** was observed indicates that the *bamb*_5915 condensation domain tolerates **178** (scheme **3.9**). Successful production of the enacyloxin analogue harbouring the desired propargyl ether, indicates that this could indeed be a viable new method of producing enacyloxin analogues utilising 'click' chemistry.

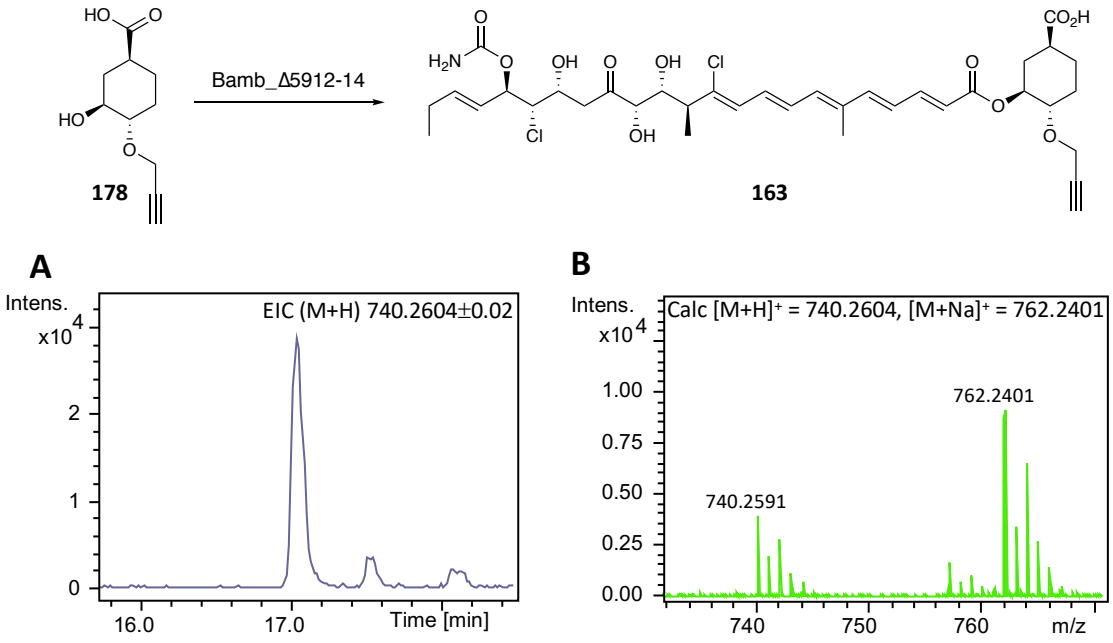

Scheme 3.9 Feeding of DHCCA analogue **178** to Bamb_Δ5912-14 blocked in DHCCA biosynthesis to produce the novel propargylated enacyloxin analogue **163**. (**A**) EIC for m/z = 740.2604 (corresponding to $[M+H]^+$ for **163**) from UHPLC-HRMS analysis of extracts of *B. ambifaria* Δ5912-14 supplemented with **178**. (**B**) HRMS data of species at 17 minutes

To determine the antimicrobial activity of **163,** and its subsequent use in a variety of 'click' reactions, a large scale feeding experiment was required followed by HPLC purification and spectroscopic analysis. The current synthetic procedure for the preparation of the DHCCA analogue **178** is limited by the low yields in the alkylation of **175.** To be a useful method of producing novel enacyloxin analogues a more efficient and cost effective synthesis would be required.

3.1.1.4.4 Attempts to optimise the alkylation of 175

Initial alkylation efforts utilised a procedure by Pereira *et al*[198] in which the alkylation of the more complex paulownin tertiary alcohol proceeded with a 91% yield. Addition of sodium hydride generates an alkoxide *in-situ* which reacts with the alkyl halide to afford the propargylated intermediate. Under these reaction conditions the alkylation of lactone **175** proceeded with a reproducible 15% yield. This was initially believed to be a result of the lactone ring opening in the presence of trace water in the anhydrous solvents and reagents. However, repetition of the reaction using freshly distilled DMF did not improve yields. Alkylations generally require aprotic solvents to prevent interactions with the alkoxide which slow the rate of reaction. The use of another aprotic solvent, THF, was investigated due to the potential reported instability of NaH/ DMF mixtures and to improve the reaction work-up conditions.[200] DMF causes difficulties in product extraction and the overall removal of the solvent is challenging. However, no alkylation was observed even using freshly distilled THF.

To conserve the valuable lactone intermediate **175** cyclohexanol was subsequently used as a mimic of **175** to continue to optimise the alkylation. Furthermore, the absence of the lactone moiety would establish whether this was the reason for the poor yields. Using cyclohexanol the reactions were repeated with freshly distilled DMF and THF separately (scheme **3.10**).

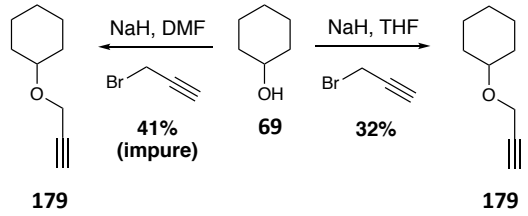

Scheme 3.10 Propargylation efforts using cyclohexanol and the solvents THF and DMF

Using THF the reaction proceeded with a 32% yield whereas in DMF the yield increased to 41%. However, NMR spectrometry revealed the presence of significant impurities after silica purification suggesting the actual yield was much lower. Propargyl bromide was substituted with 4-bromobut-1-yne, which is structurally

similar but has an additional carbon linker. The reactions were repeated as before with the new alkylating agent but neither reaction afforded any of the desired product (scheme **3.11**).

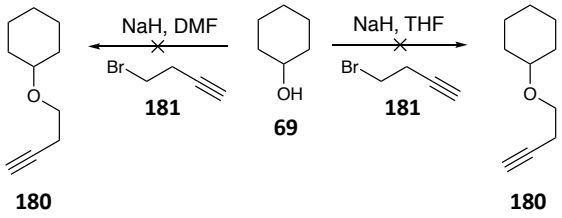

Scheme 3.11 Propargylation efforts using cyclohexanol and the solvents THF and DMF with the alkylating agent 4-bromobut-1-yne

With little success at improving the alkylation on a mimic a new approach was investigated. Conditions used by Wells *et al*[201] were used on lactone **175** due to a good substrate scope being reported, including examples with lactones and other labile functional groups. Treatment of **175** with dicobalt octacabonyl, propargyl alcohol and boron trifluoride diethyl etherate in DCM should afford a cobalt intermediate which undergoes decomplexation in the presence of ceric ammonium nitrate (CAN) (scheme **3.12**).

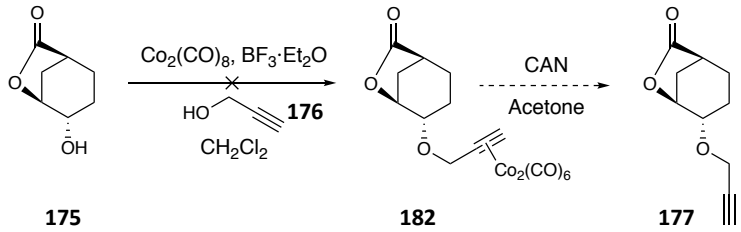

Scheme 3.12 Unsuccessful propargylation of lactone **175** attempt

Unfortunately, the cobalt intermediate could not be observed by TLC and the starting material was reisolated following work-up and purification. Due to time constraints no further optimisation efforts were possible. With little success at improving the alkylation, obtaining sufficient quantities of the DHCCA analogue required the use of the original alkylation method. To account for the poor alkylation yield, 2.5 g of **175** was used in the alkylation followed by base mediated ring opening to afford 325 mg of **178**.

Feeding of **178** to *B. ambifaria* BCC0203 Δ5912-14 blocked in DHCCA biosynthesis appeared to produce the desired enacyloxin analogue, as characteristic yellow streaks on the BSM plates were observed following incubation. Following extraction of the plates with ethyl acetate the production of **163** was confirmed by UHPLC-HRMS analysis of the crude extract but low production levels were observed (figure **3.11**).

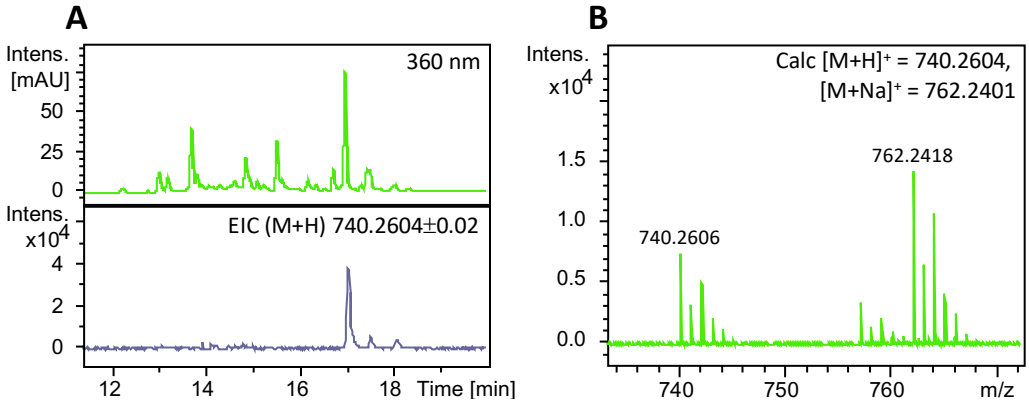

Figure 3.11 (**A - top**) UV chromatogram at 360 nm of ethyl acetate extracts of the crude product from *B. ambifaria* BCC0203 Δ5912-14 blocked in DHCCA biosynthesis supplemented with **178**, (**A-bottom**) EIC for m/z = 740.2604 (corresponding to $[M+H]^+$ for **163**) from UHPLC-HRMS (**B**) HRMS data of species at 17 minutes.

The crude extract was HPLC purified affording 0.6 mg of material. UHPLC-HRMS analysis of the purified product indicated the presence of impurities (figure **3.12**) which was confirmed by NMR spectrometry.

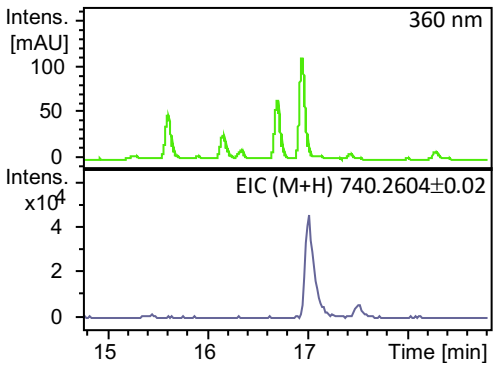

Figure 3.12 (**Top**) UV chromatogram at 360 nm of HPLC purified crude extracts from feeding of **178** to *B. ambifaria* Δ5912-14 blocked in DHCCA biosynthesis, (**bottom**) EIC for m/z = 740.2604 corresponding to $[M+H]^+$ for **163** from UHPLC-HRMS

The unusually low production levels suggests that either DHCCA analogue **178** is not accepted as well as initially thought by the *bamb*_5915 condensation domain, or that experimental errors occurred during the feeding process. To assess whether this is still a viable method of functionalising enacyloxin analogues, the feeding experiment should be repeated. However, the required re-synthesis of DHCCA analogue **178** was not possible within this project due to time constraints.

3.2 Conclusions

This chapter has explored modifications to the DHCCA moiety of enacyloxin IIa.

The Bamb_5915 condensation domain has been shown to accept a linear DHCCA moiety to produce **132** as well as 7-membered DHCCA diastereomeric analogues **143** and **144** to give **145** and **146**. However, analogues **148** and 1**51,** containing a *trans*-diol relationship, were not accepted.

A potential new method for the production of novel enacyloxin analogues through the use of 'click' chemistry has also been described. This has also presented an opportunity to modify the pharmacological properties of the enacyloxins helping them to become more amenable drug candidates. A DHCCA analogue harbouring a propargyl group tethered to the previously non-functionalised secondary hydroxyl was chemically synthesised. The overall synthesis contained a poor yielding key alkylation step, which despite optimisation efforts was unable to be resolved. Small scale feeding of **178** to *B. ambifaria* BCC0203 Δ5912-14 blocked in DHCCA biosynthesis produced the desired enacyloxin analogue which could be observed by UHPLC-HRMS analysis. Large scale feeding efforts struggled to produce the desired analogue in sufficient quantities and purity for antimicrobial activity assays. This also meant that 'click' reactions were not possible.

Propargylation of the secondary hydroxyl still needs to be optimised on cyclohexanol to reduce wastage of precious lactone material. Future efforts may use alternate bases such as ^{n}BuLi as seen by Wardrop and Fritz (scheme **3.13**).[202]

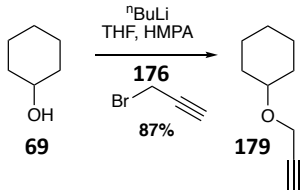

Scheme3.13 Propargylation of cyclohexanol using ^{n}BuLi and propargyl bromide mediated by HMPA

They also make use of hexamethylphosphoamide (HMPA) as a means to accelerate the S_N2 reaction of the alkoxide with propargyl bromide. HMPA could be used to try and increase the rate of reaction of the current propargylation used. If the alkylation can be optimised an alternative synthetic route may also alleviate the potential issue of the labile lactone. Under milder reaction conditions, *tert*-butyldimethyl silyl (TBS) protection of the secondary hydroxyl on **175** was achieved with a moderate yield (scheme **3.14**).

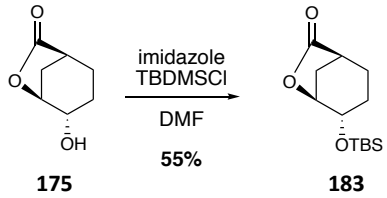

Scheme 3.14 Synthetic route for the silyl protection of the secondary alcohol.

The lactone could be opened using MeOH to form the methyl ester followed by selective protection of the alcohol using benzoyl chloride. Removal of the TBS group, using tetrabutylammonium fluoride (TBAF), would afford the free hydroxyl which, if a suitable method is found, is available for propargylation. Deprotection of the remaining groups using a mild base would produce the desired DHCCA analogue.

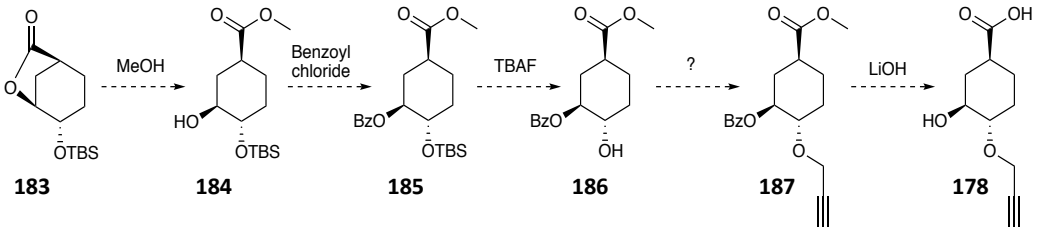

Scheme 3.15 Proposed alternate synthetic route for the production of **178** using protecting groups to facilitate the selective propargylation of the desired secondary alcohol. (? Indicates the unknown method of alkylation)

Protections and deprotections are usually high yielding therefore if the TBS protection and alkylation can be improved, this may prove to be a more suitable route with an improved overall yield compared to the currently used procedure (scheme **3.15**). Unfortunately time constraints meant this route was not fully explored.

If the propargylation step can be improved or the alternate synthetic route proves to be viable, there is the potential for the creation of a new library of enacyloxin analogues with improved solubilities, through the introduction of various PEG groups. Using previously produced mutants, which are both blocked in DHCCA biosynthesis and contain gene deletions in genes encoding tailoring enzymes, presents an opportunity to also functionalise previously produced analogues. This combined approach could result in analogues with improved activity, stability and solubility.

Chapter 4 - Results and Discussion III

4.1 Biological evaluation of compounds

4.1.1 MIC against *A. baumannii*

The activity of each compound was determined using a MIC assay as described in section **6.2.16**. Serial 2-fold dilutions of enacyloxin analogues in Mueller Hinton (MH) broth were prepared in a 96-well plate to which overnight cultures of *A. baumannii* at a specific cell density are added and incubated overnight. The lowest concentration at which bacterial growth is inhibited is determined to be the MIC value.

4.1.1.1 Brominated analogues

Di-brominated **87** has a two-fold increase in activity compared to enacyloxin (MIC = 2 µg/mL) whereas mono-brominated **85** has an 8-fold reduction in activity, suggesting halogenation at C-18 is important for antimicrobial activity. The activity of **86** is the same as enacyloxin IIa, suggesting the nature of the halogen at C-11 is not as important.

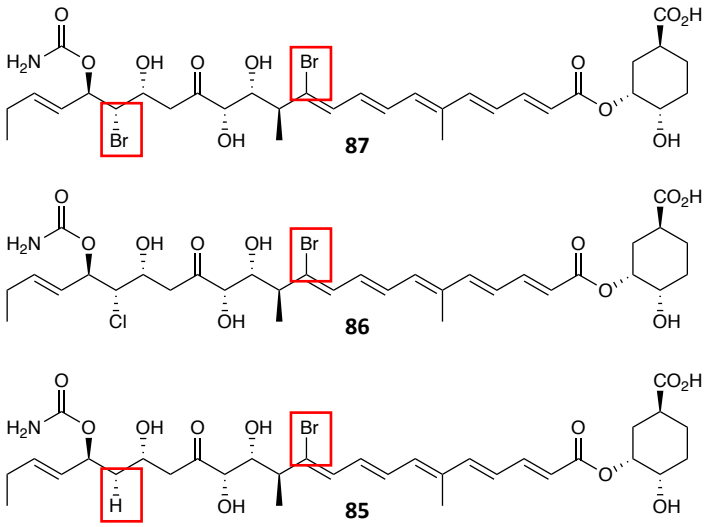

87 **86** **85**

Figure 4.1 Enacyloxin analogues isolated from *B. ambifaria* BCC0203 when bromide supplemented BSM media was used

This general trend is also observed when comparing brominated analogues isolated from *B. ambifaria* deletion mutants (figure **4.2**).

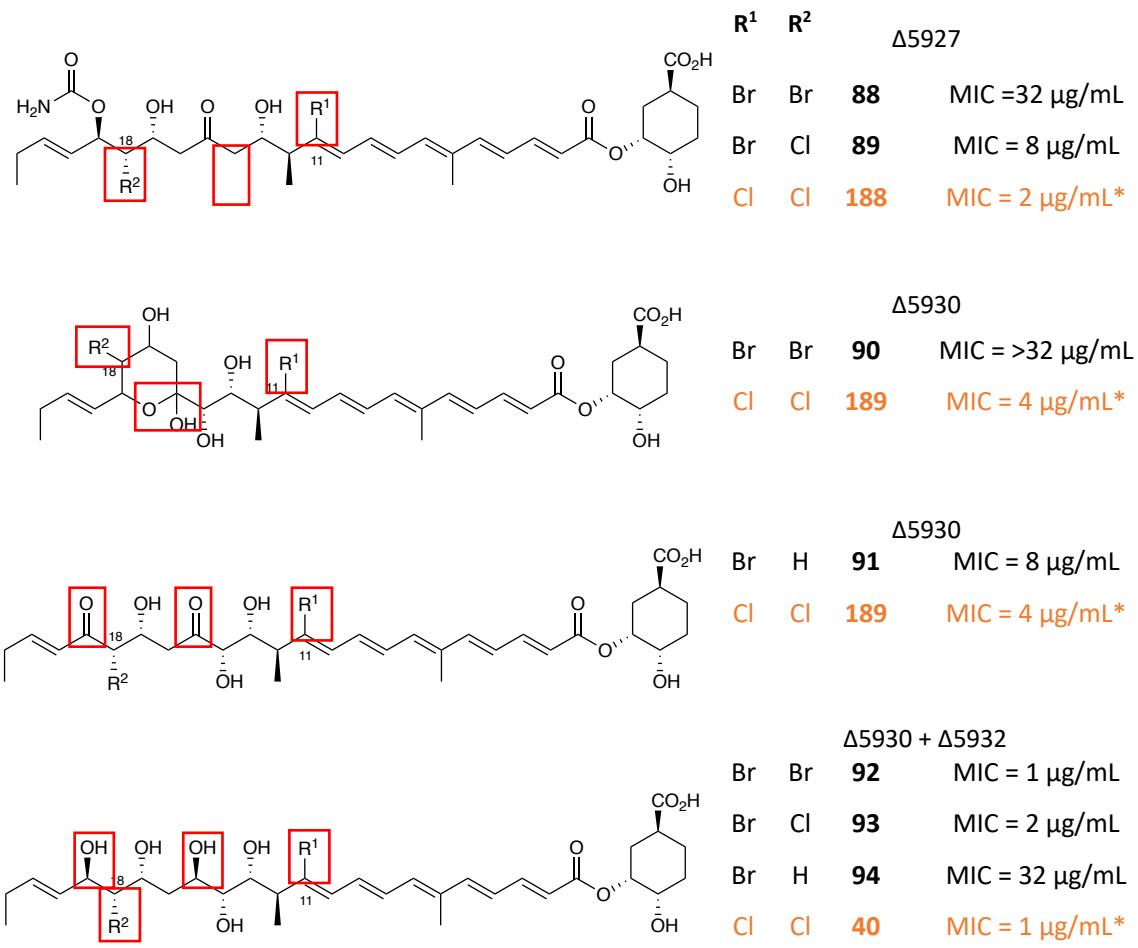

Figure 4.2 Isolated enacyloxin analogues from bromide supplemented media from mutated strains of *B. ambifaria* BCC0203 with corresponding MIC activity data. *For reference the MIC for the compounds isolated from the mutants without bromide supplementation not determined in this study are shown and highlighted orange.

Compounds without a halide present at C-18 have increased MIC against *A. baumannii* as seen in compounds **91** and **94**. A decrease in activity could also be seen when bromine was present at C-18 in the place of chlorine in analogues **88** and **90** isolated from *B. ambifaria* BCC0203_Δ5927 and Δ5930. This may be due to the disruption of the region around C-19 and therefore the binding within the active site. The replacement of chlorine at C-11 with bromine in all analogues results in a reduction or no change in activity except for **92**, suggesting that chlorination at this site may be important for antimicrobial activity. The one analogue seen to have an increased activity compared to the chlorinated WT was di-brominated analogue **92** isolated from *B. ambifaria* BCC0203_Δ5930 + Δ5932. A decrease in activity was seen

in analogue **94** when hydrogen was present at C-18 however, the activity of compound **93** remained the same as enacyloxin IIa when chlorine was present. This indicates that even though the interactions about C-19 are being interrupted the presence of bromine has a beneficial effect on activity. This is shown by compound **92** as the presence of bromine in both C-18 and C-11 causes a two-fold increase in activity.

From the crystal structure of enacyloxin IIa bound to *E.coli* EF-Tu (figure **4.3**),[149] key polar interactions can be used to rationalise the observed MIC data against *A. baumannii*. Specifically Gly386 appears to be important for halide binding, which is confirmed by the reduction in activity for analogues without a halide present at C-18. Bromination at C-18 may also affect interactions with Gly386 and nearby interactions due to the increase in size compared to chlorine. Decarbamoylation in **90** and **91** causes a notable reduction in activity, highlighting the importance of the polar contacts made with Ala96, Val125 and Gly126 but their exact role is still uncertain. Polar contacts cannot be seen between EF-Tu and the halide at C-11. However, in compound **89** when bromine is present there is a 4-fold reduction in activity compared to the chlorinated natural product despite there being no clear observable interaction causing this. This may be due to the increased size of bromine and the resultant steric hindrance caused within the active site.

X-ray crystallography of EF-Tu bound to analogues with improved, or reduced activity than enacyloxin IIa such as **92** and **88** may provide a more comprehensive understanding of the role of halogenation in enacyloxin activity. Not all changes in activity reflect what we would expect based on the crystal structure suggesting that conformation changes may occur, or that certain modifications result in greater cellular uptake, leading to an increased activity. It is known that the antibiotic kirromycin, which is structurally unrelated to enacyloxin IIa, binds to EF-Tu suggesting there may be some flexibility within the binding site. This flexibility may account for the unexpected activity data based upon the solved crystal structure.

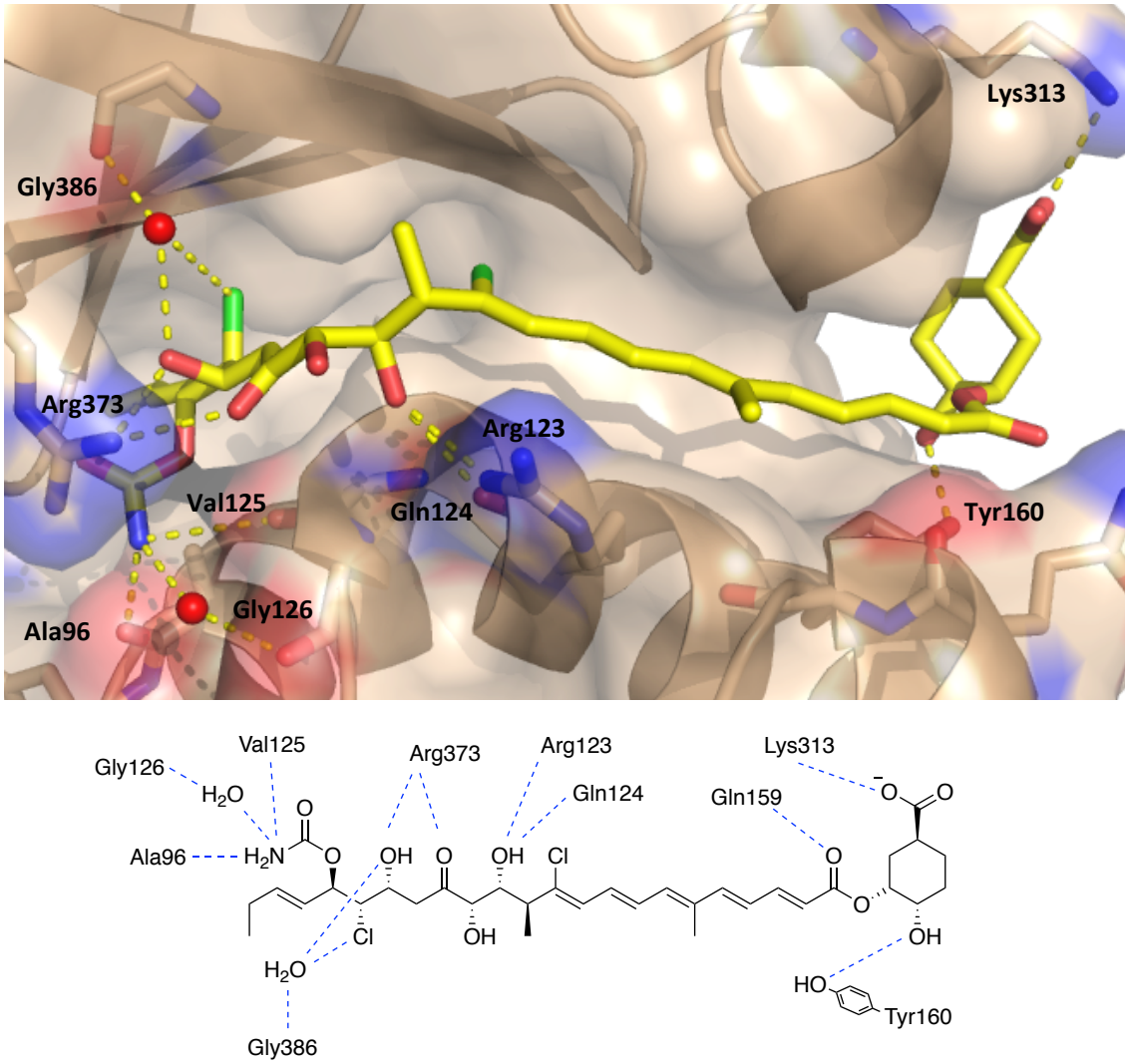

Figure 4.3 The solved crystal structure and polar contacts of enacyloxin IIa bound to EF-Tu.

Although preparation of brominated enacyloxin analogues initially appeared promising, a significant and consistent increase in activity against *A. baumannii* was not evident, so other avenues were explored to create analogues with improved activity.

4.1.1.2 Enacyloxin analogues containing chemically synthesised DHCCA analogues

The activity of **132**, containing a linear DHCCA analogue was determined as described in section **6.2.16** and the MIC value was >32 µg/mL. This suggests that, as seen previously, the cyclic DHCCA structure is important for antimicrobial activity. The lack of rigidity is likely to interfere with the polar contacts made with Lys313 and Tyr160

residues in the active site, resulting in a drop off in antimicrobial activity. Enacyloxin analogues with other linear DHCCA moieties were not therefore investigated further.

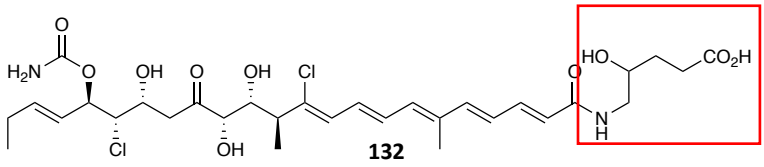

Figure 4.4 Enacyloxin analogues isolated from the feeding of **131** to *B. ambifaria* BCC0203 Δ5912-14 blocked in (DHCCA biosynthesis)

Determining the MIC of **145** and **146**, containing diasteriotopic 7-membered ring analogues showed the *anti*-configured diastereomer **145** (2 μg/ml) was twice as active as the corresponding *syn*-analogue **146** (4 μg/ml). Interestingly, **145** has the same MIC as enacyloxin IIa **1** (2 μg/ml) which also has an *anti*-conformation suggesting the increased ring size was not beneficial but the conformational relationship between the acid and diol is important in maintaining activity, and is an important factor to consider when designing future novel analogues.

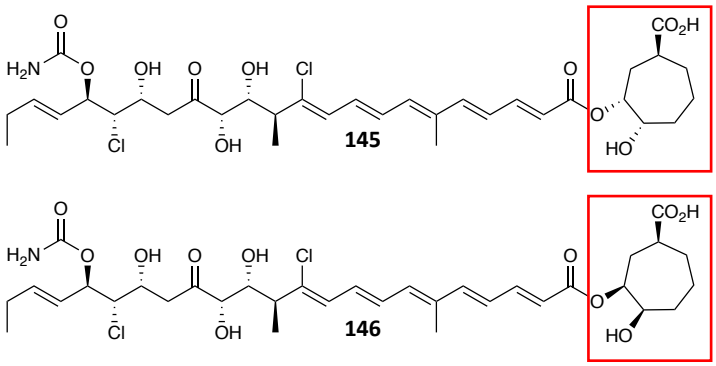

Figure 4.5 Enacyloxin analogues harbouring a 7-membered DHCCA ring produced from the feeding of **143** and **144** to *B. ambifaria* BCC0203 Δ5912-14

4.1.2 *In vivo* toxicity and efficacy investigations of enacyloxin IIa and produced analogues

4.1.2.1 Production of enacyloxin analogues for *in vivo* testing

In this and previous work a broad range of enacyloxin analogues have been produced, with an array of antimicrobial activity against *A. baumannii*, with some exhibiting a higher potency than enacyloxin IIa. High potency is only one of many factors to be considered when developing a novel pharmaceutical agent. In

collaboration with Professor Jian Li at Monash University, Australia, three target molecules were produced on scale for studies within mouse models, with the aim to gain an insight into their mammalian toxicity and efficacy (figure **4.6**). These compounds were selected as they represent the most potent compounds produced to date. Enacyloxin IIa was also used as it provides a good point of reference for the mutant analogues to be compared.

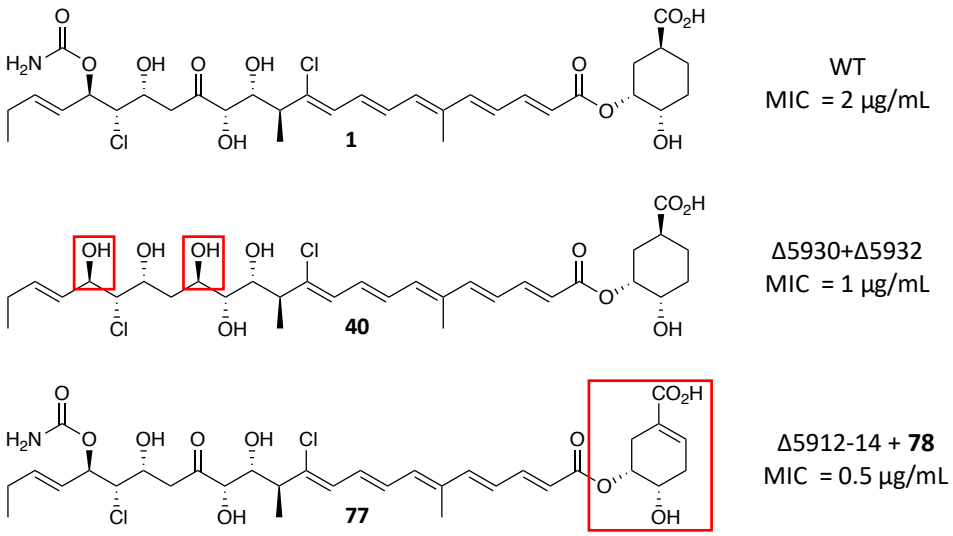

Figure 4.6 Enacyloxin analogues used for *in vivo* studies in collaboration with Professor Jian Li at Monash University.

Enacyloxin IIa, **40** and **70** were directly isolated from wild-type *B. ambifaria* BCC0203 and *B. ambifaria* BCC0203 Δ5930 + Δ5932 respectively. **40**, was isolated as described in section **6.2.13**. The structure of the products was confirmed by NMR spectrometry and MS.

4.1.2.2 *In vivo* investigations

In vivo toxicity and efficacy data were acquired by Professor Jian Li at Monash University.

Colistin (**190**), also known as polymyxin E, was used as a commercially available standard to compare efficacy data from *in vivo* studies.

Colistin is currently used as a last-line antibiotic in the clinical treatment of antibiotic resistant Gram-negative bacteria such as *A. baumannii* and *Pseudomonas aeruginosa* both of which are classified by the WHO as critical on the priority pathogens list requiring the production of new antibiotics.[203–205] The use of colistin has led to the emergence of resistance strains seen to be a critical issue requiring urgent attention. Colistin therefore is an ideal standard for comparison to enacyloxin in *in vivo* studies.

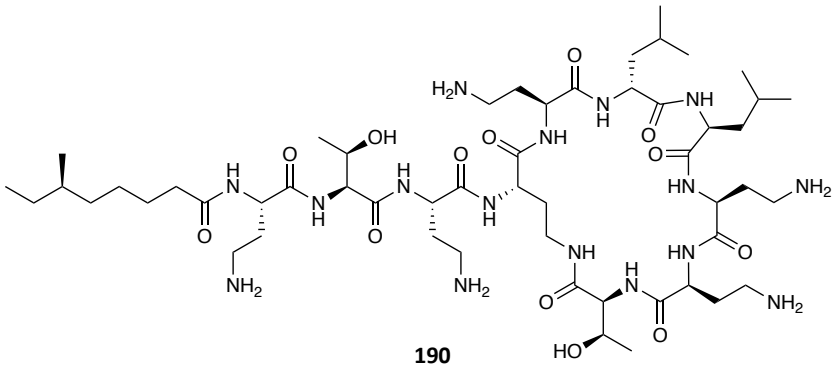

190

Figure 4.7 Chemical structure of colistin (polymyxin E) known to be active against *A. baumannii* and *P. aeruginosa*

Both intraperitoneal (IP) and blood infection models in mice were investigated in triplicate from IP administration of *A .baumanniii* DSM25645. Control points were taken upon manifestation of infection and after 4 hours with no antibiotic administered. The *in vivo* efficacy of each compound was measured after 4 hours (figure **4.8**).

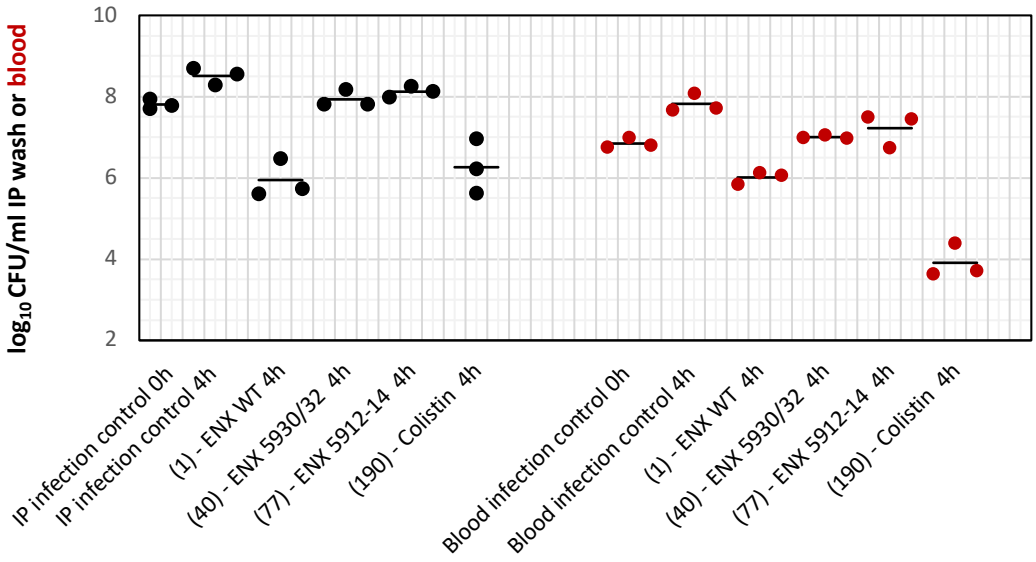

Figure 4.8 *In vivo* efficacy of enacyloxin analogues by intraperitoneal (IP) administration against *A. baumannii* DSM25645 in mouse IP and blood with a dosage of 5 mg/kg (ENX = enacyloxin).

Initial investigations suggest that wild-type enacyloxin IIa **1** has an equal if not improved effect on mouse IP infection after 4 hours compared to colistin. Unexpectedly however compounds **40** and **77** that have previously shown greater activity than enacyloxin IIa appear to have a lower IP efficacy than enacyloxin IIa and colistin within the mouse model. They do demonstrate a beneficial effect compared to the negative control after 4 hrs but not significant enough to be a competitor to the commercially available colistin. This effect is also reflected within the blood infection models. However, colistin has a much greater efficacy than all three test compounds. This unexpected lower activity of **40** and **77** compared to enacyloxin IIa could be a result of compound instability which may have been affected by the long distance shipping to Australia.

Despite the surprising lack of notable activity for the most potent enacyloxin analogue to date (**77**), these results are encouraging for further enacyloxin research. Colistin treatment can cause a range of side effects including nephrotoxicity and neurotoxicity and has only returned to clinical use due to attempts to combat the growing threat of MDR pathogens.[206] Enacyloxin is seen to mirror the efficacy of colistin in IP infections and shows a positive effect in blood infection. Importantly none of the analogues tested exhibited any obvious toxicity effects on the mice,

however current enacyloxin treatment side-effects are unknown and require further studies to determine. If they were to exhibit less toxic side-effects than current colistin treatment there is potential for enacyloxins to be novel commercially available pharmaceutical to combat AMR, specifically *A. baumannii* infections.

4.1.3 Enacyloxin and analogue binding to the *A. baumannii* EF-Tu-GDPNP complex

Difficulties with the production of the desired enacyloxin analogue **163** in sufficient quantities and purity meant that activity data against *A. baumannii* could not be obtained. Instead, through a collaboration with Professor Neil Oldham at the University of Nottingham, native mass spectrometry was used to investigate binding to EF-Tu.

Enacyloxin activity is a result of binding to EF-Tu•GTP which prevents bacterial protein synthesis as described in section **1.5.1**. Strong binding should result in an enacyloxin:EF-Tu complex which can be detected by mass spectrometry. Enacyloxin IIa **1** was produced and purified as previously reported[162] and sent to the Oldham lab at Nottingham University for native mass spectrometry binding studies. Initial data indicated that enacyloxin IIa preferentially binds to the EF-Tu•GDPNP complex (section **1.5.1**) compared to EF-Tu•GDP which was expected, given the known mode of action (figure **4.9**).

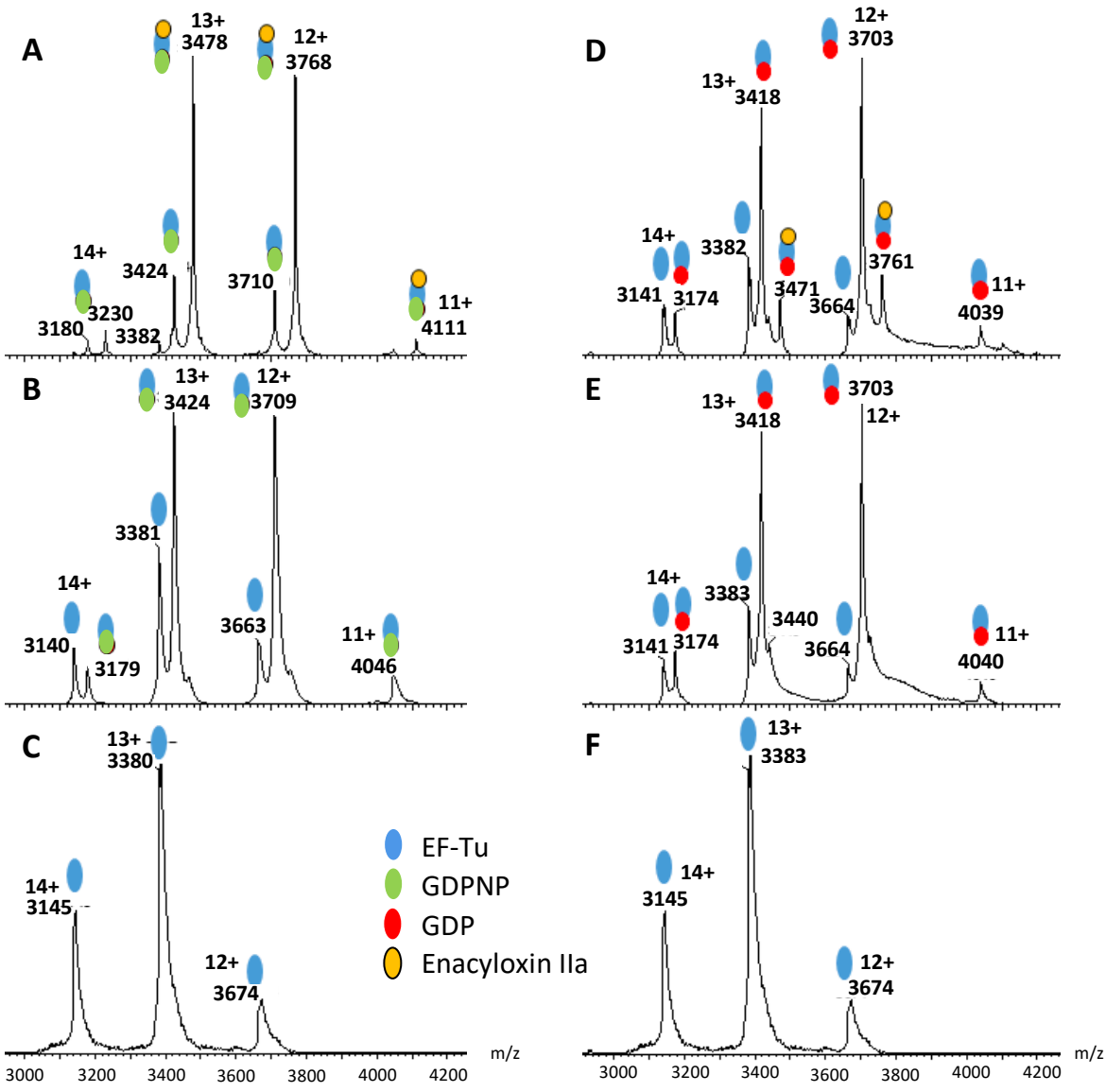

Figure 4.9 ESI mass spectra of *E. coli* EF-Tu sprayed from ammonium acetate showing preferential binding of enacyloxin IIa (5 µM) to the EF-Tu•GDPNP complex (**A**) compared to the EF-Tu•GDP complex (**D**). Charge states of each species are shown above the m/z values. Figure provided by Professor Neil J. Oldham (University of Nottingham).

Upon enacyloxin IIa addition to the EF-Tu•GDPNP complex the MS shows the appearance of high intensity peaks at 4111, 3768 and 3478 m/z indicative of enacyloxin binding. However when enacyloxin IIa is added to the EF-Tu•GDP complex the peaks indicative of enacyloxin binding are of very low intensity with high intensity peaks for the non-enacyloxin bound EF-Tu•GDPNP complex.

To confirm whether a strong binding affinity to the EF-Tu•GDPNP complex correlates to observed antimicrobial activity, a selection of analogues with a variety of MICs

against *A. baumannii* were produced and sent to Nottingham for native mass spectrometry studies. These included, enacyloxin IIa **1** (MIC = 2 µg/ml) and analogues isolated from strains containing the gene deletions; Δ5930/31 **191** (MIC = 32 µg/ml), Δ5930/32 **40** (MIC = 1 µg/ml), Δ5927-32 **39** (MIC = >64 µg/ml) and Δ5912-14 + DHCCA analogue (**78) 77** (MIC = 0.5 µg/ml) (figure **4.10**).

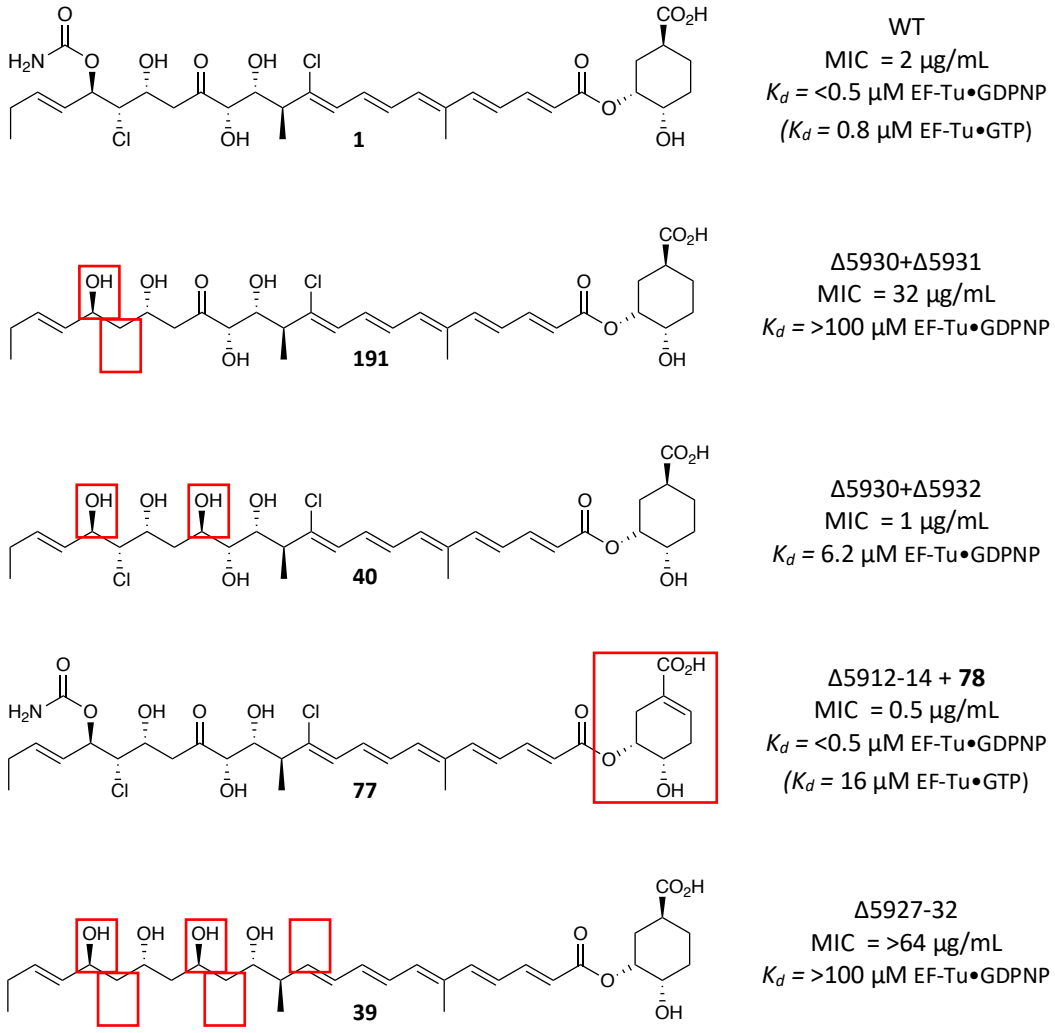

Figure 4.10 Enacyloxin analogues selected for native mass spectrometry studies at the University of Nottingham. Antimicrobial activities against *A. baumannii* are provided alongside the binding affinities for EF-Tu•GDPNP. (Values in brackets correspond to binding to EF-Tu•GDP when binding to EF-Tu•GDPNP was below <0.5 µM.)

Preliminary data regarding the enacyloxin mutant analogues reveals some interesting insights. Both analogues, from the mutant strains *B. ambifaria* BCC0203 Δ5927-32 (**39**) and Δ5930/31 (**191**), show very low binding affinities (>100 µM) to the

EF-Tu•GDPNP complex. The compounds have MIC values of >64 and 32 μg/mL respectively and are considered to have poor antimicrobial activity. Analogues from strains *B. ambifaria* BCC0203 Δ5930/32 (**40**) and Δ5912-14 + DHCCA analogue (**78**) (**77**) have MIC values of 1 and 0.5 μg/mL. Both analogues are more active than enacyloxin IIa (2 μg/mL). These results suggest a strong correlation between binding to the EF-Tu•GDPNP complex and antimicrobial activity. The only anomaly was compound **40**, which lacks the carbamoyl group and has a hydroxyl group in place of a keto group at C-15. This analogue has a weaker binding affinity (6.2 μM) compared to the natural product (<0.5 μM) despite having a lower MIC of 1 μg/mL. This may be due to the absence of the amino group present in the carbamoyl moiety which is known to bind to the active site.

4.1.3.1 Activity assessment of crude enacyloxin analogues

Native mass spectrometry could be used to obtain preliminary binding data from crude extraction mixtures from single plate extractions containing enacyloxin analogues. If successful, this would remove the need for laborious and time-consuming large scale feeding and purification processes, helping to streamline the drug-discovery process.

As large scale production of **163** was unsuccessful, the use of the crude extract from the small scale feeding experiment in section **3.1.1.4.3** was used in native mass spectrometry investigations. Crude enacyloxin IIa was also produced and sent to Nottingham for comparison. Binding of crude samples have initially suggested that enacyloxin IIa binds strongly with the EF-Tu•GDPNP complex, however the binding affinity of the propargylated analogue is less clear. The EF-Tu•GDPNP complex bound to the propargylated DHCCA analogue can be observed in the native MS alongside a fragment with the correct mass and isotopic distribution of the propargylated enacyloxin analogue **163** (figure **4.11**). The binding affinity of this analogue is still to be determined with further experiments required to fully understand how successful this method may be in predicting the viability of future analogues.

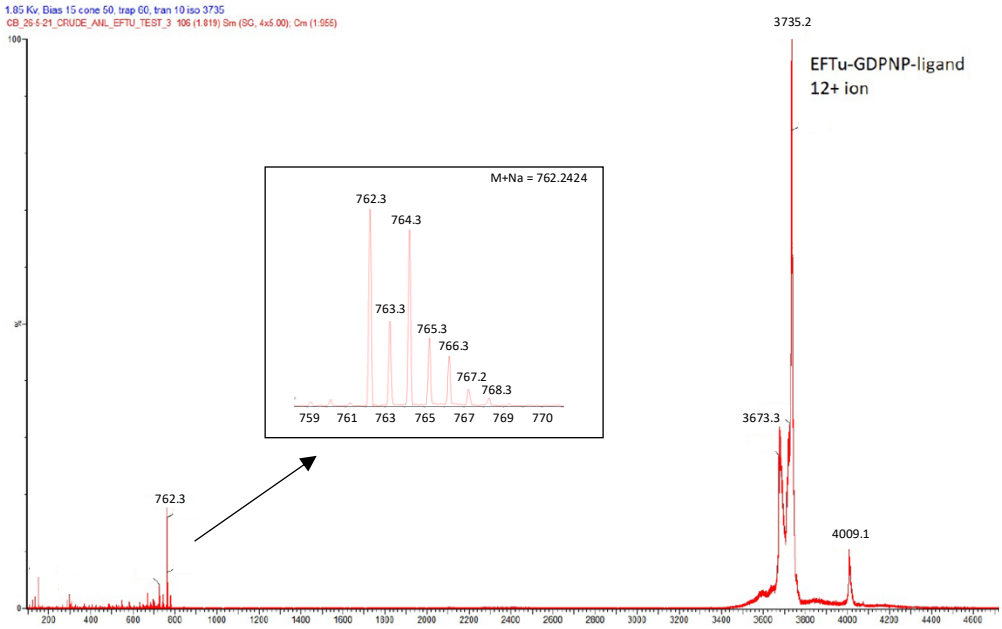

Figure 4.11 ESI mass spectrum of the 12+ charge state (*m/z* = 3735.2) of the EF-Tu•GDPNP complex. Bound to enacyloxin analogue **163**, following isolation using the quadrupole. Activation of this complex results in ejection of the enacyloxin analogue **163**, which can be observed at *m/z* = 762.3 and displays the expected isotopic distribution (inset). Figure provided by Professor Neil J. Oldham (University of Nottingham).

4.2 Conclusions

Several different methods have been used to investigate the bioactivity of enacyloxin and analogues.

Both di-brominated compounds **87** and **92** were two-fold more active than enacyloxin IIa. However, not all brominated analogues had an increased activity when compared to their chlorinated equivalent. MIC comparison of **85**, **91** and **94**, containing only halogenation at C-11 revealed that the second halogenation event at C-18 is essential for activity. Halogenation may therefore result in changes to cell permeability accounting for the changes in the observed antimicrobial activities. Therefore, whilst the production of brominated analogues is possible, further understanding of the SAR and effect on cell permeability is required to produce more potent analogues.

The high MIC of analogue **132,** containing a linear DHCCA analogue, confirmed that the ring is essential for activity. Comparing the MIC of analogues containing DHCCA analogues with 7-membered rings (**145** and **146**) showed that an *anti*-relationship between the carboxylic acid and diol was more beneficial compared to *cis*. However, neither analogues had an increased potency in comparison to the natural product, suggesting that an increased ring size was not beneficial. These results may be due to the additional degrees of rotational freedom caused by the disruption of the cyclic DHCCA moiety and increased ring size. As the rotational freedom increases, the entropic penalty associated with binding also increases accounting for the reduction in antimicrobial activity compared to analogues with more rigid DHCCA moieties.

In vivo testing of promising analogues demonstrated IP infection control of *A. baumannii* in a mouse model. However, only enacyloxin IIa proved to be as effective as the clinical standard colistin. Blood infection control of all analogues was less effective compared to colistin but some activity was observed. This suggests that enacyloxins have potential clinical applications, especially given that no obvious toxicity effects were observed.

In collaboration with Neil Oldham at the University of Nottingham, native mass spectrometry was used to determine whether binding affinity of the enacyloxins to the EF-Tu•GDPNP complex correlated with antimicrobial activity. A positive correlation was seen for purified enacyloxin IIa and a selection of purified analogues. As production of these compound required a series of time-consuming steps, it was postulated that the use of crude extracts could also be used to optimise drug discovery efforts. Crude enacyloxin IIa and propargylated analogue **163** with an unknown activity were sent to Nottingham for native mass spectrometry studies and preliminary results are promising. If successful, a series of crude analogue extracts with known activities could also be sent and used to probe the reliability of this method for the prediction of the antimicrobial activities of novel analogues using mass spectrometry.

Chapter 5 - Conclusions and Future Work

This project set out to further expand the library of enacyloxin analogues through manipulations of the biosynthetic pathway. In doing so we hoped to have a greater understanding of the SAR in order to aid the future design of novel analogues.

Firstly modifications to the polyol region were explored, through probing the substrate tolerance of the two halogenase enzymes involved in biosynthesis. Substitution of the halide source in the production media afforded a variety of brominated enacyloxin analogues in both wild-type and mutant strains. Bromination of C-11 by the flavin-dependant halogenase occurred in all analogues, whereas bromination at C-18 by the Fe(II) α-ketoglutarate-dependant halogenase was less successful, suggesting the flavin dependant halogenase is less selective. Efforts to completely remove chloride sources to abolish chlorination at C-18 were unsuccessful, indicating that even at low concentrations the Fe(II) α-ketoglutarate-dependant halogenase prefers chloride as the halogen source.

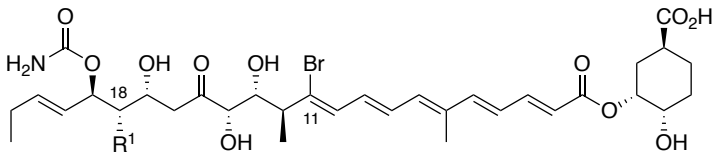

R¹ = H **85**

R¹ = Cl **86**

R¹ = Br **87**

Figure 5.1 Example of halide incorporation pattern of analogues offering insights in the halide preference of the two halogenase enzymes halogenases.

Further modifications to the polyol were investigated using mutasynthesis. The biosynthetic pathway was inactivated through production of a Ser-Ala mutation within the ACP domain of module 2 within the PKS, and restoration of natural product investigated using synthesised NAC thioester **95**. Feeding experiments failed to restore enacyloxin IIa production. However, the exact reason for this was unclear. To investigate this further an *in vitro* assay was designed to probe whether activity

of the KS domain and the KR-ACP di-domain of module 3 could be reconstituted using a NAC thioester.

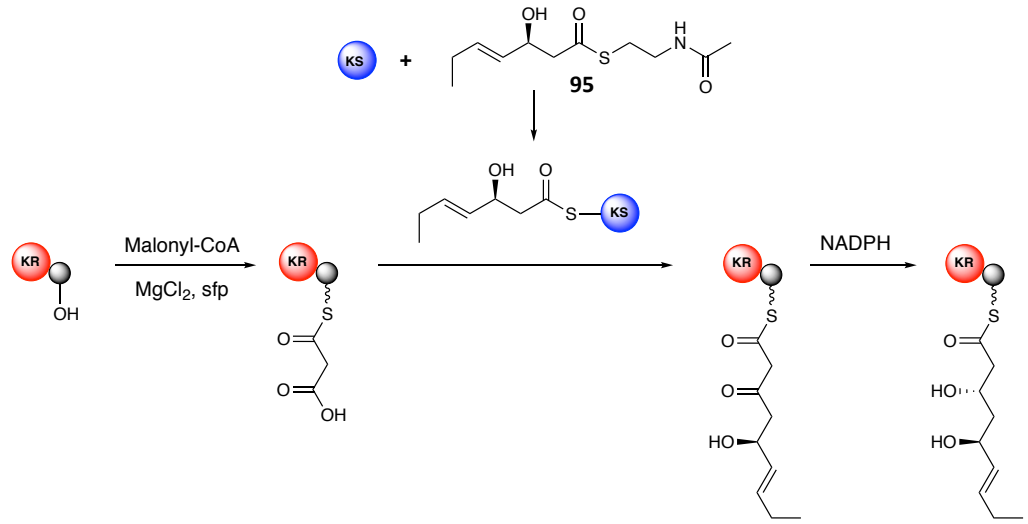

Scheme 5.1 *In vitro* assay used investigate the use of NAC thioester mimics to modify the polyol region of enacyloxins.

Acylation of the KS domain was successful, but the product resulting from condensation with the malonyl thioester on the KR-ACP didomain was rapidly hydrolysed via lactonisation. The next step would be to probe the substrate tolerance of the KS domain towards non-natural NAC thioesters such as **192** and **193** (figure **5.2**), which could be synthesised. If the KS domain is shown to have relaxed substrate specificity, improvements to the permeability of *B. ambiafaria* BCC0203 will be required to allow sufficient uptake of the NAC thioesters for the production of novel enacyloxins.

Figure 5.2 Structures of potential NAC thioester mimics to be used in the *in vitro* assay.

The second aim of this project was to incorporate novel DHCCA units into enacyloxin through mutasynthesis. This method resulted in the production of new enacyloxin analogues containing linear and 7-membered DHCCA analogues. The production of an enacyloxin analogue containing a propargylated DHCCA moiety was also investigated. This would facilitate the use of 'click' chemistry in the production of

enacyloxins with improved pharmacological properties such as increased aqueous solubility. Chemical synthesis of propargylated DHCCA (**178**) proved challenging due to the inefficient propargylation of the secondary alcohol. Despite optimisation efforts, this remains the limiting step in the synthetic procedure. However, the alternative route discussed in section **3.2** may be a suitable strategy to facilitate the efficient synthesis of **178**.

Further work would involve the feeding of **178** to *B. ambifaria* BCC0203 Δ5912-14 blocked in DHCCA biosynthesis with the final goal of producing enacyloxin analogues using 'click' chemistry.

Following the production of a variety of novel enacyloxin analogues, the final aim was to determine the antimicrobial activity of each compound. Activity data was determined using a MIC assay against cultures of *A. baumannii*. Some compounds were seen to have MIC values equal or lower than enacyloxin IIa (MIC = 2 μg/mL) indicating that the production of more potent analogues is possible using the methods described in this work. This work has provided useful insights into the SAR of enacyloxins helping to drive the design of future analogues. Complete bromination of enacyloxin was seen to increase antimicrobial activity however partial bromination did not. Mono-halogenated compounds revealed that activity is significantly decreased suggesting that halogenation – especially at C-18 – is crucial to antimicrobial activity. It has also been confirmed that cyclic DHCCA moieties are essential for antimicrobial activity but that increasing ring size is not beneficial. The relationship between the 7-memebred DHCCA diol and carboxylic acid affects the activity suggesting an *anti*-relationship is more favoured compared to *cis*.

Further, an *in vivo* mouse model was used, in collaboration with Professor Jian Li at Monash University to determine *in vivo* efficacy and to gain an insight into mammalian toxicity of enacyloxin and selected analogues. Interestingly, enacyloxin IIa displayed comparable *in vivo* activity to the industrial standard colistin. The low activity of other analogues may have been a result of compound degradation during

shipping to Australia. These experiments therefore need to be repeated, with the compounds isolated and their purities confirmed at Monash University.

Finally, through collaborations with Professor Neil Oldham at the University of Nottingham, native MS was used to evaluate the relationship between binding affinity and the antimicrobial activity of each compound. Binding affinity of selected analogues to the EF-Tu•GDPNP complex suggested in all but one compound that there is a positive correlation between activity and binding affinity. To attain a wider understanding of this relationship, binding affinity of a wider selection of enacyloxin analogues produced should be determined. This may also help to gain a greater understanding of the SAR. Further to this, the use of in-tact mass spectrometry to analyse the activity of analogues from crude production extracts has been shown to be a useful method to quickly screen for activity and avoid laborious isolation and purification procedures. This will prove invaluable in the next stage of drug development as more compounds can be generated and screened.

Long-term, future work may include modifications of the polyol region to resemble the structurally similar natural product, vibroxin **42**. Vibroxin is more active than enacyloxin IIa despite the absence of functional groups seen to be important for binding, from the crystal structure. Despite identical domain architecture of the first two modules for both enacyloxin and vibroxin the C-23 to C-18 regions differ. Replacing domains within the first two modules of the enacyloxin PKS with the corresponding vibroxin domains may provide a greater understanding of why these structural differences occur. If successful, this method could be combined with previously discussed modification strategies such as bromine incorporation and gene deletions. This would afford enacyloxin/ vibroxin analogues harbouring the C-23 to C-18 vibroxin region, alongside backbone modifications (figure **5.3**).

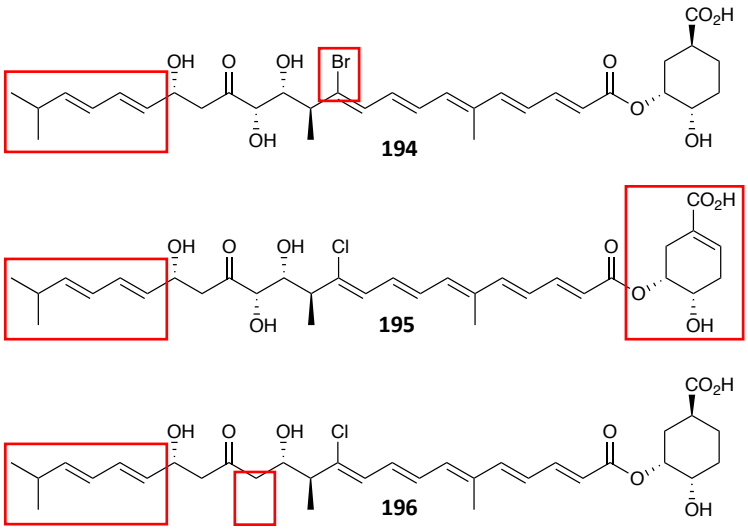

Figure 5.3 Structures of potential analogues produced by a combination of domain swapping and previously discussed backbone modification strategies.

The stability of enacyloxin IIa could be improved by modifications to the polyene region. Mutation of the DH domain in modules 8 and 9 of the PKS should result in analogues where the conjugated polyene is disrupted by the introduction of hydroxyl groups (figure **5.4**).

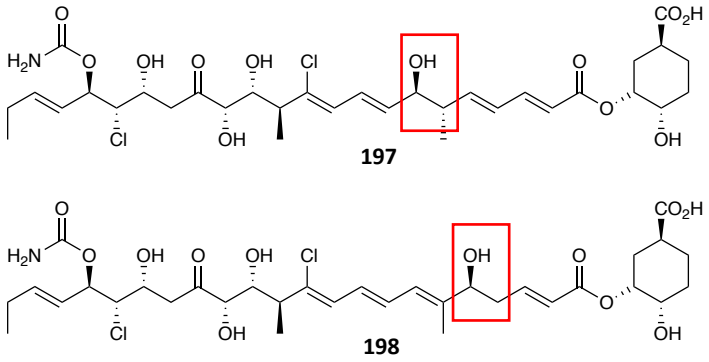

Figure 5.4 Structure of potential analogues by mutating the DH domains of module 8 and 9 in the enacyloxin PKS.

Currently, only the X-Ray crystal structure for enacyloxin IIa bound to *E. coli* EF-Tu•GDPNP has been reported.[149] Expanding this to include a selection of enacyloxin analogues would be crucial in attaining a better understanding of the SAR and therefore in the design of future compounds.

Overall, using a variety of biosynthetic methods, multiple enacyloxin analogues have been produced, with some being more potent than enacyloxin IIa. This has demonstrated the importance of natural products and how understanding biosynthetic pathways has potential to combat the fight against AMR. Further modification to enacyloxin IIa may overcome some of the issues preventing its' clinical application as an effective drug against *A. baumannii* infections.

Chapter 6 - Experimental

6.1 General Methods and equipment

All chemicals and solvents were purchased from Sigma Aldrich (UK), Thermo Fisher Scientific, Fisher Scientific or Alfa Aesar unless otherwise stated. Room temperature (RT) corresponds to ambient temperature (20 °C), 0 °C corresponds to an ice bath, -10 °C corresponds to an ice/salt bath and -78°C corresponds to an acetone/ dry ice bath. Reactions under inert conditions were first evacuated under a vacuum and purged with argon, the process repeated and an inert atmosphere maintained with argon filled balloons. Temperature dependent reactions were controlled through thermostatically controlled oil baths using IKA® RCT digital stirrer plates. The removal of solvents was performed using a BÜCHI B-490 rotary evaporator connected to a BÜCHI V-100 vacuum pump. Silica column purification was carried out on 40-60 Å silica gel purchased from Sigma Aldrich. Thin layer chromatography (TLC) was carried out using aluminium sheets coated with a layer of silica gel 60 F_{254} with appropriate solvent systems. Visualisation of TLC plates was carried out using UV light (254 nm), potassium permanganate solution or vanillin staining solution followed by heating with a heat gun. NMR spectra were recorded on Bruker Advance AV-300, HD-300, AV-400 and HD-500 MHz spectrometers as noted for each spectra. Chemical shift values are reported in parts per million (ppm) and were referenced to either $CDCl_3$ (δ_H = 7.26 ppm, δ_C = 77.2 ppm) or MeOD (δ_H = 3.31 ppm, δ_C = 49.0 ppm) with coupling constants (*J*) rounded to the nearest 0.5 Hertz (Hz). Multiplicities assigned refer to the following: multiplet (m), singlet (s), doublet (d), triplet (t), quartet (q), quintet (quin), doublet of doublets (dd), doublet of triplets (dt), doublet of doublet of doublets (ddd), doublet of doublet of triplets (ddt), triplet of doublets (td), quartet of doublets (qd). Assignments are derived from COSY, HSQC and HMBC correlations. Low resolution mass spectrometry data was collected using an open access Agilent 6130B single Quad electrospray ionisation (ESI) mass spectrometer and high resolution data collected by either Dr Lijiang Song or Jim Morris using a Bruker MaXis plus Q-TOF ESI spectrometer. Infra-red (IR) spectra were collected using a Bruker ALPHA platinum attenuated total reflection (ATR) single reflection

diamond ATR spectrometer in units of wavenumbers (cm^{-1}). Optical rotations were collected using an Optical Activity Ltd AA-1000 polarimeter at 589 nm.

Autoclaving of media was performed at 121 °C for 10 minutes at 1 bar. The handling of *Burkholderia* and *Acinetobacter* strains was conducted in a laminar flow hood within a category 2 laboratory facility. Sterile filtering was performed using Minisart® syringe filters with either a 0.22 µm or 0.45 µm pore size.

6.2 Biological material and procedures

6.2.1 Media

Luria-Bertani medium (LB)

To 25 g of LB powder was added 1L of deionised water and the mixture sterilized by autoclaving. For LB agar plates 15 g of agar was added prior to sterilisation.

Basal Salts Medium (BSM)

$K_2HPO_4 \cdot 3H_2O$ (4.25 g/L), $NaH_2PO_4 \cdot H_2O$ (1.00 g/L), NH_4Cl (2.0 g/L), $MgSO_4 \cdot 7H_2O$ (0.2 g/L), $FeSO_4 \cdot 7H_2O$ (0.012 g/L), $MnSO_4 \cdot H_2O$ (0.003 g/L), $ZnSO_4 \cdot 7H_2O$ (0.003 g/L), $CoSO_4 \cdot 7H_2O$ (0.001 g/L), nitrilotriacetic acid (0.1 g/L), Bacto CAS amino acids (0.5 g/L), Bacto yeast extract (0.5 g/L) and glycerol (4 g/L) were dissolved in deionised water and the pH adjusted to 7.0 ($\pm$ 0.2). Bacto agar (15 g/L) was added for agar plate use and the media sterilised by autoclaving. (For bromide analogue studies NH_4Cl was substituted with NH_4Br (3.66 g/L))

Mueller-Hinton broth (MH)

To 22 g of Mueller-Hinton broth powder was added 1 L of deionised water and the mixture sterilized by autoclaving.

6.2.2 Buffers and solutions

Loading Buffer:

20 mM Tris-HCl, 100 mM NaCl and 20 mM Imidazole were dissolved in deionised water, the pH adjusted to 7.8 and the solution filtered.

Stripping Buffer:

20 mM Tris-HCl, 100 mM NaCl and 50 mM EDTA were dissolved in deionised water and the solution filtered.

Elution Buffers:

20 mM Tris-HCl, 100 mM NaCl and 50-300 mM imidazole were dissolved in deionised water and the solutions filtered.

Storage Buffer:

20 mM Tris-HCl and 100 mM NaCl were dissolved in deionised water, the pH adjusted to 7.4 and the solution filtered.

10X SDS-PAGE running buffer:

250 mM Tris, 1.92 M glycine and 1% w/v SDS were dissolved in deionised water and stored at room temperature. Before use the buffer was diluted to 1X running buffer.

10X Tris/Borate/EDTA (TBE) Buffer:

890 mM Tris, 890 mM boric acid and 20 mM EDTA were dissolved in deionised water and stored at room temperature. Before use the buffer was diluted to 1X buffer.

Phosphate pH 7 Buffer:

290 mM $Na_2HPO_4 \cdot 7H_2O$ and 180 mM Na_2HPO_4 were dissolved in deionised water and the pH adjusted to 7.0

$NiSO_4$ solution:

100 mM of $NiSO_4 \cdot 6H_2O$ was dissolved in deionised water and the solution filtered.

6.2.3 Strains, and plasmids

Table 6.1 Bacterial strains used

Strain	Role
B. ambifaria BCC0203	Enacyloxin IIa producing strain
E.coli SY327	Donor strain for conjugation between *E.coli* and *B. ambifaria*
E.coli TOP10	Host for general cloning
E.coli HB101	Helper strain for conjugation between *E.coli* and *B. ambifaria*
E.coli BL21 (DE3)	Protein expression
A. baumannii ATCC 17978	Determination of MIC values for enacyloxin and analogues
A. baumannii DSM25645	Determination of MIC values for enacyloxin and analogues

Table 6.2 Plasmids used

Plasmid	Resistance	**Source**
pCR-Blunt	Kanamycin	Challis Lab Stock
pGPI-SceI	Trimethroprin	Mahenthiralingham / Challis Lab Stock
pRK2013	Kanamycin	Challis Lab Stock
pDAI-SceI	Tetracycline	Mahenthiralingham / Challis Lab Stock
pET28a(+)	Kanamycin	Novagen
pJS1	Kanamycin	Challis Lab
pJS2	Kanamycin	Challis Lab
pJS3	Tetracycline	Challis Lab
pJS4	Kanamycin	Challis Lab
pJS5	Kanamycin	Challis Lab

6.2.4 Antibiotics used

Table 6.3 Antibiotics used

Antibiotics	Solvent	Working concentration	Applied Strain
Kanamycin	H_2O	50 µg/mL	*E.coli* carrying recombinant pET28a(+) or pRK2013
Trimethroprim	DMSO	50 µg/mL	*E.coli* carrying recombinant pGPI-SceI
		150 µg/mL	*Burkholderia* carrying recombinant pGPI-SceI
Gentamycin	H_2O	50 µg/mL	*Burkholderia* carrying recombinant pGPI-SceI or pDAI-SceI
Tetracycline	70% EtOH	20 µg/mL	*E.coli* carrying recombinant pDAI-SceI
		200 µg/mL	*Burkholderia* carrying recombinant pDAI-SceI

6.2.5 Preparation of electrocompetent *E.coli* cells

For this project, electrocompetent *E.coli* SY327 cells were required and a general procedure is described. The appropriate *E.coli* strain was streaked to single colonies onto an agar plate and incubated overnight at 37 °C. A single colony was used to inoculate 5 mL of LB which was incubated at 37 °C with shaking (180 rpm). From the

overnight culture 0.5 mL was diluted in 50 mL of fresh LB in a 250 mL conical flask. This was incubated and shaken at 37 °C (180 rpm) for around 3.5 hrs until an OD_{600} of 0.4-0.6 was achieved. The culture was cooled on ice for 30 minutes and the cells harvesting by centrifugation (3000 rpm, 4 °C, 10 mins). The supernatant was discarded and the cell pellet resuspended in 50 mL of pre-cooled 15 % glycerol. The cells were again harvested by centrifugation under the same conditions. The supernatant was discarded and the cell pellet resuspended in 1 mL of pre-cooled 15 % glycerol and divided into 80 µL aliquots, flash frozen in liquid N_2 and stored at -80 °C.

6.2.6 Transformation of electrocompetent *E.coli* SY327 cells

To a thawed aliquot of 80 µL of electrocompetent *E.coli* cells was added 2 µL of plasmid DNA or ligation mixture. The solution was transferred to a Bio-Rad electroporation cuvette and shocked at 2.5 kV using a Bio-Rad Gene Pulser® II attached to a Bio-Rad Pulse Controller Plus. Immediately after electroporation 500 mL of LB was added. The solution was transferred to a sterile eppendorf tube and incubated at 37 °C in a water bath for 1 hour. 100-200 µL of transformation mixture was spread onto LB agar plates supplemented with the appropriate antibiotic and incubated at 37 °C overnight.

6.2.7 Transformation of chemically competent cells

To a thawed aliquot of 80 µL of chemically competent *E.coli* TOP10 (Thermo Fisher Scientific) or *E.coli* BL21 (DE3) (Thermo Fisher Scientific) cells was added 2 µL of plasmid DNA or ligation mixture. The mixture was kept on ice for 30 minutes followed by heat shocking at 42 °C for 60 seconds. The mixture was put back onto ice for 60 seconds and 250 µL of LB was added. This was incubated at 37 °C with mixing (180 rpm) for 1 hour. 100-200 µL of transformation mixture was spread onto LB agar plates supplemented with the appropriate antibiotic and incubated at 37 °C overnight.

6.2.8 Isolation of plasmid DNA and concentration determination

Plasmid DNA was isolated using a thermo scientific™ GeneJET Plasmid Miniprep Kit according to the manufacturer's instructions from an overnight *E.coli* culture (5 mL) supplemented with appropriate antibiotics. DNA concentration was measured using a thermo scientific NanoDrop™ Lite Spectrophotometer.

6.2.9 Polymerase Chain Reaction (PCR)

For the amplification of DNA fragments for cloning, Q5® Hot Start High Fidelity DNA polymerase was used.

Typical conditions for a 25 µL reaction are given in table **6.4** and typical thermocycling conditions shown in table **6.5**.

Table 6.4 General PCR reaction components and volumes

Component	Volume / µL
Q5 Hot Start High-Fidelity 2X Master Mix	12.5
Template DNA (10 ng/µL)	1.0
Forward Primer (10 µM)	1.25
Reverse Primer (10 µM)	1.25
Nuclease-free water	8.0
DMSO*	1.0

Table 6.5 General PCR thermocycling conditions

Step	Temperature / °C	Duration
Initial denaturation	98	3 minutes
Denaturation **Annealing** **Extension**	98 60-70 72	30 seconds 30 seconds 30 seconds/kb
Final Extension	72	10
Hold	4	

6.2.10 Agarose gel preparation and electrophoresis conditions

1 g of agarose was added to 100 mL of 1X TBE buffer and the solution heated in the microwave until completely dissolved. The solution was poured into a cast with an appropriate comb added and left to set. The gel was placed into a gel electrophoresis tank containing 1X TBE and the comb removed. The lanes were filled with FastRuler

High range or Mid-Range DNA ladder (Fisher Scientific) and DNA both containing midori green for visualisation. Gel electrophoresis was performed using a Bio Rad PowerPac™ Basic power supply at 110 V for 40-60 minutes and the results visualised using a BioDoc-it™ transilluminator.

6.2.11 DNA purification from an agarose gel

DNA was purified from an agarose gel using a thermo scientific™ GeneJET Gel Extraction Kit according to the manufacturer's instructions. DNA concentration was measured using a thermo scientific NanoDrop™ Lite Spectrophotometer.

6.2.12 Genetic Manipulation of *Burkholderia ambifaria* BCC0203

The fragment and constructs used for genetic manipulations are shown in table **6.6** and **6.7**.

Table 6.6 Isolated fragment from Burkholderia ambifaria BCC0203 genomic DNA with appropriate primers and restriction sites used

Fragment	Primer Sequence	Restriction Site
*B. ambifaria*_5924_M2_ACP (Frag_JS1)	F: 5'- ATTATCTAGACTTCCTGGCCGCGCTT R: 5' - ATATGAATTCTGTAGGCGGCCGATTC	XbaI EcoRI

***Underlined region indicates restriction sites**

Table 6.7 Constructs generated during gene deletion in Burkholderia with primer sequences when appropriate

Construct	Primer Sequence
pCR-Blunt_5924_M2_ACP (pJS1)	/
pCR-Blunt_5924_M2_ACP-S2A (pJS2)	F: 5'- CATGGATGCGCTGCTGTCG R: 5' - CCGAGTTCGAGCAGCGAGC

***Highlighted region indicates mutated region**

6.2.12.1 Ligation into pCR-Blunt

To purified PCR product *B. ambifaria*_5924_M2_ACP (Frag_JS1) (table **6.6**) (2 µL, 143 ng) and pCR-Blunt vector (1 µL, 25 ng) was added 5X T4 DNA ligase buffer (2 µL), T4 DNA ligase (1 µL) and sterile water (4 µL). The reaction mixture was incubated at

15 °C overnight to give plasmid pCR-Blunt_5924_M2_ACP (pJS1) followed by transformation of chemically competent cells *E.coli* TOP10 cells (see section **6.2.7**).

6.2.12.2 Site-directed mutagenesis in pCR-Blunt

For the creation of single point mutations throughout this project a Q5® Site-Directed Mutagenesis kit was used. PCR of pCR-Blunt_5924_M2_ACP (pJS1) (2 µL) using Q5® hot start high fidelity polymerase and the primers in **6.7**, was subsequently combined with a kinase, ligase, Dpn1 (KLD) mix (1 µL), 2X KLD buffer (5 µL) and nuclease free water (2 µL). The reaction mixture was incubated at RT for 5 minutes to give plasmid pCR-Blunt_5924_M2_ACP-S2A (pJS2) followed by transformation of chemically competent *E. coli* TOP10 cells (see section **6.2.7**).

6.2.12.3 Digestion and ligation into pGPI-SceI

Separately pCR-Blunt_5924_M2_ACP-S2A (pJS2)(4 µL, 671 ng/µL) and pGPI-SceI (17 µL, 185 ng/µL) were digested with *Xba*I (3µL) and *Eco*RI-HF (3 µL) in 10X Cutsmart buffer (5 µL) and nuclease free water (up to 50 µL) and the reaction mixture incubated at 37 °C for 2 hours. The digested DNA was visualised on an agarose gel and purified using a GeneJET Gel Extraction Kit.

The purified DNA fragment from digested pCR-Blunt_5924_M2_ACP-S2A (pJS2) (10.8 µL, 19 ng/µL) and linearised pGPI-SceI vector (6.7 µL, 27 ng/µL) were ligated using T4 DNA ligase (1 µL) and 10X T4 ligase buffer (2 µL) by incubation overnight at RT to give pGPI-SceI_5924_M2_ACP_C2A (pJS3).

pGPI-SceI_5924_M2_ACP_C2A (pJS3) was purified by the addition $\frac{1}{10} \times$ volume of 3 M NaOAc followed by addition of 2.5 × volume of pre-cooled 95 % ethanol. This was kept at -20 °C for 30 minutes followed by centrifugation (13,000 rpm, 20 mins, 4 °C). The supernatant was carefully removed and the pellet resuspended in 250 µL of pre-cooled 70 % ethanol followed by centrifugation (13,000 rpm, 10 minutes, 4 °C). The supernatant was carefully removed and the pellet air dried. Purified

pGPI-SceI_5924_M2_ACP-S2A (pJS3) was dissolved in 10-15 µL of deionised water and used to transform electrocompetent *E. coli* SY327 cells (see section **6.2.6**).

6.2.12.4 Tri-parental mating procedures

Tri-parental mating procedures incorporate the pGPI-SceI_5924_M2_ACP_C2A (pJS3) mutant plasmid into the genome of *B. ambifaria*. *E. coli* SY327/pGPI-SceI_5924_M2_ACP-S2A (pJS3) (5 mL, 37 °C , 180 rpm), *B. ambifaria* BCC0203 (5 mL, 30 °C, 180 rpm) and an *E. coli* HB101 helper strain containing the pRK2013 plasmid (5 mL, 37 °C , 180 rpm), supplemented with the appropriate antibiotics, were separately incubated at overnight. All 3 cultures were centrifuged (3000 rpm, 10 mins, 4 °C), the supernatant discarded and pellets resuspended in LB (5 mL) to remove the antibiotics. From each resuspended overnight culture, 100 µL was added to a single sterile eppendorf tube and the resulting 300 µL solution mixed gently. Onto an LB agar plate was placed a sterile nitrocellulose disk and 100 µL of the solution was spread onto the disk, followed by incubation at 30 °C overnight. The nitrocellulose disk was placed into a falcon tube and the cells washed with 1 mL of a sterile 0.9 % NaCl solution. Serial dilutions of the 1 mL solutions were made and 100 µL of each was spread onto LB agar plates supplemented with trimethroprim and gentamycin. The plates were incubated at 30 °C for 36 hours. Single colonies were selected for overnight cultures and used in a colony PCR reaction (see table **6.6** for primers) to check for correct insertion of mutated ACP fragments. Glycerol stocks of successful mating products were flash frozen and stored at -80 °C. For the second tri-parental mating procedure the *B. ambifaria* ACP mutant mating product (5 mL, 30 °C, 180 rpm), *E. coli* HB101 containing pRK2013 (5 mL, 37 °C , 180 rpm) and *E. coli* SY327 containing pDAI-SceI (5 mL, 37 °C , 180 rpm) supplemented with appropriate antibiotics were separately incubated overnight. All 3 cultures were centrifuged (3000 rpm, 4 °C, 10 mins), the supernatant discarded and pellets resuspended in LB (5 mL) to remove the antibiotics. From each resuspended overnight culture, 100 µL was added to a single

sterile eppendorf tube and the resulting 300 µL solution mixed gently. An LB agar plate containing a nitrocellulose disk spread with 100 µL of the solution was incubated at 30 °C overnight. The nitrocellulose disk was placed into a falcon tube and the cells washed with 1 mL of a sterile 0.9 % NaCl solution. Serial dilutions of the 1 mL solution were made and 100 µL of each was spread onto LB agar plates supplemented with tetracycline and gentamycin. The plates were incubated at 30 °C for 36 hours. Single colonies were selected for overnight cultures and used in a colony PCR reaction (see table **6.6** for primers) to check for correct insertion of mutated ACP fragments. The fragment DNA sequence was checked by sequence analysis following DNA purification using a thermo scientific™ GeneJET Gel Extraction Kit. Glycerol stocks of successful mating products were flash frozen and stored at -80 °C. A phenotype screen using each successful mating product combined with sequence analysis of gel purified DNA confirmed the presence of the mutation and integration into the genome of *B. ambifaria* BCC0203. Unsuccessful cross-over products were discarded. The pDAI-SceI plasmid was removed by growth on 15 % sucrose LB agar plates and confirmed by the loss of tetracycline resistance.

6.2.13 Large scale enacyloxin and analogous compound production and isolation

For small scale production and isolation or a phenotype screen a single BSM plate was used with all other conditions remaining the same. Production of characteristic yellow streaks indicated enacyloxin production.

The appropriate *B. ambifaria* strain was used to inoculate 5 mL of LB and incubated overnight (30 °C, 180 rpm). The cells were harvested by centrifugation (4000 rpm, 10 mins, 4 °C) and the supernatant discarded. The pellet was resuspended in 5 mL of a 0.9 % NaCl solution (for bromide analogues, 0.9 % NaBr solution was used.) BSM plates from 1L of media were prepared (for DHCCA feeding experiments the compound is added to cooled liquid BSM media at a concentration of 333 mg/L). The resuspended cell solution was streaked onto BSM plates in a diagonal fashion across the plates and incubated at 30 °C for 3 days. Successful enacyloxin production is indicated by the presence of yellow characteristic streaks. The agar was cut into small rectangular pieces, combined and extracted by submersion with EtOAc for 1 hour.

Organics were concentrated *in vacuo*, the extraction process repeated twice and the crude residue purified with HPLC (section **6.2.14**). (All procedures following incubation were conducted in the absence of light due to the possibility of light-induced isomerisation occurring)

6.2.14 HPLC purification of enacyloxin and analogous compounds

Crude enacyloxin extract was dissolved in 2 x 750 µL of HPLC grade MeOH and passed through a spin filter to remove solid impurities. HPLC conditions are provided in table **6.8**. Wavelengths used were 360 nm for detection of enacyloxin and 210 nm for detection of the secondary metabolite pyrrolnitrin.

Table 6.8 HPLC conditions for purification of enacyloxin and analogous analogues

Time / min	Water * (A) %	Methanol (B) %	Flow mL/min
0.00	50.0	50.0	10.00
5.00	50.0	50.0	10.00
30.00	0.0	100.0	10.00
35.00	0.0	100.0	10.00
36.00	50.0	50.0	10.00
40.00.	50.0	50.0	10.00

6.2.15 Spectroscopic analysis of enacyloxin and analogous compounds

Analyses of enacyloxin and analogous products were performed on a Bruker MaXis Impact electrospray ionisation quadrupole time-of-flight mass spectrometer (ESI-Q-TOF-MS) coupled to a Dionex Ultimate 3000 HPLC instrument fitted with a ZORBAX eclipse plus C18 column (2.1 x 100 mm, 1.8 µm). The column was eluted with a linear gradient of 5-100 % MeCN containing 0.1% formic acid over 34 minutes with a flow rate of 0.2 mL/min. The mass spectrometer was operated in positive ion mode with a scan range of 50-2500 *m/z*. Source conditions were: end plate offset at -500 V; capillary at -4500 V; nebulizer gas (N_2) at 1.4 bar; dry gas (N_2) at 8 L min^{-1}; dry

temperature at 200 °C. For calibration of samples a 20 µL injection of 1 mM sodium formate was added at the start of each run.

For NMR analysis, samples were dissolved in MeOD and ^{1}H, ^{13}C. COSY, HSQC and HMBC spectra recorded on a Bruker Advance HD-500 MHz spectrometer. Assignments of purified compounds can be found in tables **6.12** to **6.27**.

6.2.16 Minimum inhibitory concentration (MIC) value determination

Each MIC determination was performed in triplicate alongside a negative control where no antibiotic is added.

To freshly prepared MH broth (691 µL) was added an enacyloxin analogue in methanol (9 µL, 5 mg/mL). To the first column of a 96-well microtiter plate was added 100 µL of this solution. Serial 2-fold dilutions with MH broth were then made across the remaining 11 columns to leave 50 µL in each well. Overnight cultures of the test strains *Acinetobacter baumannii* ATTC17978 or DSM25645 were grown in MH broth (5mL) (section **6.2.1**) at 30 °C. The bacteria cultures were diluted with MH broth to the desired OD_{625} (0.08-0.1) giving a concentration of 10^8 cell-forming units (CFU)/mL using a McFarland turbidity standard. The cultures were further diluted 100-fold to give a concentration of 10^6 CFU/mL. 50 µL of the diluted bacteria was added to each well to give a final bacterial concentration of 5 x 10^5 CFU/mL and final well volume of 100 µL. The 96-well microtiter plate was incubated for 18 hours at 30 °C and the MIC determined as the lowest concentration at which bacterial growth is inhibited. Final concentrations of MIC values are two-fold dilutions beginning at 32 µg/mL.

6.2.17 Protein production, purification and spectroscopic analysis

6.2.17.1 Isolation of constructs used for production of proteins

For the amplification of DNA fragments for cloning, Q5® Hot Start High Fidelity DNA polymerase was used (see section **6.2.9**) with genomic *B. ambifaria* BCC0203 DNA

and the primers in table **6.9**. The PCR product was visualised on an agarose gel and purified using a GeneJET Gel Extraction Kit.

6.2.17.2 Digestion and ligation into pET28a(+)

Separately the appropriate purified DNA fragment (30 µL, 45 ng/µL) and pET28a(+) (5 µL, 90 ng/ µL) were mixed with, *Nde*I (2µL), *Hin*dIII-HF (2 µL), 10X Cutsmart buffer (5 µL) and nuclease free water (11 µL) and the reaction mixture incubated at 37 °C for 2 hours.

The digested DNA fragment (300 ng) and linearised pET28a(+) vector (100 ng) were ligated using T4 DNA ligase (1 µL) and 10X T4 ligase buffer (2µL) by incubation overnight at RT followed by transformation into chemically competent *E. coli* TOP10 cells (see section **6.2.7**).

Table 6.9 Constructs for protein production and purification

Construct	Primer Sequence
pET28a_5924_M3_KS (pJS4)	F: 5'- ATACATATGTCGAAAGAGGGCACGG R: 5'- ATAAAGCTTTTATTCGGCCTGCAAATCCT
pET28a_5923_M3_KR/ACP (pJS5)	F: 5'- ATACATATGATGGGGAGGACCGTGGCA R: 5'-ATAAAGCTTCTAGGCGGCGCCCACCC

6.2.17.3 Homology model production

A homology model of the Bamb_5924 module 3 KS domain was created using Phyre 2 alignment, using a mammalian fatty acid synthase fragment as a template from the protein data bank (PDB), (PDB code: 2vz8).

6.2.17.4 Site Directed Mutagenesis using overlap PCR in pET28a(+)

Due to the generation of the desired mutated plasmid by a Q5 directed mutagenesis approach failing, the inserted fragment to be mutated was split into two fragments.

Two sets of primers were designed to amplify the two fragments, with a 20 bp overlapping region about the point of mutation. Using Q5® hot start high fidelity polymerase, a mutation was introduced into each fragment (See table **6.10** for primers for each fragment) and both PCR products were visualised on an agarose gel and purified using a GeneJET Gel Extraction Kit. The two PCR product fragments were each used together as template DNA for a second round of PCR producing the complete fragment containing the desired mutation. This was visualised on an agarose gel and purified using a GeneJET Gel Extraction Kit.

The mutated DNA fragment was digested and ligated into pET28a(+) as seen in section **6.2.12.3**.

Table 6.10 Isolated fragment from Burkholderia genomic DNA with appropriate primers and restriction sites used

Fragment	Primer Sequence	Restriction Site
5924_M3_KS_C211A_1 (Frag_JS2)	F: 5'- ATACATATGTCGAAAGAGGGCACGG R: 5'- TCGCCATGGCGGGCCCCTGCCAGTCG	*Nde*I
5924_M3_KS_C211A_2 (Frag_JS3)	F: 5'- GCAGGGGCCCGCCATGGCGATCGACACCG R: 5'- ATAAAGCTTTTATTCGGCCTGCAAATCCT	*Hin*dIII
5924_M3_KS_C211A_3* (Frag_JS4)	F: 5'- ATACATATGTCGAAAGAGGGCACGG R: 5'- ATAAAGCTTTTATTCGGCCTGCAAATCCT	*Nde*I *Hin*dIII
5924_M3_KS_C699A_1 (Frag_JS5)	F: 5'- ATACATATGTCGAAAGAGGGCACGG R: 5'- CGCCTTCGGCCTGGTCGGCCGGCCGCA	*Nde*I
5924_M3_KS_C699A_2 (Frag_JS6)	F: 5'- GGCCGACCAGGCCGAAGGCGACGAAGGCG R: 5'- ATAAAGCTTTTATTCGGCCTGCAAATCCT	*Hin*dIII
5924_M3_KS_C699A_3* (Frag_JS7)	F: 5'- ATACATATGTCGAAAGAGGGCACGG R: 5'- ATAAAGCTTTTATTCGGCCTGCAAATCCT	*Nde*I *Hin*dIII

*5924_M3_KS_CXXXA_3 (Frag_JS4 and Frag_JS7) are the complete DNA fragments containing the desired mutation and both sets of restriction enzymes. These are digested and ligated into pET28a(+)

****Underlined region indicates restriction sites**

6.2.17.5 Protein overproduction

A single transformant of *E.coli* BL21 (DE3) containing the desired recombinant plasmid was used to inoculate sterile LB (10 mL) supplemented with the appropriate antibiotic and shaken at 37 °C (180 rpm) for 16 hours for use as a seed culture.

Following incubation the seed culture was used to sub-culture 1 L of sterile LB containing the appropriate antibiotic and this was shaken at 37 °C (180 rpm) until OD_{600} 0.6-0.8 was reached (~3.5 hours). Once the required optical density was attained, protein overproduction was induced with isopropyl β-d-1-thiogalactopyranoside (IPTG) (0.5 mL, 1 M) and the culture shaken at 15 °C for 16 hours.

6.2.17.6 Protein purification

The cells from the overnight culture were harvested through centrifugation (4000 rpm, 20 minutes, 4 °C), the supernatant discarded and cell pellet resuspended in loading buffer 10 mL/L culture) and stored on ice. The cells were lysed using a cell disrupter (one-shot mode, 20.4 KPSI) and the lysate centrifuged (17,000 rpm, 1 hour, 4 °C). The supernatant was filter sterilised and loaded onto a 1 mL HisTrap™ FF column that had been previously washed with stripping buffer (10 mL), charged with $NiSO_4$ solution (5mL, 100 mM) and equilibrated with loading buffer (5 mL). The column was washed with loading buffer (15 mL) to remove any non-specific bound proteins impurities. The protein was eluted by serial addition of elution buffers containing imidazole of concentrations; 50 mM (5 mL), 100 mM (3 mL), 200 mM (3 mL) and 300 mM (3 mL). Protein was visualised using SDS-PAGE analysis (section **6.2.17.6**). Fractions containing the desired protein were combined and concentrated via centrifugation (4000 rpm, 4 °C) using an appropriate molecular weight cut-off spin filter. Once the protein was concentrated to ~1 mL it was buffer exchanged through addition of storage buffer and concentrated as before with the final concentration determined using a thermo scientific NanoDrop™ Lite Spectrophotometer. Glycerol (final concentration 15%) was added and the protein aliquoted (50 µL), flash frozen in liquid N_2 and stored at -80 °C.

6.2.17.6 SDS-PAGE protein analysis

For size and purity determination of overexpressed proteins SDS-PAGE was used with an 8 % acrylamide SDS-PAGE gel composition suitable for 30-90 kDa proteins (table **6.11**). Elution fractions (20 µL) containing 5X SDS loading dye (5 µL) were

loaded to each well as 15 µL samples alongside 5 µL of PageRuler™ Prestained Protein ladder. The gel was run in 1X SDS-PAGE running buffer at 180 V for 50 minutes. Once complete the gel was stained with InstantBlue® protein stain and destained using deionised water.

Table 6.11 Components and volumes used in the preparation of an 8 % SDS-PAGE gel

Resolving Gel		Stacking Gel	
Component	**Volume / mL**	**Component**	**Volume / mL**
H_2O	2.3	H_2O	0.68
30 % acrylamide mix	1.3	30 % acrylamide mix	0.17
1.5 M Tris (pH 8.8)	1.3	1.5 M Tris (pH 6.8)	0.13
10 % SDS	0.05	10 % SDS	0.01
10 % Ammonium persulfate	0.05	10 % Ammonium persulfate	0.01
TEMED	0.003	TEMED	0.001

6.2.17.7 Spectroscopic analysis of intact proteins

Analyses of intact proteins were performed on a Bruker MaXis II ESI-Q-TOF MS coupled to a Dionex Ultimate 3000 HPLC instrument fitted with an ACE 3 C_4-300 reverse phase column (2.1 mm x 100, 5 µM). The column was eluted with a linear gradient of 5-100 % MeCN containing 0.1 % formic acid over 35 minutes and returned to 5 % MeCN over 10 minutes with a flow rate of 0.2 mL/min. The mass spectrometer was operated in positive ion mode with a scan range of 200-3000 *m/z*. Source conditions were: end plate offset at -500 V; capillary at -4500 V; nebulizer gas (N_2) at 1.8 bar; dry gas (N_2) at 9 L min^{-1}; dry temperature at 200 ^oC.

6.2.18 *In vitro* assays

6.2.18.1 KR/ACP activity determination

To *apo*-KR/ACP di-domain (42 µL, 200 µM) was added acetoacetyl-CoA (2 µL, 20 µM), $MgCl_2$ (5 µL, 100 mM) and Sfp (1 µL, 0.5 mM). The reaction mixture was incubated at RT for 1 hour followed by the addition of NADPH (2 µl, 50 mM) and incubation at RT

for a further 1 hour. Ketoreduction was monitored by phosphopantetheine ejection using ESI-Q-TOF-MS (MaXis II).

6.2.18.2 Malonyl-CoA loading assay

To *apo*-KR/ACP di-domain (42 µL, 200 µM) was added malonyl-CoA (2 µL, 20 µM), $MgCl_2$ (5 µL, 100 mM) and Sfp (1 µL, 0.5 mM). The reaction mixture was incubated at RT for 1 hour and conversion to malonylated-*holo* KR/ACP was monitored by ESI-Q-TOF-MS (MaXis II). (Sfp was sourced from Professor Manuela Tosin)

6.2.18.3 KS loading with chemically synthesised SNAC compound

To the KS domain (49.5 µL, 200 µM) was added chemically synthesised SNAC compound **95**, (0.5 µL, 100 mM). The reaction mixture was incubated at RT for 1 hours and 3 hours, any precipitants were removed through centrifugation (13200 g, 8 minutes) and the supernatant analysed by ESI-Q-TOF MS (MaXis II).

6.2.18.4 Elongation assay of malonylated-KR/ACP di-domain with acylated KS domain

25 µL of malonylated-KR/ACP di-domain and 25 µL of acylated KS domain were incubated at RT for 1 hour and analysed by ESI-Q-TOF MS (MaXis II)

6.2.18.5 Lactone off-loading monitoring

Elongation of malonylated-KR/ACP di-domain with acylated KS domain was performed as described in section **6.2.18.4** however after incubation at RT for 1 hour the mixture was boiled at 65 °C to precipitate the protein. The precipitate was centrifuged (13200 g, 10 minutes) and the supernatant mixed vigorously with 100 µL of EtOAc. The EtOAc layer was removed, concentrated *in vacuo* and analysed by ESI-Q-TOF MS (MaXis Impact).

6.2.18.6 Elongation assay using non-hydrolysable intermediate 111

KR/ACP di-domain (35 µL, 220 µM), Pank (1 µL), DPCK (5µL), PPat (1 µL), $MgCl_2$ (5 µL, 100 mM), Sfp (1 µL, 400 µM), ATP (2µL, 100 mM) and substrate **111** (2.5 µL, 20 mM) were incubated at RT for 1.5 hours. From this mixture was taken 25 µL and incubated with 25 µL of acylated KS from section **6.2.18.3** for a further 1 hour and analysed by ESI-Q-TOF MS (MaXis II).

6.3 NMR spectroscopic data of enacyloxin IIa and purified analogues

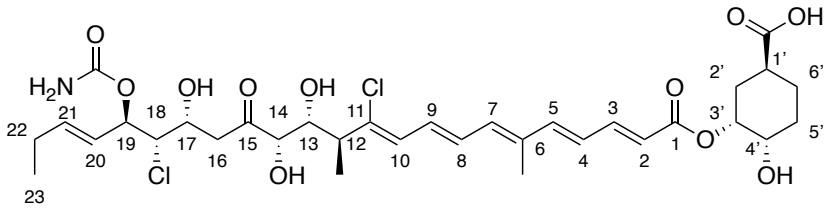

Table 6.12 NMR assignments for enacyloxin IIa **1** (d_4-MeOH, ^{1}H 500 MHz, ^{13}C 125 MHz)

Position	^{1}H (ppm)	^{13}C (ppm)
1'-COOH		179.3
1'	2.51-2.59 (m)	38.7
2'	1.71-1.77, 2.14-2.20 (m, m)	32.3
3'	5.18-5.22 (m)	73.1
4'	3.71-3.76 (m)	70.5
5'	1.78-1.84 (m)	29.4
6'	1.52-1.61, 2.00-2.06 (m, m)	27.5
1		168.5
2	6.02 (d, 15.5)	121.3
3	7.43 (dd, 15.0, 11.5)	146.8
4	6.53 (dd, 15.5, 11.5)	127.2
5	6.68-6.79 (m)	146.6
6		137.0
6-Me	1.96 (s)	12.6
7	6.42 (d, 10.5)	137.4
8	6.68-6.79 (m)	131.9
9	6.68-6.79 (m)	131.6
10	6.44 (d, 9.5)	128.4
11		140.7
12	2.94 (dq, 10.0, 6.5)	47.5
12-Me	1.19 (d, 6.5)	16.3
13	4.04 (d, 10.5)	74.1
14	4.24 (d, 1.5)	78.9
15		211.5
16	2.84, 3.04 (dd, 17.0, 4.5, dd, 17.0, 8.0)	44.5
17	4.49-4.53 (m)	66.8
18	4.03-4.07 (m)	67.9
19	5.27 (dd, 7.5,)	75.5
19-carbamate		158.6
20	5.55 (ddt, 15.5, 7.5, 1.5)	126.2
21	5.90 (dt, 15.5, 6.5)	139.2
22	2.10, (dq, 8.0, 1.5)	26.3
23	1.01 (t, 7.5)	13.6

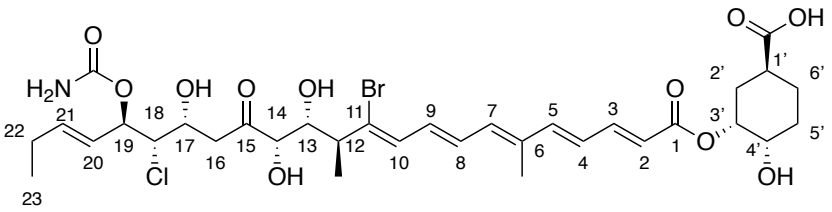

Table 6.13: NMR assignments for BrCl enacyloxin analogue **86** (d_4-MeOH, ^{1}H 500 MHz, ^{13}C 125 MHz)

Position	^{1}H (ppm)	^{13}C (ppm)
1'-COOH		
1'	2.48-2.58 (m)	39.0
2'	1.70-1.76, 2.14-2.19 (m, m)	32.5
3'	5.18-5.23 (m)	73.2
4'	3.70-3.76 (m)	70.6
5'	1.79-1.84 (m)	29.5
6'	1.50-1.62, 2.01-2.06 (m,m)	27.7
1		168.6
2	6.03 (d, 15.5)	121.4
3	7.43 (dd, 15.0, 11.0)	146.8
4	6.55 (dd, 15.0, 11.0)	127.4
5	6.76 (d, 15.0)	146.6
6		137.7
6-Me	1.96 (s)	12.7
7	6.41 (d, 11.5)	136.8
8	6.82 (dd, 13.5, 11,5)	132.3
9	6.65-6.70 (m)	133.7
10	6.34 (d, 11.5)	136.6
11		136.0
12	2.84-2.90 (m)	47.7
12-Me	1.17 (d, 6.5)	17.3
13	4.04 (dd, 2.0, 8.0)	74.7
14	4.24 (d, 1.5)	78.9
15		211.5
16	2.84, 3.04 (dd, 4.0, 17.0, dd, 17.0, 8.5)	44.6
17	4.51 (ddd, 2.5, 4.5, 7.0)	66.8
18	4.02-4.07 (m)	67.9
19	5.27 (t, 8.0)	75.5
19-carbamate		158.6
20	5.55 (ddt, 15.0, 7.5, 1.5)	126.2
21	5.90 (dt, 15.5, 6.5)	139.3
22	2.06-2.13 (m)	26.3
23	1.02 (t, 7.5)	13.6

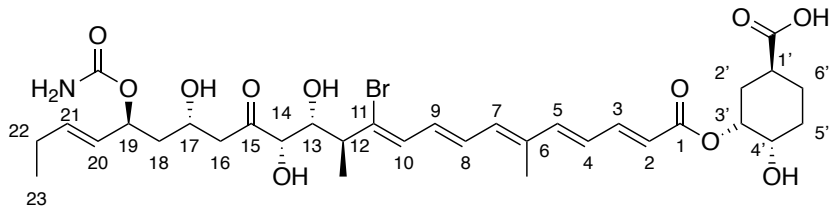

Table 6.14 NMR assignments for BrH enacyloxin analogue **85** (d_4-MeOH, ^{1}H 500 MHz, ^{13}C 125 MHz)

Position	^{1}H (ppm)	^{13}C (ppm)
1'-COOH		
1'	2.47-2.58 (m)	39.1
2'	1.71-1.75, 2.13-2.19 (m,m)	32.6
3'	5.19-5.22 (m)	73.3
4'	3.73 (ddd, 8.5, 6.0, 3.0)	70.7
5'	1.79-1.84 (m)	29.5
6'	1.50-1.57, 2.00-2.03 (m,m)	27.8
1		168.6
2	6.03 (d, 15.5)	121.5
3	7.43 (dd, 15.0, 11.5)	146.8
4	6.55 (dd, 15.0, 11.0)	127.4
5	6.76 (d, 15.0)	146.6
6		137.7
6-Me	1.95 (s)	12.7
7	6.41 (d, 12.0)	136.8
8	6.82 (dd, 13.5, 11.5)	132.2
9	6.63-6.70 (m)	133.7
10	6.35 (d, 11.5)	136.6
11		136.1
12	2.84-2.89 (m)	49.6
12-Me	1.17 (d, 7.0)	17.3
13	4.05 (dd, 10.0, 1.5)	74.6
14	4.23 (d, 1.5)	78.9
15		212.0
16	2.83, 2.66 (dd, 16.5, 8.5, dd, 16.5, 4.0)	47.2
17	4.20 (tt, 8.5, 3.5)	65.2
18	1.80, 1.65 (ddd, 14.0, 10.0, 3.23, ddd, 14.0, 9.5, 3.5)	43.8
19	5.23 (ddd, 10.0, 7.0, 3.5)	73.0
19-carbamate		159.7
20	5.45 (ddt, 15.5, 7.5, 1.5)	129.3
21	5.78 (dt, 15.5, 6.5)	135.8
22	2.05 (dq, 7.5, 1.0)	26.2
23	0.99 (t, 7.5)	13.7

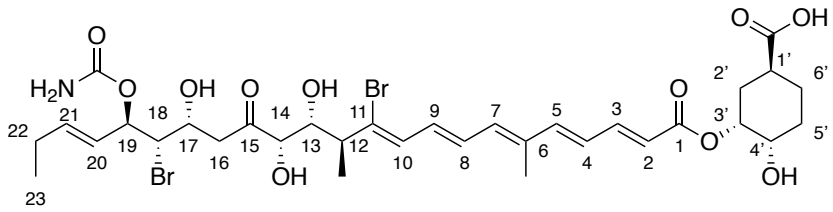

Table 6.15 NMR assignments for BrBr enacyloxin analogue **87** (d_4-MeOH, ^{1}H 500 MHz, ^{13}C 125 MHz)

Position	^{1}H (ppm)	^{13}C (ppm)
1'-COOH		
1'	2.47-2.58 (m)	
2'	1.70-1.76, 2.13-2.19 (m, m)	32.5
3'	5.18-5.23 (m)	73.2
4'	3.73 (ddd, 8.5, 6.0, 3.0)	70.6
5'	1.78-1.85 (m)	29.5
6'	1.51-1.61, 2.00-2.04 (m, m)	27.7
1		168.5
2	6.03 (d, 15.0)	121.5
3	7.43 (dd, 15.0, 11.0)	146.8
4	6.55 (dd, 15.0, 11.0)	127.4
5	6.76 (d, 15.0)	146.6
6		137.7
6-Me	1.96 (s)	12.7
7	6.41 (d, 11.5)	136.8
8	6.82 (dd, 13.5, 11.5)	132.3
9	6.63 (dd, 13.5, 11.5)	133.7
10	6.35 (d, 11.5)	136.6
11		136.0
12	2.86-2.90 (m)	49.6
12-Me	1.17, (d, 7.0)	17.3
13	4.04 (dd, 10.0, 1.5)	74.7
14	4.23 (d, 1.5)	78.9
15		211.4
16	2.84, 3.04 (dd, 14.0, 4.5, dd 17.0, 8.0)	45.9
17	4.36-4.40 (m)	66.5
18	4.17 (dd, 8.0, 2.5)	62.7
19	5.31 (t, 8.0)	75.7
19-carbamate		158.6
20	5.55 (ddt, 15.5, 7.5, 1.5)	126.9
21	5.89 (dt, 15.5, 6.5)	139.2
22	2.10 (dq, 7.5, 1.0)	26.3
23	1.02 (t, 7.5)	13.6

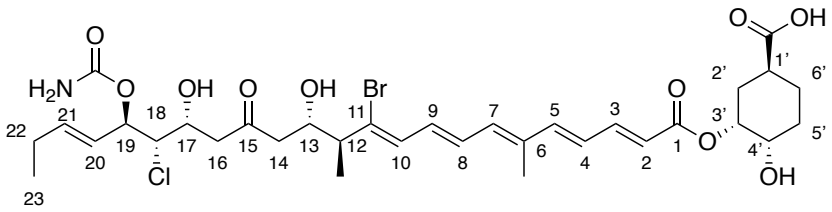

Table 6.16 NMR assignments for Δ5927_Br/Cl enacyloxin analogue **89** (d_4-MeOH, ^{1}H 500 MHz, ^{13}C 125 MHz)

Position	^{1}H (ppm)	^{13}C (ppm)
1'-COOH		
1'	2.46-2.55 (m)	
2'	1.69-1.76, 2.14-2.19 (m, m)	32.6
3'	5.18-5.23 (m)	73.3
4'	3.73 (ddd, 8.5, 6.0, 3.0)	70.8
5'	1.79-1.83 (m)	29.6
6'	1.47-1.64, 1.99-2.06 (m, m)	26.3
1		168.5
2	6.03 (d, 15.5)	121.5
3	7.43 (dd, 15.0, 11.0)	146.7
4	6.55 (dd, 15.0, 11.0)	127.4
5	6.76 (d, 15.0)	146.5
6		137.8
6-Me	1.96 (s)	12.7
7	6.41 (d, 11.5)	136.8
8	6.83 (dd, 14.0, 11.5)	132.4
9	6.60-6.65 (m)	133.7
10	6.35 (d, 11.5)	136.5
11		134.6
12	2.58-2.70 (m)	51.8
12-Me	1.13 (d, 7.0)	16.5
13	4.24 (td, 8.0, 3.5)	70.7
14	2.58-2.70 (m)	Solvent
15		209.6
16	2.90, 2,78 (dd, 17.0, 8.0, dd, 17.0, 5.0)	Solvent
17	4.44-4.48 (m)	66.6
18	3.99 (dd, 8.0, 2.5)	67.8
19	5.26 (t, 8.0)	75.5
19-carbamate		158.6
20	5.54 (ddt, 15.5, 7.5, 1.5)	126.2
21	5.89 (dt, 15.5, 6.5)	139.2
22	2.10 (dq, 7.5, 1.0)	26.3
23	1.01 (t, 7.5)	13.6

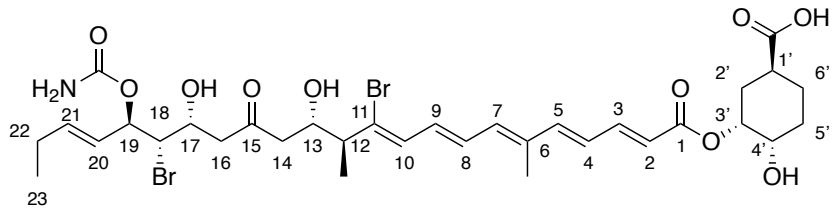

Table 6.17 NMR assignments for ∆5927_Br/Br enacyloxin analogue **88** (d_4-MeOH, ^{1}H 500 MHz, ^{13}C 125 MHz)

Position	^{1}H (ppm)	^{13}C (ppm)
1'-COOH		
1'	2.49-2.58	38.8
2'	1.69-1.77, 2.13-2.20 (m,m)	32.4
3'	5.17-5.24 (m)	73.1
4'	3.73 (ddd, 8.5, 6.0, 3.0)	70.7
5'	1.78-1.85 (m)	29.5
6'	1.51-1.62, 2.00-2.07 (m,m)	27.6
1		168.5
2	6.03 (d, 15.0)	121.5
3	7.43 (dd, 15.0, 11.0)	146.9
4	6.55 (dd, 15.0, 11.0)	127.4
5	6.76 (d, 15.0)	146.6
6		137.8
6-Me	1.96 (s)	12.7
7	6.41 (d, 11.5)	136.8
8	6.83 (dd, 13.5, 11.5)	132.4
9	6.61-6.68 (m)	133.8
10	6.35 (d, 11.5)	136.5
11		134.7
12	2.58-2.71 (m)	51.8
12-Me	1.13 (d, 7.0)	16.5
13	4.24 (td, 8.0, 3.5)	70.5
14	2.58-2.71 (m)	Solvent
15		209.5
16	2.90, 2.78 (dd, 17.0, 8.0, dd, 17.0, 4,5)	50.4
17	4.31-4.35 (m)	66.3
18	4.12 (dd, 8.0, 2.5)	62.6
19	5.30 (t, 8.0)	75.7
19-carbamate		158.6
20	5.54 (ddt, 15.5, 7.5, 1.5)	126.9
21	5.89 (dt, 15.5, 6.5)	139.2
22	2.10 (dq, 7.5, 1.0)	26.3
23	1.01 (t, 7.5)	13.6

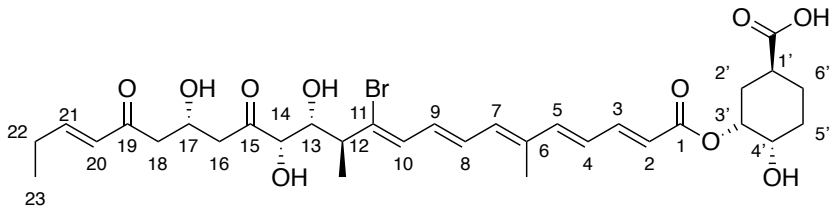

Table 6.18 NMR assignments for Δ5930_Br/H enacyloxin analogue **91** (d_4-MeOH, ^{1}H 500 MHz, ^{13}C 125 MHz)

Position	^{1}H (ppm)	^{13}C (ppm)
1'-COOH		
1'	2.46-2.58 (m)	
2'	1.69-1.79, 2.13-2.19 (m, m)	32.8
3'	5.18-5.23 (m)	73.4
4'	3.72 (ddd, 8.5, 6.0, 3.0)	70.8
5'	1.78-1.83 (m)	29.6
6'	1.49-1.63, 1.99-2.06 (m, m)	26.6
1		168.6
2	6.03 (d, 15.5)	121.5
3	7.43 (dd, 15.0, 11.0)	146.7
4	6.55 (dd, 15.0, 11.0)	127.4
5	6.76 (d, 15.0)	146.5
6		137.7
6-Me	1.96 (s)	12.6
7	6.41 (d, 11.5)	136.8
8	6.82 (dd, 14.0, 11.5)	132.2
9	6.62-6.65 (m)	133.7
10	6.35 (d, 11.5)	136.6
11		136.0
12	2.79-2.81 (m)	46.6
12-Me	1.17 (d, 6.5)	17.3
13	4.05 (dd, 10.0, 2.0)	74.7
14	4.23 (d, 1.5)	78.9
15		212.1
16	2.87 (dd, 16.5, 7.0)	47.6
17	2.79-2.82 (m)	47.5
18	4.55-4.61 (m)	65.5
19		201.3
20	6.14 (dt, 16.0, 1.5)	131.2
21	7.01 (dt, 16.0, 6.5)	151.8
22	2.28 (dq, 7.5, 1.5)	26.6
23	1.10 (t, 7.5)	12.7

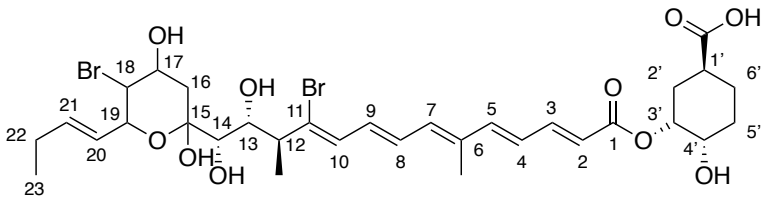

Table 6.19 NMR assignments for Δ5930_Br/Br enacyloxin analogue **90** (d_4-MeOH, ^{1}H 500 MHz, ^{13}C 125 MHz)

Position	^{1}H (ppm)	^{13}C (ppm)
1'-COOH		
1'	2.49-2.58 (m)	
2'	1.69-1.77, 2.16-2.20 (m, m)	32.5
3'	5.18-5.22 (m)	73.2
4'	3.73 (ddd, 8.5, 6.0, 3.0)	70.6
5'	1.78-1.85 (m)	29.5
6'	1.52-1.61, 2.00-2.06 (m, m)	27.7
1		168.5
2	6.03 (d, 15.0)	121.4
3	7.43 (dd, 15.0, 11.0)	146.8
4	6.55 (dd, 15.0, 11.0)	127.3
5	6.76 (d, 15.0)	146.6
6		137.6
6-Me	1.95 (s)	12.7
7	6.41 (d, 11.5)	136.9
8	6.81 (dd, 14.0, 11.5)	132.1
9	6.64-6.71 (m)	133.8
10	6.35 (d, 11.5)	136.6)
11		137.3
12	2.82 (dq, 9.5, 6.5)	49.6
12-Me	1.10 (d, 6.5)	17.1
13	4.16 (d, 9.5)	73.3
14	3.45 (d, 0.5)	73.4
15		100.5
16	2.44, 1.54 (dd, 13.0, 5.0, dd, 13.0, 1.5)	43.0
17	3.49 (t, 10.0)	61.5
18	4.01-4.08 (m)	70.9
19	4.46 (dd, 10.0, 7.0)	74.9
20	5.54 (ddt, 15.5, 7.0, 1.5)	128.0
21	5.83 (dt, 15.5, 6.5)	137.8
22	2.10 (dq, 7.5, 1.5)	26.4
23	1.02 (t, 7.5)	13.8

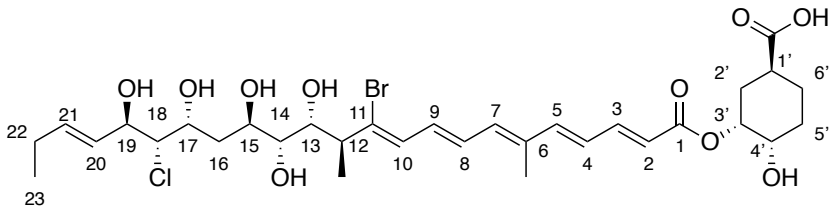

Table 6.20 NMR assignments for Δ5930 + Δ5932_Br/Cl enacyloxin analogue **93** (d_4-MeOH, ^{1}H 500 MHz, ^{13}C 125 MHz)

Position	^{1}H (ppm)	^{13}C (ppm)
1'-COOH		
1'	2.47-2.59 (m)	
2'	1.70-1.76, 2.17-2.19 (m,m)	32.5
3'	5.18-5.22 (m)	73.2
4'	3.70-3.74 (m)	70.6
5'	1.79-1.85 (m)	29.5
6'	1.54-1.61, 2.01-2.05 (m,m)	27.7
1		168.5
2	6.03 (d, 15.0)	121.4
3	7.43 (dd, 15.0, 11.0)	146.8
4	6.55 (dd, 15.0, 11.5)	127.3
5	6.76 (d, 15.0)	146.6
6		137.5
6-Me	1.96 (s)	12.7
7	6.42 (d, 11.5)	137.0
8	6.81 (dd, 14.5, 11.5)	131.9
9	6.65-6.73 (m)	134.0
10	6.35 (d, 11.5)	136.7
11		137.4
12	2.80 (dq, 9.5, 6.5)	49.6
12-Me	1.11 (d, 6.5)	17.2
13	3.95 (d, 9.5)	72.9
14	3.36 (d, 8.5)	74.1
15	3.88-3.93 (m)	69.6
16	1.46, 2.20-2.24 (ddd, 14.0, 10.0, 2.5, m)	40.5
17	4.27 (t, 7.5)	74.4
18	3.74 (dd, 7.5, 2.5)	71.1
19	4.43-4.47 (m)	67.8
20	5.59 (ddt, 15.5, 7.0, 1.5)	130.6
21	5.82 (dt, 15.3, 6.5)	136.6
22	2.10 (dq, 7.5, 1.5)	26.4
23	1.03 (t, 7.5)	13.8

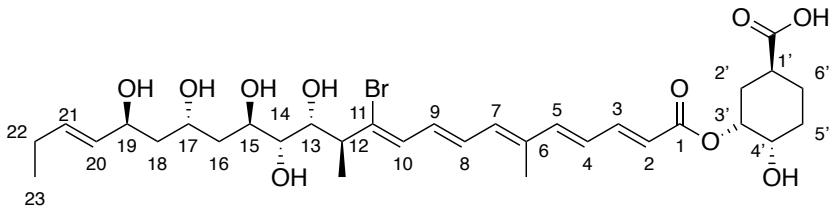

Table 6.21 NMR assignments for Δ5930 + Δ5932_Br/H enacyloxin analogue **94** (d_4-MeOH, ^{1}H 500 MHz, ^{13}C 125 MHz)

Position	^{1}H (ppm)	^{13}C (ppm)
1'-COOH		
1'	2.48-2.59 (m)	38.8
2'	1.70-1.76, 2.13-2.20 (m,m)	32.4
3'	5.18-5.22 (m)	73.1
4'	3.70-3.75 (m)	70.5
5'	1.79-1.84 (m)	29.5
6'	1.57-1.63, 2.00-2.03 (m,m)	27.6
1		168.5
2	6.03 (d, 15.0)	121.4
3	7.43 (dd, 15.0, 11.0)	146.8
4	6.54 (dd, 15.0, 11.0)	127.2
5	6.76 (d, 15.0)	146.6
6		137.5
6-Me	1.96 (s)	12.7
7	6.41 (d, 11.5)	137.0
8	6.81 (dd, 14.0, 11.5)	131.9
9	6.63-6.72 (m)	133.6
10	6.35 (d, 11.5)	136.7
11		137.5
12	2.80 (dq, 10.0, 6.5)	49.6
12-Me	1.11 (d, 6.5)	17.2
13	3.95 (d, 9.5)	72.8
14	3.36 (d, 8.0)	74.0
15	3.89-3.93 (m)	69.9
16	1.52, 1.90 (ddd, 14.0, 9.5, 2.5, ddd, 14.0, 10.0, 2.5)	42.7
17	4.12 (tt, 10.0, 3.0)	66.3
18	1.57-1.66 (m)	46.5
19	4.28 (dt, 6.5, 6.0)	70.3
20	5.50 (ddt, 15.5, 7.0, 1.5)	133.4
21	5.71 (dt, 15.5, 6.5)	134.0
22	2.06 (dq, 7.5, 1.0)	26.3
23	1.01 (t, 7.5)	14.0

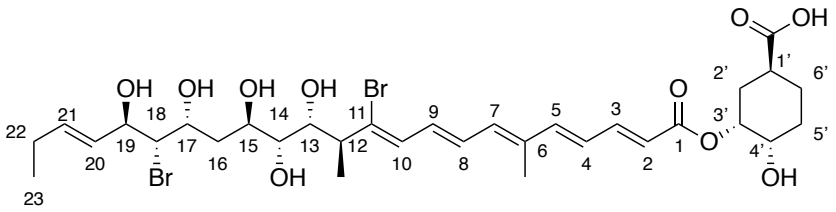

Table 6.22 NMR assignments for Δ5930 + Δ5932_Br/Br enacyloxin analogue **92** (d_4-MeOH, ^{1}H 500 MHz, ^{13}C 125 MHz)

Position	^{1}H (ppm)	^{13}C (ppm)
1'-COOH		
1'	2.48-2.61 (m)	38.8
2'	1.69-1.76, 2.14-2.17 (m,m)	32.4
3'	5.18-5.24 (m)	73.2
4'	3.73 (ddd, 8.5, 6.0, 3.0)	70.6
5'	1.78-1.85 (m)	29.5
6'	1.52-1.62, 2.01-2.06 (m,m)	27.6
1		168.5
2	6.03 (d, 15.5)	121.4
3	7.43 (dd, 15.0, 11.0)	146.8
4	6.55 (dd, 15.0, 11.0)	127.3
5	6.76 (d, 15.0)	146.6
6		137.5
6-Me	1.96 (s)	12.7
7	6.42 (d, 11.5)	137.0
8	6.81 (dd, 14.5, 11.5)	131.9
9	6.65-6.72 (m)	134.0
10	6.35 (d, 11.5)	136.7
11		137.3
12	2.80 (dq, 9.5, 6.5)	49.6
12-Me	1.11 (d, 6.5)	17.2
13	3.95 (d, 9.5)	72.9
14	3.36 (d, 8.0)	74.1
15	3.88-3.90 (m)	69.5
16	1.46, 2.21 (ddd, 14.0, 10.0, 2.4, ddd, 14.0, 10.0, 2.5)	41.8
17	4.29-4.35 (m)	67.6
18	3.92 (dd, 7.5, 2.5)	66.7
19	4.29-4.35 (m)	74.7
20	5.59 (ddt, 15.5, 7.0, 1.5)	130.7
21	5.81 (dt, 15.5, 6.5)	136.6
22	2.10 (dq, 7.5, 1.5)	26.3
23	1.03 (t, 7.5)	13.8

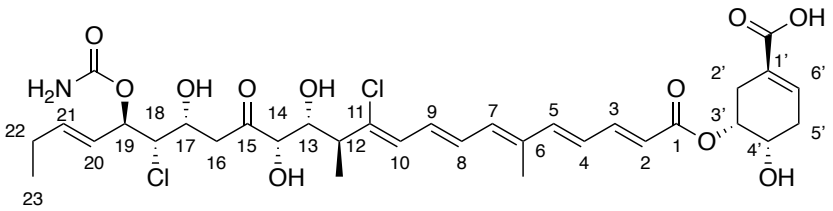

Table 6.23 NMR assignments for Δ5912-14 enacyloxin analogue **77** (d_4-MeOH, ^{1}H 500 MHz, ^{13}C 125 MHz)

Position	^{1}H (ppm)	^{13}C (ppm)
1'-COOH		
1'		
2'	2.58-2.42 (m)	32.7
3'	5.12 (td, *J* = 5.0, 2.0 Hz)	72.8
4'	4.08-4.02 (m)	66.9
5'	2.65-2.58 (m)	28.5
6'	6.90 (br s)	137.0
1		168.5
2	5.99 (d, *J* = 15.0 Hz)	121.1
3	7.42 (dd, *J* = 15.0, 11.0 Hz)	146.7
4	6.51 (dd, *J* = 15.0, 11.0 Hz)	128.4
5	6.78-6.68 (m)	147.0
6		137.4
6-Me	1.95 (s)	12.6
7	6.41 (d, *J* = 10.0. Hz)	137.0
8	6.78-6.68 (m)	131.6
9	6.78-6.68 (m)	131.6
10	6.43 (d, *J* = 10.0 Hz)	127.2
11		140.7
12	2.94 (dq, *J* = 9.5, 6.5 Hz)	47.5
12-Me	1.19 (d, *J* =7.0 Hz)	16.3
13	4.08-4.02 (m)	74.1
14	4.24 (d, *J* = 1.5 Hz)	78.9
15		211.4
16	3.05 (dd, *J* = 17.0, 8.0 Hz,), 2.84 (dd, dd, *J* = 17.0, 4.5 Hz)	44.5
17	4.51 (ddd, *J* = 7.5, 4.5, 2.5 Hz)	66.8
18	4.08-4.02 (m)	67.9
19	5.27 (t, *J* = 7.5 Hz)	75.5
19-carbamate		158.6
20	5.55 (ddt, *J* = 15.5, 7.5, 1.5 Hz)	126.2
21	5.89 (dt, *J* = 15.5, 6.5 Hz)	139.2
22	2.09 (qdd, *J* = 7.5, 6.5, 1.5 Hz)	26.3
23	1.01 (t, *J* = 7.5 Hz)	13.6

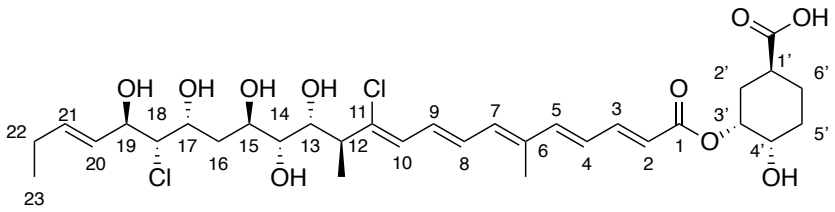

Table 6.24 NMR assignments for Δ5930 + Δ5932 enacyloxin analogue **40** (d_4-MeOH, ^{1}H 500 MHz, ^{13}C 125 MHz)

Position	^{1}H (ppm)	^{13}C (ppm)
1'-COOH		
1'	2.59-2.50 (m)	38.8
2'	2.19-2.14 (m), 1.74 (ddd, *J* = 14.0, 11.5, 2.0 Hz)	32.4
3'	5.22-5.18 (m)	73.1
4'	3.74-3.70 (m)	71.1
5'	1.85-1.77 (m)	29.4
6'	2.07-2.01 (m), 1.61-1.52 (m)	27.6
1		168.5
2	6.02 (d, *J* = 15.0 Hz)	121.3
3	7.43 (dd, *J* = 15.0, 11.0 Hz)	146.6
4	6.52 (dd, *J* = 15.0, 11.0 Hz)	127.9
5	6.76 (d, *J* = 15.0 Hz)	146.8
6		137.2
6-Me	1.96 (s)	12.7
7	6.41 (d, *J* = 9.5 Hz)	137.1
8	6.75-6.72 (m)	131.7
9	6.75-6.72 (m)	131.3
10	6.43 (d, *J* = 9.5 Hz)	127.1
11		142.0
12	2.88 (dq, *J* = 9.5, 7.0 Hz)	47.4
12-Me	1.13 (d, *J* = 7.0 Hz)	16.2
13	3.96 (d, *J* = 10.0 Hz)	72.2
14	3.37 (d, *J* = 8.0 Hz)	74.1
15	3.91 (ddd, *J* = 10.0, 8.0, 2.0 Hz)	69.5
16	2.21 (ddd, *J* = 14.0, 10.0, 2.0 Hz), 1.46 (ddd, *J* = 14.0, 10.0, 2.5 Hz)	40.4
17	4.45 (dt, *J* = 10.0, 2.0 Hz)	67.7
18	3.75 (dd, *J* = 7.5, 2.0 Hz)	70.5
19	4.27 (t, *J* = 7.5 Hz)	74.4
20	5.59 (ddt, *J* = 15.5, 7.0, 1.5 Hz)	130.1
21	5.82 (dt, *J* = 15.5, 7.0 Hz)	136.6
22	2.09 (qdd, *J* = 7.5, 6.5, 1.5 Hz)	26.3
23	1.02 (t, *J* = 7.5 Hz)	13.8

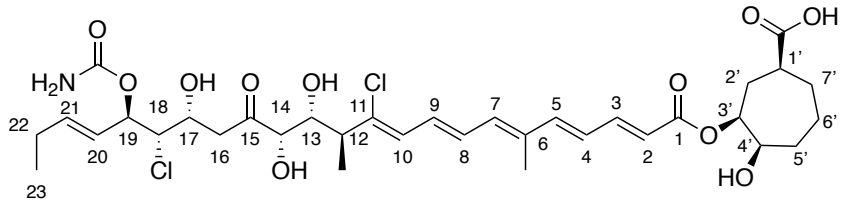

Table 6.25 NMR assignments for 7-membered enacyloxin analogue **146** (d_4-MeOH, ^{1}H 500 MHz, ^{13}C 125 MHz)

Position	^{1}H (ppm)	^{13}C (ppm)
1'-COOH		180.1
1'	2.73-2.64 (m)	40.4
2'	2.34 (ddd, *J* = 14.5, 8.0, 5.5), 2.04-1.97 (m)	33.3
3'	5.20 (dt, *J* = 8.4, 2.0 Hz)	76.3
4'	3.91 (dt, *J* = 8.4, 2.5 Hz)	73.8
5'	1.93-1.84 (m), 1.79-1.69 (m)	30.7
6'	1.79-1.69 (m), 1.69-1.60 (m)	22.1
7'	1.93-1.84 (m), 1.79-1.69 (m)	30.6
1		168.4
2	6.01 (d, *J* = 15.5 Hz)	121.2
3	7.43 (dd, *J* = 15.0, 11.5 Hz)	146.9
4	6.52 (dd, *J* = 15.0, 11.5 Hz)	127.2
5	6.79-6.69 (m)	146.6
6		137.4
6-Me	1.95 (s)	12.7
7	6.41 (d, *J* = 10.0 Hz)	137.0
8	6.79-6.68 (m)	131.5
9	6.79-6.68 (m)	131.6
10	6.44 (d, *J* = 9.5 Hz)	128.4
11		140.7
12	2.94 (dq, *J* = 10.0, 6.5 Hz)	47.5
12-Me	1.19 (d, *J* = 6.5 Hz)	16.3
13	4.06 (dd, *J* = 9.5, 1.5 Hz)	74.0
14	4.24 (d, *J* = 1.5 Hz)	78.9
15		211.4
16	3.05 (dd, *J* = 17.0, 8.0 Hz), 2.84 (dd, *J* = 17.0, 4.5 Hz)	44.5
17	4.51 (ddd, *J* = 7.5, 4.5, 2.5 Hz)	66.7
18	4.05 (dd, *J* = 8.0, 2.5 Hz)	67.9
19	5.27 (t, *J* = 7.5 Hz)	75.5
19-carbamate		158.6
20	5.55 (ddt, *J* = 15.5, 7.5, 1.5 Hz)	126.1
21	5.90 (dt, *J* = 15.5, 6.5 Hz)	139.2
22	2.09 (qdd, *J* = 7.5, 6.5, 1.5 Hz)	26.3
23	1.01 (t, *J* = 7.5 Hz)	13.6

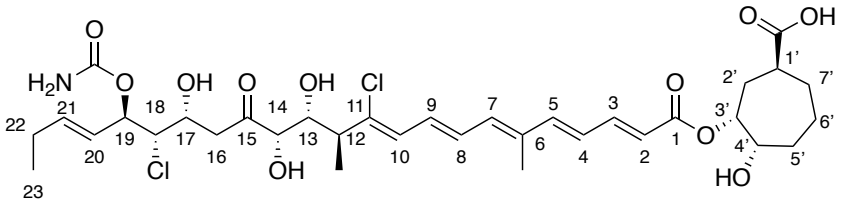

Table 6.26 NMR assignments for 7-membered enacyloxin analogue **145** (d_4-MeOH, ^{1}H 500 MHz, ^{13}C 125 MHz)

Position	^{1}H (ppm)	^{13}C (ppm)
1'-COOH		
1'	2.87-2.78 (m)	40.1
2'	2.20 (ddd, *J* = 14.5, 8.0, 5.0 Hz), 1.88 (ddd, *J* = 14.5, 9.0, 2.5 Hz)	34.6
3'	4.97 (dt, *J* = 8.5, 2.5 Hz)	78.8
4'	4.13 (dt, *J* = 7.5, 2.5 Hz)	70.9
5'	2.04-1.97 (m), 1.74-1.65 (m)	29.2
6'	1.74-1.65 (m)	22.3
7'	2.04-1.97 (m), 1.74-1.65 (m)	30.6
1		168.4
2	5.99 (d, *J* = 15.0 Hz)	121.4
3	7.43 (dd, *J* = 15.0, 11.5 Hz)	146.8
4	6.52 (dd, *J* = 15.0, 11.5 Hz)	127.2
5	6.79-6.68 (m)	146.6
6		137.4
6-Me	1.95 (s)	12.7
7	6.41 (d, *J* = 10.0 Hz)	137.0
8	6.79-6.68 (m)	131.6
9	6.79-6.68 (m)	131.6
10	6.43 (d, *J* = 9.5 Hz)	128.4
11		140.7
12	2.96 (dq, *J* = 10.0, 6.5 Hz)	47.6
12-Me	2.21 (d, *J* = 6.5 Hz)	16.3
13	4.07 (dd, *J* = 9.5, 1.5 Hz)	74.1
14	4.25 (d, *J* = 1.5 Hz)	78.9
15		211.5
16	3.07 (dd, *J* = 17.0, 8.0 Hz), 2.84 (dd, *J* = 17.0, 4.5 Hz)	44.6
17	4.53 (ddd, *J* = 7.5, 4.5, 2.5 Hz)	66.8
18	4.06 (dd, *J* = 8.0, 2.5 Hz)	67.9
19	5.29 (t, *J* = 7.5 Hz)	75.5
19-carbamate		158.6
20	5.57 (ddt, *J* = 15.5, 7.5, 1.5 Hz)	126.2
21	5.91 (dt, *J* = 15.5, 6.5 Hz)	139.3
22	2.10 (qdd, *J* = 8.5, 7.5, 1.5 Hz)	26.3
23	1.03 (t, *J* = 7.5 Hz)	13.6

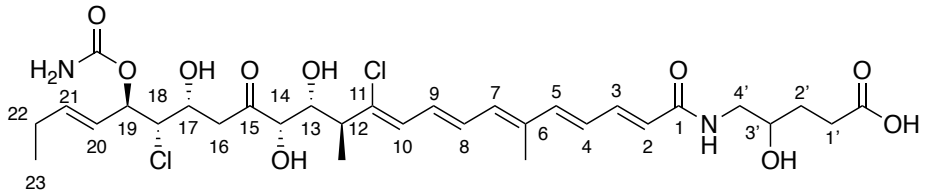

Table 6.27 NMR assignments for Δ5912-14 enacyloxin analogue **132** (d_4-MeOH, ^{1}H 500 MHz, ^{13}C 125 MHz)

Position	^{1}H (ppm)	^{13}C (ppm)
1'-COOH		
1'	1.11-1.03 (m)	23.2
2'	1.33-1.28 (m)	30.1
3'	3.75-3.57 (m)	69.7
4'	3.41-3.35 (m)	46.6
1		
2	6.10 (d, *J* = 15.5 Hz)	120.4
3	7.24 (dd, *J* = 14.5, 10.5 Hz)	142.4
4	6.47 (dd, *J* = 15.0, 11.0 Hz)	128.4
5	6.79-6.65 (m)	145.0
6		137.5
6-Me	1.95 (s)	12.6
7	6.37 (d, *J* = 10.0 Hz)	136.0
8	6.79-6.65 (m)	131.6
9	6.79-6.65 (m)	131.6
10	6.42 (d, *J* = 10.0 Hz)	127.5
11		140.4
12	2.93 (dq, *J* = 9.5, 6.5 Hz)	47.6
12-Me	1.19 (d, *J* = 7.0 Hz)	16.3
13	4.07-4.02 (m)	74.1
14	4.23 (d, *J* = 1.5 Hz)	79.0
15		211.5
16	3.04 (dd, *J* = 17.0, 8.0 Hz) 2.83 (dd, *J* = 17.0, 4.5 Hz)	44.6
17	4.51 (ddd, *J* = 7.5, 4.5, 2.5 Hz)	66.8
18	4.07-4.02 (m)	68.0
19	5.27 (t, *J* = 7.5 Hz)	75.5
19-carbamate		158.5
20	5.55 (ddt, *J* = 15.5, 7.5, 1.5 Hz)	126.2
21	5.90 (dt, *J* = 15.5, 6.5 Hz)	139.2
22	2.10 (qdd, *J* = 7.5, 6.5, 1.5 Hz)	26.3
23	1.02 (t, *J* = 7.5 Hz)	13.6

6.4 Chemical Synthesis

(*S*)-4-benzyl-3-(2-chloroacetyl)oxazolidin-2-one (98)

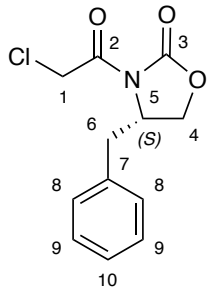

To a stirred solution of (*S*)-4-benzyloxazolidin-2-one (**96**) (10.00 g, 56.4 mmol) in anhydrous THF (115 mL) at -78 ^{o}C was added a 2.5 M solution of ^{n}BuLi (22.5 mL, 56.4 mmol) dropwise. The reaction mixture was stirred at -78 ^{o}C for 15 minutes followed by the addition of a solution of chloroacetyl chloride (8.1 mL, 101.6 mmol) in anhydrous THF (35mL). The solution was stirred for a further 30 minutes after which the cooling bath was removed and the reaction mixture allowed to warm to RT and stirred for a further 1 hour at RT. The reaction was quenched with sat.NH_4Cl (150 mL) and acidified with 1 M HCl (75 mL). The organics were extracted with EtOAc (2 x 200 mL), washed with brine (100 mL), dried with $MgSO_4$, filtered and concentrated *in vacuo* to afford a white solid. The crude material was purified using flash chromatography using silica gel (1:1 EtOAc: hexane) to afford a white powdered solid. The ^{1}H NMR spectrum of the product showed residual starting material remained so the solid was stirred in THF (75 mL) and sat.$NaHCO_3$ (75 mL) for 1 hour. The THF was removed *in vacuo* and organics extracted with EtOAc (2 x 150 mL), dried with $MgSO_4$ and concentrated *in vacuo* to give a white solid (12.41g, 49.1 mmol, 87 %, m.p. 77-78°C).

ν_{max}/cm^{-1} (neat) 1765 (C=O), 1600 (C=C), 1209 (C-N), 718 (C-Cl). **^{1}H NMR (500 MHz, $CDCl_3$):** δ = 7.37-7.32 (m, 2H; **H9**), 7.32-7.27 (m, 1H; **H10**), 7.23-7.19 (m, 2H; **H8**), 4.75 (s, 2H; **H1**), 4.71 (ddt, *J* = 7.5, 7.0, 3.0 Hz, 1H; **H5**), 4.32-4.24 (m, 2H; **H4**), 3.35 (dd, *J* = 13.5, 3.0 Hz, 1H; **H6**), 2.82 (dd, *J* = 13.5, 9.5 Hz, 1H; **H6**). **^{13}C NMR (125 MHz, $CDCl_3$):** δ = 166.3 (**C2**), 153.6 (**C3**), 134.8 (**C7**), 129.6 (**C9**), 129.3 (**C8**), 127.7 (**C10**), 67.2 (**C4**), 55.6 (**C5**), 43.9 (**C1**), 37.8 (**C6**). **HR MS (ESI, +ve, MeOH):** m/z calculated for $[C_{12}H_{12}ClNO_3 + Na]^+$; 276.0403, Found; 276.0397. $[\alpha]_D^{27}$ (c 0.27, $CHCl_3$); +76.0

(*S*)-4-benzyl-3-((2*S*,3*R*,*E*)-2-chloro-3-hydroxyhept-4-enoyl)oxazolidin-2-one (199)

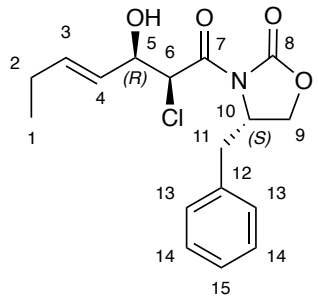

Procedure adapted from Son *et al*.[207] To a stirred solution of (*S*)-4-benzyl-3-(2-chloroacetyl)oxazolidin-2-one (**98**) (12.41 g, 49.0 mmol), in anhydrous CH_2Cl_2 (137 mL) at -78 °C was added diisopropylethylamine (11.41 mL, 66.7 mmol) and a solution of Bu_2BOTf (1.0 M in CH_2Cl_2, 58.9 mL, 58.9 mmol). The reaction mixture was stirred at RT for 1.5 hours followed by cooling to -78 °C and addition of trans-2-pentanal (7.2 mL, 73.6 mmol) solution in CH_2Cl_2 (26 mL). The solution was further stirred at -78 °C for 1 hour and 0 °C for 2 hrs. The reaction mixture was diluted with MeOH (235 mL) at 0 °C followed by a phosphate pH 7 buffer solution (section **6.2.2**) (118 mL) and 30% hydrogen peroxide (118 mL) and stirring continued for a further 1 hour. The organics were extracted with CH_2Cl_2 (2 x 150 mL), washed with brine (75 mL), dried over $MgSO_4$, filtered and concentrated *in vacuo*. The crude material was purified using flash chromatography using silica gel (1:2 EtOAc: hexane) to afford a pale oil (12.11 g, 35.9 mmol, 73 %).

ν_{max}/cm^{-1} (neat) 3300 (OH), 1774 (C=O), 1650 (C=C), 1209 (C-O), 700 (C-Cl). **^{1}H NMR (500 MHz, $CDCl_3$):** δ = 7.37-7.32 (m, 2H; **H14**), 7.31-7.27 (m, 1H; **H15**), 7.24-7.20 (m, 2H; **H13**), 5.91 (dt, *J* = 15.5, 6.5 Hz, 1H; **H3**), 5.71 (d, *J* = 5.0 Hz, 1H; **H6**), 5.53 (dd, *J* = 15.5, 6.5 Hz, 1H; **H4**), 4.70 (ddt, *J* = 6.5, 6.0, 4.0 Hz, 1H; **H10**), 4.63-4.59 (m, 1H; **H5**), 4.24 (d, *J* = 4.5 Hz, 2H; **H9**), 3.31 (dd, *J* = 13.5, 3.0 Hz, 1H; **H11**), 2.84 (dd, *J* = 13.5, 9.5 Hz, 1H; **H11**), 2.08 (dq, *J* = 7.0, 7.0 Hz, 2H; **H2**), 1.00 (t, *J* = 7.5 Hz, 3H; **H1**). **^{13}C NMR (125 MHz, $CDCl_3$):** δ = 168.0 (**C7**), 152.8 (**C8**), 137.9 (**C3**), 134.7 (**C12**), 129.6 (**C14**), 129.2 (**C13**), 127.7 (**C15**), 125.7 (**C4**), 72.9 (**C5**), 66.6 (**C9**), 59.8 (**C6**), 55.6 (**C10**), 37.4 (**C11**), 25.4 (**C2**), 13.3 (**C1**). **HR MS (ESI, +ve, MeOH):** m/z calculated for $[C_{17}H_{20}ClNO_4 + Na]^+$; 360.0979, Found; 360.0976. $[\alpha]_D^{27}$ (c 0.15, $CHCl_3$); +55.2

(*S*)-4-benzyl-3-((*S*,*E*)-3-hydroxyhept-4-enoyl)oxazolidin-2-one (100)

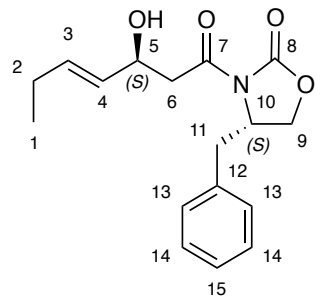

Procedure adapted from Son *et al*.[207] To a solution of (**199**) (100 mg, 0.3 mmol) in methanol (2 mL) was added activated zinc powder (77 mg, 1.2 mmol) and ammonium chloride (64 mg, 1.2 mmol). The suspensions were stirred vigorously for 5 minutes at RT. The reaction mixture was filtered, concentrated *in vacuo* and analysed by ^{1}H NMR. If starting material doublet for **H6** present, procedure repeated. The crude reaction product was purified using flash chromatography using silica gel (1:2 EtOAc: hexane) to afford a white solid (50.2 mg, 0.2 mmol, 56 %, m.p. 78-79°C).

Note: Upon addition of solvent system for column loading an off white precipitate formed. This was filtered, confirmed to not contain desired product and the filtrate concentrated *in vacuo* and purified.

ν_{max}/cm^{-1} (neat) 3439 (OH), 1784 (C=O) 1650 (C=C), **^{1}H NMR (500 MHz, $CDCl_3$):** δ = 7.37-7.32 (m, 2H; **H14**), 7.31-7.27 (m, 1H; **H15**), 7.24-7.20 (m, 2H; **H13**), 5.82 (dt, *J* = 15.5, 6.5 Hz, 1H; **H3**), 5.56 (dd, *J* = 15.5, 6.5 Hz, 1H; **H4**), 4.71 (ddt, *J* = 6.5, 6.0, 4.0 Hz, 1H; **H10**), 4.64-4.58 (m, 1H; **H5**), 4.25-4.17 (m, 2H; **H9**), 3.29 (dd, *J* = 13.5, 3.0 Hz, 1H; **H11**), 3.23 (dd, *J* = 17.5, 8.5 Hz, 2H; **H6**), 3.13 (dd, *J* = 17.5, 3.0 Hz, 2H; **H6**), 2.81 (dd, *J* = 13.5, 9.5 Hz, 1H; **H11**), 2.08 (qd, *J* = 7.0, 7.0 Hz, 2H; **H2**), 1.01 (t, *J* = 7.5 Hz, 3H; **H1**). **^{13}C NMR (125 MHz, $CDCl_3$):** δ = 172.5 (**C7**), 153.6 (**C8**), 135.2 (**C12**), 134.5 (**C3**), 129.6 (**C14** and **C4**), 129.2 (**C13**), 127.6 (**C15**), 69.0 (**C5**), 66.5 (**C9**), 55.2 (**C10**), 42.9 (**C6**), 38.0 (**C11**), 25.3 (**C2**), 13.4 (**C1**). **HR MS (ESI, +ve, MeOH):** m/z calculated for $[C_{17}H_{21}NO_4 + Na]^+$; 326.1368, Found; 326.1366. $[\alpha]_D^{27}$ (c 0.14, $CHCl_3$); +56.2

(*S*)-4-benzyl-3-((*S*,*E*)-3-((*tert*-butyldimethylsilyl)oxy)hept-4-enoyl)oxazolidin-2-one (101)

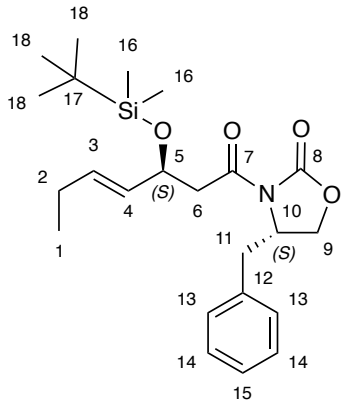

To a stirred solution of (*S*)-4-benzyl-3-((*S*,*E*)-3-hydroxyhept-4-enoyl)oxazolidin-2-one (100) (1.0 g, 3.3 mmol) in anhydrous DMF (11 mL) was added imidazole (337 mg, 5.0 mmol). To this solution was added *tert*-butyldimethylsilyl chloride (597 mg, 4.0 mmol) and the reaction stirred at RT overnight. The reaction mixture was diluted with diethyl ether (75 mL) and water (75 mL), The organics were extracted (2 x 100 mL), washed with brine (25 mL), dried with $MgSO_4$ and concentrated *in vacuo*. The crude reaction product was purified using flash chromatography using silica gel (1:2 EtOAc: hexane) to afford a white crystalline solid (1.30 g, 3.1 mmol, 94 %, m.p. 82-83°C). ν_{max}/cm^{-1} (neat) 1782 (C=O), 1650 (C=C). **^{1}H NMR (500 MHz, $CDCl_3$):** δ = 7.36-7.31 (m, 2H; **H14**), 7.30-7.27 (m, 1H; **H15**), 7.23-7.19 (m, 2H, **H13**), 5.68 (dt, *J* = 15.5, 6.5 Hz, 1H; **H3**), 5.49 (dd, *J* = 15.5, 7.5, 1H; **H4**), 4.71-4.67 (m, 2H; **H5, H10**), 4.19-4.12 (m, 2H; **H9**), 3.30 (dd, *J* = 13.5, 3.0 Hz, 1H; **H11**), 3.28 (d, *J* = 15.5 Hz, 1H; **H6**), 3.04 (dd, *J* = 15.5, 5.1 Hz, 1H; **H6**), 2.74 (dd, *J* = 13.5, 9.5 Hz, 1H; **H11**), 2.03 (qd, *J* = 7.0, 7.0 Hz, 2H; **H2**), 0.98 (t, *J* = 7.5 Hz, 3H; **H1**), 0.87 (s, 9H; **H18**), 0.06 (d, *J* = 9.0 Hz, 6H; **H16**). **^{13}C NMR (125 MHz, $CDCl_3$):** δ = 170.7 (**C7**), 153.5 (**C8**), 135.5 (**C12**), 133.3 (**C3**), 131.4 (**C4**), 129.6 (**C14**), 129.1 (**C13**), 127.5 (**C15**), 70.3 (**C10**), 66.2 (**C9**), 55.3 (**C5**), 44.7 (**C6**), 38.1 (**C11**), 26.0 (**C18**), 25.2 (**C2**), 13.5 (**C1**), -4.7 (**C16**). **HR MS (ESI, +ve, MeOH):** m/z calculated for $[C_{23}H_{35}NO_4Si + Na]^+$; 440.2233, Found; 440.2223. $[\alpha]_D^{27}$ (c 0.09, $CHCl_3$); +49.7

(*S*,*E*)-3-((*tert*-butyldimethylsilyl)oxy)hept-4-enoic acid (102)

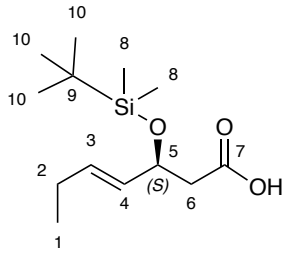

Procedure adapted from Liddle *et al*.[208] To a stirred solution of (*S*)-4-benzyl-3-((*S*,*E*)-3-((*tert*-butyldimethylsilyl)oxy)hept-4-enoyl)oxazolidin-2-one (**101**) (1.30 g, 3.1 mmol) in a mixture of THF (69 mL) and water (21 mL) (4:1) at 0 °C was added, 30% H_2O_2 solution (2.5 mL, 17.1 mmol) and LiOH (430 mg, 18.0 mmol). The reaction mixture was stirred at RT and monitored by TLC for conversion to desired product. At 0 °C Na_2SO_3 (3.12 g, 24.7 mmol) was added and the mixture quenched by stirring at RT for 15 minutes. The THF was removed *in vacuo* and the aqueous layer washed with CH_2Cl_2 (2 x 75 mL), acidified to pH 1 with conc.HCl then extracted with diethyl ether (2 X 75 mL). Organics were washed with brine (50 mL), dried with $MgSO_4$ and concentrated *in vacuo* to afford a colourless oil which used in the subsequent step without further purification (690 mg, 2.7 mmol, 86%).

ν_{max}/cm^{-1} (neat) 2998 (OH), 1694 (C=O), 1640 (C=C). **^{1}H NMR (500 MHz, $CDCl_3$):** δ = 5.70 (dt, *J* = 15.5, 6.5 Hz, 1H; **H3**), 5.43 (dd, *J* = 15.5, 7.5 Hz, 1H; **H4**), 4.56- 4.53 (m, 1H; **H5**), 2.60- 2.52 (m, 2H; **H6**), 2.04 (qd, *J* = 7.0, 7.0 Hz, 2H, **H2**), 0.98 (t, *J* = 7.5 Hz, 3H; **H1**), 0.88 (s, 9H; **H10**), 0.10-0.06 (m, 6H; **H8**). **^{13}C NMR (125 MHz, $CDCl_3$):** δ = 175.1 (**C7**), 134.3 (**C3**), 130.1 (**C4**), 70.8 (**C5**), 43.3 (**C6**), 30.0 (**C9**), 25.9 (**C10**), 25.2 (**C2**), 13.4 (**C1**), -4.0 (**C8**). **HR MS (ESI, +ve, MeOH):** m/z calculated for $[C_{13}H_{26}O_3Si + Na]^+$; 281.1549, Found; 281.1540. $[\alpha]_D^{27}$ (c 0.03, $CHCl_3$); -22.7

***S*-(2-acetamidoethyl) (*S*,*E*)-3-((*tert*-butyldimethylsilyl)oxy)hept4-enethioate (103)**

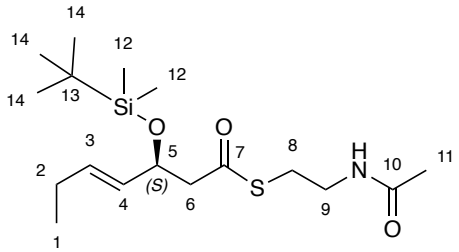

Procedure adapted from Liddle *et al*.[208] To a stirred solution of (*S*,*E*)-3-((*tert*-butyldimethylsilyl)oxy)hept-4-enoic acid (**102**) (683 mg, 2.7 mmol) in anhydrous CH_2Cl_2 (8 mL) at 0°C was added EDC·HCl (558 mg, 2.9 mmol) and DMAP (65 mg, 0.2 mmol). The reaction mixture was stirred at 0 °C for 15 minutes and a solution of *N*-acetylcysteamine (**27**) (346 mg, 2.9 mmol) in dry CH_2Cl_2 (2 mL) was added. The reaction was warmed to RT and stirred overnight. The reaction was diluted with water (25 mL), the organics extracted with CH_2Cl_2 (2 x 50 mL), dried with $MgSO_4$ and concentrated *in vacuo*. The crude product was purified using flash chromatography using silica gel (100% EtOAc) to afford a colourless oil (950.3 mg, 2.7 mmol, 54 %). ν_{max}/cm^{-1} (neat) 3310 (NH), 1743 (C=O), 1650 (C=C), 1200 (C-N). **^{1}H NMR (500 MHz, $CDCl_3$):** δ = 5.66 (dt, *J* = 15.5, 6.5 Hz, 1H; **H3**), 5.38 (dd, *J* = 15.5, 7.0 Hz, 1H; **H4**), 4.56 (td, *J* = 7.5, 5.0 Hz, 1H; **H5**), 3.46-3.37 (m, 2H; **H9**), 3.06-2.96 (m, 2H; **H8**), 2.80 (dd, *J* = 14.0, 8.0 Hz, 1H; **H6**), 2.62 (dd, *J* = 14.0, 4.5 Hz, 1H; **H6**), 2.02 (qd, *J* = 7.0, 7.0 Hz, 2H; **H2**), 1.96 (s, 3H; **H11**), 0.97 (t, *J* = 7.5 Hz, 3H; **H1**), 0.91 (s, 9H; **H14**), 0.10 (s, 6H; **H12**). **^{13}C NMR (125 MHz, $CDCl_3$):** δ = 197.9 (**C7**), 170.3 (**C10**), 133.6 (**C3**), 130.8 (**C4**), 71.1 (**C5**), 53.0 (**C6**), 39.8 (**C9**), 29.8 (**C13**), 28.9 (**C8**), 25.9 (**C14**), 25.8 (**C11**), 25.2 (**C2**), 13.5 (**C1**), -3.4 (**C12**). **HR MS (ESI, +ve, MeOH):** m/z calculated for $[C_{17}H_{33}NO_3SSi + Na]^+$; 382.1848, Found; 382.1839. $[\alpha]_D^{27}$ (c 0.04, $CHCl_3$); -53.8

_S_-(2-acetamidoethyl) (_S_,_E_)-3-hydroxyhept-4-enethioate (95)

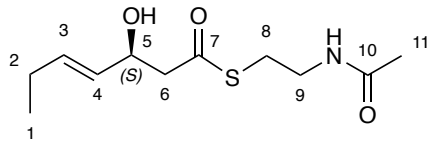

Procedure adapted from Liddle *et al*.[208] To a stirred solution of *S*-(2-acetamidoethyl) (*S*,*E*)-3-((*tert*-butyldimethylsilyl)oxy)hept-4-enethioate (**103**) (512 mg, 1.4 mmol) in THF (5) and water (5 mL) was added acetic acid (13.3 mL). The reaction mixture was stirred and reaction followed by TLC. Upon completion the reaction mixture was concentrated *in vacuo* whilst azeotroping with toluene. The crude product was purified using flash chromatography using silica gel (5% MeOH/EtOAc) to afford a colourless oil (304 mg, 1.2 mmol, 87%).

ν_{max}/cm^{-1} (neat) 3285 (OH), 1690 (C=O), 1650 (C=C). **^{1}H NMR (500 MHz, $CDCl_3$):** δ = 5.78 (dt, *J* = 15.5, 6.5 Hz, 1H; **H3**), 5.46 (dd, *J* = 15.5, 7.0 Hz, 1H; **H4**), 4.56 (td, *J* = 6.0, 5.5 Hz, 1H; **H5**), 3.48-3.41 (m, 2H; **H9**), 3.10-3.00 (m, 2H; **H8**), 2.83-2.78 (m, 2H; **H6**), 2.05 (qd, *J* = 7.0, 7.0 Hz, 2H; **H2**), 1.97 (s, 3H; **H11**), 0.99 (t, *J* = 7.5 Hz, 3H; **H1**). **^{13}C NMR (125 MHz, $CDCl_3$):** δ = 199.0 (**C7**), 170.5 (**C10**), 134.9 (**C3**), 129.4 **(C4**), 69.8 (**C5**), 51.2 (**C6**), 39.5 (**C9**), 29.0 (**C8**), 25.3 (**C2**), 23.4 (**C11**), 13.4 (**C1**). **HR MS (ESI, +ve, MeOH):** m/z calculated for $[C_{11}H_{19}NO_3S + Na]^+$; 268.0983, Found; 268.0976. $[\alpha]_D^{27}$ (c 0.09, $CHCl_3$); -27.3

S-(2-acetamidoethyl) ethanethioate (200)

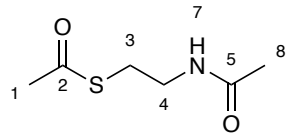

Procedure adapted from Jenner *et al*[209] and Wang *et al*.[210] To 0 °C stirred solution of cisteamine hydrochloride (3.5 g, 30.8 mmol) in water (20 mL) was added 6M KOH until pH 8 was reached. To this was added acetic anhydride (8.7 mL, 92.4 mmol) dropwise with a constant pH 8 being maintained using 6M KOH. Upon complete addition of acetic anhydride the pH was adjusted to pH 7 with 2M HCl and the reaction mixture stirred at 0 °C for 1.5 hours. The reaction mixture was saturated with NaCl and the organics were extracted with CH_2Cl_2 (2 x 75 mL), dried with $MgSO_4$ and concentrated *in vacuo* to give a colourless oil (4.4 g, 88%).

^{1}H NMR (500 MHz, $CDCl_3$): δ = 5.93 (br s, 1H; **H7**), 3.42 (q, *J* = 6.5 Hz, 2H; **H4**), 3.01 (t, *J* = 6.5 Hz, 2H; **H3**), 2.35 (s, 3H; **H1**), 1.96 (s, 3H; **H6**). **^{13}C NMR (125 MHz, $CDCl_3$):** δ = 196.5 (**C2**), 170.4 (**C5**), 39.7 (**C4**), 30.8 (**C1**), 28.9 (**C3**), 23.3 (**C6**). **HR MS (ESI, +ve, MeOH):** m/z calculated for $[C_6H_{11}NO_2S + Na]^+$; 184.0408, Found; 184.0404. Spectroscopic data was consistent with that of the literature.[209,210]

N-acetyl cisteamine (27)

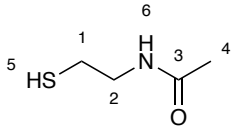

Procedure adapted from Li *et al*.[211] To a 0 °C stirred solution of S-(2-acetamidoethyl) ethanethioate (**200**) (800 mg, 5.0 mmol) in water (5 mL) was added KOH (892 mg, 15.9 mmol). The reaction mixture was warmed to RT and stirred for 50 minutes. The reaction was subsequently cooled to 0 °C and the pH adjusted to pH 5 with 2M HCl, The reaction mixture was saturated with NaCl and the organics were extracted with CH_2Cl_2, dried with $MgSO_4$ and concentrated *in vacuo* to give a colourless oil (430 mg, 73%).

^{1}H NMR (500 MHz, $CDCl_3$): δ = 5.96 (br s, 1H; **H6**), 3.43 (q, *J* = 6.5 Hz, 2H; **H2**), 2,67 (dt, *J* = 8.5, 6.5 Hz, 2H; **H1**), 2.01 (s, 3H; **H4**), 1.35 (t, *J* = 8.5 Hz, 1H; **H5**). **^{13}C NMR (125 MHz, $CDCl_3$):** δ = 170.4 (**C3**), 42.6 (**C2**), 24.8 (**C1**), 23.4 (**C4**). **HR MS (ESI, +ve, MeOH):** m/z calculated for $[C_4H_9NOS + Na]^+$; 142.0303, Found; 142.0293. Spectroscopic data was consistent with that of the literature.[211]

Synthesis of (*S*,*E*)-1-((*S*)-4-benzyl-2-oxooxazolidin-3-yl)-1-oxohept-4-en-3-yl (*S*)-3,3,3-trifluoro-2-methoxy-2-phenylpropanoate (201)

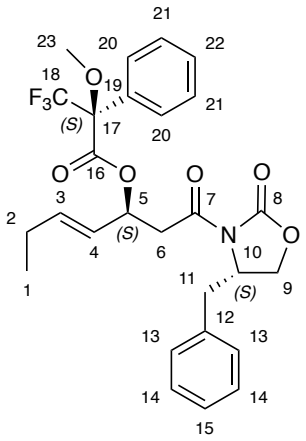

To a solution of (*R*)-(−)-α-Methoxy-α-(trifluoromethyl)phenylacetyl chloride (37 mg, 0.14 mmol) in CH_2Cl_2 (8 ml) was added DMAP (16mg, 0.13 mmol).The reaction mixture stirred at room temperature for 10 minutes after which (*S*)-4-benzyl-3-((*S*,*E*)-3-hydroxyhept-4-enoyl)oxazolidin-2-one (**100**) (40 mg, 0.13 mmol) was added. Stirring was continued for 24 hours with TLC monitoring. The crude mixture was concentrated *en vacuo* and purified using flash chromatography using silica gel (1:1, EtOAc:Hexane) to afford a colourless oil (15 mg, 22%).

^{1}H NMR (500 MHz, $CDCl_3$): δ = 7.54-7.49 (m, 2H; **H20**), 7.35-7.28 (m, 6H; **H14, H15, H21, H22**), 7.23-7.20 (m, 2H; **H13**), 6.05 (dt, *J* = 15.5, 6.1 Hz, 1H; **H3**), 5.56 (ddt, *J* = 15.4, 8.0, 1.5 Hz, 1H; **H4**), 4.75 (ddt, *J* = 9.6, 8.1, 3.3 Hz, 1H; **H5**), 4. 60 (ddt, *J* = 12.8, 11.2, 3.3 Hz, 1H; **H10**), 4.22-4.19 (m, 2H; **H9**), 3.57 (s, 3H; **H23**), 3.33 (dd, *J*= 13.65, 3.2 Hz, 1H; **H11**), 3.30-3.08 (m, 2H; **H6**), 2.81 (dd, *J* = 13.4, 9.6 Hz, 1H; **H11**), 2.12-2.05 (m, 2H; **H2**), 1.00 (t, *J* = 7.5 Hz, 3H; **H1**). **^{13}C NMR (125 MHz, $CDCl_3$):** δ = 168.8 (**C7**), 165.5 (**C16**), 153.5 (**C8**), 139.4 (**C3**), 135.4 (**C12**), 132.5 (**C19**), 129.5 (**C14**), 129.0 (**C13**, **C21**), 128.1 (**C15**, **C22**), 127.3 (**C20**), 124.6 (**C4**), 124.5 (**C18**), 66.1 (**C9**), 55.5 (**C5**), 55.4 (**C23**), 54.9 (**C10**), 40.4 (**C6**), 38.0 (**C11**), 25.2 (**C2**), 12.8 (**C1**). **HR MS (ESI, +ve, MeOH):** m/z calculated for $[C_{27}H_{28}F_3NO_6 + Na]^+$; 542.1766, Found; 542.1759

Synthesis of (*S*,*E*)-1-((*S*)-4-benzyl-2-oxooxazolidin-3-yl)-1-oxohept-4-en-3-yl (*R*)-3,3,3-trifluoro-2-methoxy-2-phenylpropanoate (202)

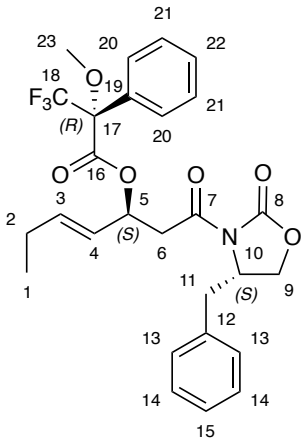

To a solution of (*S*)-4-benzyl-3-((*S*,*E*)-3-hydroxyhept-4-enoyl)oxazolidin-2-one (**100**) (25 mg, 0.082 mmol) in anhydrous CH_2Cl_2 (5 ml) was added (*R*)-(+)-α-Methoxy-α-trifluoromethylphenylacetic acid (22 mg, 0.091 mmol), EDC·HCl (18 mg, 0.091 mmol) and DMAP (11 mg, 0.082 mmol). The reaction mixture was stirred at RT for 24 hours and the reaction acidified with 1M HCl (5 ml). The organics were extracted with CH_2Cl_2, dried with $MgSO_4$ and concentrated *en vacuo*. The crude product was purified using flash chromatography using silica gel (1:1 EtOAc: hexane) to afford a colourless oil (15 mg, 0.03 mmol, 35%). **^{1}H NMR (500 MHz, $CDCl_3$):** δ = 7.53-7.51 (m, 2H; **H20**), 7.41-7.29 (m, 6H; **H14, H15, H21, H22**), 7.21-7.15 (m, 2H; **H13**), 5.98 -5.94 (m, 1H; **H3**), 5.42 (dd, *J* = 15.5, 7.5 Hz, 1H; **H4**), 4.78-4.70 (m, 1H; **H5**), 4.69-4.63 (m, 1H; **H10**),

4.24-4.15 (m, 2H; **H9**), 3.56 (s, 3H, **H23**), 3.36 (dd, *J* = 13.5, 3.2 Hz, 1H; **H11**), 3.24-3.19 (m, 2H; **H6**), 2.72 (dd, *J* = 13.4, 9.5 Hz, 1H; **H11**), 2.08-2.01 (m, 2H; **H2**), 0.97 (t, *J* = 7.5 Hz, 3H; **H1**). **^{13}C NMR (125 MHz, $CDCl_3$):** δ = 169.5 (**C7**), 165.8 (**C16**), 153.6 (**C8**), 137.8 (**C3**), 135.0 (**C12**), 129.6 (**C14**), 129.5 (**C19**), 129.2 (**C13**), 128.6 (**C21**), 127.6 (**C15**, **C22**), 127.4 (**C20**), 124.6 (**C4**), 124.1 (**C18**), 66.5 (**C9**), 56.1 (**C10**), 55.7 (**C5**), 55.5 (**C23**), 40.8 (**C6**), 37.8 (**C11**), 25.3 (**C2**), 13.1 (**C1**). **HR MS (ESI, +ve, MeOH):** m/z calculated for $[C_{27}H_{28}F_3NO_6 + Na]^+$; 542.1766, Found; 542.1758

Synthesis of (*R*)-*N*-(3-((2-aminoethyl)amino)-3-oxopropyl)-2,2,5,5-tetramethyl-1,3-dioxane-4-carboxamide (107)

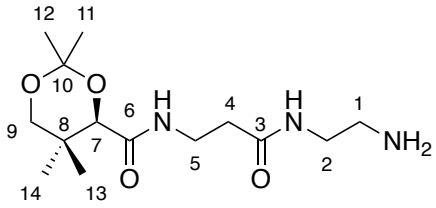

Procedure adapted from Weeks *et al*.[212] To a stirred solution of benzyl (*R*)-(2-(3-(2,2,5,5-tetramethyl-1,3-dioxane-4-carboxamido)propanamido)ethyl)carbamate (**106**) (3.027 g, 6.9 mmol) in MeOH (60 mL) was added Pd/C (10 wt%, 303 mg) and the reaction placed under an atmosphere of argon. The solution was sparged with hydrogen for 10 minutes and the reaction mixture stirred under an atmosphere of hydrogen for 16 hours. Upon completion the reaction mixture was filtered through celite and washed with EtOAc. The organics were concentrated *in* vacuo to yield a white gum (2.04 g, 98%).

^{1}H NMR (500 MHz, $CDCl_3$): δ = 7.04 (br t, *J* = 5.5 Hz, 1H; **NH**), 6.34 (br t, *J* = 5.5 Hz, 1H; **NH**), 4.07 (s, 1H; **H7**), 3.68 (d, *J* = 11.5 Hz, 1H; **H9**), 3.62-3.55 (m, 1H; **H5**), 3.55 -3.49 (m, 1H; **H5**), 3.34-3.28 (m, 2H; **H2**), 3.27 (d, *J* = 11.5 Hz, 1H; **H9**), 2.82 (t, *J* = 6.0 Hz, 2H; **H1**), 2.45 (t, *J* = 6.0 Hz, 2H; **H4**), 1.53 (br s, 2H; **NH_2**), 1.46 (s, 3H; **H13** or **H14**), 1.41 (s, 3H; **H14** or **H13**), 1.03 (s, 3H; **H11** or **H12**), 0.97 (s, 3H; **H12** or **H11**).**^{13}C NMR (125 MHz, $CDCl_3$):** δ = 171.4 (**C3** or **C6**), 170.3 (**C6** or **C3**), 99.2 (**C10**), 77.3 (**C7**), 71.6 (**C9**), 42.2 (**C2**), 41.5 (**C1**), 36.3 (**C4**), 35.0 (**C5**), 33.1 (**C8**), 29.6 (**C13** or **C14**), 22.3 (**C11** or **C12**), 19.0 (**C12** or **C11**), 18.8 (**C14** or **C13**). **HR MS (ESI, +ve, MeOH):** m/z calculated for $[C_{14}H_{27}N_3O_4 + Na]^+$; 324.1899, Found; 324.1897. Spectroscopic data was consistent with that of the literature.[212]

Synthesis of ethyl (*R*)-3-oxo-3-((2-(3-(2,2,5,5-tetramethyl-1,3-dioxane-4-carboxamido)propanamido)ethyl)amino)propanoate (109)

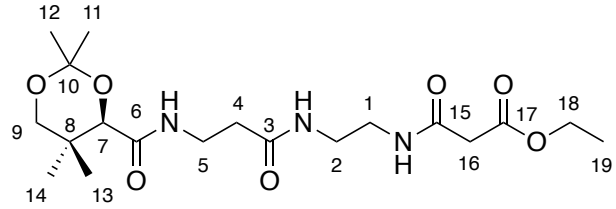

Procedure adapted from Tosin *et al*.[176] To a 0 °C cooled stirred solution of **107** (500 mg, 1.67 mmol), DIPEA (0.4 ml, 2.32 mmol) and mono-ethyl malonate (**108**) (0.25 ml, 2.16 mmol) in anhydrous THF (35 ml) was added HATU (694 mg, 1.83 mmol) and the reaction mixture stirred for 16 hours at 0 °C. The reaction mixture was concentrated *in vacuo* and the crude residue purified using flash chromatography using silica gel (17:3, CH_2Cl_2: MeOH) to afford **109** as a pale white gum (632.2 mg, 92 %).

ν_{max}/cm^{-1} (neat)1739 (C=O), 1639 (C=C), 1249 (C-N), 1197 (C-O); **^{1}H NMR (500 MHz, $CDCl_3$):** δ = 7.48 (s, 1H; **NH**), 7.04 (s, 1H; **NH**), 6.54 (s, 1H, **NH**), 4.21 (q, *J* = 7.0 Hz, 2H; **H18**), 4.08 (s, 1H; **H7**), 3.68 (d, *J* = 11.5 Hz, 1H; **H9**), 3.61-3.55 (m, 1H; **H5**), 3.54-3.48 (m, 1H; **H5**), 3.46-3.37 (m, 4H; **H1** and **H2**), 3.31 (s, 2H; **H16**), 3.28 (d, *J* = 11.5 Hz, 1H; **H9**), 2.46 (t, *J* = 6.0 Hz, 2H; **H4**), 1.46 (s, 3H; **H13** or **H14**), 1.42 (s, 3H; **H14** or **H13**), 1.29 (t, *J* = 7.5 Hz, 3H; **H19**), 1.03 (s, 3H; **H11** or **H12**), 0.97 (s, 3H; **H12** or **H11**). **^{13}C NMR (125 MHz, $CDCl_3$):** δ = 171.8 (**C3**), 170.4 (**C17** or **C15**), 169.5 (**C6**), 166.5 (**C15** or **C17**), 99.3 (**C10**), 77.3 (**C7**), 71.6 (**C9**), 61.9 (**C18**), 41.5 (**C16**), 40.0 (**C1** or **C2**), 39.8 (**C2** or **C1**), 36.5 (**C4**), 35.1 (**C5**), 33.1 (**C8**), 29.6 (**C13** or **C14**), 22.3 (**C11** or **C12**), 19.0 (**C12** or **C11**), 18.8 (**C14** or **C13**), 14.2 (**C19**). **HR MS (ESI, +ve, MeOH):** m/z calculated for $[C_{19}H_{33}N_3O_7 + Na]^+$; 438.2216, Found; 438.2211. $[\alpha]_D^{30}$ (c 0.10, $CHCl_3$); +37.5.

Synthesis of ethyl (*R*)-3-((2-(3-(2,4-dihydroxy-3,3-dimethylbutanamido)propanamido)ethyl)amino)-3-oxopropanoate (110)

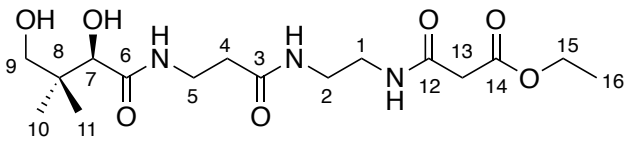

109 (20 mg, 0.048 mmol) was stirred in a solution of AcOH:H_2O (6ml, 2:1) at RT for 16 hours. The RM was concentrated *in vacuo* and purified using flash chromatography using silica gel (17:3, CH_2Cl_2: MeOH) to afford **110** as a pale white gum (13.5 mg, 75%).

ν_{max}/cm^{-1} (neat) 3271 (OH), 1621 (C=C), 1235 (C-N); **^{1}H NMR (500 MHz, MeOD):** δ = 4.12 (q, *J* = 7.0 Hz, 2H; **H15**), 3.91 (s, 1H; **H7**), 3.53-3.48 (m, 2H; **H5**), 3.48-3.38 (m, 2H; **H9**), 3.35-3.30 (m, 6H; **H1**, **H2** and **H13**), 2.44 (t, *J* = 6.5 Hz, 2H; **H4**), 1.29 (t, *J* = 7.0 Hz, 3H; **H16**), 0.94 (s, 6H; **H10** and **H11**).**^{13}C NMR (125 MHz, MeOD):** δ = 176.1 (**C6**), 174.2 (**C3**), 170.0 (**C14**), 168.9 (**C12**), 77.3 (**C7**), 70.3 (**C9**), 62.4 (**C15**), 40.4 (**C13**), 40.1 (**C1** or **C4**), 39.9 (**C2** or **C5**), 36.6 **(C4** or **C1**), 36.4 (**C5** or **C2**), 21.3 (**C10** or **C11**), 20.9 (**C11** or **C10**), 14.4 (**C16**). **HR MS (ESI, +ve, MeOH):** m/z calculated for $[C_{16}H_{29}N_3O_7 + Na]^+$; 398.1903, Found; 398.1884. $[\alpha]_D^{30}$ (c 0.02, MeOH); +28.0.

Synthesis of (*R*)-3-((2-(3-(2,4-dihydroxy-3,3-dimethylbutanamido)propanamido)ethyl)amino)-3-oxopropanoic acid (111)

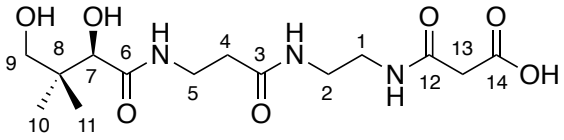

Procedure adapted from Tosin *et al*.[176] To a solution of **110** (5 mg, 0.0133 mmol) in wet methanol (2 ml) was added K_2CO_3 (6 mg, 0.043 mmol) and the RM stirred at RT for 16 hours. The RM was concentrated *in vacuo* and water removed by lyophilisation to afford **111** as a white gum in a quantitative yield.

^{1}H NMR (500 MHz, MeOD): δ = 3.91 (s, 1H; **H7**), 3.52-3.46 (m, 2H; **H5**), 3.47 (d, *J* = 11.0 Hz, 1H; **H9**), 3.38 (d, *J* = 11.0 Hz, 1H; **H9**), 3.32-3.30 (m, 6H; **H1**,**H2** and **H13**), 2.42 (t, *J* = 6.5 Hz, 2H; **H4**), 0.92 (s, 6H; **H10** and **H11**). **^{13}C NMR (125 MHz, MeOD):** δ = 175.1 (**C6**), 173.4 (**C14**), 173.0 (**C3**), 170.8 (**C12**), 77.3 (**C7**), 70.3 (**C9**), 40.4 (**C13**), 40.1 (**C1** or **C4**), 39.9 (**C2** or **C5**), 36.6 (**C4** or **C1**), 36.4 (**C5** or **C2**), 21.4 (**C10**), 21.0 (**C11**). **HR MS (ESI, -ve, MeOH):** m/z calculated for $[C_{14}H_{24}N_3O_7]^-$; 346.1614, Found; 346.1634

Spectroscopic data is consistent with that found in the literature.[213]

Synthesis of 6-(but-1-en-1-yl)dihydro-2*H*-pyran-2,4(3*H*)-dione (117)

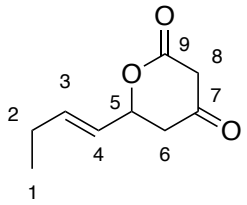

Synthesis adapted from Friedrich *et* al.[214] Under an atmosphere of argon, sodium hydride (60% oil suspension, 900 mg, 22.2 mmol) was suspended in anhydrous THF (40 mL) and cooled to 0 °C. To the stirred solution was added methyl acetoacetate (2 mL,. 18.5 mmol) dropwise. Once gas evolution ceased the solution cooled to -78 °C followed by dropwise addition of ^{n}BuLi (1.6 M in hexanes, 13 mL, 20.4 mmol). The reaction mixture was warmed to 0 °C and stirred for 30 minutes before being subsequently cooled to -78 °C. To the cooled solution was added *trans*-2-pentenal (2.0 mL, 20.4 mmol) dropwise and the reaction mixture stirred for 30 minutes at RT. The reaction was quenched with the addition of NH_4Cl (40 mL) at 0 °C, the aqueous layer washed with EtOAc and acidified to pH 1 with concentrated HCl. The organics were extracted with EtOAc, dried with $MgSO_4$ and concentrated *in vacuo* to afford the desired product as pale yellow gum (143 mg, 5%).

ν_{max}/cm^{-1} (neat) 1697 (C=O), 1650 (C=C), 1102 (C-O); **^{1}H NMR (500 MHz, $CDCl_3$):** δ = 5.94 (dtd, *J* = 15.5, 6.0, 1.0 Hz, 1H; **H3**), 5.55 (ddt, *J* = 15.5, 6.0, 1.5 Hz, 1H; **H4**), 5.12 (ddd, *J* = 9.5, 6.0, 3.5 Hz, 1H; **H5**), 3.54 (d, *J* = 20.0 Hz, 1H; **H8**), 3.45 (d, *J* = 20.0 Hz, 1H; **H8**), 2.77 (dd, *J* = 18.0, 3.5 Hz, 1H; **H6**), 2.64 (dd, *J* = 18.0, 9.5 Hz, 1H; **H6**), 2.13 (quin, *J* = 7.0 Hz, 2H; **H2**), 1.03 (t, *J* = 7.5 Hz, 3H; **H1**). (4:1 trans : cis). **^{13}C NMR (125 MHz, $CDCl_3$):** δ = 200.0 (**C7**), 167.2 (**C9**), 138.6 (**C3**), 124.4 (**C4**), 75.7 (**C5**), 47.1 (**C8**), 43.6 (**C6**), 25.4 (**C2**), 13.0 (**C1**). **HR MS (ESI, +ve, MeOH):** m/z calculated for $[C_9H_{12}O_3 + Na]^+$; 191.0684, Found; 191.0680. $[\alpha]_D^{30}$ (c 0.08, $CHCl_3$); +4.7.

Synthesis of (3a*R*,4*R*,7*S*,8a*R*)-7-hydroxy-2,2-dimethyltetrahydro-4,7-methano[1,3]dioxolo[4,5-*c*]oxepin-6(4*H*)-one (120)

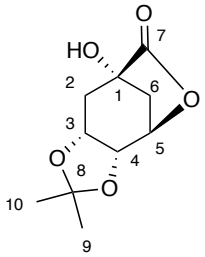

Procedure adapted from Kawashima *et al*[215] and Wang *et al*.[216,217] To a solution of D-(−)-Quinic acid (8.00 g, 41.6 mmol) (**119**) in acetone (120 mL) was added 2,2-dimethoxypropane (16.0 mL, 130 mmol) and *p*-toluenesulfonic acid monohydrate (80 mg, 0.4 mmol) and stirred under reflux for 4 hours. The reaction mixture was concentrated *in vacuo*, the crude residue dissolved in EtOAc (100 mL), washed with sat.$NaHCO_3$ (50 mL), brine (50 mL), dried with $MgSO_4$ and the combined organics concentrated *in vacuo* to leave a white solid (8.57g, 40.0 mmol, 96%).

^{1}H NMR (500 MHz, $CDCl_3$): δ = 4.73 (dd, *J* = 6.0, 2.0 Hz, 1H; **H5**), 4.50 (td, *J* =7.5, 5.0 Hz, 1H; **H3**), 4.32-4.29 (m, 1H; **H4**), 2.65 (d, *J* = 12.0 Hz, 1H; **H6**), 2.39-2.33 (m, 1H; **H2**), 2.33-2.27 (m, 1H; **H6**), 2.18 (dd, *J* = 15.0, 3.0 Hz, 1H; **H2**), 1.52 (s, 3H; **H9/10**), 1.33 (s, 3H; **H10/9**). **^{13}C NMR (125 MHz, $CDCl_3$):** δ = 178.8 (**C7**), 110.0 (**C8**), 76.0 (**C5**), 72.3 (**C4**), 71.7 (**C3**), 71.6 (**C1**), 38.4 (**C2**), 34.4 (**C6**), 27.1 (**C10/9**), 24.4 (**C9/10**). **HR MS (ESI, +ve, MeOH):** m/z calculated for $[C_{10}H_{14}O_5 + Na]^+$; 237.0739, Found; 237.0731. Spectroscopic data was consistent with that of the literature.

Synthesis of methyl (3a*R*,5*R*,7*R*,7a*S*)-5,7-dihydroxy-2,2-dimethylhexahydrobenzo[*d*][1,3]dioxole-5-carboxylate (121)

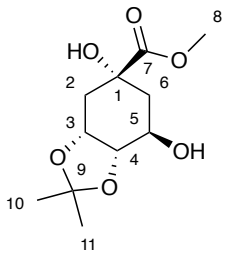

Procedure adapted from Wang *et al*.[216,217] To a stirred solution of **120** (8.57 g, 40.0 mmol), in methanol (237 mL) was added NaOMe (2.16 g, 40.0 mmol) and the reaction mixture stirred at RT for 3 hours. The reaction was quenched with the addition of

acetic acid (2.3 mL) and the methanol removed *in vacuo*. The crude material was extracted with EtOAc, washed with water, brine, dried with $MgSO_4$ and concentrated *in vacuo*. The crude product was purified using flash chromatography using silica gel (100% EtOAc) to afford a colourless oil (5.00g, 51%) alongside recovered lactone starting material (820 mg, 3.3 mmol, 9.6 %).

^{1}H NMR (500 MHz, $CDCl_3$): δ = 4.47 (dt, *J* = 5.5, 4.0 Hz, 1H; **H5**), 4.17-4.12 (m, 1H; **H4**), 3.98 (t, *J* = 6.5 Hz, 1H; **H3**), 3.81 (s, 3H; **H8**), 2.26 (d, *J* = 3.5 Hz**,** 2H; **H6**), 2.07 (dd, *J* = 13.5, 4.0 Hz, 1H; **H2**), 1.88 (dd, *J* = 11.0, 3.0 Hz, 1H; **H2**), 1.54 (s, 3H; **H11/10**), 1.37 (s, 3H; **H10/11**). **^{13}C NMR (125 MHz, $CDCl_3$):** δ = 175.8 (**C7**), 109.4 (**C9**), 79.9 (**C3**), 74.0 (**C1**), 73.5 (**C5**), 68.3 (**C4**), 53.3 (**C8**), 39.0 (**C2**), 34.8 (**C6**), 28.3 (**C11/10**), 25.9 (**C10/11**). **HR MS (ESI, +ve, MeOH):** m/z calculated for $[C_{11}H_{18}O_6 + Na]^+$; 269.1001, Found; 269.0992. Spectroscopic data was consistent with that of the literature.

Synthesis of methyl (3a*R*,7a*R*)-2,2-dimethyl-7-oxo-3a,4,7,7a-tetrahydrobenzo[*d*][1,3]dioxole-5-carboxylate (122)

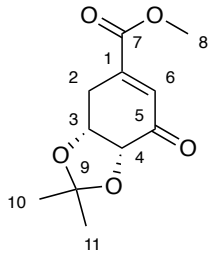

Procedure adapted from Wang *et al*.[216,217] To a stirred solution of **121** (5.00 g, 20.3 mmol), 3Å molecular sieves (10 g) anhydrous pyridine (5.04 mL, 62.3 mmol) in anhydrous CH_2Cl_2 was added pyridinium chlorochromate (17.2 g, 79.8 mmol). The reaction mixture was stirred at RT for 24 hours and filtered through celite. The filtrate was washed with brine (50 mL), dried with $MgSO_4$ and the organics concentrated *in vacuo*. The crude product was purified with flash chromatography using silica gel (50% EtOAc:Hexane) to afford a white powder (2.30 g, 10.2 mmol, 50%).

^{1}H NMR (500 MHz, $CDCl_3$): δ = 6.85 (d, *J* = 2.5 Hz, 1H; **H6**), 4.70 (td, *J* = 5.0, 1.0 Hz, 1H; **H3**), 4.31 (d, *J* = 5.0 Hz, 1H; **H4**), 3.86 (s, 3H; **H8**), 3.22 (d, *J* = 20.0 Hz, 1H; **H2**), 2.88 (ddd, *J* = 20.0, 5.0, 3.0 Hz, 1H; **H2**), 1.41 (s, 3H; **H10**), 1.33 (s, 3H; **H11**). **^{13}C NMR (125 MHz, $CDCl_3$):** δ = 197.6 (**C5**), 166.3 (**C7**), 144.4 (**C1**), 131.4 (**C6**), 109.8 (**C9**), 75.3 (**C4**),

72.7 (**C3**), 53.1 (**C8**), 26.8 (**C2**), 26.0 (**C10**), 27.5 (**C11**). **HR MS (ESI, +ve, MeOH):** m/z calculated for $[C_{11}H_{14}O_5 + Na]^+$; 249.0739, Found; 249.0735. Spectroscopic data was consistent with that of the literature.

Methyl (3a*R*,7a*S*)-7-hydroxy-2,2-dimethyl-3a,4,7,7a-tetrahydrobenzo[*d*][1,3]dioxole-5-carboxylate (123)

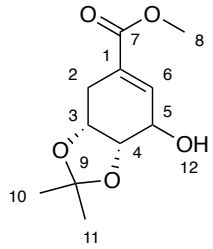

Procedure adapted from Wang *et al*.[216,217] To a solution of **122** (2.25 g, 10.0 mmol) in methanol (20 mL) at 0 ^oC was added $NaBH_4$ (414 mg, 10.9 mmol) and the reaction mixture stirred for 30 minutes. The reaction was quenched with sat.NH_4Cl (50 mL) and methanol removed *in vacuo*. The organics were extracted with CH_2Cl_2 (2 x 100 mL), washed with brine (50 mL), dried with $MgSO_4$ and concentrated *in vacuo* to afford a colourless oil which was not further purified (2.16 g, 9.5 mmol, 95%).

^{1}H NMR (500 MHz, $CDCl_3$): δ = 6.94 (s, 1H; **H6**), 4.64 (ddd, *J* = 7.5, 4.0, 2.5 Hz, 1H; **H3**), 4.56 (ddd, *J* = 6.5, 5.0, 1.0 Hz, 1H; **H5**), 4.07 (ddt, *J* = 10.0, 4.5, 2.5 Hz, 1H; **H4**), 3.77 (s, 3H; **H8**), 3.04 (dd, *J* = 16.5, 1.5 Hz, 1H; **H2**), 2.70 (d, *J* = 11.0 Hz, 1H; **H12**), 1,95 (ddd, *J* = 16.5, 7.0, 3.0 Hz, 1H; **H2**), 1.33 (s, 3H, **H11**), 1.32 (s, 3H; **H10**). **^{13}C NMR (125 MHz, $CDCl_3$):** δ = 166.3 (**C7**), 142.6 (**C6**), 128.5 (**C1**), 109.2 (**C9**), 76.2 (**C5**), 72.5 (**C3**), 68.1 (**C4**), 52.1 (**C8**), 26.6 (**C2**), 26.0 (**C11**), 24.5 (**C10**). **HR MS (ESI, +ve, MeOH):** m/z calculated for $[C_{11}H_{16}O_5 + Na]^+$; 251.0895, Found; 251.0890. Spectroscopic data was consistent with that of the literature.

methyl (3a*R*,7a*R*)-2,2-dimethyl-7-((methylsulfonyl)oxy)-3a,4,7,7a-tetrahydrobenzo[*d*][1,3]dioxole-5-carboxylate (124)

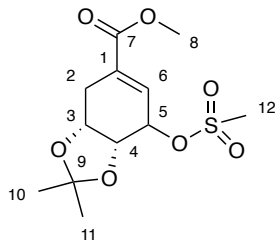

To a stirred solution of **123** (2.14 g, 9.4 mmol) in CH_2Cl_2 (60 mL) at 0 °C was added Et_3N (1.31 mL, 93.8 mmol) and MsCl (3.62 mL, 46.9 mmol). The reaction mixture was stirred at 0 °C for 2 hours and monitored by TLC. Upon completion the reaction was quenched with water (50 mL), acidified with 1M HCl (25 mL) and organics extracted with DCM (2 x 100 mL). The organics were washed with brine (50 mL), dried with $MgSO_4$ and concentrated *in vacuo* affording a colourless oil. The crude product was purified with flash chromatography using silica gel (50% EtOAc:Hexane) to afford a white powder (2.48 g, 8.1 mmol, 86%, m.p. 88-99 °C)

ν_{max}/cm^{-1} (neat) 1701 (C=O), 1351 (S=O), 1063 (C-O); **^{1}H NMR (500 MHz, $CDCl_3$):** δ = 6.95 (s, 1H; **H6**), 5.06 (ddd, *J* = 4.5, 2.5, 2.5 Hz, 1H; **H5**), 4.76-4.71 (m, 1H; **H4**), 4.68-4.64 (m, 1H; **H3**), 3.79 (s, 3H; **H8**), 3.17 (s, 3H; **H12**), 3.08 (dd, *J* = 16.5, 1.5 Hz, 1H; **H2**), 2.00 (ddd, *J* = 16.5, 6.5, 3.0 Hz, 1H; **H2**), 1.35 (s, 3H; **H11**), 1.33 (s, 3H; **H10**). **^{13}C NMR (125 MHz, $CDCl_3$):** δ = 165.5 (**C7**), 136.2 (**C6**), 130.8 (**C1**), 109.9 (**C9**), 75.7 (**C5**), 75.5 (**C4**), 72.6 (**C3**), 52.4 (**C8**), 39.2 (**C12**), 27.3 (**C2**), 25.9 (**C11**), 24.4 (**C10**). **HR MS (ESI, +ve, MeOH):** m/z calculated for $[C_{12}H_{18}O_7S + Na]^+$; 329.0671, Found; 329.0664

methyl (3a*R*,7a*S*)-2,2-dimethyl-3a,4,7,7a-tetrahydrobenzo[*d*][1,3]dioxole-5-carboxylate (125)

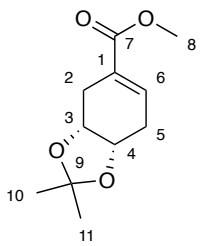

Procedure adapted from Nakuamura *et al*.[218]To a solution of $Pd_2(dba)_3{\cdot}CHCl_3$ (414 mg, 0.4 mmol), PBu_3 (0.1 mL, 0.4 mmol), and **124** (2.45 g, 8.0 mmol) in dioxane (57 mL) under an atmosphere of argon was added a suspension of $NaBH_4$ (303 mg, 8.0

mmol) in water (4.5 mL). The reaction mixture was stirred at RT for 2 hrs after which brine (25 mL) was added. The organics were extracted with Et_2O (2 x 100 mL), dried with $MgSO_4$ and concentrated *in vacuo*. The crude product was purified with flash chromatography using silica gel (25% EtOAc:Hexane) to afford a colourless oil (1.58 g, 7.5 mmol, 93%) Seen by NMR to be a mixture of isomers (9:1) due to vinyl proton presence.

ν_{max}/cm^{-1} (neat) 2985 (C=C-H), 1711 (C=O), 1092 (C-O); **^{1}H NMR (500 MHz, $CDCl_3$):** δ = 7.03 (t, *J* = 5.5 Hz, 1H; **H6**), 4.50-4.46 (m, 1H; **H3**), 4.44-4.40 (m, 1H; **H4**), 3.75 (s, 3H; **H8**), 2.74 (dd, *J* = 16.5, 3.0 Hz, 1H; **H2**), 2.51 (ddd, *J* = 17.5, 5.5, 3.0 Hz, 1H; **H5**), 2.39-2.33 (m, 1H; **H2**), 2.33-2.26 (m, 1H; **H5**), 1.37 (s, 3H; **H11**), 1.32 (s, 3H; **H10**). **^{13}C NMR (125 MHz, $CDCl_3$):** δ = 166.9 (**C7**), 137.7 (**C6**), 129.6 (**C1**), 108.1 (**C9**), 73.4 (**C3**), 72.6 (**C4**), 51.9 (**C8**), 29.5 (**C5**), 27.4 (**C2**), 26.9 (**C11**), 24.8 (**C10**). **HR MS (ESI, +ve, MeOH):** m/z calculated for $[C_{11}H_{16}O_4 + Na]^+$; 235.0946, Found; 235.0940. $[\alpha]_D^{25}$ (c 0.1, CH_3OH); +33.8.

(4*S*,5*R*)-4,5-dihydroxycyclohex-1-ene-1-carboxylic acid (78)

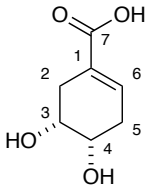

Procedure adapted from Akkala *et al*.[219] To a stirred solution of **125** (1.51 g, 7.4 mmol) in methanol 150 mL) was added a catalytic amount of TsOH (142 mg, 0.7 mmol) and the reaction mixture stirred for 2-4 hours with TLC monitoring. The reaction mixture was concentrated *in vacuo* to remove methanol and the crude product purified with flash chromatography using silica gel (100% EtOAc) to afford the diol as a white solid. To a stirred solution of the diol (800 mg, 4.7 mmol) in THF (30 mL) and water (30 mL) was added LiOH (210 mg, 8.8 mmol) and the reaction mixture stirred at RT for 16 hours. The reaction was quenched with addition of 2M HCl and reaction mixture concentrated *in vacuo* to remove the THF and subsequently lyophilized to remove remaining water with no further purification required to produce a pale solid in quantitative yield (725 mg, 4.6 mmol, 66% (two steps))

ν_{max}/cm^{-1} (neat) 3287 (OH), 2927 (C=C-H), 1709 (C=O), 1089 (C-O); **^{1}H NMR (500 MHz, $CDCl_3$):** δ = 6.87-6.84 (m, 1H; **H6**), 3.89 (dt, *J* = 9.0, 5.5 Hz, 2H; **H3, H4**), 2.54-2.35 (m, 4H; **H2, H5**). **^{13}C NMR (125 MHz, $CDCl_3$):** δ = 170.3 (**C7**), 137.8 (**C6**), 128.9 (**C1**), 69.6 (**C3**), 68.9 (**C4**), 32,3 (**C2**), 31.0 (**C5**). **HR MS (ESI, -ve, MeOH):** m/z calculated for $[C_7H_9O_4]^-$; 157.0501 Found; 157.0505. $[\alpha]_D^{25}$ (c 0.5, CH_3OH); +18.0

Synthesis of 5-(((benzyloxy)carbonyl)amino)-4-oxopentanoic acid (127)

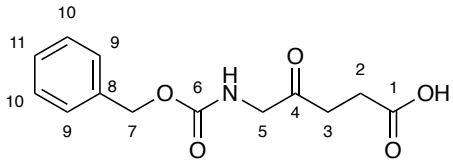

Procedure adapted from Battah *et al*.[220] A solution of 5-aminolevulinic acid hydrochloride (**126**) (1.00 g, 6.0 mmol) in water (14 mL) was pH adjusted to pH 8-10 with sodium carbonate solution. To this was added a solution of benzyl chloroformate (0.92 mL, 6.4 mmol) in 1,4-dioxane (14 mL) and the reaction mixture was stirred at RT for 18 hours. The reaction mixture was concentrated *in vacuo*, 0.1 M NaOH added and the mixture washed with diethyl ether. The aqueous layer was acidified to pH 6, organics extracted with CH_2Cl_2, dried with $MgSO_4$ and concentrated *in vacuo* to afford the desired product as a white solid (667 mg, 42%, m.p 105-107 °C).

^{1}H NMR (500 MHz, $CDCl_3$): δ = 7.37-7.33 (m, 5H; **H11**, **H10**, and **H9**), 5.11 (s, 2H; **H7**), 4.15 (d, *J* = 4.5 Hz, 2H; **H5**), 2.74-2.70 (m, 4H; **H3** and **H2**). **^{13}C NMR (125 MHz, $CDCl_3$):** δ = 203.7 (**C4**), 176.3 (**C1**), 156.3 (**C6**), 136.3 (**C8**), 128.7 (**C10**), 128.4 (**C11**), 128.3 (**C9**), 67.3 (**C7**), 50.7 (**C5**), 34.3 (**C3**), 27.4 (**C2**). **HR MS (ESI, -ve, MeOH):** m/z calculated for $[C_{13}H_{14}NO_5]^-$; 264.0872, Found; 264.0874. Spectroscopic data was consistent with that of the literature.

Synthesis of methyl 5-(((benzyloxy)carbonyl)amino)-4-oxopentanoate (128)

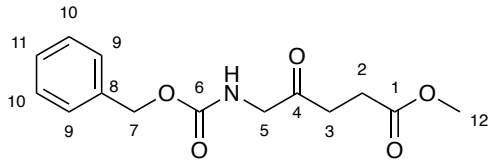

Procedure adapted from Campbell *et al*.[221] To a 0 °C solution of **127** (360 mg, 1.4 mmol) in MeOH (4 mL) was added thionyl chloride (0.29 mL, 4.00 mmol) dropwise and the reaction mixture stirred for 16 hours. The reaction mixture was concentrated *in vacuo* and the crude residue purified using flash chromatography using silica gel (3:1, EtOAc: Hexane) to afford a white solid (263 mg, 69%)

ν_{max}/cm^{-1} (neat) 1716 (C=O), 1690 (C=C), 1248 (N-H), 1161 (C-O); **^{1}H NMR (500 MHz, $CDCl_3$):** δ = 7.37-7.30 (m, 5H; **H11**, **H10**, and **H9**), 5.46 (br s, 1H; **NH**), 5.11 (s, 2H; **H7**), 4.15 (d, *J* = 5.0 Hz, 2H; **H5**), 3.67 (s, 3H; **H12**), 2.73 (t, *J* = 6.0 Hz, 2H; **H3**), 2.66 (t, *J* = 6.0 Hz, 2H; **H1**). **^{13}C NMR (125 MHz, $CDCl_3$):** δ = 203.9 (**C4**), 173.0 (**C1**), 156.2 (**C6**), 136.4 (**C8**), 128.7 (**C10**), 128.3 (**C11**), 128.2 (**C9**), 67.2 (**C7**), 52.1 (**C12**), 50.8 (**C5**), 34.5 (**C3**), 27.7 (**C2**). **HR MS (ESI, +ve, MeOH):** m/z calculated for $[C_{14}H_{17}NO_5 + Na]^+$; 302.1004, Found; 302.1001. $[\alpha]_D^{30}$ (c 0.09, $CHCl_3$); -15.1.

Synthesis of methyl 5-(((benzyloxy)carbonyl)amino)-4-hydroxypentanoate (129)

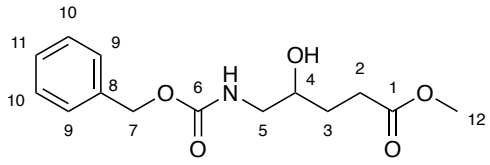

Synthesis adapted from Edoo *et al*.[222] To a 0 °C solution of **128** (260 mg, 0.9 mmol) in methanol was added $NaBH_4$ (70.5 mg, 1.9 mmol) and the solution stirred for 2 hours. The reaction was warmed to RT and quenched with water. The organics were extracted with EtOAc, washed with brine, dried over $MgSO_4$ and concentrated *in vacuo*. The crude residue was purified using flash chromatography using silica gel (3:1, EtOAc: Hexane) to afford a colourless oil seen to be the desired product with the presence of lactonised product (220 mg, 84%).

ν_{max}/cm^{-1} (neat) 3312 (OH), 1766 (C=O), 1690 (C=C), 1250 (N-H), 1143 (C-O); **^{1}H NMR (500 MHz, $CDCl_3$):** δ = 7.37-7.29 (m, 5H; **H11, H10** and **H9**), 5.21 (br s, 1H; **NH**), 5.10 (s, 2H; **H7**), 3.78-3.71 (m, 1H; **H4**), 3.67 (s, 3H; **H12**), 3.37 (dd, *J* = 14.0, 3.5 Hz, 1H; **H5**), 3.14-3.09 (m, 1H; **H5**), 2.85 (br s, 1H; **OH**), 2.49 (t, *J* = 7.0 Hz, 2H; **H2**), 1.79 (ddt, *J* = 17.0, 13.0, 8.0 Hz, 1H; **H3**), 1.75 (dq, *J* = 14.0, 7.0 Hz, 1H; **H3**). **^{13}C NMR (125 MHz,**

$CDCl_3$): δ = 174.7 (**C1**), 157.3 (**C6**), 136.5 (**C8**), 128.7 (**C10**), 128.3 (**C11** and **C9**), 70.9 (**C4**), 67.1 (**C7**), 52.0 (**C12**), 47.1 (**C5)**, 30.5 (**C2**), 29.5 (**C3**). **HR MS (ESI, +ve, MeOH):** m/z calculated for $[C_{14}H_{19}NO_5 + Na]^+$; 304.1161, Found; 304.1155. $[\alpha]_D^{30}$ (c 0.09, $CHCl_3$); -7.5.

Synthesis of 5-hydroxypiperidin-2-one (130)

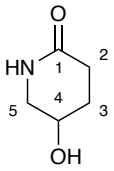

Synthesis adapted from Herdeis *et* al.[223] To a stirred solution of **129** (100 mg, 0.4 mmol) in MeOH (2 mL) was added Pd/C (10 mg) and the reaction placed under an atmosphere of argon. The solution was sparged with hydrogen for 10 minutes. The reaction mixture was stirred at RT under an atmosphere of hydrogen for 16 hours. Upon completion the reaction mixture was filtered through celite and washed with EtOAc. The organics were concentrated *in vacuo* to yield a white gum (40 mg, 97%). **^{1}H NMR (500 MHz, $CDCl_3$):** δ = 4.06 (dq, *J* = 7.5, 4.5 Hz, 1H; **H4**), 3.41 (dd, *J* = 12.5, 4.0 Hz, 1H; **H5**), 3.18 (dd, *J* = 12.5, 4.5 Hz, 1H; **H5**), 2.49 (ddd, *J* = 15.5, 8.5, 7.0 Hz, 1H; **H3**), 2.30 (dt, *J* = 18.0, 6.0 Hz, 1H; **H3**), 1.98-1.85 (m, 2H; **H2**). **^{13}C NMR (125 MHz, $CDCl_3$):** δ = 174.5 (**C1**), 63.7 (**C4**), 49.3 (**C5**), 28.7 (**C2**), 28.0 (**C3**). **HR MS (ESI, +ve, MeOH):** m/z calculated for $[C_5H_9NO_2 + Na]^+$; 138.0531, Found; 138.0528. Spectroscopic data was consistent with that of the literature

Synthesis of 5-amino-4-hydroxypentanoic acid (131)

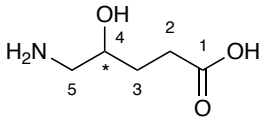

Synthesis adapted from Herdeis *et* al.[223] To a stirred solution of **130** (35 mg, 0.3 mmol) in water (10 mL) was added $Ba(OH)_2$ (60 mg, 0.4 mmol) and the reaction mixture stirred at reflux for 16 hours. Upon completion the reaction mixture was filtered, adjusted to pH 6.5 with 3N H_2SO_4 and concentrated *in vacuo*. This was seen

to be the undesired lactonized product due to over acidification. The resultant product was stirred in THF/water (14 mL, 1:1) and LiOH added (10 mg, 0.4 mmol). The reaction mixture was stirred at RT until completion by TLC monitoring, the solvent removed *in vacuo* and residual water removed via lyophilization to yield the desired product as the lithium salt (quant).

^{1}H NMR (500 MHz, D_2O): δ = 4.90 (dtd, *J* = 10.0, 7.5, 2.5 Hz, 1H; **H4**), 3.36 (dd, *J* = 14.0, 2.5 Hz, 1H; **H5**), 3.22 (dd, *J* = 14.0, 9.5 Hz, 1H; **H5**), 2.76-2.63 (m, 2H; **H2**), 2.47 (dddd, *J* = 13.0, 10.0, 7.0, 4.0 Hz, 1H; **H3**), 2.47 (dq, *J* = 13.0, 9.0 Hz, 1H; **H3**). **^{13}C NMR (125 MHz, D_2O):** δ = 180.7 (**C1**), 77.8 (**C4**), 42.7 (**C5**), 28.0 (**C2**), 24.3 (**C3**). Spectroscopic data was consistent with that of the literature

(*R*)-4-benzyl-3-(hept-6-enoyl)oxazolidin-2-one (134)

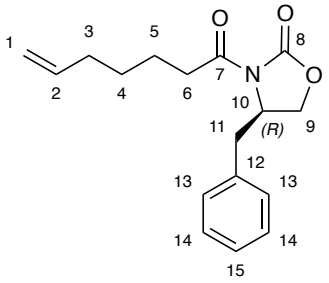

Procedure adapted from Kaliappan *et al.*[224] To a -10 °C solution of 6-heptanoic acid (**133**) (2.64 mL, 19.5 mmol) and Et_3N (7.07 mL, 50.7 mmol) in anhydrous THF (100 mL) under and argon atmosphere was added pivaloyl chloride (2.4 mL, 19.5 mmol) and the resultant solution stirred for 1 hour. This was followed by the addition of LiCl (910 mg, 21.5 mmol) and (*R*)-4-Benzyl-2-oxazolidinone (3.28 g, 18.5 mmol) and the solution warmed to RT and stirring continued for 12 hours. The reaction was quenched with $NaHCO_3$ (50 mL) and concentrated *in vacuo* to remove the THF. The organics were extracted with EtOAc (2 x 100 mL), washed with brine (50 mL), dried with $MgSO_4$ and concentrated *in vacuo*. The crude product was purified using flash chromatography using silica gel (1:9, EtOAc: Petroleum ether)) to afford a colourless oil (5.16 g, 18.0 mmol, 92%).

ν_{max}/cm^{-1} (neat) 1777, 1694 (C=O), 1654 (C=C), 1232, 1187 (C-N), 1112 (C-O); **^{1}H NMR (500 MHz, $CDCl_3$):** δ = 7.36-7.31 (m, 2H; **H14**), 7.30-7.27 (m, 1H; **H15**), 7.23-7.19 (m,

2H; **H13**), 5.82 (ddt, *J* = 17.0, 10.5, 6.5 Hz, 1H; **H2**), 5.03 (dd, *J* = 17.0, 1.5 Hz, 1H; *cis*-**H1**), 4.97 (dd, *J* = 10.5, 1.5 Hz, 1H; *trans*-**H1**), 4.67 (ddt, *J* = 10.0, 7.5, 3.0 Hz, 1H; **H10**), 4.22-4.15 (m, 2H; **H9**), 3.30 (dd, *J* = 13.5, 3.5 Hz, 1H; **H11**), 2.98 (dt, *J* = 17.0, 7.5 Hz, 1H; **H6**), 2.91 (dt, *J* = 17.0, 7.5 Hz, 1H; **H6**), 2.77 (dd, *J* = 13.5, 10.0 Hz, 1H; **H11**), 2.11 (q, *J* = 7.0 Hz, 2H; **H3**), 1.72 (ddt, *J* = 15.0, 7.5, 2.5 Hz, 2H; **H5**), 1.49 (quin *J* = 8.0 Hz, 2H; **H4**). **^{13}C NMR (125 MHz, $CDCl_3$):** δ = 173.4 (**C7**), 153.6 (**C8**), 138.6 (**C2**), 135.4 (**C12**), 129.6 (**C13**), 129.1 (**C14**), 127.5 (**C15**), 114.9 (**C1**), 66.3 (**C9**), 55.3 (**C10**), 38.1 (**C11**), 35.5 (**C6**), 33.6 (**C3**), 28.4 (**C4**), 23.8 (**C5**). **HR MS (ESI, +ve, MeOH):** m/z calculated for $[C_{17}H_{21}NO_3 + Na]^+$; 310.1419, Found; 310.1418. $[\alpha]_D^{29}$ (c 0.80, CH_3OH); -51.7.

(*R*)-3-((*S*)-2-allylhept-6-enoyl)-4-benzyloxazolidin-2-one (136)

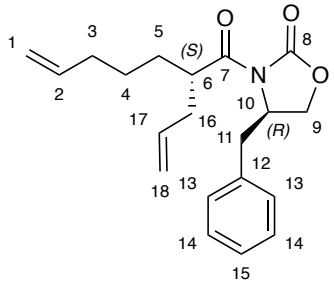

Procedure adapted from Davidson *et al*.[225] To a -78 °C stirred solution of (*R*)-4-benzyl-3-(hept-6-enoyl)oxazolidin-2-one (**134**) (5.10 g, 17.8 mmol) in anhydrous THF (55 mL) under an argon atmosphere was added LiHMDS (21.3 mL, 1M in THF), The reaction mixture stirred for 1 hour at -78 °C after which ally bromide (**135**) (3.07 mL, 35.5 mmol) was added dropwise and the resultant solution allowed to warm to RT and further stirred for 16 hours. The reaction mixture was saturated with sat.NH_4Cl (40 mL) and concentrated *in vacuo* to remove the THF. The organics were extracted with CH_2Cl_2 (2 x 50 mL), washed with brine (50 mL), dried with $MgSO_4$ and concentrated *in vacuo*. The crude product was purified using flash chromatography using silica gel (1:4, EtOAc: Petroleum ether)) to afford a colourless oil (5.03 g, 15.4 mmol, 87%). ν_{max}/cm^{-1} (neat) 1779, 1697 (C=O), 1640 (C=C), 1243, 1208 (C-N), 1102 (C-O); **^{1}H NMR (500 MHz, $CDCl_3$):** δ = 7.36-7.31 (m, 2H; **H14**), 7.30-7.26 (m, 1H; **H15**), 7.24-7.20 (m, 2H; **H13**), 5.83 (ddt, *J* = 17.0, 10.5, 7.0 Hz, 1H; **H17**), 5,78 (ddt, *J* = 17.0, 10.0, 6.5 Hz,

1H; **H2**), 5.09 (dd, *J* = 17.0, 1.5 Hz, 1H; *cis*-**H18**), 5.05 (dd, *J* = 10.0, 1.5 Hz, 1H; *trans*-**H18**), 5.00 (dd, *J* = 17.0, 1.5 Hz, 1H; *cis*-**H1**), 4.95 (dd, *J* = 10.0, 1.5 Hz, 1H; *trans*-**H1**), 4.69 (ddt, *J* = 10.0, 7.5, 3.0 Hz, 1H; **H10**), 4.20-4.13 (m, 2H; **H9**), 3.92 (tt, *J* = 8.0, 6.0 Hz, 1H; **H6**), 3.30 (dd, *J* = 13.5, 3.5 Hz, 1H; **H11**), 2.66 (dd, *J* = 13.5, 10.0 Hz, 1H; **H11**), 2.47 (dt, *J* = 14.0, 7.5 Hz, 1H; **H16**), 2.33 (dt, *J* = 13.5, 6.0 Hz, 1H; **H16**), 2.05 (q, *J* = 7.0 Hz, 2H; **H3**), 1.75 (ddd, *J* = 16.0, 14.0, 8.0 Hz, 1H; **H5**), 1.52 (ddd, *J*= 13.5, 9.5, 6.0 Hz, 1H; **H5**), 1.40 (quin, *J* = 7.5 Hz,2H; **H4**). **^{13}C NMR (125 MHz, $CDCl_3$):** δ = 176.1 (**C7**), 153.3 (**C8**), 138.5 (**C17**), 135.6 (**C12**), 135.4 (**C2**), 129.6 (**C13**), 129.1 (**C14**), 127.5 (**C15**), 117.3 (**C18**), 114.9 (**C1**), 66.1 (**C9**), 55.7 (**C10**), 42.4 (**C6**), 38.3 (**C11**), 36.9 (**C16**), 33.9 (**C3**), 31.1 (**C5**), 26.6 (**C4**). **HR MS (ESI, +ve, MeOH):** m/z calculated for $[C_{20}H_{25}NO_3 + Na]^+$; 350.1752, Found; 350.1724. $[\alpha]_D^{29}$ (c 0.47, CH_3OH); -100.3.

(*R*)-4-benzyl-3-(cycloheptanecarbonyl)oxazolidin-2-one (137)

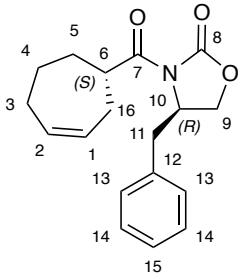

Procedure adapted from Xiao *et al*.[226] Argon was bubbled through a stirred solution of (*R*)-3-((*S*)-2-allylhept-6-enoyl)-4-benzyloxazolidin-2-one (**136**) (5.00g, 15.3 mmol) in CH_2Cl_2 (285 mL) after which Grubbs 2nd generation catalyst (35 mg, 0.04 mmol) was added and the resultant solution stirred under reflux under an argon atmosphere for 16 hrs. The reaction mixture was cooled and concentrated *in vacuo* and the crude mixture purified using flash chromatography using silica gel (1:4 EtOAc: Petroleum ether) to afford a white solid (3.09 g, 10.3 mmol, 68%, m.p. 92-93 °C) ν_{max}/cm^{-1} (neat) 1777, 1694 (C=O), 1604 (C=C), 1232, 1197 (C-N), 1112 (C-O); **^{1}H NMR (500 MHz, $CDCl_3$):** δ = 7.36-7.31 (m, 2H; **H14**), 7.30-7.27 (m, 1H; **H15**), 7.23-7.20 (m, 2H; **H13**), 5.90 (dddd, *J* = 11.0, 7.0, 5.0, 2.0 Hz, 1H; **H2**), 5.82 (dddd, *J* = 11.0, 7.0, 4.5, 2.0 Hz, 1H; **H1**), 4.65 (ddt, *J* = 10.0, 7.5, 3.5 Hz, 1H; **H10**), 4.22-4.14 (m, 2H; **H9**), 3.61 (tt, *J* = 10.5, 2.5 Hz, 1H; **H6**), 3.29 (dd, *J* = 13.5, 3.5 Hz, 1H; **H11**), 2.75 (dd, *J* = 13.5,

10.0 Hz, 1H; **H11**), 2.46-2.32 (m, 2H; **H16**), 2.28-2.20 (m, 1H; **H3**), 2.17-2.08 (m, 2H; **H3** and **H5**), 1.88-1.81 (m, 1H; **H4**), 1.81-1.73 (m, 1H; **H5**), 1.50-1.39 (m, 1H; **H4**). **^{13}C NMR (125 MHz, $CDCl_3$):** δ = 176.7 (**C7**), 153.2 (**C8**), 135.5 (**C12**), 133.7 (**C2**), 129.6 (**C13**), 129.4 (**C1**), 129.1 (**C14**), 127.5 (**C15**), 68.2 (**C9**), 55.5 (**C10**), 42.2 (**C6**), 38.1 (**C11**), 34.5 (**C5**), 31.2 (**H16**), 28.6 (**C3**), 25.5 (**C4**). **HR MS (ESI, +ve, MeOH):** m/z calculated for $[C_{18}H_{21}NO_3 + Na]^+$; 322.1419, Found; 322.1417. $[\alpha]_D^{29}$ (c 0.47, CH_3OH); -51.3.

Synthesis of (*S*)-cyclohept-3-ene-1-carboxylic acid (138)

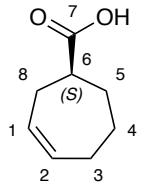

Procedure adapted from Liddle *et al*.[208] To a stirred solution of (*R*)-4-benzyl-3-((*S*)-cyclohept-3-ene-1-carbonyl)oxazolidin-2-one (**137**) (1.68 g, 5.6 mmol) in THF:H_2O (17.5 mL, 4:1) at 0 °C was added 30% H_2O_2 solution (3.16 mL, 30.85 mmol) and LiOH (544 mg, 22.6 mmol) and the reaction mixture stirred at RT to completion with TLC monitoring. Upon completion the RM was cooled to 0 °C, Na_2SO_3 (4.04 g, 32.0 mmol) added and the mixture stirred for 15 minutes at RT. The THF was removed *in vacuo* and the aqueous layer washed with CH_2Cl_2 (2 x 75 mL). The aqueous layer was acidified to pH 2 with conc.HCl and extracted with Et_2O (2 x 100 mL). The organics were washed with brine (50 mL), dried over $MgSO_4$ and concentrated *in vacuo* to afford a white solid (500 mg, 63%, m.p. 74-75 °C).

ν_{max}/cm^{-1} (neat) 3000 (br, OH), 1704 (C=O), 1654 (C=C), 1193 (C-O); **^{1}H NMR (500 MHz, MeOD):** δ = 5.85 (dt, *J* = 11.0, 6.0 Hz, 1H; **H2**), 5.76 (dt, *J* = 11.0, 6.0 Hz, 1H; **H1**), 2.39 (tt, *J* = 10.0, 3.0 Hz, 1H; **H6**), 2.38-2.30 (m, 2H; **H8**), 2.24-2.06 (m, 3H; **H5** and **H3**), 1.86-1.80 (m, 1H; **H5**), 1.80-1.73 (m, 1H; **H4**), 1.46-1.37 (m, 1H; **H4**). **^{13}C NMR (125 MHz, MeOD):** δ = 179.8 (**C7**), 134.4 (**C2**), 130.5 (**C1**), 44.6 (**C6**), 35.6 (**C5**), 31.6 (**C8**), 29.5 (**C3**), 26.5 (**C4**). **HR MS (ESI, +ve, MeOH):** m/z calculated for $[C_8H_{11}O_2]^-$; 139.0759, Found; 139.0765. $[\alpha]_D^{29}$ (c 0.33, CH_3OH); + 11.1.

Synthesis of ethyl (*S*)-cyclohept-3-ene-1-carboxylate (139)

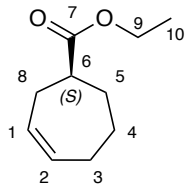

Procedure adapted from Ching *et* al.[227] To a stirred solution of (*S*)-cyclohept-3-ene-1-carboxylic acid (**138**) (500 mg, 3.6 mmol) in ethanol (30 mL) at 0 °C was added thionyl chloride (2.8 mL, 38.0 mmol) dropwise and the solution stirred at RT for 3 hrs The solvent was removed *in vacuo* and the crude residue was purified using flash chromatography using silica gel (1:4 Et_2O: Petroleum ether) to afford a colourless oil (460 mg, 76%).

ν_{max}/cm^{-1} (neat) 1732 (C=O), 1678 (C=C), 1162 (C-O); **^{1}H NMR (500 MHz, $CDCl_3$):** δ = 5.84 (dt, *J* = 11.0, 6.0 Hz, 1H; **H2**), 5.75 (dt, *J* = 11.0, 6.0 Hz, 1H; **H1**), 4.12 (q, *J* = 7.0 Hz, 2H; **H9**), 2.46-2.39 (m, 1H; **H6**), 2.38-2.35 (m, 2H, **H8**), 2.22- 2.06 (m, 3H; **H5** and **H3**), 1.86-1.79 (m, 1H; **H5**), 1.79-1.72 (m, 1H; **H4**), 1.45- 1.35 (m, 1H; **H4**), 1.25 (t, *J* =7.0 Hz, 3H; **H10**). **^{13}C NMR (125 MHz, $CDCl_3$):** δ = 176.2 (**C7**), 133.5 (**C2**), 129.5 (**C1**), 60.3 (**C9**), 43.6 (**C6**), 34.4 (**C5**), 30.8 (**C8**), 28.6 (**C3**), 25.5 (**C4**), 14.4 (**C10**). **HR MS (ESI, +ve, MeOH):** m/z calculated for $[C_{10}H_{16}O_2 + Na]^+$; 191.1048, Found; 191.1043. $[\alpha]_D^{29}$ (c 0.12, CH_3OH); +34.6.

Synthesis of ethyl (1*S*,3*R*,4*S*)-3,4-dihydroxycycloheptane-1-carboxylate (140) and ethyl (1*S*,3*S*,4*R*)-3,4-dihydroxycycloheptane-1-carboxylate (141)

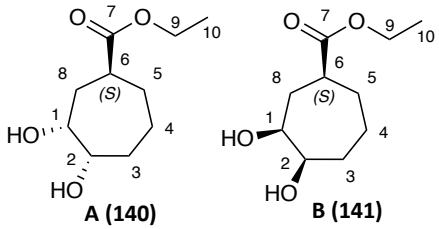

To a stirred solution of ethyl (*S*)-cyclohept-3-ene-1-carboxylate (**139**) (97 mg, 2.7 mmol) in Me_2CO: H_2O (4 mL, 3:1) was added N-methylmorpholine-N-oxide (143 mg, 1.2 mmol) and $K_2OsO_4 \cdot H_2O$ (1.5 mg, catalytic) and the solution stirred for 5 hours at RT. The reaction mixture was quenched with sat·$NaHSO_3$ and the organics extracted with EtOAc (2 x 50 mL), dried over $MgSO_4$ and concentrated *in vacuo*. The crude

residue was purified using flash chromatography using silica gel (100% EtOAc) to afford a 3:2 mixture of diastereomers **140** and **141** as a colourless oil (62 mg, 53%). ν_{max}/cm^{-1} (neat) 3405 (br OH), 1728 (C=O), 1181 (C-O). **Anti-Diastereomer A : ^{1}H NMR (500 MHz, $CDCl_3$):** δ = 4.13 (q, *J* = 7.0 Hz, 2H; **H9**), 3.82-3.74 (m, 2H; **H1** and **H2**), 2.95-2.84 (m, 1H; **H6**), 2.22 (dd, *J* = 7.5, 3.5 Hz, 1H; **H8**), 2.04-1.88 (m, 2H; **H3**), 1.86-1.62 (m, 4H; **H8**, **H5** and **H4**), 1.52-1.44 (m, 1H; **H4**), 1.25 (t, *J* = 7.0 Hz, 3H; **H10**); **Anti-Diastereomer A: ^{13}C NMR (125 MHz, $CDCl_3$):** δ = 176.2 (**C7**), 74.6 (**C2**), 71.8 (**C1**), 60.2 (**C9**), 40.5 (**C6**), 34.2 (**C8**), 30.7 (**C5**), 30.6 (**C3**), 21.4 (**C4**), 14.3 (**C10**). **Syn-Diastereomer B: ^{1}H NMR (500 MHz, $CDCl_3$):** δ = 4.14 (q, *J* = 7.0 Hz, 2H; **H9**), 3.92-3.84 (m, 2H; **H1** and **H2**), 2.95-2.84 (m, 1H; **H6**), 2.27 (dd, *J* = 7.5, 3.5 Hz, 1H; **H8**), 2.04-1.88 (m, 2H; **H3**), 1.86-1.62 (m, 4H; **H8**, **H5** and **H4**), 1.52-1.44 (m, 1H; **H4**), 1.26 (t, *J* = 7.0 Hz, 3H; **H10**); **Syn-Diastereomer B: ^{13}C NMR (125 MHz, $CDCl_3$):** δ = 176.2 (**C7**), 74.2 (**C2**), 72.1 (**C1**), 60.2 (**C9**), 42.3 (**C6**), 33.7 (**C8**), 31.3 (**C5**), 31.2 (**C3**), 21.0 (**C4**), 14.3 (**C10**). **HR MS (ESI, +ve, MeOH):** m/z calculated for $[C_{10}H_{18}O_4 + Na]^+$; 225.1103, Found; 225.1097. $[\alpha]_D^{30}$ (c 0.20, CH_3OH); +3.8.

Synthesis of ethyl (3a*R*,5*S*,8a*S*)-2,2-dimethylhexahydro-4*H*-cyclohepta[*d*][1,3]dioxole-5-carboxylate (142) and ethyl (3a*S*,5*S*,8a*R*)-2,2-dimethylhexahydro-4*H*-cyclohepta[*d*][1,3]dioxole-5-carboxylate (147)

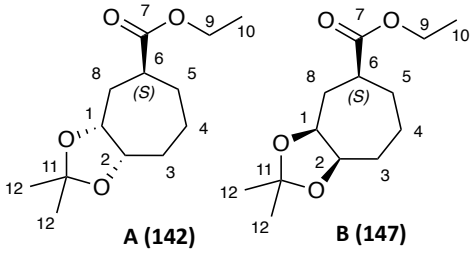

Procedure adapted from Kawashima *et al*[215] and Kusama *et al*[228]. To a stirred solution of **140** and **141** (18 mg, 0.1 mmol) in CH_2Cl_2 (2 mL) was added *p*-toluenesulfonic acid (2 mg, 0.01 mmol) and 2,2-dimethoxypropane (0.5 mL, 4.1 mmol). The solution was stirred at RT for 4 hrs with TLC monitoring and the solvent was removed *in vacuo*. The crude residue was purified using flash chromatography using silica gel (1:9 EtOAC: petroleum ether) to give diastereomer **142 (A)** (8.0 mg, 0.05 mmol, 37%) and a mixture of **142** (**A**) and **147 (B)** as colourless oils (8.7 mg, 0.5 mmol, 77%).

ν_{max}/cm^{-1} (neat) 1728 (C=O), 1171 (C-O). **Anti-Diastereomer A : ^{1}H NMR (500 MHz, $CDCl_3$):** δ = 4.46-4.42 (m, 1H; **H1**), 4.39-4.35 (m, 1H; **H2**), 4.12 (q, *J* = 7.0 Hz, 2H; **H9**), 2.79 (t, *J* = 10.5 Hz, 1H; **H6**), 2.26 (dd, *J* = 15.5, 6.0, 1H; **H8**), 2.02-1.95 (m, 2H; **H5** and **H3**), 1.80 (ddd, *J* = 15.0, 10.0, 1.5 Hz, 1H; **H8**), 1.75-1.69 (m, 1H; **H4**), 1.63-1.58 (m, 2H; **H5** and **H4**), 1.50 (s, 3H; **H12**), 1.47-1.45 (m, 1H; **H3**), 1.35 (s, 3H; **H12**), 1.25 (t, *J* = 7.0 Hz, 3H; **H10**). **Anti-Diastereomer A: ^{13}C NMR (125 MHz, $CDCl_3$):** δ = 176.3 (**C7**), 106.7 (**C11**), 76.4 (**C2**), 75.4 (**C1**), 60.5 (**C9**), 40.1 (**C6**), 33.9 (**C3**), 33.3 (**C8**), 31.2 (**C5**), 26.5 (**C12**), 24.0 (**C12**), 21.1 (**C4**), 14.4 (**C10**). **Syn-Diastereomer B: ^{1}H NMR (500 MHz, $CDCl_3$):** δ = 4.53-4.47 (m, 1H; **H1**), 4.41-4.34 (m, 1H; **H2**), 4.12 (q, *J* = 7.0 Hz, 2H; **H9**), 2.72-2.65 (m, 1H; **H6**), 2.28 (dd, *J* = 15.0, 6.0 Hz, 1H; **H8**), 2.03-1.94 (m, 2H; **H5 and H3**), 1.84-1.76 (m, 1H; **H8**), 1.76-1.68 (m, 1H; **H4**), 1.64-1.54 (m, 2H; **H5** and **H4**), 1.50 (s, 3H; **H12**),1.44-1.42 (m, 1H; **H3**), 1.33 (s, 3H; **H12**), 1.25 (t, 3H; *J* = 7.0 Hz, **H10**). **Syn-Diastereomer B: ^{13}C NMR (125 MHz, $CDCl_3$):** δ = 176.2 (**C7**), 106.5 (**C11**), 76.2 (**C2**), 75.5 (**C1**), 60.3 (**C9**), 40.4 (**C6**), 34.0 (**C3**), 33.4 (**C8**), 31.0 (**C5**), 26.1 (**C12**), 23.7 (**C12**), 20.8 (**C4**), 14.3 (**C10**). **HR MS (ESI, +ve, MeOH):** m/z calculated for $[C_{12}H_{22}O_4 + Na]^+$; 265.1416, Found; 265.1411. $[\alpha]_D^{30}$ (c 0.53, $CHCl_3$); +2.9.

Synthesis of (1*S*,3*R*,4*S*)-3,4-dihydroxycycloheptane-1-carboxylic acid (143)

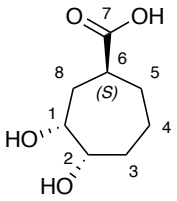

Procedure adapted from Akkala *et al*.[219] To a stirred solution of **142** (32 mg, 0.1 mmol) in methanol (4 mL) was added a catalytic amount of TsOH (3 mg, 0.02 mmol) and the reaction mixture stirred for 2-4 hours with TLC monitoring. The methanol was removed *in vacuo* and the crude product purified with flash chromatography using silica gel (100% EtOAc). To a stirred solution of the purified product (11 mg, 0.05 mmol) in THF/H_2O (4 mL 1:1) was added LiOH (2.3 mg, 0.1 mmol). The reaction mixture was stirred at RT for 16 hours and subsequently quenched with 2M HCl. The reaction mixture was concentrated *in vacuo* to remove the THF and lyophilized to

afford an off white gum that was used without further purification (7 mg, 44% (two steps)).

ν_{max}/cm^{-1} (neat) 3358 (br OH), 1711 (C=O), 1169 (C-O). **^{1}H NMR (500 MHz, MeOD):** δ = 4.04-3.99 (m, 1H; **H1**), 3.76-3.71 (m, 1H; **H2**), 2.66-2.59 (m, 1H; **H6**), 2.16-2.09 (m, 1H; **H8**), 1.97-1.82 (m, 2H; **H3** and **H5**), 1.80-1.70 (m, 1H; **H8**), 1.70-1.53 (m, 4H; **H5**, **H4** and **H3**). **^{13}C NMR (125 MHz, MeOD):** δ = 184.8 (**C7**), 74.5 (**C2**), 71.8 (**C1**), 41.4 (**C6**), 34.1 (**C8**), 30.6 (**C3** or **C5**), 30.5 (**C3** or **C5**), 21.2 (**C4**).

Synthesis of (1*S*,3*R*,4*S*)-3,4-dihydroxycycloheptane-1-carboxylic acid (143) and (1*S*,3*S*,4*R*)-3,4-dihydroxycycloheptane-1-carboxylic acid (144)

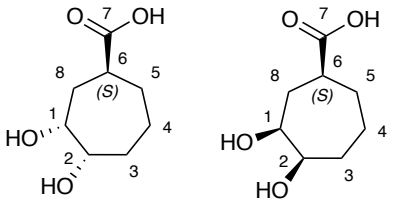

A **B**

To a stirred solution of a mixture of **140** and **141** (200 mg, 1.0 mmol) in THF/H_2O (50 ml 1:1) was added LiOH (28.5 mg, 1.2 mmol). The reaction mixture was stirred at RT for 16 hours and subsequently quenched with 2M HCl. The reaction mixture was concentrated *in vacuo* to remove the THF and lyophilized to afford a mixture of diastereomers **143** and **144** as a white solid (157 mg, 91%).

ν_{max}/cm^{-1} (neat) 3358 (br OH), 1711 (C=O), 1169 (C-O). **Anti-Diastereomer A : ^{1}H NMR (500 MHz, MeOD):** δ = 4.04-3.99 (m, 1H; **H1**), 3.76-3.71 (m, 1H; **H2**), 2.66-2.59 (m, 1H; **H6**), 2.16-2.09 (m, 1H; **H8**), 1.97-1.82 (m, 2H; **H3** and **H5**), 1.80-1.70 (m, 1H; **H8**), 1.70-1.53 (m, 4H; **H5**, **H4** and **H3**). **Anti-Diastereomer A: ^{13}C NMR (125 MHz, MeOD):** δ = 184.8 (**C7**), 74.5 (**C2**), 71.8 (**C1**), 41.4 (**C6**), 34.1 (**C8**), 30.6 (**C3** or **C5**), 30.5 (**C3** or **C5**), 21.2 (**C4**).

Syn-Diastereomer B: ^{1}H NMR (500 MHz, MeOD): δ = 3.87-3.82 (m, 1H; **H1**), 3.77-3.72 (m, 1H; **H2**), 2.48-2.41 (m, 1H; **H6**), 2.10-2.04 (m, 1H; **H8**), 1.97-1.82 (m, 4H; **H3** and **H5**), 1.80-1.70 (m, 1H; **H8**), 1.70-1.53 (m, 2H; **H4**). **Syn-Diastereomer B: ^{13}C NMR (125 MHz, MeOD):** δ = 184.8 (**C7**), 74.1 (**C2**), 73.5 (**C1**), 45.3 (**C6**), 33.1 (**C8**), 31.8 (**C3** or **C5**),

31.5 (**C3** or **C5**), 20.9 (**C4**). **HR MS (ESI, +ve, MeOH):** m/z calculated for $[C_8H_{13}O_4]^-$; 173.0814, Found; 173.0818. $[\alpha]_D^{30}$ (c 0.07, CH_3OH); +0.00

Synthesis of (1*S*,5*S*,6*S*)-5-hydroxy-7-oxabicyclo[4.2.1]nonan-8-one (147)

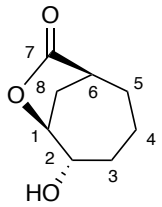

Procedure adapted from Corey *et al*.[229] To a stirred solution of **138** (100 mg, 0.7 mmol) in $CHCl_3$ (2.50 mL) at 0 °C was added mCPBA (136 mg, 0.8 mmol). The reaction mixture stirred for 4 hours followed by the addition of triethylamine (1.0 mL) and the resultant solution was stirred at 55 °C for 3 hours. The solvent removed *in vacuo* and the crude residue purified using flash chromatography using silica gel (1:9, petroleum ether: EtOAc) to yield a colourless oil (78 mg, 70%).

ν_{max}/cm^{-1} (neat) 3405 (br OH), 1753 (C=O) and 1143 (C-O). **^{1}H NMR (500 MHz, $CDCl_3$):** δ = 4.67 (dd, *J* = 8.0, 3.0 Hz, 1H; **H1**), 4.11-4.06 (m, 1H; **H2**), 2.75 (tt, *J* = 5.5, 2.5 Hz, 1H; **H6**), 2.40-2.30 (m, 1H; **H8**), 2.29-2.23 (m, 1H; **H8**), 2.04-1.96 (m, 1H; **H3**), 1.95-1.82 (m, 2H; **H5** and **H4**), 1.81-1.72 (m, 1H; **H3**), 1.71-1.62 (m, 1H; **H5**), 1.52-1.44 (m, 1H; **H4**). **^{13}C NMR (125 MHz, $CDCl_3$):** δ = 180.6 (**C7**), 81.6 (**C1**), 70.3 (**C2**), 38.1 (**C6**), 31.7 (**C5**), 30.5 (**C3**), 26.7 (**C8**), 18.8 (**C4**). **HR MS (ESI, +ve, MeOH):** m/z calculated for $[C_8H_{12}O_3 + Na]^+$; 179.0684, Found; 179.0677. $[\alpha]_D^{30}$ (c 0.07, CH_3OH); +3.8

Synthesis of (1*S*,3*S*,4*S*)-3,4-dihydroxycycloheptane-1-carboxylic acid (148)

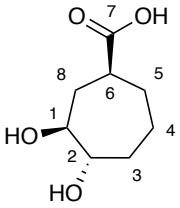

To a stirred solution of **147** (60 mg, 0.9 mmol) in THF/H_2O (4 mL, 2:1) was added 6M HCl (0.40 mL) and the reaction mixture stirred at RT until completion with TLC monitoring. The reaction mixture was concentrated *in vacuo* and water removed by

lyophilisation to afford the crude product as a colourless oil which was used without further purification (52.9 mg, 79%).

ν_{max}/cm^{-1} (neat) 3340 (br, OH), 1710 (C=O) and 1169 (C-O). **^{1}H NMR (500 MHz, MeOD):** δ = 3.93-3.86 (m, 1H; **H1**), 3.49-3.43 (m, 1H; **H2**), 2.76-2.68 (m, 1H; **H6**), 2.29-2.24 (m, 1H; **H8**), 1.94-1.74 (m, 2H; **H3** and **H4**), 1.74-1.62 (m, 2H; **H3** and **H8**), 1.62-1.54 (m, 2H; **H5**), 1.42-1.32 (m, 1H, **H4**). **^{13}C NMR (125 MHz, MeOD):** δ = 181.8 (**C7**), 70.4 (**C2**), 69.7 (**C1**), 38.3 (**C6**), 31.0 (**C8**), 29.5 (**C3**), 28.9 (**C5**), 18.7 (**C4**). **HR MS (ESI, +ve, MeOH):** m/z calculated for $[C_8H_{13}O_4]^-$; 173.0814, Found; 173.0813. $[\alpha]_D^{30}$ (c 0.40, CH_3OH); +12.1.

Synthesis of (*S*)-4-benzyl-3-(hept-6-enoyl)oxazolidin-2-one (203)

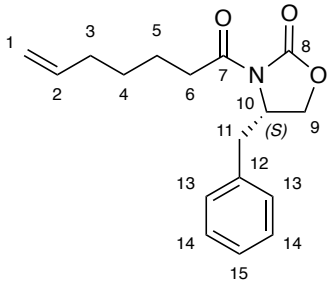

Compound **203** was synthesised using the same procedure used in the synthesis of **134** using 6-heptenoic acid (4 mL, 29.7 mmol) and (*S*)-4-Benzyl-2-oxazolidinone (5.00 g, 28.2 mmol) to afford **203** as a colourless oil oil (8.1 g, 28.2 mmol, 95%).

ν_{max}/cm^{-1} (neat) 1776, 1697 (C=O), 1639 (C=C), 1288 (C-N), 1102 (C-O); **^{1}H NMR (500 MHz, $CDCl_3$):** δ = 7.35-7.31 (m, 2H; **H14**), 7.30-7.26 (m, 1H; **H15**), 7.23-7.19 (m, 2H; **H13**), 5.82 (ddt, *J* = 17.0, 10.0, 6.5 Hz, 1H; **H2**), 5.03 (dd, *J* = 17.0, 1.5 Hz, 1H; *cis*-**H1**), 4.97 (dd, *J* = 10.0, 1.5 Hz, 1H; *trans*-**H1**), 4.67 (ddt, *J* = 10.5, 6.5, 3.5 Hz, 1H; **H10**), 4.22-4.15 (m, 2H; **H9**), 3.28 (dd, *J* = 13.5, 3.0 Hz, 1H; **H11**), 2.99 (dt, *J* = 17.0, 7.5 Hz, 1H; **H6**), 2.91 (dt, *J* = 17.0, 7.5 Hz, 1H; **H6**), 2.77 (dd, *J* = 13.0, 9.5 Hz, 1H; **H11**), 2.11 (q, *J* = 7.0 Hz, 2H; **H3**), 1.72 (ddt, *J* = 15.0, 7.5, 2.5 Hz, 2H; **H5**), 1.49 (quin, *J* = 7.5 Hz, 2H; **H4**). **^{13}C NMR (125 MHz, $CDCl_3$):** δ = 173.3 (**C7**), 153.5 (**C8**), 138.5 (**C2**), 135.3 (**C12**), 129.5 (**C13**), 129.0 (**C14**), 127.4 (**C15**), 114.8 (**C1**), 66.2 (**C9**), 55.2 (**C10**), 38.0 (**C11**), 35.4 (**C6**), 33.5 (**C3**), 28.3 (**C4**), 23.7 (**C5**). **HR MS (ESI, +ve, MeOH):** m/z calculated for $[C_{17}H_{21}NO_3 + Na]^+$; 310.1419, Found; 310.1417. $[\alpha]_D^{30}$ (c 0.10, $CHCl_3$); +28.9.

Synthesis of (*S*)-3-((*R*)-2-allylhept-6-enoyl)-4-benzyloxazolidin-2-one (204)

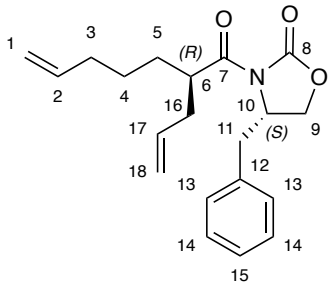

Compound **204** was synthesised using the same procedure used in the synthesis of **136** using **203** (8.1 g, 28.2 mmol) to afford **204** as a colourless oil (6.64 g, 20.3 mmol, 72%).

ν_{max}/cm^{-1} (neat) 1775, 1694 (C=O), 1639 (C=C), 1240, 1206 (C-N), 1101 (C-O); **^{1}H NMR (500 MHz, $CDCl_3$):** δ = 7.35-7.30 (m, 2H; **H14**), 7.29-7.26 (m, 1H; **H15**), 7.24-7.20 (m, 2H; **H13**), 5.83 (ddt, *J* = 17.0, 10.0, 7.0 Hz, 1H; **H17**), 5,78 (ddt, *J* = 17.0, 10.0, 7.0 Hz, 1H; **H2**), 5.09 (dd, *J* = 17.0, 1.5 Hz, 1H; *cis*-**H18**), 5.05 (dd, *J* = 10.0, 1.5 Hz, 1H; *trans*-**H18**), 5.00 (dd, *J* = 17.0, 1.5 Hz, 1H; *cis*-**H1**), 4.95 (dd, *J* = 10.0, 1.5 Hz, 1H; *trans*-**H1**), 4.69 (ddt, *J* = 10.0, 7.5, 3.0 Hz, 1H; **H10**), 4.20-4.13 (m, 2H; **H9**), 3.90 (tt, *J* = 8.0, 6.0 Hz, 1H; **H6**), 3.30 (dd, *J* = 13.5, 3.5 Hz, 1H; **H11**), 2.66 (dd, *J* = 13.5, 10.0 Hz, 1H; **H11**), 2.47 (dt, *J* = 14.0, 7.5 Hz, 1H; **H16**), 2.33 (dt, *J* = 13.5, 6.0 Hz, 1H; **H16**), 2.05 (q, *J* = 7.0 Hz, 2H; **H3**), 1.75 (ddd, *J* = 16.0, 14.0, 8.0 Hz, 1H; **H5**), 1.57-1.48 (m, 1H; **H5**), 1.40 (quin, *J* = 7.5 Hz, 2H; **H4**). **^{13}C NMR (125 MHz, $CDCl_3$):** δ = 176.0 (**C7**), 153.2 (**C8**), 138.4 (**C17**), 135.5 (**C12**), 135.3 (**C2**), 129.5 (**C13**), 129.0 (**C14**), 127.4 (**C15**), 117.2 (**C18**), 114.8 (**C1**), 66.0 (**C9**), 55.6 (**C10**), 42.2 (**C6**), 38.2 (**C11**), 36.8 (**C16**), 33.7 (**C3**), 31.0 (**C5**), 26.5 (**C4**). **HR MS (ESI, +ve, MeOH):** m/z calculated for $[C_{20}H_{25}NO_3 + Na]^+$; 350.1732, Found; 350.1725. $[\alpha]_D^{30}$ (c 0.10, $CHCl_3$); +27.1.

Synthesis of (*S*)-4-benzyl-3-((*R*)-cyclohept-3-ene-1-carbonyl)oxazolidin-2-one (205)

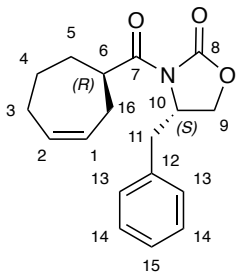

Compound **205** was synthesised using the same procedure used in the synthesis of **137** using **204** (6.64 g, 20.3 mmol) to afford **205** as a white solid (4.17 g, 69%). ν_{max}/cm^{-1} (neat) 1776, 1693 (C=O), 1605 (C=C), 1232, 1196 (C-N), 1111 (C-O); **^{1}H NMR (500 MHz, CDCl$_3$):** δ = 7.36-7.31 (m, 2H; **H14**), 7.30-7.26 (m, 1H; **H15**), 7.23-7.19 (m, 2H; **H13**), 5.90 (dddd, *J* = 11.0, 7.0, 5.0, 2.0 Hz, 1H; **H2**), 5.82 (dddd, *J* = 12.5, 7.5, 4.5, 2.0 Hz, 1H; **H1**), 4.65 (ddt, *J* = 10.0, 7.0, 3.0 Hz, 1H; **H10**), 4.22-4.14 (m, 2H; **H9**), 3.61 (tt, *J* = 10.5, 3.0 Hz, 1H; **H6**), 3.29 (dd, *J* = 13.5, 3.5 Hz, 1H; **H11**), 2.75 (dd, *J* = 13.5, 10.0 Hz, 1H; **H11**), 2.45-2.29 (m, 2H; **H16**), 2.29-2.20 (m, 1H; **H3**), 2.18-2.09 (m, 2H; **H3** and **H5**), 1.87-1.81 (m, 1H; **H4**), 1.81-1.73 (m, 1H; **H5**), 1.50-1.40 (m, 1H; **H4**). **^{13}C NMR (125 MHz, CDCl$_3$):** δ = 176.6 (**C7**), 153.1 (**C8**), 135.4 (**C12**), 133.6 (**C2**), 129.5 (**C13**), 129.3 (**C1**), 129.0 (**C14**), 127.4 (**C15**), 66.1 (**C9**), 55.4 (**C10**), 42.1 (**C6**), 38.0 (**C11**), 34.4 (**C5**), 31.1 (**H16**), 28.5 (**C3**), 25.4 (**C4**). **HR MS (ESI, +ve, MeOH):** m/z calculated for $[C_{18}H_{21}NO_3 + Na]^+$; 322.1419, Found; 322.1415. $[\alpha]_D^{30}$ (c 0.09, $CHCl_3$); +5.4.

Synthesis of (*R*)-cyclohept-3-ene-1-carboxylic acid (149)

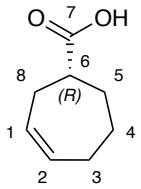

Compound **149** was synthesised using the same procedure used in the synthesis of **138** using **2-5** (4.17 g, 13.9 mmol) to afford **149** as a white solid (1.3 g, 67%, m.p. 74-75 °C)

ν_{max}/cm^{-1} (neat) 2989 (OH), 1695 (C=O), 1195 (C-O); **^{1}H NMR (500 MHz, MeOD):** δ = 11.0 (br s, 1H; **OH**), 5.87 (dt, *J* = 11.0, 6.0 Hz, 1H; **H2**), 5.76 (dt, *J* = 11.0, 6.0 Hz, 1H; **H1**), 2.50 (tt, *J* = 10.0, 3.0 Hz, 1H; **H6**), 2.44-2.36 (m, 2H; **H8**), 2.21-2.10 (m, 3H; **H5** and **H3**), 1.86 (dtd, *J* = 17.0, 10.0, 3.5, 1H; **H5**), 1.81-1.73 (m, 1H; **H4**), 1.43 (dtt, *J* = 18.0, 9.0, 3.0, 1H; **H4**). **^{13}C NMR (125 MHz, MeOD):** δ = 181.5 (**C7**), 133.7 (**C2**), 129.2 (**C1**), 43.2 (**C6**), 34.2 (**C5**), 30.4 (**C8**), 28.6 (**C3**), 25.3 (**C4**). **HR MS (ESI, +ve, MeOH):** m/z calculated for $[C_8H_{11}O_2]^-$; 139.0759, Found; 139.0764. $[\alpha]_D^{30}$ (c 0.09,) $CHCl_3$; -23.6.

Synthesis of (1*R*,5*R*,6*R*)-5-hydroxy-7-oxabicyclo[4.2.1]nonan-8-one (150)

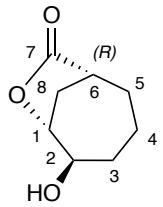

Compound **150** was synthesised using the same procedure used in the synthesis of **147** using **149** (1.3 g, 9.3 mmol) to afford **150** as a white solid (864 mg, 60%, m.p. 73-74 °C).

ν_{max}/cm^{-1} (neat) 3428 (OH), 1740 (C=O), 1145 (C-O); **^{1}H NMR (500 MHz, $CDCl_3$):** δ = 4.67 (dd, *J* = 8.0, 3.0 Hz, 1H; **H1**), 4.10-4.05 (m, 1H; **H2**), 2.75 (tt, *J* = 5.5, 2.5 Hz, 1H; **H6**), 2.36-2.31 (m, 1H; **H8**), 2.27-2.24 (m, 1H; **H8**), 2.02-1.96 (m, 1H; **H3**), 1.94-1.87 (m, 1H; **H5**), 1.87-1.81 (m, 1H; **H4**), 1.80-1.74 (m, 1H; **H3**), 1.66 (ddd, *J* = 17.5, 10.0, 7.0 Hz, 1H; **H5**), 1.50-1.41 (m, 1H; **H4**). **^{13}C NMR (125 MHz, $CDCl_3$):** δ = 180.9 (**C7**), 81.9 (**C1**), 70.3 (**C2**), 38.2 (**C6**), 31.8 (**C5**), 30.6 (**C3**), 26.9 (**C8**), 18.9 (**C4**). **HR MS (ESI, +ve, MeOH):** m/z calculated for $[C_8H_{12}O_3 + Na]^+$;179.0684, Found; 179.0677. $[\alpha]_D^{30}$ (c 0.09, $CHCl_3$); -30.7.

Synthesis of (1*R*,3*R*,4*R*)-3,4-dihydroxycycloheptane-1-carboxylic acid (151)

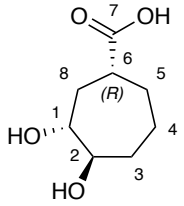

To a stirred solution of **150** (150 mg, 0.9 mmol) in THF/H_2O (9 mL, 2:1) was added 6M KOH (2mL) and the reaction mixture stirred at RT until completion with TLC monitoring. The reaction mixture was concentrated *in vacuo* and water removed by lyophilisation to afford the crude product which was used without further purification (quantitative). (NOTE: Upon acidification to pH<6 formation of the lactone starting material occurs which upon addition of KOH to pH>7 is converted to acid product)

ν_{max}/cm^{-1} (neat) 3351 (br OH), 1553 (C=O), 1125 (C-O); **^{1}H NMR (500 MHz, d$_6$-DMSO):** δ = 4.22 (br s, 1H; **OH**), 3.46-3.38 (m, 2H; **H1** and **H2**), 2.16 (dq, *J* = 11.0, 5.5 Hz, 1H; **H6**), 1.89 (ddd, *J* = 15.0, 5.0, 2.5 Hz, 1H; **H8**), 1.70 (dtd, *J* = 17.0, 10.0, 3.0 Hz, 1H; **H5**), 1.65-1.53 (m, 3H; **H8**, **H5**, **H3**), 1.48-1.35 (m, 3H; **H4** and **H3**). **^{13}C NMR (125 MHz, d$_6$-DMSO):** δ = 179.8 (**C7**), 74.6 (**C2**), 74.4 (**C1**), 45.4 (**C6**), 33.5 (**C5**), 32.2 (**C3**), 32.0 (**C8**), 21.0 (**C4**). **HR MS (ESI, +ve, MeOH):** m/z calculated for [$C_8H_{13}O_4$]$^-$; 173.0814, Found; 173.0833. $[\alpha]_D^{30}$ (c 0.03, $CHCl_3$); -3.2.

Synthesis of (*R*)-4-benzyl-3-(hex-5-enoyl)oxazolidin-2-one (171)

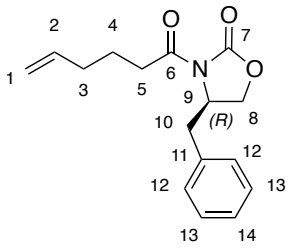

Procedure adapted from Kaliappan *et al.*[224] To a -10 °C solution of 5-hexanoic acid (**170**) (5.2 ml, 43.8 mmol) and Et_3N (15.9 ml, 113.9 mmol) in anhydrous THF (197 ml) under an atmosphere of argon was added pivaloyl chloride (5.4 ml, 43.8 mmol) and the solution stirred for 1 hour. To the reaction mixture were added LiCl (2.0 g, 48.2 mmol) and (*R*)-4-Benzyl-2-oxazolidinone (7.4 g, 41.62 mmol) and the solution warmed to RT and stirred for 16 hours. The reaction was quenched with $NaHCO_3$ (100 mL) and concentrated *in vacuo* to remove the THF. The organics were extracted with EtOAc (2 x 200 mL), washed with brine (100 mL), dried with $MgSO_4$ and concentrated *in vacuo*. The crude product was purified using flash chromatography using silica gel (1:5, EtOAc: Petroleum ether)) to afford a colourless oil (10.74 g, 39.3 mmol, 90%).
^{1}H NMR (500 MHz, $CDCl_3$): δ = 7.36-7.28 (m, 2H; **H13**), 7.28-7.25 (m, 1H; **H14**), 7.22-7.18 (m, 2H; **H12**), 5.82 (ddt, *J* = 17.0, 10.0, 6.5 Hz, 1H; **H2**), 5.06 (dd, *J* = 17.0, 1.5 Hz, 1H; *cis*-**H1**), 5.00 (dd, *J* = 10.0, 1.5 Hz, 1H; *trans*-**H1**), 4.67 (ddt, *J* = 10.0, 7.5, 3.0 Hz, 1H; **H9**), 4.22-4.14 (m, 2H; **H8**), 3.30 (dd, *J* = 13.5, 3.0 Hz, 1H; **H10**), 3.03-2.87 (m, 2H; **H5**), 2.77 (dd, *J* = 13.5, 10.0 Hz, 1H; **H10**), 2.16 (q, *J* = 7.0 Hz, 2H; **H3**), 1.87-1.75 (m, 2H; **H4**). **^{13}C NMR (125 MHz, $CDCl_3$):** 173.3 (**C6**), 153.6 (**C7**), 137.9 (**C2**), 135.4 (**C11**), 129.6 (**C12**), 127.5 (**C14**),129.1 (**C13**), 115.5 (**C1**), 66.3 (**C8**), 55.3 (**C9**), 38.1 (**C10**), 35.0

(**C5**), 33.1 (**C3**), 23.5 (**C4**). **HR MS (ESI, +ve, MeOH):** m/z calculated for $[C_{16}H_{19}NO_3 + Na]^+$; 296.1263, Found; 296.1256. Spectroscopic data is consistent with that reported in the literature.[230,231]

Synthesis of (*R*)-3-((*S*)-2-allylhex-5-enoyl)-4-benzyloxazolidin-2-one (172)

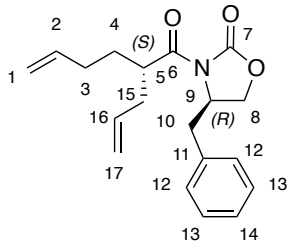

Procedure adapted from Davidson *et al*.[225] To a -78 °C stirred solution of (*R*)-4-benzyl-3-(hex-5-enoyl)oxazolidin-2-one (**171**) (10.7 g, 39.2 mmol) in anhydrous THF (153 ml) under an atmosphere of argon was added LiHMDS (47 ml, 1M in THF). The reaction mixture was stirred for 30 minutes at -78 °C after which allyl bromide (6.8 ml, 78.3 mmol) was added dropwise and the solution allowed to warm to RT and stirred for 16 hours at this temperature. The reaction was quenched with sat.NH_4Cl and concentrated *in vacuo* to remove the THF. The organics were extracted with CH_2Cl_2 (2 x 100 ml), washed with brine (100 ml), dried with $MgSO_4$ and concentrated *in vacuo*. The crude product was purified using flash chromatography using silica gel (1:9, EtOAc: Petroleum ether)) to afford a colourless oil (9.77 g, 31.20 mmol, 80%). **^{1}H NMR (500 MHz, $CDCl_3$):** δ = 7.36-7.30 (m, 2H; **H13**), 7.30-7.26 (m, 1H; **H14**), 7.24-7.20 (m, 2H; **H12**), 5.83 (ddt, *J* = 17.0, 10.0, 7.0 Hz, 1H; **H2**), 5.78 (ddt, *J* = 17.0, 10.0, 7.0 Hz, 2H; **H16**), 5.08 (dd, *J* = 17.0, 1.5 Hz, 1H; *cis*-**H1**), 5.06 (dd, *J* = 10.5, 1.5 Hz, 1H; *trans*-**H1**), 5.00 (dd, *J* = 17.0, 1.5 Hz, 1H; *cis*-**H17**), 4.95 (dd, *J* = 10.5, 1.5 Hz, 1H; *trans*-**H17**), 4.68 (ddt, *J* = 10.0, 7.5, 3.0 Hz, 1H; **H9**), 4.19-4.13 (m, 2H; **H8**), 3.94 (tt, *J* = 7.5, 5.5 Hz, 1H; **H5**), 3.30 (dd, *J* = 13.5, 3.0 Hz, 1H; **H10**), 2.67 (dd, *J* = 13.5, 10.0 Hz, 1H; **H10**), 2.48 (dt, *J* = 14.0, 7.5 Hz, 1H; **H15**), 2.33 (dt, *J* = 14.0, 7.5 Hz, 1H; **H15**), 2.08 (q, *J* = 7.5 Hz, 2H; **H4**), 1.92-1.81 (m, 1H; **H3**), 1.66-1.58 (m, 1H; **H3**). **^{13}C NMR (125 MHz, $CDCl_3$):** 176.0 (**C6**), 153.3 (**C7**), 138.2 (**C16**), 135.6 (**C11**), 135.2 (**C2**), 129.6 (**C12**), 129.1 (**C13**), 127.5 (**C14**),117.5 (**C17**), 115. 1 (**C1**), 66.1 (**C8**), 55.7 (**C9**), 42.0 (**C5**), 38.3 (**C10**), 37.1 (**C15**), 31.7 (**C3**), 30.7 (**C4**). **HR MS (ESI, +ve, MeOH):** m/z calculated for

$[C_{19}H_{23}NO_3 + Na]^+$; 336.1576, Found; 336.1566. Spectroscopic data is consistent with that reported in the literature.[162]

Synthesis of (*R*)-4-benzyl-3-((*S*)-cyclohex-3-ene-1-carbonyl)oxazolidin-2-one (173)

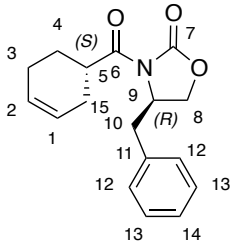

Procedure adapted from Xiao *et al*.[226] A solution of (*R*)-3-((*S*)-2-allylhex-5-enoyl)-4-benzyloxazolidin-2-one (**172**) (7.00 g, 23.35 mmol) in CH_2Cl_2 (58 ml) was sparged for 5 minutes under an atmosphere of argon. To the solution was added Grubbs 2nd generation catalyst (100 mg, 0.12 mmol) and the reaction mixture heated at reflux for 5 hours. The reaction mixture was concentrated *in vacuo* followed by purification using flash chromatography using silica gel (1:9 EtOAc: Petroleum ether) to afford a white solid (4.9 g, 77 %).

^{1}H NMR (500 MHz, $CDCl_3$): δ = 7.36-7.31 (m, 2H; **H13**), 7.30-7.27 (m, 1H; **H14**), 7.23-7.19 (m, 2H; **H12**), 5.76-5.70 (m, 2H; **H1** and **H2**), 4.68 (ddt, *J* = 10.0, 7.5, 3.0 Hz, 1H; **H9**), 4.24-4.16 (m, 2H; **H8**), 3.76 (dddd, *J* = 11.5, 9.5, 6.5, 2.5 Hz, 1H; **H5**), 3.28 (dd, *J* = 13.5, 3.0 Hz, 1H; **H10**), 2.78 (dd, *J* = 13.5, 3.0 Hz, 1H; **H10**), 2.35-2.27 (m, 2H; **H15**), 2.20-2.12 (m, 2H; **H3**), 1.97-1.91 (m, 1H; **H4**), 1.73 (qd, *J* = 11.5, 7.0 Hz, 1H; **H4**). **^{13}C NMR (125 MHz, $CDCl_3$):** δ = 176.6 (**C6**), 153.2 (**C7**), 135.4 (**C11**), 129.6 (**C12**), 129.1 (**C13**), 127.5 (**C14**), 126.8 (**C1**), 125.2 (**C2**), 66.2 (**C8**), 55.5 (**C9**), 38.6 (**C5**), 38.1 (**C10**), 27.6 (**C15**), 25.5 (**C3**), 24.8 (**C4**). **HR MS (ESI, +ve, MeOH):** m/z calculated for $[C_{17}H_{19}NO_3 + Na]^+$; 308.1263, Found; 308.1257 Spectroscopic data is consistent with that reported in the literature.[232]

Synthesis of (*S*)-cyclohex-3-ene-1-carboxylic acid (174)

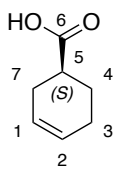

Procedure adapted from Liddle *et al*.[208] To a stirred solution of (*R*)-4-benzyl-3-((*S*)-cyclohex-3-ene-1-carbonyl)oxazolidin-2-one (**173**) (4.9 g, 17.2 mmol) in THF:H_2O (50 ml, 4:1) at 0 °C was added 30% H_2O_2 (8.10 ml, 85.9 mmol) and LiOH (1.66 g, 85.9 mmol) and the reaction mixture stirred at RT upon completion as indicated by TLC analysis. Upon completion the RM was cooled to 0 °C, Na_2SO_3 (9.8 g, 77.75 mmol) added cautiously and mixture stirred for and additional 15 minutes at RT. The THF was removed *in vacuo* and the aqueous layer washed with CH_2Cl_2 (2 x 225 mL). The aqueous layer was acidified to pH 2 with conc.HCl and extracted with Et_2O (2 x 300 mL). The organics were washed with brine (150 mL), dried over $MgSO_4$ and concentrated *in vacuo* to afford a white solid (1.98 g, 91%).

^{1}H NMR (500 MHz, $CDCl_3$): δ = 5.73-5.66 (m, 2H; **H1** and **H2**), 2.61 (dddd, *J* = 11.5, 9.5, 6.5, 2.5 Hz, 1H; **H5**), 2.32-2.25 (m, 2H; **H7**), 2.18-2.02 (m, 3H; **H3** and **H4**), 1.77-1.67 (m, 1H; **H5**). **^{13}C NMR (125 MHz, $CDCl_3$):** δ = 182.2 (**C6**), 126.9 (**C1**), 125.1 (**C2**), 39.2 (**C5**), 27.3 (**C7**), 25.0 (**C3**), 24.4 (**C4**). **HR MS (ESI, +ve, MeOH):** m/z calculated for $[C_7H_{10}O_2 + Na]^+$; 149.0578, Found; 149.0572. Spectroscopic data is consistent with that reported in the literature.[233]

Synthesis of (1*S*,4*S*,5*S*)-4-hydroxy-6-oxabicyclo[3.2.1]octan-7-one (175)

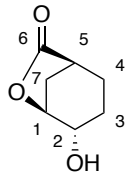

Procedure adapted from Corey *et al*.[229] To a stirred solution of (*S*)-cyclohex-3-ene-1-carboxylic acid (**174**) (1.21 g, 9.60 mmol) in $CHCl_3$ (50 ml) under an argon atmosphere was added *m*-CPBA (3.64 g, 21.12 mmol) and the RM stirred at 0 °C for 4 hours. Triethylamine (6.7 ml, 48.0 mmol) was added and the RM heated to 65 °C for a further 4 hours. The RM was diluted with $CHCl_3$, washed with 1M HCl (15 ml), brine (15 ml), dried over $MgSO_4$ and concentrated *in vacuo*. The crude mixture was purified using flash chromatography using silica gel (3:1, EtOAc: petroleum ether) to yield a colourless oil (680 mg, 4.79 mmol, 50%).

^{1}H NMR (500 MHz, $CDCl_3$): δ = 4.67 (t, *J* = 5.5 Hz, 1H; **H1**), 4.20 (t, *J* = 4.5 Hz, 1H; **H2**), 2.61 (t, *J* = 5.0 Hz, 1H; **H5**), 2.39 (d, *J* = 12.0 Hz, 1H; **H7**), 2.21 (dt, *J* = 11.5, 5.5 Hz, 1H;

H7). **^{13}C NMR (125 MHz, $CDCl_3$):** δ = 178.8 (**C6**), 79.1 (**C1**), 65.3 (**C2**), 38.5 (**C5**), 31.3 (**C7**), 27.5 (**C4**), 22.8 (**C3**). **HR MS (ESI, +ve, MeOH):** m/z calculated for $[C_7H_{10}O_3 + Na]^+$; 165.0528, Found; 165.0523. Spectroscopic data is consistent with that reported in the literature.[162]

Synthesis of (1*S*,4*S*,5*S*)-4-(prop-2-yn-1-yloxy)-6-oxabicyclo[3.2.1]octan-7-one (177)

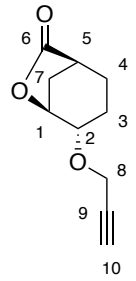

Procedure adapted from Pereira *et al*.[198] To a stirred solution of (1*S*,4*S*,5*S*)-4-hydroxy-6-oxabicyclo[3.2.1]octan-7-one (**175**) (660 mg, 4.65 mmol) in anhydrous DMF (8 ml) containing 3Å molecular sieves was added NaH (0.2 g, 60% oil dispersion) and the RM stirred at RT for 30 minuets. The flask was cooled to 0 °C followed by addition of propargyl bromide (**176**) (0.66 ml, 80% (w/w) toluene) and subsequently stirred at RT for 16 hours. The RM was quenched with sat.NH_4Cl (1ml), the organics extracted with EtOAc (2 x 20 ml), washed with brine (2 x 5 ml), dried over $MgSO_4$ and concentrated *in vacuo*. The crude mixture was purified using flash chromatography using silica gel (3:2, EtOAc: petroleum ether) to yield **177** as a yellow oil (127 mg, 0.71 mmol, 15%).

ν_{max}/cm^{-1} (neat) 2150 (C≡C), 1780 (C=O), 1100 (C-O); **^{1}H NMR (500 MHz, $CDCl_3$):** δ = 4.77 (t, *J* = 5.0 Hz, 1H; **H1**), 4.23 (dd, *J* = 16.0, 2.0 Hz, 1H; **H8**), 4.15 (dd, *J* = 16.0, 2.0 Hz, 1H; **H8**), 3.94 (t, *J* = 4.0 Hz, 1H; **H2**), 2.59 (t, *J* = 5.0 Hz, 1H; **H5**), 2.45 (t, *J* = 2.0 Hz, 1H; **H10**), 2.32 (d, *J* = 12.0 Hz, 1H; **H7**), 2.21 (dt, *J* = 11.5, 5.5 Hz, 1H; **H7**), 1.98-1.89 (m, 1H; **H3**), 1.86-1.76 (m, 3H; **H3** and **H4**). **^{13}C NMR (125 MHz, $CDCl_3$):** δ = 178.9 (**C6**), 77.6 (**C1**), 74.8 (**C9**), 72.4 (**C2**), 57.1 (**C8**), 38.2 (**C5**), 31.7 (**C7**), 23.6 (**C3**), 23.0 (**C4**). **HR MS (ESI, +ve, MeOH):** m/z calculated for $[C_{10}H_{12}O_3 + Na]^+$; 203.0684, Found; 203.0684 $[\alpha]_D^{30}$ (c 0.07, $CHCl_3$); +34.3.

Synthesis of (1*S*,3*S*,4*S*)-3-hydroxy-4-(prop-2-yn-1-yloxy)cyclohexane-1-carboxylic acid (178)

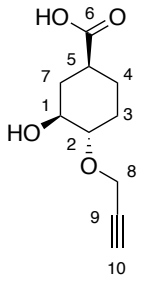

To a solution of (1*S*,4*S*,5*S*)-4-(prop-2-yn-1-yloxy)-6-oxabicyclo[3.2.1]octan-7-one (**177**) (126 mg, 0.70 mmol) in THF:H_2O (8 ml, 5:3) was added LiOH and the RM stirred for 16 hours at RT. The RM was acidified to pH 2.0 with 1M HCl and concentrated *in vacuo* to afford **178** as a colourless oil (138 mg, quant, 0.70 mmol).

ν_{max}/cm^{-1} (neat) 3366 (OH), 2117 (CΞC), 1693 (C=O), 1141 (C-O); **^{1}H NMR (500 MHz, MeOD):** δ = 4.31 (d, *J* = 2.0 Hz, 2H; **H8**), 3.45 (ddd, *J* = 13.0, 9.0, 4.5 Hz, 1H; **H1**), 3.27 (ddd, *J* = 13.0, 9.0, 4.5 Hz, 1H; **H2**), 2.81 (t, *J* = 2.0 Hz, 1H; **H10**), 2.37 (tt, *J* = 12.5, 3.5 Hz, 1H; **H5**), 2.21-2.13 (m, 2H; **H3** and **H7**), 2.00-1.93 (m, 1H; **H4**), 1.50-1.35 (m, 2H; **H4** and **H7**), 1.30-1.19 (m, 1H; **H3**). **^{13}C NMR (125 MHz, MeOD):** δ = 83.1 (**C2**), 75.3 (**C9**), 74.0 (**C1**), 57.9 (**C8**), 42.4 (**C5**), 36.9 (**C7**), 30.0 (**C3**), 28.1 (**C4**). **HR MS (ESI, +ve, MeOH):** m/z calculated for $[C_{10}H_{14}O_4 + Na]^+$; 221.0790, Found; 221.0789 $[\alpha]_D^{30}$ (c 0.11, $CHCl_3$); +5.1.

Synthesis of (prop-2-yn-1-yloxy)cyclohexane (179)

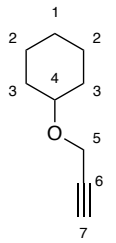

Procedure adapted from Trost *et al*.[234] To a 0 °C stirred solution of cyclohexanol (**69**) (0.25 mL, 2.37 mmol) in anhydrous THF (10 mL) containing 3Å molecular sieves was added NaH (0.12 g, 60% oil dispersion) and the RM stirred at 0 °C for 5 minuets. The flask was warmed to RT followed by addition of propargyl bromide (**176**) (0.216 mL,

80% (w/w) toluene) and subsequently stirred at RT for 16 hours. The RM was quenched with sat.NH_4Cl (1ml), the organics extracted with Et_2O (2 x 20 ml), washed with brine (2 x 5 ml), dried over $MgSO_4$ and concentrated *en vacuo*. The crude mixture was purified using flash chromatography using silica gel (1:9, Et_2O: petroleum ether) to yield as a colourless oil (106 mg, 32%).

Synthesis of **179** using DMF was carried out under the same conditions using 0.11 mL of cyclohexanol, 50 mg of NaH (60% oil disoersion), 0.91 mL of propargyl bromide (80% (w/w) toluene) and 5mL of DMF. The reaction afforded **179** as a yellowish oil (56 mg, 41% - impure by NMR).

^{1}H NMR (500 MHz, $CDCl_3$): δ = 4.17 (d, *J* = 2.5 Hz, 2H; **H6**), 3.51-3.42 (m, 1H; **H4**), 2.38 (t, *J* = 2.5 Hz, **H7**), 1.96-1.87 (m, 2H; **H3**), 1.79-1.69 (m, 2H; **H2**), 1.57-1.49 (m, 1H; **H1**), 1.34-1.18 (m, 5H; **H1**, **H2** and **H3**). **^{13}C NMR (125 MHz, $CDCl_3$):** δ = 80.8 (**C4**), 76.8 (**C6**), 73.7 (**C7**), 55.1 (**C5**), 32.0 (**C3**), 25.5 (**C1**), 24.2 (**C2**). Spectroscopic data is consistent with that reported in the literature.

Synthesis of (1*S*,3*S*,4*S*)-4-((*tert*-butyldimethylsilyl)oxy)-3-hydroxycyclohexane-1-carboxylic acid (183)

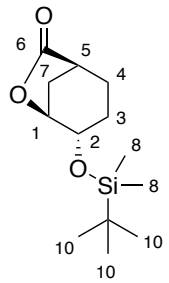

To a 0 °C solution of **175** (49 mg, 0.35 mmol) and imidazole (35 mg, 0.52 mmol) in anhydrous DMF (5 ml) was added *tert*-butyldimethylsilyl chloride (62 mg, 0.41 mmol) and the reaction mixture stirred for 16 hours at RT. The reaction mixture was diluted with diethyl ether (15 mL) and water (15 mL), The organics were extracted (2 x 100 mL), washed with brine (25 mL), dried with $MgSO_4$ and concentrated *in vacuo*. The crude reaction product was purified using flash chromatography using silica gel (1:2 EtOAc: hexane) to afford a white crystalline solid (99 mg, 55 %, m.p. 70-71 °C).

ν_{max}/cm^{-1} (neat) 1787 (C=O), 1100 (C-O); **^{1}H NMR (500 MHz, $CDCl_3$):** δ =4.51 (t, *J* = 5.5 Hz, 1H; **H1**), 4.08 (t, *J* = 4.5 Hz, 1H; **H2**), 2.56 (t, *J* = 5.0 Hz, 1H; **H5**), 2.40 (d, *J* = 12.0

Hz, 1H; **H7**), 2.15 (dt, *J* = 11.5, 5.5 Hz, 1H; **H7**), 1.93-1.67 (m, 4H; **H3** and **H4**), 0.90 (s, 9H; **H10**), 0.07 (d, *J* = 7.5 Hz, 6H; **H8**). **^{13}C NMR (125 MHz, $CDCl_3$):** δ = 179.6 (**C6**), 79.6 (**C1**), 65.8 (**C2**), 38.6 (**C5**), 31.4 (**C7**), 30.1 (**C9**), 27.7 (**C4**), 25.8 (**C10**), 22.9 (**C3**), -4.0 (**C8**). **HR MS (ESI, +ve, MeOH):** m/z calculated for $[C_{13}H_{24}O_3Si + Na]^+$; 279.1392, Found; 279.1387. $[\alpha]_D^{30}$ (c 0.12, $CHCl_3$); +14.3.

Synthesis of methyl (1*S*,3*S*,4*S*)-3-hydroxy-4-(prop-2-yn-1-yloxy)cyclohexane-1-carboxylate (206)

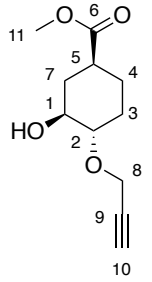

Procedure adapted from Campbell *et al*.[221] To a 0 °C solution (**178**) (108 mg, 0.55 mmol) in MeOH (4 ml) was added thionyl chloride (0.06 ml, 0.82 mmol) dropwise and the reaction mixture stirred at RT for 16 hours. The solution was concentrated *in vacuo* and the crude residue purified using flash chromatography using silica gel (3:1, EtOAc: Hexane) to afford **206** as a white gum (94.2 mg, 82%).

^{1}H NMR (500 MHz, $CDCl_3$): δ = 4.31 (dd, *J* = 16.0, 2.0 Hz, 1H; **H8**), 4.20 (dd, *J* = 16.0, 2.0 Hz, 1H; **H8**), 3.68 (s, 3H; **H11**), 3.51 (ddd, *J* = 13.0, 9.0, 4.5 Hz, 1H; **H1**), 3.30 (ddd, *J* = 13.0, 9.0, 4.5 Hz, 1H; **H2**), 2.46 (t, *J* = 2.0 Hz, 1H; **H10**), 2.41 (tt, *J* = 12.5, 3.5 Hz, 1H; **H5**), 2.30-2.24 (m, 1H; **H7**), 2.20-2.13 (m, 1H; **H3**), 2.05-1.98 (m, 1H; **H4**), 1.59-1.41 (m, 2H; **H4** and **H7**), 1.30-1.20 (m, 1H; **H3**). **^{13}C NMR (125 MHz, $CDCl_3$):** δ = 175.1 (**C6**), 82.1 (**C2**), 74.8 (**C9**), 72.6 (**C1**), 56.6 (**C8**), 52.0 (**C11**), 41.1 (**C5**), 34.3 (**C7**), 27.8 (**C3**), 26.9 (**C4**). **HR MS (ESI, +ve, MeOH):** m/z calculated for $[C_{11}H_{16}O_4 + Na]^+$; 235.0946, Found; 235.0958

Synthesis of 5 *S*-(2-acetamidoethyl) heptanethioate (192)

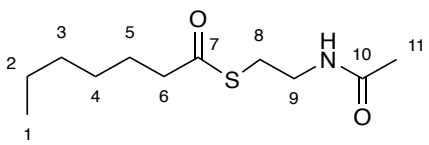

To a stirred solution of heptanoic acid (**133**) (0.43 mL, 3.1 mmol) in anhydrous CH_2Cl_2 (6 mL) at 0 °C under an atmosphere of argon was added EDC·HCl (645 mg, 3.4 mmol) and DMAP (75 mg, 0.6 mmol). The reaction mixture was stirred for 15 minutes and a solution *N*-acetylcisteamine (**27**) (400 mg, 3.4 mmol) in CH_2Cl_2 (2 mL) was added and the reaction mixture warmed to RT. The reaction mixture was stirred for 16 hours at RT. Upon completion the reaction mixture was diluted with water (10 mL), organics extracted with CH_2Cl_2 (25 mL), dried with $MgSO_4$ and concentrated *in vacuo* to afford a colourless oil (651 mg, 92%).

ν_{max}/cm^{-1} (neat) 1687 (C=O), 1635 (C=C); **^{1}H NMR (500 MHz, $CDCl_3$):** δ = 5.81 (br s, 1H; **NH**), 3.43 (q, *J* = 6.0 Hz, 2H; **H9**), 3.02 (t, *J* = 6.5 Hz, 2H; **H8**), 2.57 (t, *J* = 7.5 Hz, 2H; **H6**), 1.96 (s, 3H; **H11**), 1.65 (quin, *J* = 7.5 Hz, 2H; **H5**), 1.35-1.25 (m, 6H; **H2**, **H3** and **H4**), 0.88 (t, *J* = 7.0 Hz, 3H; **H1**). **^{13}C NMR (125 MHz, $CDCl_3$):** δ = 200.5 (**C7**), 170.4 (**C10**), 44.3 (**C6**), 39.9 (**C9**), 31.5 (**C3**), 28.7 (**C4**), 28.6 (**C8**), 25.8 (**C5**), 23.4 (**C11**), 22.6 (**C2**), 14.1 (**C1**). **HR MS (ESI, +ve, MeOH):** m/z calculated for $[C_{11}H_{21}NO_2S + Na]^+$; 254.1191, Found; 254.1186. $[\alpha]_D^{30}$ (c 0.25, $CHCl_3$); +1.0.

References

1 E. J. Bassett, M. S. Keith, G. J. Armelagos, D. L. Martin and A. R. Villanueva, *Science*, 1980, **209**, 1532–4.

2 F. Winau, O. Westphal and R. Winau, *Microbes Infect.*, 2004, **6**, 786–789.

3 R. I. Aminov, *Front. Microbiol.*, 2010, **1**, 134.

4 P. Ehrlich and S. Hata, *Die experimentelle Chemotherapie der Spirillosen*, Springer Berlin Heidelberg, Berlin, Heidelberg, 1910.

5 K. Gould, *J. Antimicrob. Chemother.*, 2016, **71**, 572–575.

6 N. C. Lloyd, H. W. Morgan, B. K. Nicholson and R. S. Ronimus, *Angew. Chemie Int. Ed.*, 2005, **44**, 941–944.

7 B. R. da Cunha, L. P. Fonseca and C. R. C. Calado, *Antibiotics*, 2019, 8, 45.

8 R. Gaynes, *Emerg. Infect. Dis.*, 2017, **23**, 849–853.

9 A. Fleming, *Br. J. Exp. Pathol.*, 1929, **10**, 226.

10 R. Bentley, *J. Chem. Educ.*, 2004, **81**, 1462.

11 G. Domagk, *Dtsch. Medizinische Wochenschrift*, 1935, **61**, 250–3.

12 G. E. SHAMBAUGH, *Arch. Otolaryngol. - Head Neck Surg.*, 1966, **83**, 1–2.

13 R. Bentley, *J. Ind. Microbiol. Biotechnol.*, 2009, **36**, 775–786.

14 S. A. Waksman and H. B. Woodruff, *Exp. Biol. Med.*, 1940, **45**, 609–614.

15 S. A. Waksman and H. B. Woodruff, *Exp. Biol. Med.*, 1942, **49**, 207–210.

16 K. Lewis, *Nature*, 2012, **485**, 439–440.

17 J. H. Comroe, *Am. Rev. Respir. Dis.*, 1978, **117**, 773–781.

18 H. B. Woodruff, *Appl. Environ. Microbiol.*, 2014, **80**, 2–8.

19 A. Schatz, E. Bugle and S. A. Waksman, *Exp. Biol. Med.*, 1944, **55**, 66–69.

20 M. O. Griffin, E. Fricovsky, G. Ceballos and F. Villarreal, *Am. J. Physiol. Cell Physiol.*, 2010, **299**, C539-48.

21 B. Hamad, *Nat. Rev. Drug Discov.*, 2010, **9**, 675–676.

22 L. Kakoullis, E. Papachristodoulou, P. Chra and G. Panos, *Antibiotics*, 2021, **10**, 415.

23 L. Dijkshoorn, A. Nemec and H. Seifert, *Nat. Rev. Microbiol.*, 2007, **5**, 939–51.

24 W. C. Reygaert, *AIMS Microbiol.*, 2018, **4**, 482–501.

25 T. J. Foster, *FEMS Microbiol. Rev.*, 2017, **41**, 430–449.

26 F. D. Lowy, *J. Clin. Invest.*, 2003, **111**, 1265.

27 P. D. Stapleton and P. W. Taylor, *Sci. Prog.*, 2002, **85**, 57–72.

28 A. Cassini, L. D. Högberg, D. Plachouras, A. Quattrocchi, A. Hoxha, G. S. Simonsen, M. Colomb-Cotinat, M. E. Kretzschmar, B. Devleesschauwer, M. Cecchini, D. A. Ouakrim, T. C. Oliveira, M. J. Struelens, C. Suetens, D. L. Monnet, R. Burden of AMR Collaborative Group, K. Mertens, T. Struyf, B. Catry, K. Latour, I. N. Ivanov, E. G. Dobreva, A. T. Andraševic, S. Soprek, A. Budimir, N. Paphitou, H. Žemlicková, S. S. Olsen, U. W. Sönksen, P. Märtin, M. Ivanova, O. Lyytikäinen, J. Jalava, B. Coignard, T. Eckmanns, M. A. Sin, S. Haller, G. L. Daikos, A. Gikas, S. Tsiodras, F. Kontopidou, Á. Tóth, Á. Hajdu, Ó. Guólaugsson, K. G. Kristinsson, S. Murchan, K. Burns, P. Pezzotti, C. Gagliotti, U. Dumpis, A. Liuimiene, M. Perrin, M. A. Borg, S. C. de Greeff, J. C. Monen, M. B. Koek, P. Elstrøm, D. Zabicka, A. Deptula, W. Hryniewicz, M. Caniça, P. J. Nogueira, P. A. Fernandes, V. Manageiro, G. A. Popescu, R. I. Serban, E. Schréterová, S. Litvová, M. Štefkovicová, J. Kolman, I. Klavs, A. Korošec, B. Aracil, A. Asensio, M. Pérez-Vázquez, H. Billström, S. Larsson, J. S. Reilly, A. Johnson and S. Hopkins, *Lancet. Infect. Dis.*, 2019, **19**, 56–66.

29 J. Davies, *Can. J. Infect. Dis. Med. Microbiol.*, 2006, **17**, 287–90.

30 J. M. Hamilton-Miller, *Br. J. Clin. Pharmacol.*, 1984, **18**, 469–74.

31 M. Mendelson, *S. Afr. Med. J.*, 2015, **105**, 414–8.

32 J. G. Bartlett, D. N. Gilbert and B. Spellberg, *Clin. Infect. Dis.*, 2013, **56**, 1445–50.

33 M. J. Martin, S. E. Thottathil and T. B. Newman, *Am. J. Public Health*, 2015, **105**, 2409–10.

34 J. Davies and D. Davies, *Microbiol. Mol. Biol. Rev.*, 2010, **74**, 417–33.

35 M. S. Mulani, E. E. Kamble, S. N. Kumkar, M. S. Tawre and K. R. Pardesi, *Front. Microbiol.*, 2019, **10**, 539.

36 W. H. Organization, WHO publishes list of bacteria for which new antibiotics are urgently needed, https://www.who.int/news/item/27-02-2017-who-publishes-list-of-bacteria-for-which-new-antibiotics-are-urgently-needed, (accessed 22 June 2021).

37 A. Howard, M. O'Donoghue, A. Feeney and R. D. Sleator, *Virulence*, 2012, **3**, 243–50.

38 M. Beijerinck, *Versl K. Akad Wetensch Amsterdam*, 1911, 1092–1103.

39 J. Brisou and A. R. Prevot, *Ann. Inst. Pasteur (Paris).*, 1954, **86**, 722–8.

40 P. Baumann, M. Doudoroff and R. Y. Stanier, *J. Bacteriol.*, 1968, **95**, 1520–41.

41 P. Baumann, *J. Bacteriol.*, 1968, **96**, 39–42.

42 I. Kusradze, S. M. Diene, M. Goderdzishvili and J.-M. Rolain, *Int. J. Antimicrob. Agents*, 2011, **38**, 164–168.

43 F. Perez, R. Ponce-Terashima, M. D. Adams and R. A. Bonomo, *Virulence*, 2011, **2**, 86–90.

44 P. Scott, G. Deye, A. Srinivasan, C. Murray, K. Moran, E. Hulten, J. Fishbain, D. Craft, S. Riddell, L. Lindler, J. Mancuso, E. Milstrey, C. T. Bautista, J. Patel, A. Ewell, T. Hamilton, C. Gaddy, M. Tenney, G. Christopher, K. Petersen, T. Endy and B. Petruccelli, *Clin. Infect. Dis.*, 2007, **44**, 1577–84.

45 P. J. Sebeny, M. S. Riddle and K. Petersen, *Clin. Infect. Dis.*, 2008, **47**, 444–9.

46 A. Y. Peleg, H. Seifert and D. L. Paterson, *Clin. Microbiol. Rev.*, 2008, **21**, 538–82.

47 I. V. Rocha, D. E. Xavier, K. R. H. de Almeida, S. R. de Oliveira and N. C. Leal, *Braz. J. Infect. Dis.*, 2018, **22**, 438–441.

48 P. Espinal, S. Martí and J. Vila, *J. Hosp. Infect.*, 2012, **80**, 56–60.

49 M. Asif, I. A. Alvi and S. U. Rehman, *Infect. Drug Resist.*, 2018, **11**, 1249–1260.

50 J. Liu, Y. Shu, F. Zhu, B. Feng, Z. Zhang, L. Liu and G. Wang, *J. Glob. Antimicrob. Resist.*, 2021, **24**, 136–147.

51 W. F. Penwell, A. B. Shapiro, R. A. Giacobbe, R.-F. Gu, N. Gao, J. Thresher, R. E. McLaughlin, M. D. Huband, B. L. M. DeJonge, D. E. Ehmann and A. A. Miller, *Antimicrob. Agents Chemother.*, 2015, **59**, 1680–9.

52 R. Vázquez-López, S. G. Solano-Gálvez, J. J. Juárez Vignon-Whaley, J. A. Abello Vaamonde, L. A. Padró Alonzo, A. Rivera Reséndiz, M. Muleiro Álvarez, E. N. Vega López, G. Franyuti-Kelly, D. A. Álvarez-Hernández, V. Moncaleano Guzmán, J. E. Juárez Bañuelos, J. Marcos Felix, J. A. González Barrios and T. Barrientos Fortes, *Antibiot. (Basel, Switzerland)*, 2020, **9**, 205.

53 M. Mohammadi, H. Khayat, K. Sayehmiri, S. Soroush, F. Sayehmiri, S. Delfani,

L. Bogdanovic and M. Taherikalani, *Open Microbiol. J.*, 2017, **11**, 63–71.

54 R. Tewari, D. Chopra, R. Wazahat, S. Dhingra and M. Dudeja, *Malays. J. Med. Sci.*, 2018, **25**, 129–134.

55 B. Y. Lee, S. M. McGlone, Y. Doi, R. R. Bailey and L. H. Harrison, *Infect. Control Hosp. Epidemiol.*, 2010, **31**, 1087–9.

56 E. Becerra, G. F. R. Magallanes, D. Murrieta, M. Gonzalez, N. Castellano, V. E. N. Roman and J. Rodríguez, *Int. J. Infect. Dis.*, 2020, **101**, 148.

57 X. Zhen, C. S. Lundborg, X. Sun, X. Hu and H. Dong, *Antimicrob. Resist. Infect. Control*, 2019, **8**, 137.

58 D. J. Newman and G. M. Cragg, *J. Nat. Prod.*, 2020, **83**, 770–803.

59 D. J. Newman and G. M. Cragg, *J. Nat. Prod.*, 2007, **70**, 461–77.

60 H. C. Neu, *Science (80-.).*, 1992, **257**, 1064–1073.

61 D. J. Payne, M. N. Gwynn, D. J. Holmes and D. L. Pompliano, *Nat. Rev. Drug Discov.*, 2007, **6**, 29–40.

62 A. L. Harvey, R. Edrada-Ebel and R. J. Quinn, *Nat. Rev. Drug Discov.*, 2015, **14**, 111–129.

63 P. F. Chan, D. J. Holmes and D. J. Payne, *Drug Discov. Today Ther. Strateg.*, 2004, **1**, 519–527.

64 C. A. Lipinski, F. Lombardo, B. W. Dominy and P. J. Feeney, *Adv. Drug Deliv. Rev.*, 1997, **23**, 3–25.

65 K. Lewis, *Nat. Rev. Drug Discov.*, 2013, **12**, 371–387.

66 M. N. Thaker, W. Wang, P. Spanogiannopoulos, N. Waglechner, A. M. King, R. Medina and G. D. Wright, *Nat. Biotechnol.*, 2013, **31**, 922–7.

67 M. Zerikly and G. L. Challis, *Chembiochem*, 2009, **10**, 625–33.

68 G. L. Challis, *J. Med. Chem.*, 2008, **51**, 2618–28.

69 C. Corre and G. L. Challis, *Chem. Biol.*, 2007, **14**, 7–9.

70 C. Walsh, *Nat. Rev. Microbiol.*, 2003, **1**, 65–70.

71 I. B. Seiple, Z. Zhang, P. Jakubec, A. Langlois-Mercier, P. M. Wright, D. T. Hog, K. Yabu, S. R. Allu, T. Fukuzaki, P. N. Carlsen, Y. Kitamura, X. Zhou, M. L. Condakes, F. T. Szczypiński, W. D. Green and A. G. Myers, *Nature*, 2016, **533**, 338–345.

72 P. M. Wright, I. B. Seiple and A. G. Myers, *Angew. Chem. Int. Ed. Engl.*, 2014,

53, 8840–69.

73 R. Leclercq, *Clin. Infect. Dis.*, 2002, **34**, 482–492.

74 F. Liu and A. G. Myers, *Curr. Opin. Chem. Biol.*, 2016, **32**, 48–57.

75 C. Sun, Q. Wang, J. D. Brubaker, P. M. Wright, C. D. Lerner, K. Noson, M. Charest, D. R. Siegel, Y.-M. Wang and A. G. Myers, *J. Am. Chem. Soc.*, 2008, **130**, 17913–17927.

76 J. A. Sutcliffe, W. O'Brien, C. Fyfe and T. H. Grossman, *Antimicrob. Agents Chemother.*, 2013, **57**, 5548–58.

77 P. Li, J. Li, F. Arikan, W. Ahlbrecht, M. Dieckmann and D. Menche, *J. Am. Chem. Soc.*, 2009, **131**, 11678–11679.

78 M. A. Fischbach and C. T. Walsh, *Science*, 2009, **325**, 1089–93.

79 S. Morimoto, Y. Takahashi, Y. Watanabe and S. Omura, *J. Antibiot. (Tokyo).*, 1984, **37**, 187–9.

80 P. Kurath, P. H. Jones, R. S. Egan and T. J. Perun, *Experientia*, 1971, **27**, 362–362.

81 T. Cachet, G. Van den Mooter, R. Hauchecorne, C. Vinckier and J. Hoogmartens, *Int. J. Pharm.*, 1989, **55**, 59–65.

82 G. M. Bright, A. A. Nagel, J. Bordner, K. A. Desai, J. N. Dibrino, J. Nowakowska, L. Vincent, R. M. Watrous, F. C. Sciavolino and A. R. English, *J. Antibiot. (Tokyo).*, 1988, **41**, 1029–47.

83 S. D. Putnam, M. Castanheira, G. J. Moet, D. J. Farrell and R. N. Jones, *Diagn. Microbiol. Infect. Dis.*, 2010, **66**, 393–401.

84 R. L. Peck, C. E. Hoffhin and K. Folkers, *J. Am. Chem. Soc.*, 1946, **68**, 1390.

85 L. H. Conover, W. T. Moreland, A. R. English, C. R. Stephens and F. J. Pilgrim, *J. Am. Chem. Soc.*, 1953, **75**, 4622–4623.

86 1956, (US Patent 2734018).

87 S. Deng, X. Ma, E. Su and D. Wei, *J. Biotechnol.*, 2016, **219**, 142–148.

88 S. S. Ospina, A. Lopez-Munguia, R. L. Gonzalez and R. Quintero, *J. Chem. Technol. Biotechnol.*, 1992, **53**, 205–14.

89 S. Dutta, J. R. Whicher, D. A. Hansen, W. A. Hale, J. A. Chemler, G. R. Congdon, A. R. H. Narayan, K. Håkansson, D. H. Sherman, J. L. Smith and G. Skiniotis, *Nature*, 2014, **510**, 512–517.

90 D. E. Cane and C. C. Yang, *J. Am. Chem. Soc.*, 1987, **109**, 1255–1257.

91 D. E. Cane, H. Hasler and T.-C. Liang, *J. Am. Chem. Soc.*, 1981, **103**, 5960–5962.

92 J. Staunton and B. Wilkinson, *Chem. Rev.*, 1997, **97**, 2611–2630.

93 E. J. N. Helfrich and J. Piel, *Nat. Prod. Rep.*, 2016, **33**, 231–316.

94 J. Piel, *Nat. Prod. Rep.*, 2010, **27**, 996.

95 L. E. N. Quadri, P. H. Weinreb, M. Lei, M. M. Nakano, P. Zuber and C. T. Walsh, *Biochemistry*, 1998, **37**, 1585–1595.

96 J. Beld, E. C. Sonnenschein, C. R. Vickery, J. P. Noel and M. D. Burkart, *Nat. Prod. Rep.*, 2014, **31**, 61–108.

97 R. H. Lambalot, A. M. Gehring, R. S. Flugel, P. Zuber, M. LaCelle, M. A. Marahiel, R. Reid, C. Khosla and C. T. Walsh, *Chem. Biol.*, 1996, **3**, 923–36.

98 D. I. Chan and H. J. Vogel, *Biochem. J*, 2010, **430**, 1–19.

99 C. Khosla, Y. Tang, A. Y. Chen, N. A. Schnarr and D. E. Cane, *Annu. Rev. Biochem.*, 2007, **76**, 195–221.

100 B. S. Moore and C. Hertweck, *Nat. Prod. Rep.*, 2002, **19**, 70–99.

101 Y. A. Chan, A. M. Podevels, B. M. Kevany and M. G. Thomas, *Nat. Prod. Rep.*, 2009, **26**, 90–114.

102 T. Robbins, J. Kapilivsky, D. E. Cane and C. Khosla, *Biochemistry*, 2016, **55**, 4476–84.

103 A. T. Keatinge-Clay and R. M. Stroud, *Structure*, 2006, **14**, 737–48.

104 P. Caffrey, *ChemBioChem*, 2003, **4**, 654–657.

105 A. T. Keatinge-Clay, *Chem. Biol.*, 2007, **14**, 898–908.

106 J. Zheng and A. T. Keatinge-Clay, *J. Mol. Biol.*, 2011, **410**, 105–117.

107 J. Zheng, S. K. Piasecki and A. T. Keatinge-Clay, *ACS Chem. Biol.*, 2013, **8**, 1964–71.

108 X. Xie and D. E. Cane, *Org. Biomol. Chem.*, 2018, **16**, 9165–9170.

109 B. Sedgwick, C. Morris and S. J. French, *J. Chem. Soc. Chem. Commun.*, 1978, 193.

110 D. M. Roberts, C. Bartel, A. Scott, D. Ivison, T. J. Simpson and R. J. Cox, *Chem. Sci.*, 2017, **8**, 1116–1126.

111 D. H. Kwan, Y. Sun, F. Schulz, H. Hong, B. Popovic, J. C. C. Sim-Stark, S. F.

Haydock and P. F. Leadlay, *Chem. Biol.*, 2008, **15**, 1231–1240.

112 T. Pavkov-Keller, K. Steiner, M. Faber, M. Tengg, H. Schwab, M. Gruber-Khadjawi and K. Gruber, *PLoS One*, 2017, **12**, e0171056.

113 D. K. Liscombe, G. V. Louie and J. P. Noel, *Nat. Prod. Rep.*, 2012, **29**, 1238.

114 M. A. Skiba, M. M. Bivins, J. R. Schultz, S. M. Bernard, W. D. Fiers, Q. Dan, S. Kulkarni, P. Wipf, W. H. Gerwick, D. H. Sherman, C. C. Aldrich and J. L. Smith, *ACS Chem. Biol.*, 2018, **13**, 3221–3228.

115 M. A. Skiba, A. P. Sikkema, W. D. Fiers, W. H. Gerwick, D. H. Sherman, C. C. Aldrich and J. L. Smith, *ACS Chem. Biol.*, 2016, **11**, 3319–3327.

116 P. A. Storm, D. A. Herbst, T. Maier and C. A. Townsend, *Cell Chem. Biol.*, 2017, **24**, 316–325.

117 M. Köksal, W. K. W. Chou, D. E. Cane and D. W. Christianson, *Biochemistry*, 2012, **51**, 3003–3010.

118 L. Du and L. Lou, *Nat. Prod. Rep.*, 2010, **27**, 255–278.

119 S.-C. Tsai, H. Lu, D. E. Cane, C. Khosla and R. M. Stroud, *Biochemistry*, 2002, **41**, 12598–606.

120 T. Kornfuehrer and A. Eustaquio, *Medchemcomm*, 2019, **10**, 1256–1272.

121 U. R. Awodi, J. L. Ronan, J. Masschelein, E. L. C. de los Santos and G. L. Challis, *Chem. Sci.*, 2017, **8**, 411–415.

122 M. W. Mullowney, R. A. McClure, M. T. Robey, N. L. Kelleher and R. J. Thomson, *Nat. Prod. Rep.*, 2018, **35**, 847–878.

123 R. F. Little and C. Hertweck, *Nat. Prod. Rep.*, 2021, Advance Article.

124 J. Masschelein, P. K. Sydor, C. Hobson, R. Howe, C. Jones, D. M. Roberts, Z. Ling Yap, J. Parkhill, E. Mahenthiralingam and G. L. Challis, *Nat. Chem.*, 2019, **11**, 906–912.

125 S. Kosol, A. Gallo, D. Griffiths, T. R. Valentic, J. Masschelein, M. Jenner, E. L. C. de los Santos, L. Manzi, P. K. Sydor, D. Rea, S. Zhou, V. Fülöp, N. J. Oldham, S.-C. Tsai, G. L. Challis and J. R. Lewandowski, *Nat. Chem.*, 2019, **11**, 913–923.

126 C. Olano, C. Méndez and J. A. Salas, *Nat. Prod. Rep.*, 2010, **27**, 571.

127 J. L. R. Anderson and S. K. Chapman, *Mol. Biosyst.*, 2006, **2**, 350.

128 L. C. Blasiak and C. L. Drennan, *Acc. Chem. Res.*, 2009, **42**, 147–155.

129 F. H. Vaillancourt, D. A. Vosburg and C. T. Walsh, *ChemBioChem*, 2006, **7**,

748–752.

130 J. Cortes, K. E. Wiesmann, G. A. Roberts, M. J. Brown, J. Staunton and P. F. Leadlay, *Science*, 1995, **268**, 1487–9.

131 C. M. Kao, M. McPherson, R. N. McDaniel, H. Fu, D. E. Cane and C. Khosla, *J. Am. Chem. Soc.*, 1997, **119**, 11339–11340.

132 C. M. Kao, G. Luo, L. Katz, D. E. Cane and C. Khosla, *J. Am. Chem. Soc.*, 1995, **117**, 9105–9106.

133 C. M. Kao, G. Luo, L. Katz, D. E. Cane and C. Khosla, *J. Am. Chem. Soc.*, 1996, **118**, 9184–9185.

134 S. Kushnir, U. Sundermann, S. Yahiaoui, A. Brockmeyer, P. Janning and F. Schulz, *Angew. Chem. Int. Ed. Engl.*, 2012, **51**, 10664–9.

135 A. Bhatt, C. B. W. Stark, B. M. Harvey, A. R. Gallimore, Y. A. Demydchuk, J. B. Spencer, J. Staunton and P. F. Leadlay, *Angew. Chemie Int. Ed.*, 2005, **44**, 7075–7078.

136 B. Kusebauch, N. Brendel, H. Kirchner, H.-M. Dahse and C. Hertweck, *ChemBioChem*, 2011, **12**, 2284–2288.

137 T. Kornfuehrer and A. S. Eustáquio, *Medchemcomm*, 2019, **10**, 1256–1272.

138 T. Watanabe, K. Izaki and H. Takahashi, *J. Antibiot. (Tokyo).*, 1982, **35**, 1141–7.

139 T. Watanabe, T. Sugiyama and K. Izaki, *J. Antibiot. (Tokyo).*, 1994, **47**, 496–498.

140 T. Watanabe, T. Sugiyama, M. Takahashi, J. Shima, K. Yamashita, K. Izaki, K. Furihata and H. Seto, *Agric. Biol. Chem.*, 1990, **54**, 259–261.

141 H. Furukawa, H. Kiyota, T. Yamada, M. Yaosaka, R. Takeuchi, T. Watanabe and S. Kuwahara, *Chem. Biodivers.*, 2007, **4**, 1601–1604.

142 T. Watanabe, T. Sugiyama, M. Takahashi, J. Shima, K. Yamashita, K. Izaki, K. Furihata and H. Seto, *J. Antibiot. (Tokyo).*, 1992, **45**, 470–5.

143 T. Watanabe, T. Sugiyama, K. Chino, T. Suzuki, S. Wakabayashi, H. Hayashi, R. Itami, J. Shima and K. Izaki, *J. Antibiot. (Tokyo).*, 1992, **45**, 476–484.

144 R. Takeuchi, H. Kiyota, M. Yaosaka, T. Watanabe, K. Enari, T. Sugiyama and T. Oritani, *J. Chem. Soc. Perkin Trans. 1*, 2001, 2676–2681.

145 T. Watanabe, J. Shima, K. Izaki and T. Sugiyama, *J. Antibiot. (Tokyo).*, 1992,

45, 575–576.

146 E. Mahenthiralingam, L. Song, A. Sass, J. White, C. Wilmot, A. Marchbank, O. Boaisha, J. Paine, D. Knight and G. L. Challis, *Chem. Biol.*, 2011, **18**, 665–677.

147 T. Watanabe, T. Suzuki and K. Izaki, *J. Antibiot. (Tokyo).*, 1991, **44**, 1457–1459.

148 T. Watanabe, N. Okubo, T. Suzuki and K. Izaki, *J. Antibiot. (Tokyo).*, 1992, **45**, 572–4.

149 A. Parmeggiani, I. M. Krab, T. Watanabe, R. C. Nielsen, C. Dahlberg, J. Nyborg and P. Nissen, *J. Biol. Chem.*, 2006, **281**, 2893–900.

150 R. Cetin, I. M. Krab, P. H. Anborgh, R. H. Cool, T. Watanabe, T. Sugiyama, K. Izaki and A. Parmeggiani, *EMBO J.*, 1996, **15**, 2604–11.

151 M. Warias, H. Grubmüller and L. V. Bock, *Biophys. J.*, 2020, **118**, 151–161.

152 L. Gu, T. W. Geders, B. Wang, W. H. Gerwick, K. Håkansson, J. L. Smith and D. H. Sherman, *Science*, 2007, **318**, 970–4.

153 J. Masschelein, M. Jenner and G. L. Challis, *Nat. Prod. Rep.*, 2017, **34**, 712–783.

154 R. Oyama, T. Watanabe, H. Hanzawa, T. Sano, T. Sugiyama and K. Izaki, *Biosci. Biotechnol. Biochem.*, 1994, **58**, 1914–7.

155 S. Dachwitz, C. Widmann, M. Frese, H. H. Niemann and N. Sewald, Royal Society of Chemistry, 2020, pp. 1–43.

156 C. Bergt, X. Fu, N. P. Huq, J. Kao and J. W. Heinecke, *J. Biol. Chem.*, 2004, **279**, 7856–66.

157 A. J. Mitchell, Q. Zhu, A. O. Maggiolo, N. R. Ananth, M. L. Hillwig, X. Liu and A. K. Boal, *Nat. Chem. Biol.*, 2016, **12**, 636–640.

158 M. Voss, S. Honda Malca and R. Buller, *Chem. – A Eur. J.*, 2020, **26**, 7336–7345.

159 B. Mennenga, C. W. M. Kay and H. Görisch, *Arch. Microbiol.*, 2009, **191**, 361–367.

160 S. I. Chan, P. Chuankhayan, P. K. Reddy Nareddy, I.-K. Tsai, Y.-F. Tsai, K. H.-C. Chen, S. S.-F. Yu and C.-J. Chen, *J. Am. Chem. Soc.*, 2021, **143**, 3359–3372.

161 C. W. M. Kay, B. Mennenga, H. Görisch and R. Bittl, *Proc. Natl. Acad. Sci. U. S. A.*, 2006, **103**, 5267–72.

162 C. Hobson, PhD Thesis, University of Warwick, 2019.

163 J. Masschelein, C. Hobson, X. Jian, J. Sargeant, H. G. Smith, N. Bali, C. Heffernan and G. L. Challis, *Biosynthetic engineering illuminates the structure activity relationship of enacyloxin IIa (Manuscript in preparation)*, .

164 S. A. Shepherd, C. Karthikeyan, J. Latham, A.-W. Struck, M. L. Thompson, B. R. K. Menon, M. Q. Styles, C. Levy, D. Leys and J. Micklefield, *Chem. Sci.*, 2015, **6**, 3454–3460.

165 B. F. Fisher, H. M. Snodgrass, K. A. Jones, M. C. Andorfer and J. C. Lewis, *ACS Cent. Sci.*, 2019, **5**, 1844–1856.

166 P. R. Neubauer, C. Widmann, D. Wibberg, L. Schröder, M. Frese, T. Kottke, J. Kalinowski, H. H. Niemann and N. Sewald, *PLoS One*, 2018, **13**, e0196797.

167 V. Agarwal, A. A. El Gamal, K. Yamanaka, D. Poth, R. D. Kersten, M. Schorn, E. E. Allen and B. S. Moore, *Nat. Chem. Biol.*, 2014, **10**, 640–647.

168 M. Ismail, M. Frese, T. Patschkowski, V. Ortseifen, K. Niehaus and N. Sewald, *Adv. Synth. Catal.*, 2019, **361**, 2475–2486.

169 J. Peed, I. Periñán Domínguez, I. R. Davies, M. Cheeseman, J. E. Taylor, G. Kociok-Köhn and S. D. Bull, *Org. Lett.*, 2011, **13**, 3592–3595.

170 N. R. Curtis, A. B. Holmes, M. G. Looney, N. D. Pearson and G. C. Slim, *Tetrahedron Lett.*, 1991, **32**, 537–540.

171 J. A. Dale, D. L. Dull and H. S. Mosher, *J. Org. Chem.*, 1969, **34**, 2543–2549.

172 J. A. Dale and H. S. Mosher, *J. Am. Chem. Soc.*, 1973, **95**, 512–519.

173 T. R. Hoye, C. S. Jeffrey and F. Shao, *Nat. Protoc.*, 2007, **2**, 2451–2458.

174 P. C. Dorrestein, S. B. Bumpus, C. T. Calderone, S. Garneau-Tsodikova, Z. D. Aron, P. D. Straight, R. Kolter, C. T. Walsh and N. L. Kelleher, *Biochemistry*, 2006, **45**, 12756–12766.

175 M. Jenner, *Using Mass Spectrometry for Biochemical Studies on Enzymatic Domains from Polyketide Synthases*, Springer International Publishing, Cham, 2016.

176 M. Tosin, L. Betancor, E. Stephens, W. M. Ariel Li, J. B. Spencer and P. F. Leadlay, *ChemBioChem*, 2010, **11**, 539–546.

177 M. Tosin, Y. Demydchuk, J. S. Parascandolo, C. Blasco Per, F. J. Leeper and P. F. Leadlay, *Chem. Commun.*, 2011, **47**, 3460.

178 M. Tosin, D. Spiteller and J. B. Spencer, *ChemBioChem*, 2009, **10**, 1714–1723.

179 D. Spiteller, C. L. Waterman and J. B. Spencer, *Angew. Chemie Int. Ed.*, 2005, **44**, 7079–7082.

180 H. C. Kolb and K. B. Sharpless, *Drug Discov. Today*, 2003, **8**, 1128–1137.

181 C. D. Hein, X.-M. Liu and D. Wang, *Pharm. Res.*, 2008, **25**, 2216–2230.

182 H. C. Kolb, M. G. Finn and K. B. Sharpless, *Angew. Chemie Int. Ed.*, 2001, **40**, 2004–2021.

183 H. C. Kolb, M. G. Finn and K. B. Sharpless, *Angew. Chemie Int. Ed.*, 2001, **40**, 2004–2021.

184 V. V Rostovtsev, L. G. Green, V. V Fokin and K. B. Sharpless, *Angew. Chem. Int. Ed. Engl.*, 2002, **41**, 2596–9.

185 Christian W. Tornøe, A. Caspar Christensen and M. Meldal, *J. Org. Chem*, 2002, **67**, 3057–3064.

186 B. T. Worrell, J. A. Malik and V. V Fokin, *Science*, 2013, **340**, 457–60.

187 R. Ramkumar and P. Anbarasan, in *Copper Catalysis in Organic Synthesis*, Wiley, 2020, pp. 177–207.

188 V. D. Bock, H. Hiemstra and J. H. van Maarseveen, *European J. Org. Chem.*, 2006, **2006**, 51–68.

189 J. E. Hein and V. V. Fokin, *Chem. Soc. Rev.*, 2010, **39**, 1302.

190 G. Turan-Zitouni, Z. A. Kaplancikli, M. T. Yildiz, P. Chevallet and D. Kaya, *Eur. J. Med. Chem.*, 2005, **40**, 607–13.

191 C. Gill, G. Jadhav, M. Shaikh, R. Kale, A. Ghawalkar, D. Nagargoje and M. Shiradkar, *Bioorg. Med. Chem. Lett.*, 2008, **18**, 6244–7.

192 B. S. Holla, M. Mahalinga, M. S. Karthikeyan, B. Poojary, P. M. Akberali and N. S. Kumari, *Eur. J. Med. Chem.*, 2005, **40**, 1173–8.

193 J. N. Sangshetti, R. R. Nagawade and D. B. Shinde, *Bioorg. Med. Chem. Lett.*, 2009, **19**, 3564–7.

194 I. Bennett, N. J. Broom, G. Bruton, S. Calvert, B. P. Clarke, K. Coleman, R. Edmondson, P. Edwards, D. Jones and N. F. Osborne, *J. Antibiot. (Tokyo).*, 1991, **44**, 331–7.

195 R. D. Padmaja and K. Chanda, *Org. Process Res. Dev.*, 2018, **22**, 457–466.

196 R. Kharb, P. C. Sharma and M. S. Yar, *J. Enzyme Inhib. Med. Chem.*, 2011, **26**,

1–21.

197 S. M. Silverman, J. E. Moses and K. B. Sharpless, *Chem. - A Eur. J.*, 2017, **23**, 79–83.

198 G. R. Pereira, A. C. G. Ferreira, F. Costa, V. Munhoz, D. Alvarenga, B. M. Silva, A. C. C. Reis and G. C. Brandão, *Nat. Prod. Res.*, 2020, 1–4.

199 F. M. Veronese and G. Pasut, *Drug Discov. Today*, 2005, **10**, 1451–8.

200 Q. Yang, M. Sheng, J. J. Henkelis, S. Tu, E. Wiensch, H. Zhang, Y. Zhang, C. Tucker and D. E. Ejeh, *Org. Process Res. Dev.*, 2019, **23**, 2210–2217.

201 S. M. Wells, J. C. Widen, D. A. Harki and K. M. Brummond, *Org. Lett.*, 2016, **18**, 4566–4569.

202 D. J. W. and and J. Fritz, *Org. Lett*, 2006, **8**, 3659–3662.

203 B. A. Napier, E. M. Burd, S. W. Satola, S. M. Cagle, S. M. Ray, P. McGann, J. Pohl, E. P. Lesho and D. S. Weiss, *MBio*, 2013, **4**, e00021-13.

204 I. Caniaux, A. van Belkum, G. Zambardi, L. Poirel and M. F. Gros, *Eur. J. Clin. Microbiol. Infect. Dis.*, 2017, **36**, 415–420.

205 M. E. Falagas, S. K. Kasiakou and L. D. Saravolatz, *Clin. Infect. Dis.*, 2005, **40**, 1333–1341.

206 A. Ordooei Javan, S. Shokouhi and Z. Sahraei, *Eur. J. Clin. Pharmacol.*, 2015, **71**, 801–810.

207 Jung Beom Son, Min-ho Hwang, A. Wonsun Lee and D.-H. Lee, *Org. Lett*, 2007, **9**, 3897–3900.

208 E. Liddle, A. Scott, L.-C. Han, D. Ivison, T. J. Simpson, C. L. Willis and R. J. Cox, *Chem. Commun.*, 2017, **53**, 1727–1730.

209 M. Jenner, S. Frank, A. Kampa, C. Kohlhaas, P. Pöplau, G. S. Briggs, J. Piel and N. J. Oldham, *Angew. Chemie Int. Ed.*, 2013, **52**, 1143–1147.

210 F. Wang, Y. Wang, J. Ji, Z. Zhou, J. Yu, H. Zhu, Z. Su, L. Zhang and J. Zheng, *ACS Chem. Biol.*, 2015, **10**, 1017–1025.

211 Y. Li, W. Zhang, H. Zhang, W. Tian, L. Wu, S. Wang, M. Zheng, J. Zhang, C. Sun, Z. Deng, Y. Sun, X. Qu and J. Zhou, *Angew. Chemie*, 2018, **130**, 5925–5929.

212 A. M. Weeks, N. Wang, J. G. Pelton and M. C. Y. Chang, *Proc. Natl. Acad. Sci. U. S. A.*, 2018, **115**, E2193–E2201.

213 R. B. Hamed, L. Henry, J. R. Gomez-Castellanos, A. Asghar, J. Brem, T. D. W.

Claridge and C. J. Schofield, *Org. Biomol. Chem.*, 2013, **11**, 8191.

214 S. Friedrich, F. Hemmerling, F. Lindner, A. Warnke, J. Wunderlich, G. Berkhan and F. Hahn, *Molecules*, 2016, **21**, 1443.

215 H. Kawashima, M. Sakai, Y. Kaneko and Y. Kobayashi, *Tetrahedron*, 2015, **71**, 2387–2392.

216 Z.-X. Wang and Y. Shi, *J. Org. Chem*, 1997, **62**, 8622–8623.

217 Z.-X. Wang, S. M. Miller, O. P. Anderson and Y. Shi, *J. Org. Chem*, 1999, **64**, 6443–6458.

218 H. Nakamura, M. Ono, Y. Shida and H. Akita, *Tetrahedron: Asymmetry*, 2002, **13**, 705–713.

219 B. Akkala and K. Damera, *Arkivoc*, 2013, **2013**, 164.

220 S. Battah, R. C. Hider, A. J. MacRobert, P. S. Dobbin and T. Zhou, *J. Med. Chem.*, 2017, **60**, 3498–3510.

221 C. D. Campbell, C. Concellón and A. D. Smith, *Tetrahedron: Asymmetry*, 2011, **22**, 797–811.

222 Z. Edoo, L. Iannazzo, F. Compain, I. Li de la Sierra Gallay, H. van Tilbeurgh, M. Fonvielle, F. Bouchet, E. Le Run, J.-L. Mainardi, M. Arthur, M. Ethève-Quelquejeu and J.-E. Hugonnet, *Chem. - A Eur. J.*, 2018, **24**, 8081–8086.

223 C. Herdeis, *Synthesis (Stuttg).*, 1986, 232–233.

224 K. P. K. and and V. Ravikumar, *J. Org. Chem*, 2007, **72**, 6116–6126.

225 S. J. Davidson, A. N. Pearce, B. R. Copp and D. Barker, *Org. Lett.*, 2017, **19**, 5368–5371.

226 D. Xiao, M. D. Vera, B. Liang and M. M. Joullié, *J. Org. Chem*, 2001, **66**, 2734–2742.

227 K.-C. Ching, Y.-W. Kam, A. Merits, L. F. P. Ng and C. L. L. Chai, *J. Med. Chem.*, 2015, **58**, 9196–9213.

228 T. Kusama, T. Soga, E. Shioya, K. Nakayama, H. Nakajima, Y. Osada, Y. Ono, S. Kusumoto and T. Shiba, *Chem. Pharm. Bull. (Tokyo).*, 1990, **38**, 3366–72.

229 E. . Corey and H.-C. Huang, *Tetrahedron Lett.*, 1989, **30**, 5235–5238.

230 A. D. Steele, K. W. Knouse, C. E. Keohane and W. M. Wuest, *J. Am. Chem. Soc.*, 2015, **137**, 7314–7317.

231 A. K. Ghosh and G. Gangli, *J. Org. Chem*, 2006, **71**, 1085–1093.

232 K. Miyashita, T. Tsunemi, T. Hosokawa, M. Ikejiri and T. Imanishi, *Tetrahedron Lett.*, 2007, **48**, 3829–3833.

233 X. Wang, M. Ma, A. G. K. Reddy and W. Hu, *Tetrahedron*, 2017, **73**, 1381–1388.

234 B. M. Trost, J. Xie and J. D. Sieber, *J. Am. Chem. Soc.*, 2011, **133**, 20611–20622.

Appendices

Previously produced enacyloxin analogues

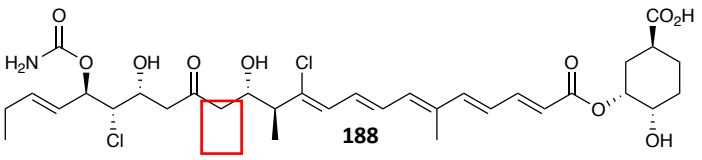

Δ5927
MIC = 2 µg/mL

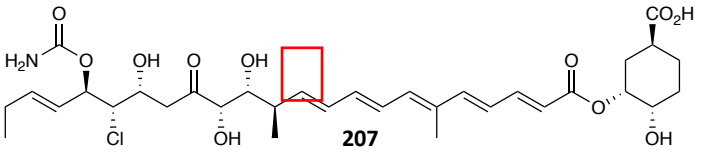

Δ5928
MIC = 4 µg/mL

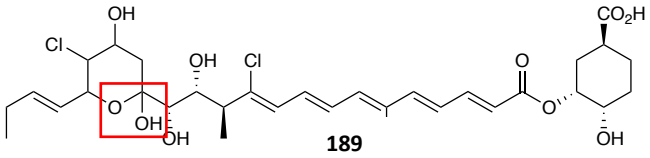

Δ5930
MIC = 4 µg/mL

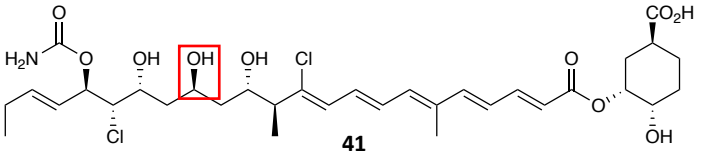

Δ5932
MIC = 8 µg/mL

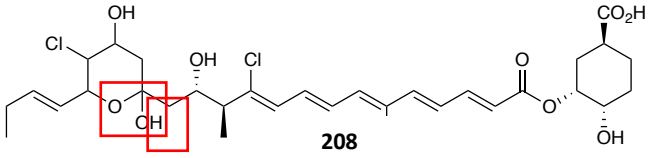

Δ5927 + Δ5930
MIC = 8 µg/mL

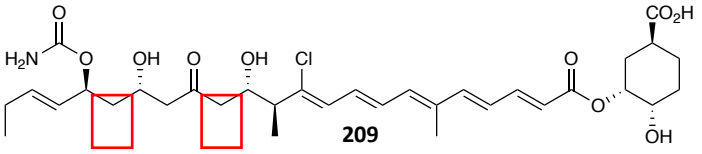

Δ5927 + Δ5931
MIC = 8 µg/mL

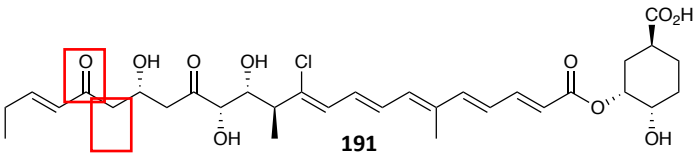

Δ5930 + Δ5931
MIC = 32 µg/mL

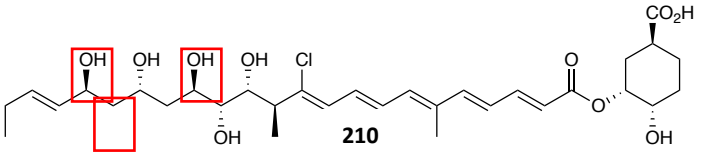

Δ5930 - Δ5932
MIC = 8 µg/mL

Appendix 1.1 Structures of previously produced enacyloxin analogues through deletions of genes encoding the tailoring enzymes with corresponding activities against *A. baumannii*..

HRMS of enacyloxin and analogues produced in this work

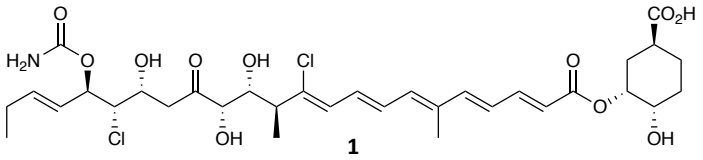

1

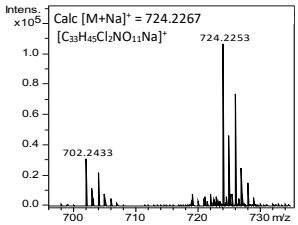

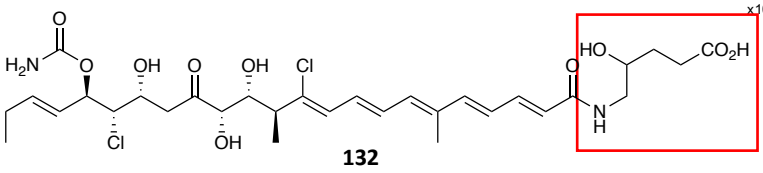

132

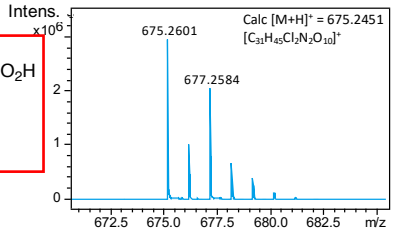

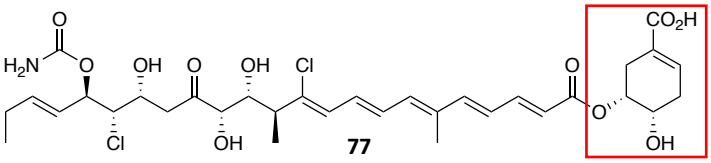

77

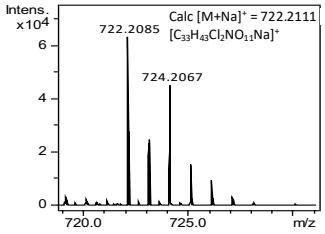

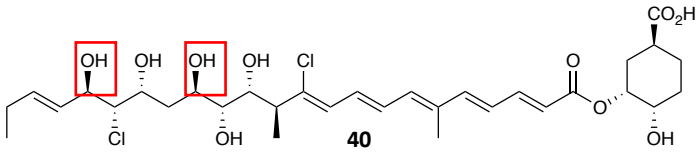

40

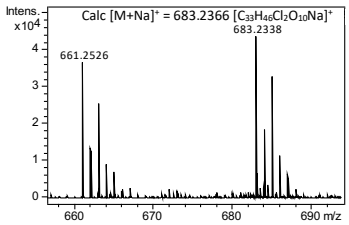

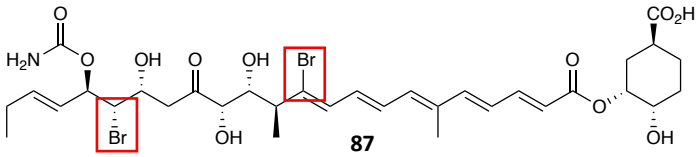

87

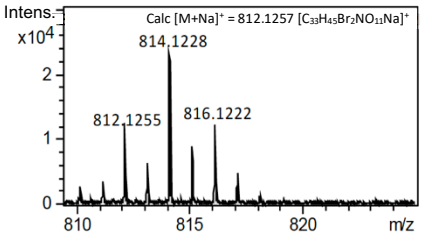

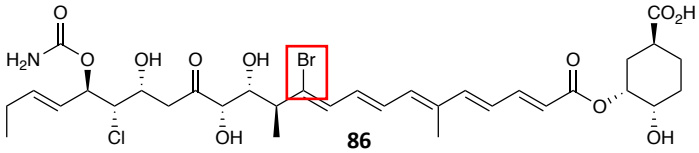

86

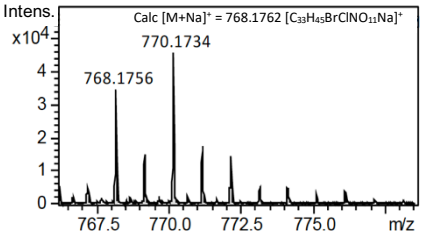

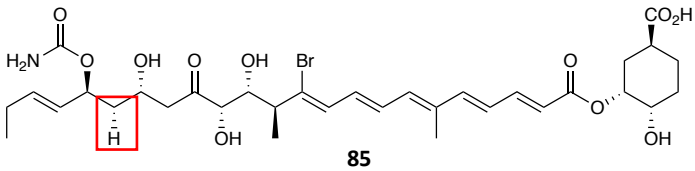

85

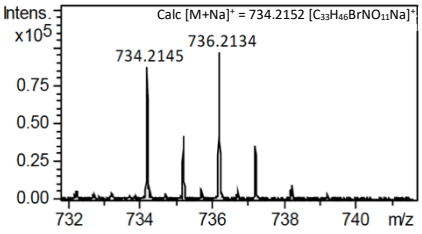

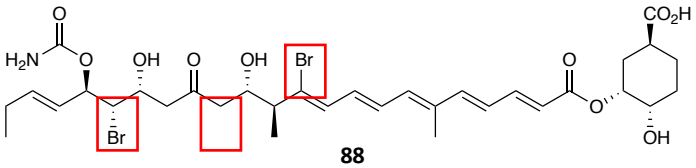

88

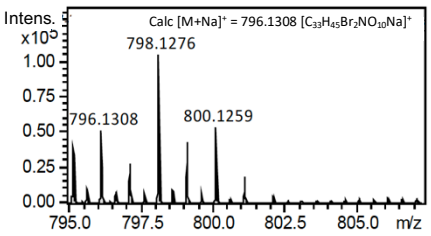

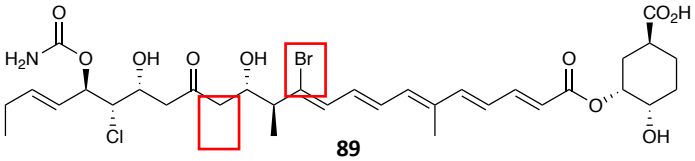

89

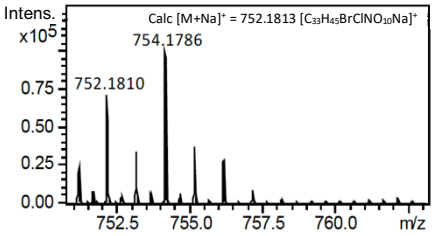

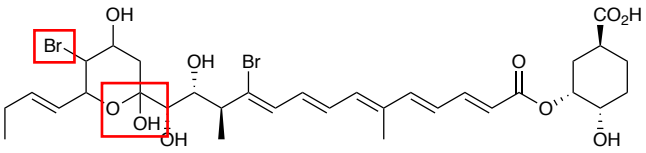

90

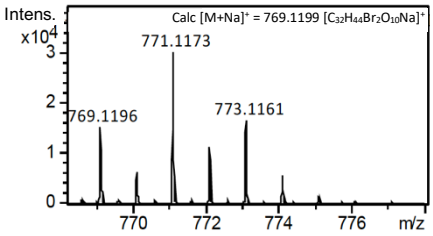

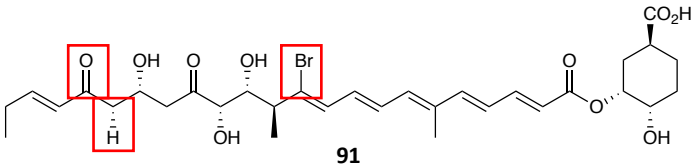

91

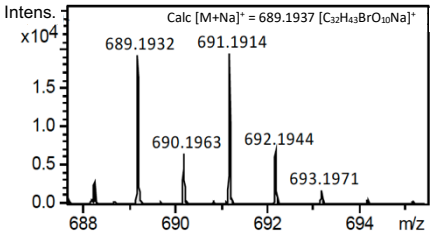

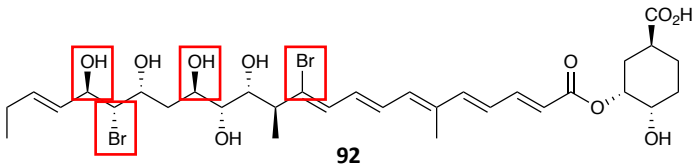

92

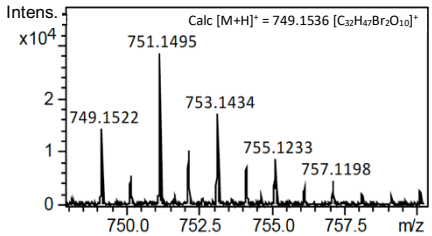

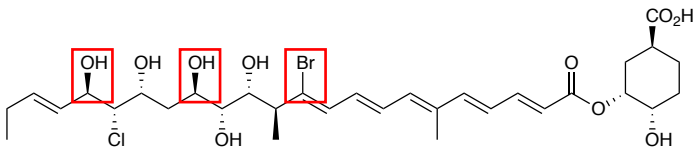

93

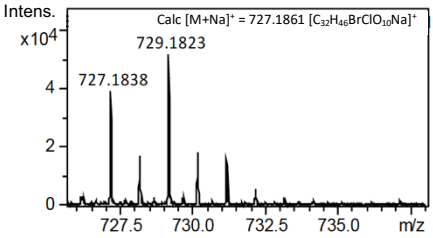

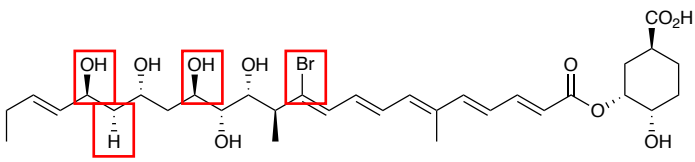

94

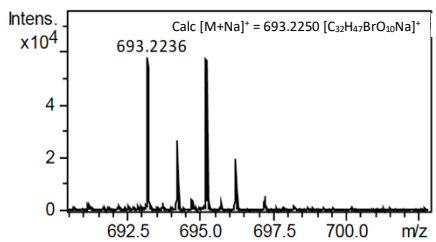

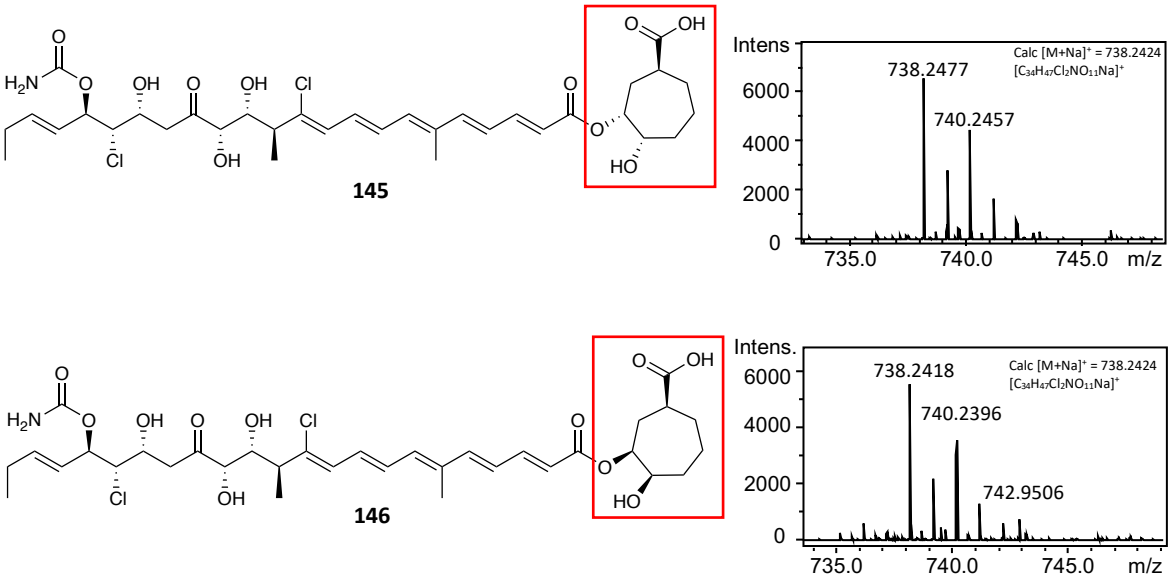

Appendix 1.2 HR-MS data for enacyloxin IIa and analogues produced

Homology Model

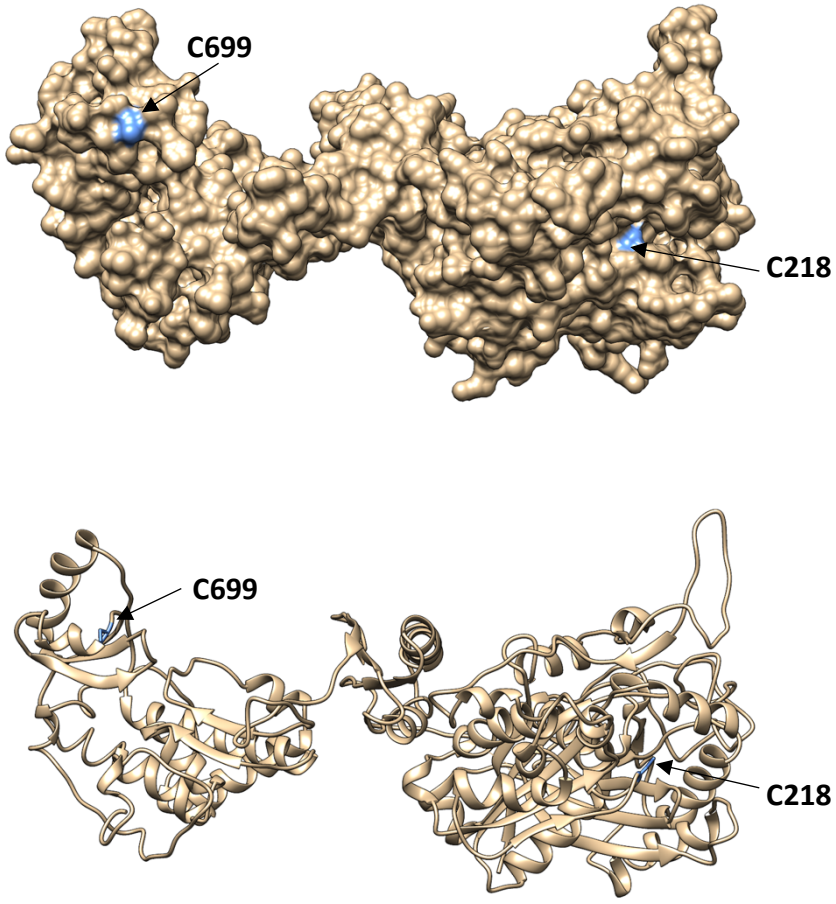

Appendix 1.3 Homology model of the *bamb*_5924 module 3 KS domain from a mammalian fatty acid synthase as a template. PDB code: 2vz8